

Sacred Heart Journal of Science and Humanities

(Bi - annual Journal of Science and Humanities)

Editor - in - Chief

C.M. Varghese

Principal, Sacred Heart College, Tirupattur, Vellore Dt

Editor

T. Jeyabalan

Director, Abraham Panampara Research Centre, Sacred Heart College, Tirupattur, Vellore Dt

Editorial Board

E. Thandapani, RIAS in Mathematics, University of Madras

S. Kalainathan, Dept. of Physics, VIT University, Vellore

K. Srinivasan, School of Chemistry, Bharathidasan University, Tiruchirappalli

E. George Dharma Prakash Raj, Dept. of Computer Science & Engineering, Bharathidasan University, Trichy

A. Gokulakrishnan, Dept. of Biochemistry, Islamiah College, Vaniyambadi

A. Joseph Jayapaul, Dept. of Economics, Loyola College, Chennai

R.S. Mani, VIT Business School, VIT University, Vellore

Sethurama Subbiah, Dept. of Social Work, Bharathiar University, Coimbatore

R. Srinivasan, Dept. of Tamil, Presidency College, Chennai

S. Joseph Arul Jayraj, Dept. of English, St. Joseph's College, Trichy

J. Henry Rozario, Dept. of Social Work, Sacred Heart College, Tirupattur

T. Jeyabalan, Dept. of Chemistry, Sacred Heart College, Tirupattur

S. Sagayaraj, Dept. of Computer Science, Sacred Heart College, Tirupattur

S. Mariappan, Dept. of Tamil, Sacred Heart College, Tirupattur

Editorial Office

Editor

Sacred Heart Journal of Science and Humanities

Sacred Heart College (Autonomous)

Tirupattur, Vellore Dt. 635 601, Tamil Nadu

Tel: 04179 - 220553, Fax: 04179-226423

Email: ceeyemv@yahoo.co.uk

Website: www.shcpt.edu

Subscription Rate:

Institution Rs. 400/- per annum

All contents including text, tables, figures, photographs, and all other information are the property of "Sacred Heart Journal of Science and Humanities", protected by copyright. The contents of pages should not be reproduced, copied, published or printed all or any part of contents in any form by any one, by any means electronic, photocopying or otherwise without the written permission of the "Sacred Heart Journal of Science and Humanities".

In case of any dispute or breach of agreement, matters will be settled in jurisdiction of Vellore.

Editor

From the Desk of Chief Editor

Greetings from Sacred Heart College, Tirupattur. The editorial board is happy to publish another issue of the journal. As the year comes to a close, this is a moment of introspection and evaluation enabling us to venture into new resolutions for the year ahead. The dictum 'Publish or Perish' is catching up with the academia. We are glad that these authors have made it after being put through a strict selection by the review board members.

We are concluding the year of Mathematics. In the early 20th century, Srinivasa Ramanujam (1887-1920) stated results in Mathematics that were both original and highly unconventional, such as the Ramanujan prime and the Ramanujan theta function, which have inspired a vast amount of further research.. In 1930, Sir C. V. Raman was the first 'non-white', Asian and Indian to receive the Nobel prize in physics for his work on scattering of light and discovery of the Raman effect. These great scientists reached such heights with minimum facilities of the times, whereas in this modern technologically advanced era we need to raise the bar and set benchmarks to leave a legacy for posterity. It is imperative that we vibrate with the same passionate zeal of scientists of yesteryears.

I am happy to put on record my heartfelt gratitude to all the authors and reviewers of these articles. I would like to thank the committee members for their unstinted efforts to make this issue see the light of day.

C. M. Varghese

CONTENTS

Part - A

SYNTHESIS AND CHARACTERIZATION OF NANOSIZED PHOSPHOMOLYBDATES AND PHOSPHOTUNGSTATES

T.Jeyabalan, S.Elavarasan and S.Kalaiyarasan

NATURAL DYE SENSITIZED TITANIUM DIOXIDE NANO PARTICLES FOR DYE SENSITIZED SOLAR CELL APPLICATIONS

S. Ananth, T. Arumanayagam and P. Murugakoothan

GROWTH, SPECTRAL AND DIELECTRIC STUDIES ON NEW ORGANIC NLO CRYSTAL: GUANIDINIUM SALICILATE (GuSL)

T. Arumanayagam, S. Ananth and P. Murugakoothan

STUDIES ON GOWTH AND OPTICAL PROPERTIES OF AN ORGANIC NLO CRYSTAL: GUANIDINIUM 3-NITROBENZOATE

A. Suvitha and P. Murugakoothan

EFFECT OF THICKNESS ON THE BAND GAP OF SELENIUM THIN FILMS

M.Pandiaraman and N.Soundararajan

NON LINEAR EFFECTS ON PHONON POLARITON MODES IN FERROELECTRIC SUPERLATTICES

K.S. Joseph Wilson and V. Revathy

CRYSTAL AND MOLECULAR STRUCTURE OF DIETHYL 5-{(4-CHLOROPHENYL) SULFINYL}-4-{(4-CHLOROPHENYL) SULFINYL} METHYL-6-HYDROXY-2-(4-METHYLPHENYL)-3,6-CYCLOHEXADIENE-1,3-DICARBOXYLATE

J. Suresh, P.S. Harikrishnan, R. Vishnu Priya and R. Nagalakshmi

SOLUTION OF A CONJECTURE ON SKOLEM MEAN GRAPH OF STARS

$K_{1,1} \cup K_{1,1} \cup K_{1,m} \cup K_{1,n}$

V. Balaji, D. S. T. Ramesh and V. Maheswari

A DYNAMIC APPROACH OF GENERALIZED DIFFERENCE OPERATOR TO n -MULTIPLE SERIES

G.Britto Antony Xavier, H.Nasira Begum, S.U.Vasantha Kumar and .Govindan

APPLICATION OF K MEANS CLUSTERING ALGORITHM FOR PASSWORD AUTHENTICATION THROUGH KEYSTROKE BIOMETRICS

Nisha Raj Nair

**A LOCAL MONITORING APPROACH WITH SCHEDULING IN WIRELESS
SENSOR NETWORKS**

K.J Eldh

**SYNTHESIS, SPECTROSCOPIC CHARACTERIZATION OF MANGANESE
AND VANADIUM SUBSTITUTED KEGGIN-TYPE
HETEROPOLYMOLYBDATES**

T. Jeyabalan and U. Anto Maria Jeraldin

**MIXED CONVECTION IN TWO-SIDED LID-DRIVEN DIFFERENTIALLY
HEATED SQUARE CAVITY USING NANOFLUID**

Nitesh Mittal, A. Satheeshand D. Santhosh Kumar

**AN *M/G/I//N* GATED VACATION QUEUEING SYSTEM WITH MARKOV
REGENERATIVE APPROACH**

R. Jayaraman

**ENHANCED INFORMATION RETRIEVAL AND STORAGE OF RDF GRAPH
IN CLOUDS**

Pramod Mathew Jacob and S. Jagadeesan

Part - B

RESIDENTIAL WATER CONSUMPTION

- A Urban Perspective

K. Sathyamurthi

WORK MOTIVATION AMONG THE PRIMARY SCHOOL TEACHERS

M. Govindan

கைப்பொருளும் மெய்ப்பொருளும் : பொருள்வயிற் பிரிதல் அடிப்படையில் ஒரு
விவாதம்

கி.பார்த்திபராஜா

ஜி.நாகராஜன் - மாற்று ஒழுக்கத்தை முன்வைத்த கலைஞன்

சு.இரமேஷ்

சங்க கால வரலாற்றில் திருமுடிக்காரி

க. மோகன்காந்தி

Synthesis and Characterization of Nanosized Phosphomolybdates and Phosphotungstates

T.Jeyabalan*, S.Elavarasan and S.Kalaiyaran.

APRC, Department of Chemistry,
Sacred Heart College, Tirupattur 635601, India.

Abstract

The Phosphomolybdates (PA1) and Phosphotungstates (PA2) nanomaterials were synthesized using CTAB as structure directing agent. The XRD and SEM results show the formation of nanostructures. The FT-IR results make known the framework of polyoxometalates. The optical absorption and E_g value extracted from DRS spectra.

Keywords Fourier Transform Infrared Spectra (FT-IR), X-Ray Diffraction (XRD), Scanning Electron Microscopy (SEM) and Diffused Reflectance Spectroscopy (DRS).

1. Introduction

The early transition metals (V, Nb, Ta, Mo, W) in their highest oxidation states are able to form metal oxygen cluster anions, commonly referred to as polyoxometalates¹. The chemistry of polyoxometalates anions, an important subarea of modern inorganic chemistry, is dominated by molybdenum and tungsten in their +6 oxidation state. During the last two decades this class of compounds has received much attention because of their interesting properties, importance as reagents in analytical procedures and wide applications in catalysis, biology, material science and medicine as inorganic drugs.¹⁻⁴

The measurement of the band gap of materials is important in the semiconductor, nanomaterial and solar industries. The term "band gap" refers to the energy difference between the top of the valence band to the bottom of the conduction band electrons are able to jump from one band to another. In order for an electron to jump from a valence band to a conduction band, it requires a specific minimum amount of energy for the transition, the band gap energy.⁵ Measuring the band gap is important in the semiconductor and nanomaterial industries. The band gap energy of insulators is large ($> 4\text{eV}$), but lower for semiconductors ($< 3\text{eV}$).

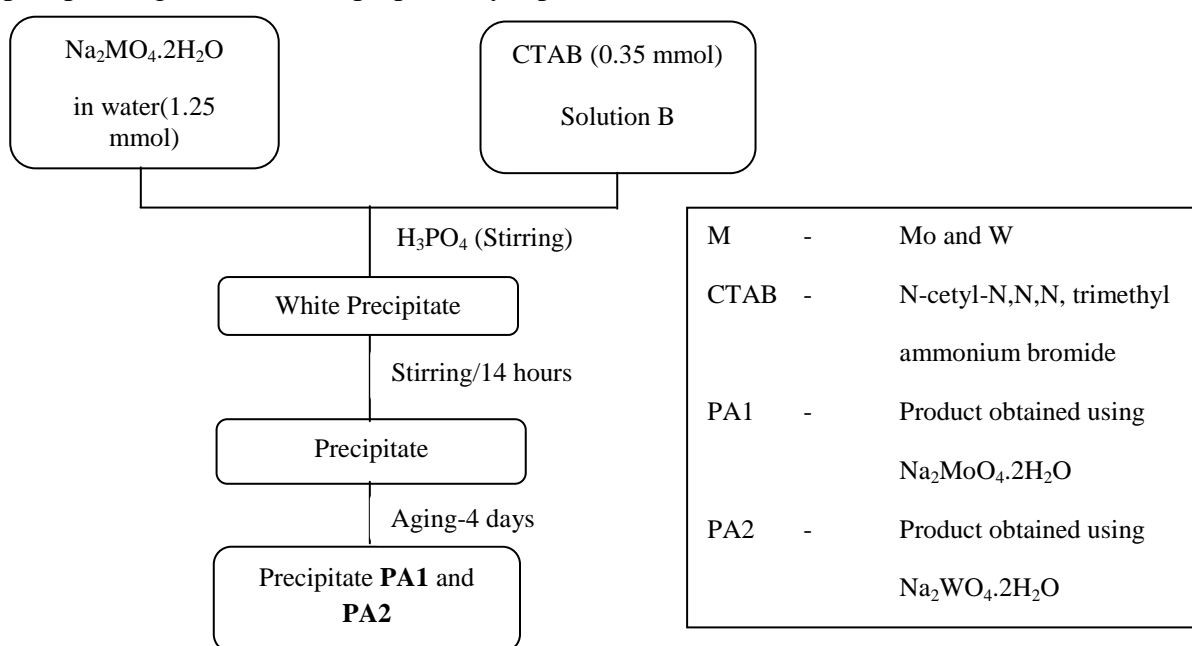
Based on these reflectance spectra the absorption edge was determined. Using these absorption edge values, the band gap energy was calculated. The present study aimed to directly measure the absorption edge and band-gap energies of these nanostructured materials, based on the onset of diffuse reflectance spectra. This investigation forms part of the semiconductor and microdevice chemistry.

* Corresponding author

In this paper, we present our results on how molybdenumoxide frameworks are modified upon substitution by phosphate units under acidic aqueous conditions at room temperature resulted in $\{H_xP_2Mo_{12}O_{40}\}^{(6-x)-}$ cluster based solids while the presence of transition metal ions result in nano-sized multidimensional framework solids.⁶ Here, we have investigated the growth of phosphomolybdate and phosphotungstate solids in the presence of N-cetyl-N,N,N, trimethyl ammonium bromide (CTAB). Reacting molybdate, tungstate and phosphate precursors with CTAB under acidic conditions at room temperature resulted in nanostructure of high aspect ratio. The size, structure and optical property were established by powder X-ray diffraction, Fourier transform infrared spectroscopy and Diffuse reflectance spectroscopy. The work is therefore significant in terms of understanding the self assembly of solids.

2. Synthesis

All reagents were purchased from Merck and used as received. Initially two different solutions were prepared. $Na_2MoO_4 \cdot 2H_2O$ and was dissolved in water (Solution A). N-cetyl-N,N,N, trimethyl ammonium bromide (CTAB) was dissolved in water (solution B) and the pH of the reaction medium was adjusted to ~2-4 using phosphoric acid. Consequently, solution A was added slowly to solution B with vigorous stirring. Instantaneously white precipitate was obtained upon mixing of the two solutions. The resultant solution was stirred for 14 hours and there after left undisturbed for four days. Scheme 1 shows the experimental procedure for synthesis of phosphomolybdate. Similarly phosphotungstate was also prepared by replace of $Na_2MoO_4 \cdot 2H_2O$ to $Na_2WO_4 \cdot 2H_2O$.



Scheme 1: Synthesis of Phosphomolybdate. and Phosphotungstate.

3. Characterization

Fourier transform infrared (FTIR) spectra were recorded on KBR pellets using a Nicolet 5DX spectrophotometer. Powder X-ray diffraction data was collected on a Bruker D8 advance diffractometer for 2 theta values ranging from 5° to 90° using CuK α radiation at 1.5406 Å. The diffuse reflectance spectra of the samples were recorded using Cary100 UV-Visible spectrophotometer to estimate the band gap energy.

4. Result and discussion

4.1 Infrared spectral studies

FTIR of the synthesized samples PA1 & PA2 are shown in figure 1 and 2. The presence of strong bands around 1080-1060 and 990-960 cm⁻¹ were recognized to PO₄ groups, peaks around 900-870 and 810-760 cm⁻¹ were attributed to M-O_b-M and M-O_c-M vibrations, respectively (M =

Mo and W).

Two absorption peaks at 2923 and near 2850 cm⁻¹ corresponded to the aliphatic C-H vibrations of CTAB. Bands near at 1635 and 1470, cm⁻¹ were attributed to extending vibrations of N-H and C-H respectively of CTAB moiety. A broad peak at 3448 cm⁻¹ was due to O-H stretching vibrations of the adsorbed water on the surface of the powders.^{7,8}

4.2 X-Ray diffraction analysis

The size of the samples PA1 and PA2 were determined by X-ray diffraction studies. Figure 3 and 4

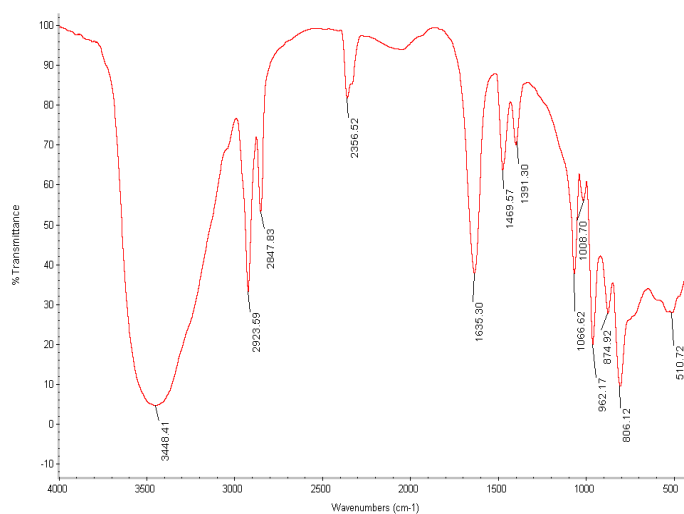


Figure 1: FTIR spectra of PA1 sample

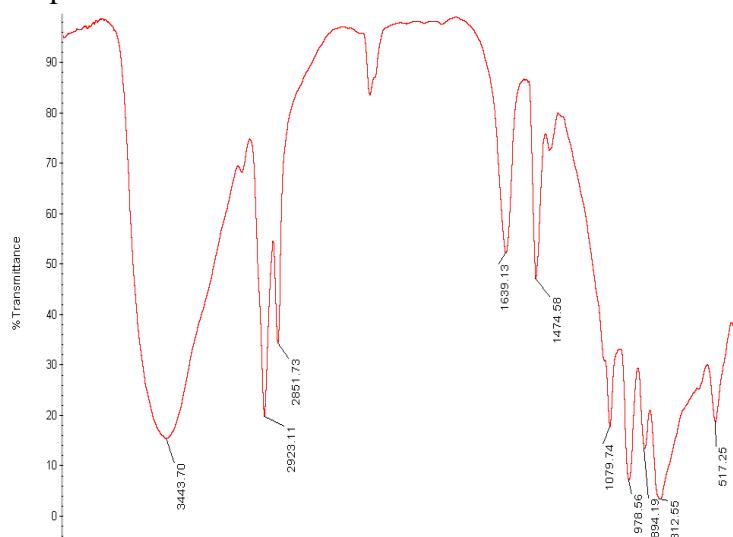


Figure 2: FTIR spectra of PA2 sample

shows the XRD peaks of the tested samples. The average crystallite size was calculated using Scherrer formula⁹ given in equation following equation.

$$L = \frac{0.89\lambda}{\beta \cos \theta}$$

Where L is the crystallite size, λ , the X-ray wavelength, θ , the Bragg diffraction angle and β , the peak width at half maximum (FWHM). The crystallite size for PA1 was found to be 1.42 nm and for PA2 was 23 nm

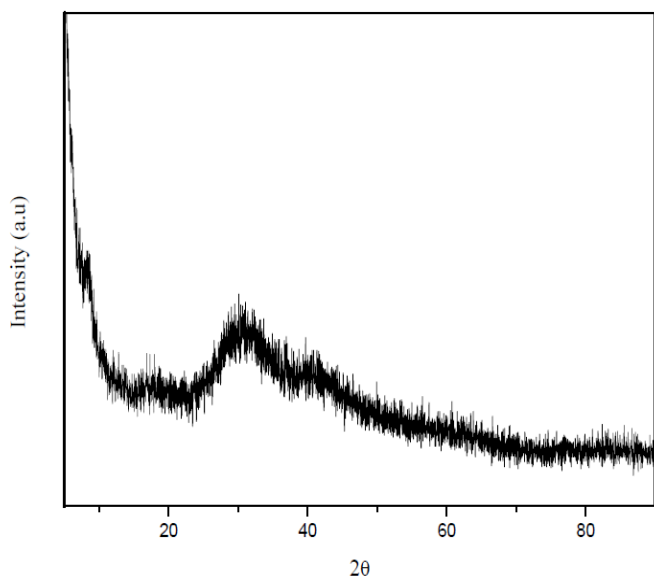


Figure 3: XRD spectra of PA1 sample

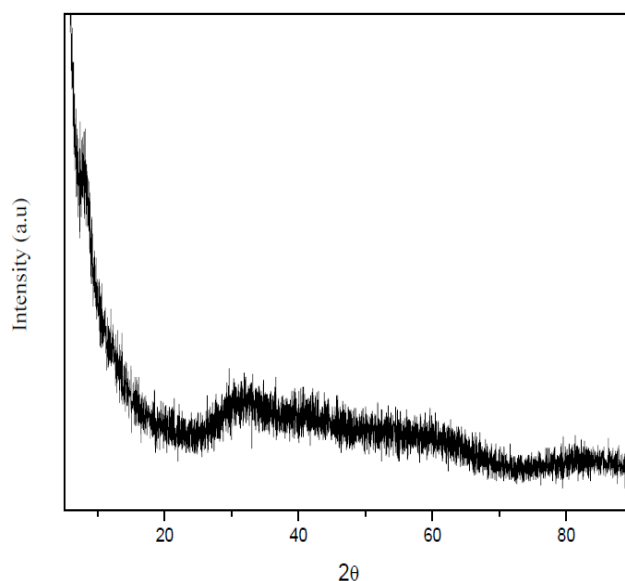


Figure 4: XRD spectra of PA2 sample

4.3 Morphology of PA1 and PA2

The morphologies of phosphomolybdates and phosphotungstates obtained from scanning electron micrograph are shown in figure 5 and 6

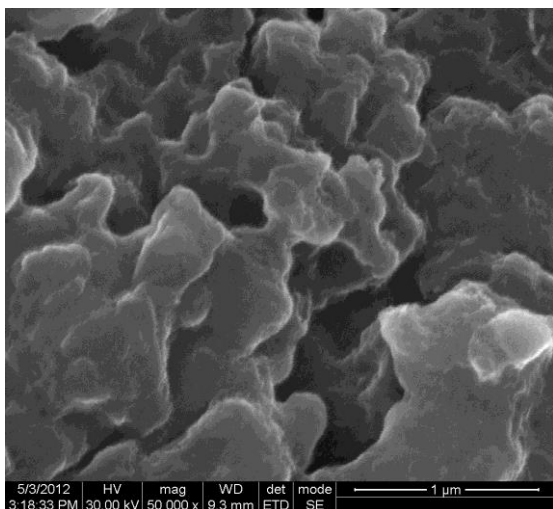


Figure 3: SEM image of PA1 sample

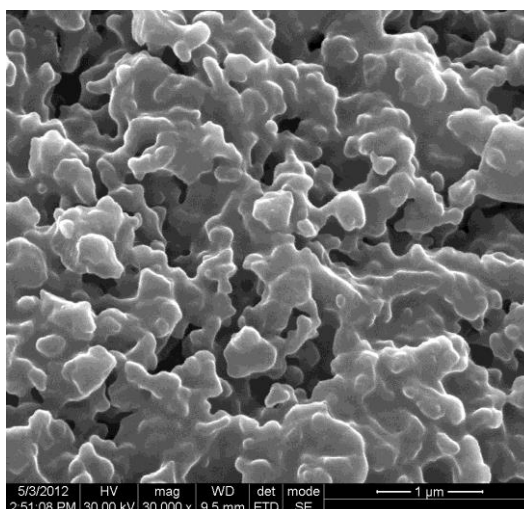


Figure 6: SEM image of PA2 sample

4.4 Diffused reflectance spectroscopy (DRS)

Diffuse Reflectance Spectroscopy (DRS) is a more convenient technique to characterize nanomaterials than UV-Vis absorption spectroscopy, since it takes advantage of the enhanced scattering phenomenon in powder materials. Moreover the effects of light scattering in the absorption spectra of powder samples dispersed in liquid media can be avoided using DRS¹⁰.

Diffuse reflectance spectral (DRS) studies in the UV-Visible region were carried out to investigate the band gap energy (E_g) of the PA1 and PA2 samples. The spectra are shown in figure 7 and 8. In order to assign the band gap with certainty, the diffuse reflectance (R) of the sample were transformed using Kubelka-Munk function $F(R)$. The definition of Kubelka-Munk function^{11,12} is enumerated as follows

$$F(R) = \frac{(1 - R^2)}{2R}$$

Where R is the diffuse-reflection factor.

The E_g of the nanomaterials was obtained by plotting of between $[F(R)E]^2$ versus energy of the incident light and extrapolating the linear region to the zero. The E_g value of samples obtained from DRS is about 3.11 eV(398 nm) and 3.67 eV(337nm).

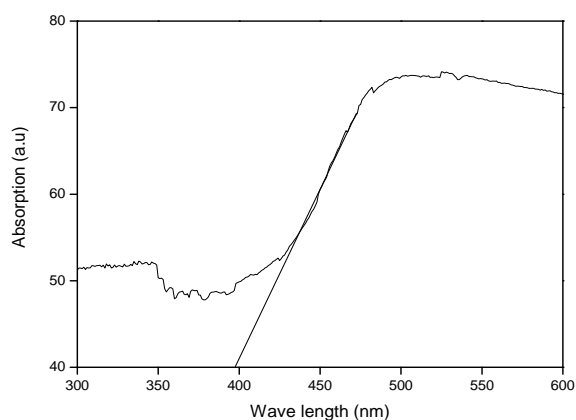


Figure 7: DRS spectra of PA2 sample

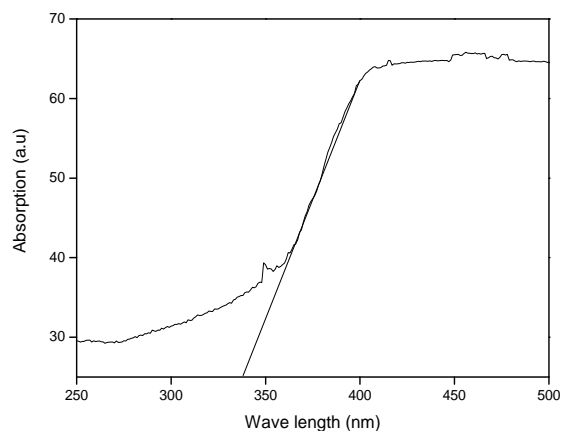


Figure 8: DRS spectra of PA2 sample

5. Conclusion

Phosphomolybdate(PA1) and phosphotungstate(PA2) were successfully synthesized via microemulsion method using CTAB as structure directing agent. Diffuse reflectance spectra indicated maximum absorption at 398 nm (3.11 eV) and 337 nm (3.67 eV) respectively. The morphology of PA1 and PA2 nanomaterials obtained from scanning electron micrograph. The crystallite size (L) of synthesized samples was found to be 1.42 nm and 23 nm respectively.

Acknowledgments

The authors duly acknowledge the APRC, Sacred Heart college, Tirupattur, India for providing research facility. We thank the Environmental Technology Division, (CLRI), Adiyar, Chennai for recording DRS facility. S.E Thanks the IIT, Roorkee for FTIR and XRD analysis.

6. References

1. M.T. Pope, *Heteropoly and Isopolyoxometalates*, Springer, New York, 1983.
2. M.T. Pope, A. Muller (Eds.), *Polyoxometalates: From Platonic Solids to Anti-Retroviral Activity*, Kluwer Academic, Dordrecht, 1994.
3. J.T. Rhule, C.L. Hill, D.A. Judd, R.F. Schinazi, *Chem. Rev.* 98 (1) (1998) 327.
4. D.E. Katsoulis, *Chem. Rev.* 98 (1) (1998) 359.
5. Hoffman, M., Martin, S., Choi, W., & Bahnemann, D.(1995). "Environmental applications of semiconductor photo catalysis," *Chemical Review*, vol. 95, pp. 69-96.
6. Thomas J and Ramanan A 2008 *Cryst. Growth Des.* 8 3390
7. Thomas J, Kannan K R and Ramanan A *J. Chem. Sci.*, Vol. 120, No. 6, November 2008, pp. 529–536.
8. Ahmed Aouissi, Salem S. Al-Deyab, Ahmad Al-Owais and Amro Al-Amro *Int. J. Mol. Sci.* 2010, 11, 2770-2779
9. H.Y. Chang, Y.H. Park, and C.R. Park, *Carbon* 39, 559 (2001).
10. Jong Dae Han and Seong Ihl Woo, *Korean J. of Chem. Eng.* 8(4), 235-239, (1991).
11. L.C.Nehru, V.Swaminathan, and C. Sanjeeviraja, *powder Technol.* 226, 29 (2012).
12. N. Serpone, D. Lawless, and R. Khairutdinov, *J. Phys. Chem.* 99, 16646 (1995).

Natural Dye Sensitized Titanium Dioxide Nano particles for Dye Sensitized Solar Cell applications

S. Ananth, T. Arumanayagam and P. Murugakoothan*

MRDL, PG and Research Department of Physics, Pachaiyappa's College, Chennai 600 030, India

Abstract

In the present work, a natural dye extracted from *Opuntia ficus-indica* fruit was used as dye sensitizer for Titanium dioxide (TiO_2) nano particles for the fabrication of dye-sensitized solar cell. The TiO_2 nano particles in anatase phase were synthesized using Sol – Gel method. The natural dye was extracted using water as solvent and mixed with TiO_2 nano particles to yield photo anode material for the fabrication of dye sensitized solar cell. The powder XRD and SEM analysis of natural dye mixed TiO_2 and UV-vis spectra, and E-DAX analysis of pure and natural dye mixed TiO_2 were taken to study their structural, morphological and optical properties.

Keywords: Sol-Gel, Natural Dye, Photo Anode, *Opuntia ficus-indica*.

Introduction

Dye sensitized solar cells (DSSC) have been widely investigated due to their low production cost and good light to electron conversion efficiency. In DSSC, the photons were converted into electric current by charge injection of excited dye molecules into a wide band gap semiconductor which is in contrast to the conventional silicon based solar cells, where the semiconductor performs both task of light absorption and charge separation [1]. The light was absorbed by a sensitizer (dye) which is available on the surface of the metal oxide semiconductor. Charge separation takes place at the interface due to the photo-induced electron injection from dye to the conduction band of the semiconductor [2]. The dye molecule is regenerated by a redox ($\text{I}^+ / \text{I}_3^-$) system, which itself is regenerated at the counter electrode by electrons passed through the load [3]. The sensitizer can be a natural dye or a chemical one. The chemical dyes have higher life time and light to electron conversion efficiency. Due to their toxic and high

* Corresponding author

synthesis cost, the natural dyes gained much attention. The natural dyes are very cheap and environment friendly. TiO_2 is the successful semiconductor used in DSSC due to its superior properties. The photo catalytic activity of TiO_2 was dependent on its crystalline nature, defects on the surface, photon absorption ability, particle size and surface area [4]. Using sol–gel hydrolysis route, anatase phase TiO_2 nano particles were synthesized and mixed with the natural dye extracted from *Opuntia ficus-indica* fruit to obtain photo anode material for DSSC.

1.1 Natural dye

Opuntia ficus-indica fruit extracted in water contains a red betacyanin pigment (betanin), betalamic acid, the yellow betaxanthin and red-violet betacyanin [5]. Betanin is the major pigment present in *Opuntia ficus-indica* fruit. The structure of betanin, betaxanthin and betacyanin dye is shown in Fig. (1). The outer cover of the fresh *Opuntia* fruit is removed and the flesh part is cut into small pieces without crushing. To extract the betanin dye, 100 grams of fruit pieces was mixed with 200 mL of double distilled water and the mixture was kept for six hours. The mixture was filtered to obtain natural dye solution by removing the solid fruit pieces.

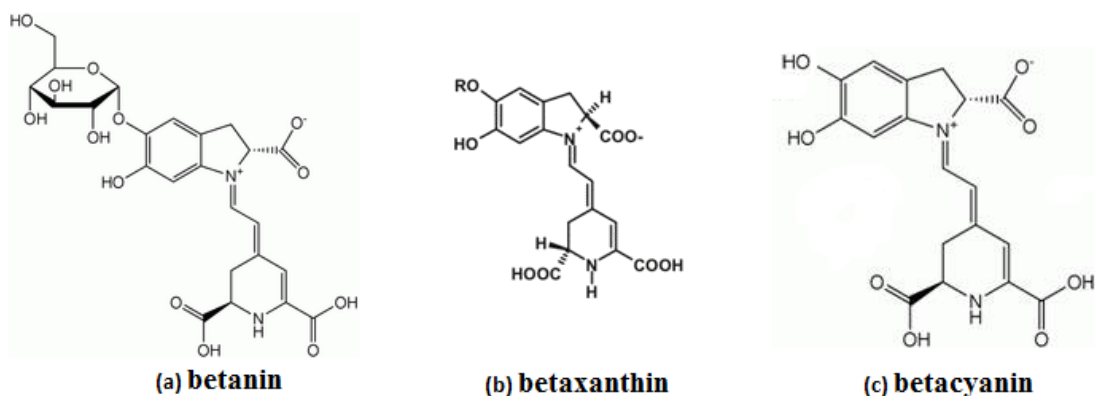


Fig. (1). Structure of betanin (a), betaxanthin (b) and betacyanin (c)

1.2 Experimental

Titanium isopropoxide was used as the precursor for the sol–gel synthesis of TiO_2 nano particles. A thoroughly mixed solution of distilled water with an alcohol was used

for the hydrolysis of titanium isopropoxide solution. A 250 cc solution of distilled water with 15 cc isopropanol was mixed well and the pH was noted as 8.75. The pH of solution has a strong influence on the size distribution of nano particles [6]. When the pH level of the solution is higher than 2, a white suspension of rough precipitants was formed immediately as the hydrolysis reactions was started. On the other hand, when the pH level of the solution is 2, a homogeneous suspension of fine particles is formed. The pH value was adjusted to 2 by adding concentrated nitric acid drop wise. This solution was stirred vigorously and the titanium isopropoxide solution of 5cc is added gradually to result a white precipitation containing nano TiO₂. After the hydrolysis process was over, the turbid solution containing the TiO₂ precipitation was heated up to 80°C for about 5 to 6 hours. After this, the mixture was kept for aging for 1 hour at room temperature. This yields a high viscous white suspension which is washed in distilled water first and then in ethanol to remove the byproduct impurities. Thus prepared precipitate was dried around 150°C for 15 to 20 hours to get fine white nano particles of TiO₂.

2. Characterization Studies

2.1 Powder XRD

The Powder XRD pattern of natural dye mixed TiO₂ nano particles is shown in Fig. 2. The nano crystalline anatase structure was confirmed by (1 0 1), (0 0 4), (2 0 0), (2 1 1), (0 0 2) and (3 0 1) diffraction peaks. The lack of orientation corresponding to the plane (110) confirms the absence of rutile phase. Particle size was calculated by Debye-Scherrer's formula given by equation $D = K\lambda / (\beta\cos\theta)$ where, D is the particle size; λ is the wavelength of the X-ray radiation ($\lambda=0.15406$ nm) for CuK α ; K is usually taken as 0.94 and β is the line width at half-maximum height [7]. The particle size obtained using this formula is approximately 23 nm for TiO₂ nano particles.

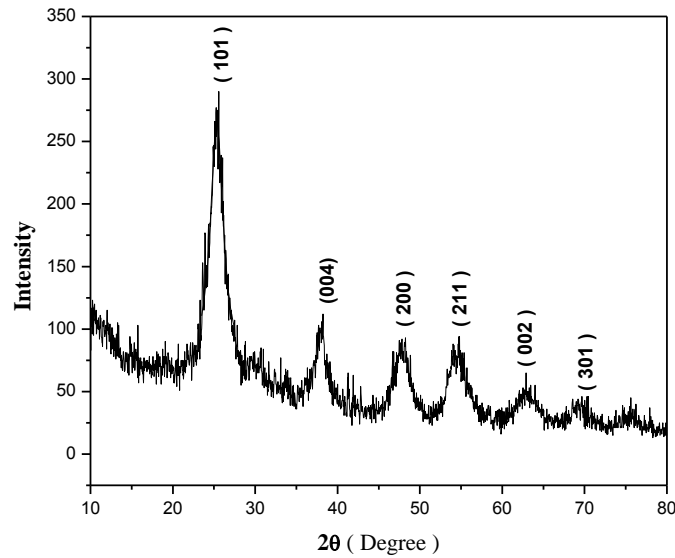


Fig. (2). Powder XRD pattern of dye mixed TiO_2

2.2 UV-VIS Spectral Analysis

The absorption spectra of TiO_2 nano particles are shown in Fig.3. The ideal sensitizer for a single junction photovoltaic cell converting standard global AM 1.5 sunlight to electricity should absorb all light below a threshold wavelength of about 920 nm [2]. From the spectra, it is clear that TiO_2 nano particle's cutoff wavelength is 356 nm. TiO_2 nano particles absorbs only in UV and nearby region only. That's why we need a separate dye sensitizer attached with TiO_2 for making it suitable for solar cell applications. The band gap of pure TiO_2 nano particles was found to be 3.48 eV. The band gap of normal or bulk TiO_2 is 3.2 eV and this variation is due to the change in particle size. The band gap increases with decreasing particle size and the absorption edge is shifted to a higher energy with decreasing particle size [8].

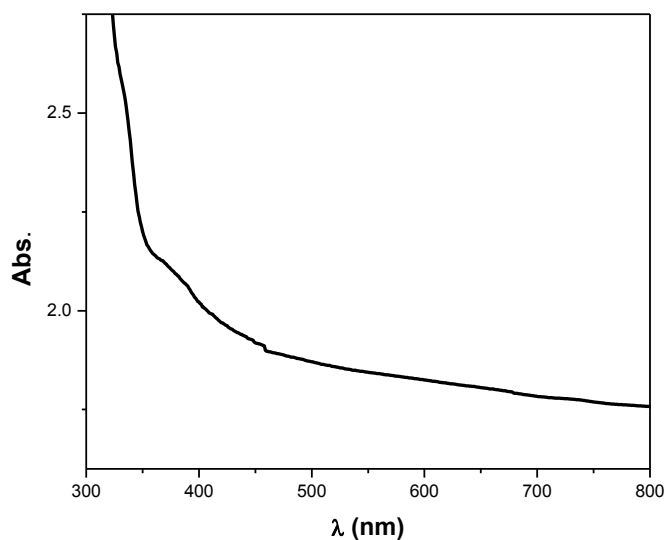


Fig. (3). Absorption spectra of pure TiO₂

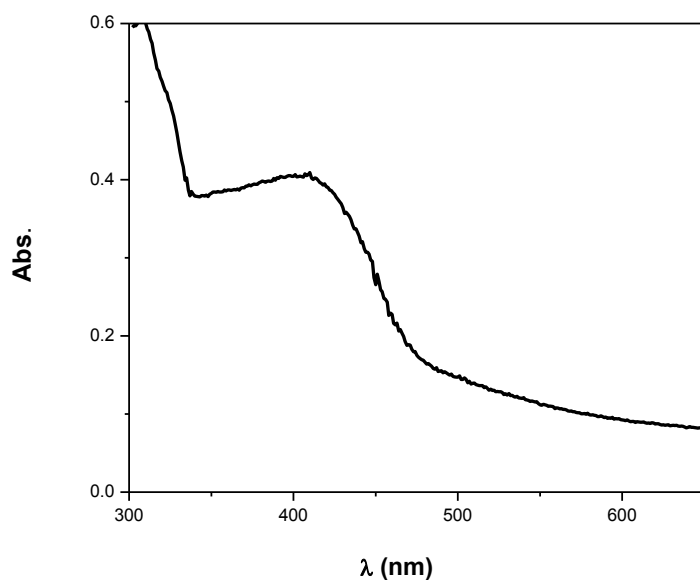


Fig. (4). Absorption spectra of natural dye mixed TiO₂

The absorption spectra of natural dye mixed TiO₂ nano particles are shown in Fig.4. The introduction of a new absorption peak is due to the natural dye adsorbed on the TiO₂ nano particles. The UV cutoff wavelength of betanin dye sensitized TiO₂ nano particle is 411 nm. The effective band gap of the natural dye and TiO₂ nano particle

combination was calculated as 3.02 eV. So, this reduction in the band gap boosts the photo catalytic activity of TiO₂.

2.3 SEM

The Scanning Electron Microscope image of TiO₂ nano particles synthesized by sol-gel technique is shown in Fig.5. Spherical nanostructures can be observed having grain size of approximately 30 nm. It should be noted that having higher surface area is one of the essential property of TiO₂ nano particles for its suitability to DSSC.

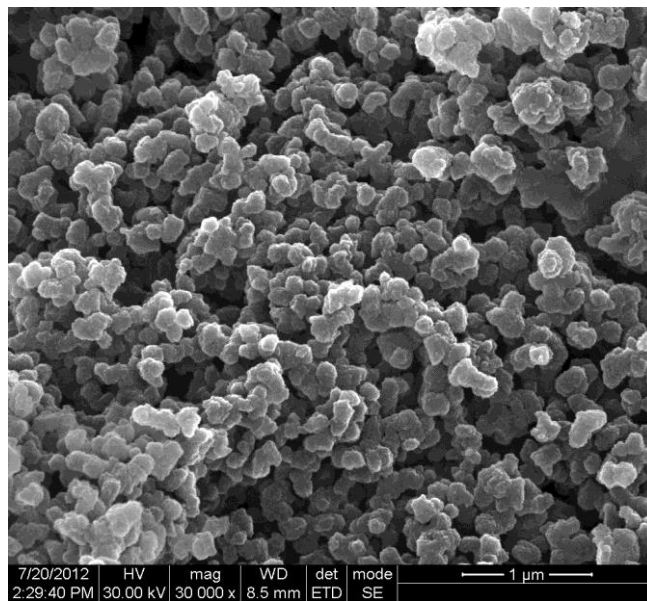


Fig. (5). SEM image of natural dye mixed TiO₂

2.4 E-DAX analysis

The E-DAX spectrum of TiO₂ nano particles is given in Fig. 6(a). The spectrum has prominent peaks of Ti and O. There is a less intense peak available for K. This may be due to the additional impurities. From the peaks, it was confirmed that the nano particles synthesized by sol-gel technique using optimal growth parameters belongs to pure TiO₂. The weight contributions are 33.83 and 61.45 percentage for Oxygen and Titanium respectively. Together they contribute 96.56 percentage of the total weight. This indicates the purity of TiO₂. Fig. 6(b) shows the E-DAX spectrum of TiO₂ nano

particles mixed with betanin dye. The weight contributions are 30.51, 30.50 and 29.84 percentages for Oxygen, Titanium and natural dye functional group(C) respectively. As a whole, they contribute 90.85 percentage of the total weight. Table 1 gives the E-DAX data.

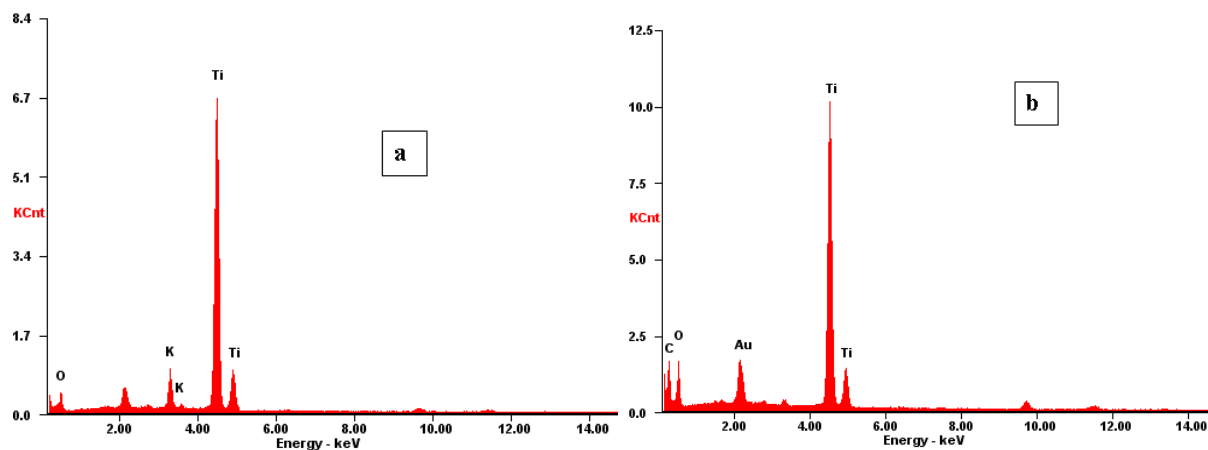


Fig. (6). E-DAX spectra a: pure TiO₂ b: TiO₂ mixed with betanin dye.

Table 1. E-DAX data

Pure TiO ₂			Dye mixed TiO ₂		
Element	Wt. %	At. %	Element	Wt. %	At. %
Ti	61.45	36.46	Ti	30.50	12.55
O	33.83	60.10	O	30.51	37.58
K	04.73	03.44	C	29.84	48.96

Conclusion

Pure TiO₂ nano particles were synthesized using sol-gel technique efficiently. A natural dye extracted from *Opuntia ficus-indica* fruit was used as dye sensitizer for TiO₂. The structural, optical and morphological properties were analyzed

using PXRD, UV-vis-NIR Spectroscopy, SEM and E-DAX. The TiO₂ nano particles prepared were highly crystalline and comparatively smaller particle size and spherical morphology. The band gap of pure TiO₂ nano particles was 3.48 eV and it was reduced to 3.02 eV due to the mixing of natural dye. The E-DAX study confirms the purity of TiO₂ and thus confirming the results obtained by XRD and SEM. The Opuntia ficus-indica fruit dye sensitized TiO₂ nano particles can be used as a potential photo anode material for the fabrication of Dye Sensitized Solar Cell.

Referenes

- [1] O'Regan, M. Graetzel, Nature 335 (1991) 737.
- [2] M. Graetzel, J. Photochem. 4 (2003) 145 – 153.
- [3] M. Graetzel, J. Photochem. 164 (2004) 3 - 14.
- [4] K. Kalyanasundaram, M. Graetzel. J. copbio. 21 (2010) 298 – 310.
- [5] D. Sreekanth , M. K. Arunasree , K. R. Roy , T. Chandramohan Reddy , G. V. Reddy , P. Reddanna Phytomedicine. 2007 Nov; 14(11):739-46.
- [6] S. Mahshid, M. Sasani Ghamsari et. al. Semiconductor Physics, Quantum Electronics & Optoelectronics. 9 (2006) 65-68.
- [7] G. Calogero, G. D. Marco (2008) Sol.EnergyMater. Sol.Cells 92: 1341-1346.
- [8] K.Madhusudan Reddy, S.V.Manorama, A.Ramachandra Reddy, Materials Chemistry and Physics 78 (2002) 239.
- [9] C. Kormann, D. W. Bahnemann, M. R. Hoffmann (1988) Journal of Phycical Chemistry 92: 5196-5201.

Growth, Spectral and Dielectric Studies on New Organic NLO Crystal: Guanidinium Salicylate (GuSL)

T. Arumanayagam, S. Ananth, P. Murugakoothan*

PG and Research Department of Physics, Pachaiyappa's College, Chennai-600 030, India.

Abstract

A potential organic nonlinear optical (NLO) single crystal guanidinium salicylate (GuSL) was successfully grown by slow evaporation technique. The crystal structure and morphology were confirmed by X-ray diffraction analysis. Formation of synthesized compound was confirmed by FTIR analysis. Wide band gap of 5.6 eV with optical window from 225 nm to 1100 nm were observed for the grown crystal in UV-Vis-NIR spectral analysis. The second harmonic generation efficiency of the grown crystal was tested by Kurtz-Perry powder technique. The dielectric measurement on GuSL single crystal was carried out for various "frequencies" and temperatures.

Keywords: Growth from solution; Nonlinear optic materials; Recrystallization; Dielectric properties

1. Introduction

"An" extensive research of suitable new nonlinear optical (NLO) materials is an important task because of their applications in optoelectronics, such as second harmonic generation (SHG), electro-optic modulation, optical switching and high data storage [1]. Recently the study of organic nonlinear optical materials has attracted a great attention due to their large optical susceptibilities, inherent ultra fast response time and high optical threshold for laser power as compared with inorganic materials [2]. One of the advantages in working with organic materials is that they allow to fine-tune the chemical structure and hence the properties for the desired nonlinear optical applications [3]. Guanidine is an important compound which has many biological, chemical and medical applications. Strong base guanidinium cation may be easily protonated by most organic and inorganic acids because of the presence of six potential donor sites for hydrogen bonding interactions which makes guanidine compounds are potential material for nonlinear optical applications [4]. Thus researchers are very much interested in searching guanidine based organic compounds with good nonlinear properties, such as guanidinium L-tartrate monohydrate [5], aminoguanidinium(1+) hydrogen L-tartrate monohydrate [6] and etc. "Recently, we have reported synthesis and characterization of Zinc guanidinium sulfate [7], guanidinium 4-aminobenzoate [8] and guanidinium 4-nitrobenzoate [9]." "In the present work, we report crystal growth, optical, spectral and dielectric properties of guanidinium salicylate (GuSL) were analyzed."

* Corresponding author

2. Experimental

2.1 Synthesis and Crystal growth

Guanidinium salicylate crystal was synthesized using high purity guanidine carbonate and salicylic acid in the ratio 1:2. The calculated quantities of guanidine carbonate and salicylic acid were dissolved in water. The reaction that has taken place is given below:



The saturated solution of GuSL was filtered and the filtered solution was allowed to dry at room temperature. The synthesized GuSL was subjected "to solubility studies. Solubility study has been carried out using a constant temperature bath, controlled at an accuracy of ± 0.01 °C attached with a temperature indicator and a programmer. The solubility of GuSL in water and water-methanol (1:1) solvents has been determined for the temperature range 35-50 °C by the gravimetric method. The solubility of GuSL as a function of temperature is depicted in figure 1(a) which shows that the GuSL exhibits high solubility in water-methanol (1:1) solvent with positive slope than water. The recrystallized solution of GuSL in water-methanol (1:1) solvent" was filtered in to a clean glass beaker and it was covered by a clean polythene sheet, so as to reduce the rate of evaporation of solvent. Optically transparent and good quality single crystal of dimension 40 x 9 x 6 mm³ was harvested in a period of 23 days. The as grown GuSL single crystal is shown in figure 1(b).

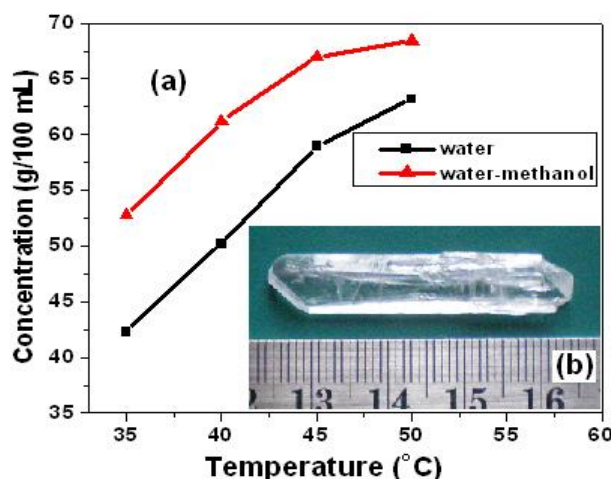


Fig. 1(a) Variation of solubility with temperature **1(b)**. Photograph of as grown GuSL crystal.

3. Characterization

3.1. X-ray diffraction analysis

The single crystal X-ray diffraction studies for GuSL crystal were carried out using Enraf Nonius-CAD4 single crystal X-ray diffractometer. It is observed that the title compound belongs to orthorhombic crystal system with space group *Pbca*. The unit cell parameters obtained are $a = 9.215 (11) \text{ \AA}$, $b = 9.876 (6) \text{ \AA}$, $c = 20.781 (2) \text{ \AA}$ and the cell volume is $1891.2 (3) \text{ \AA}^3$. The obtained lattice parameter values are in good agreement with the reported literature values [10]. Powder X-ray diffraction pattern of the grown crystal is shown in figure 2. The appearance of sharp peak confirmed the good crystallinity of the GuSL crystal.

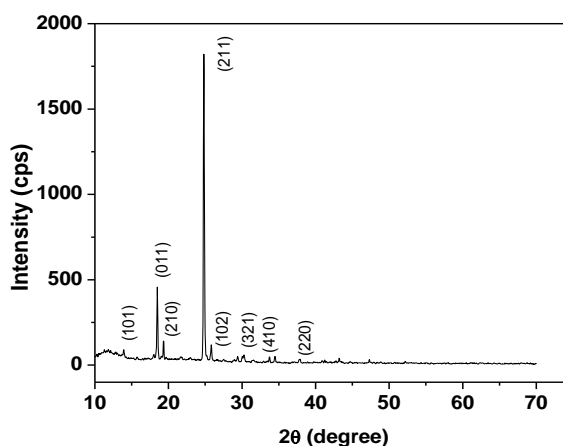


Fig. 2. Powder XRD pattern of GuSL crystal.

3.2. Spectroscopic analysis

Fourier transform infrared (FT-IR) spectrum was recorded in the range $4000\text{-}400 \text{ cm}^{-1}$ using Perkin Elmer FTIR spectrometer by KBr pellet technique to identify the various functional groups present in the title compound. The recorded spectrum for GuSL is presented in figure 3. The high frequency peak observed at around 3471 cm^{-1} and 3367 cm^{-1} are assigned to NH_2 asymmetric and symmetric stretching mode [4]. The broad band at 3126 cm^{-1} in the IR spectrum indicates the aromatic C–OH symmetric stretching.

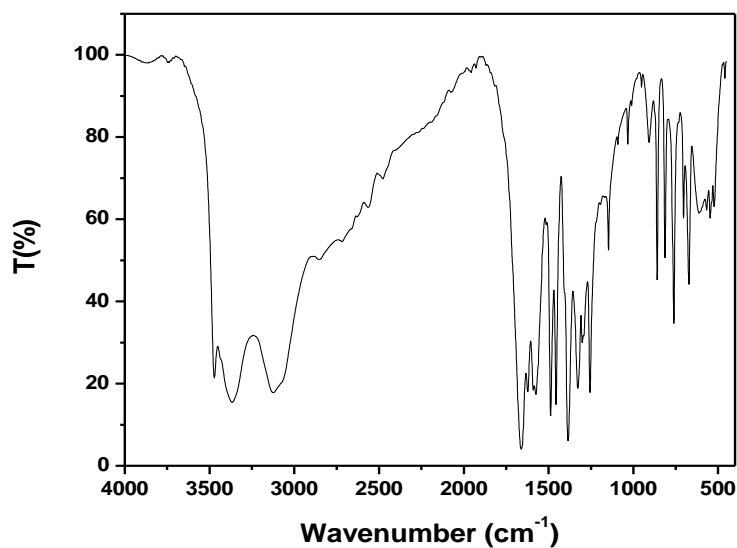


Fig. 3. FTIR spectra of GuSL.

The strong characteristic peak found at around 1661 cm^{-1} probably corresponds to stretching vibration of C=O bond in COOH group [11,12]. The sharp intense peak observed at around 1488 cm^{-1} is due to the deformation of C-H of the benzene ring. The intense peak found at 1258 cm^{-1} is characterized by bending mode NH_2 . The characteristic weak absorption band in the FTIR arises at around 1009 cm^{-1} is assigned as the symmetric C-N stretching mode of the guanidinium compound [13]. The characteristic IR bands for different molecular groups present in the GuSL have been identified and their assignments are given in Table 1.

Table 1 Vibrational band assignments of GuSL crystal

Assignment	FTIR
$\text{v}^{\text{as}}\text{NH}_2$	3471 s
$\text{v}^{\text{s}}\text{NH}_2$	3367 b
v^{NH_2}	31246 b
$\text{v}^{\text{C=O}}$	1661 s
$\text{v}^{\text{C=O}}$	1617 s
δ^{NH_2}	1574 s
$\text{v}^{\text{C=N}}$	1488 s
δ^{CH_2}	1435 s
$\text{v}^{\text{as}}(\text{COO}^-)$	1385 s
δ^{OH}	1327 s
$\text{v}^{\text{s}}(\text{COO}^-)$	1255 m
δ^{NH_2}	1146 w
τ^{CH_2}	1073 m
v^{CN}	1007 w
$\text{v}^{\text{C-C}}$	924 w
ω^{NH_2}	817 w
τ^{NH_2}	672 m
τ^{NH_2}	627 m
δ^{CCN}	548 m

Abbreviations: s, strong; m, medium; w, weak; ν_s , symmetric stretching; ν_{as} , asymmetric stretching; δ , bending in-plane; ω , wagging; ρ , rocking; τ , twisting.

3.3. Linear and nonlinear optical studies

Transmittance spectra are very important for any NLO material because nonlinear optical material can be practically useful only if it has wide transparency window. The UV-vis- NIR transmission spectrum was recorded in the range 200 – 1100 nm employing a Perkin Elmer Lambda 35 UV-vis spectrophotometer. The grown crystal of 2 mm thickness was used for recording the spectrum. The recorded spectrum is shown in figure 4(a) “which” indicates the cutoff wavelength at 225 nm. The percentage of transmission of about 75 % in visible region is attributed to better quality of the grown crystal. As this crystal “exhibits” wide transmission range, starting from 225 nm to 1100 nm, it can be used for optical applications including the second harmonic generation of Nd: YAG laser of fundamental wavelength $\lambda=1064$ nm. The energy dependence of optical absorption coefficient on photon energy in high absorption region can be expressed by $(\alpha h\nu) = \beta (h\nu - E_g)^\gamma$, where β is an energy independent constant, E_g is the optical band gap and γ is a constant which determines the type of optical transition [14, 15]. From the functional dependence obtained for the absorption coefficient on photon energy of title compound, the value of γ is close to $\frac{1}{2}$, which suggest that the optical transition is a direct one. The graph between $(\alpha h\nu)^2$ and photon energy ($h\nu$) has been plotted and is shown in figure 4(b). The intercept obtained by the extrapolation of the linear portion of the plot gives the band gap energy of the crystal as 5.6 eV.

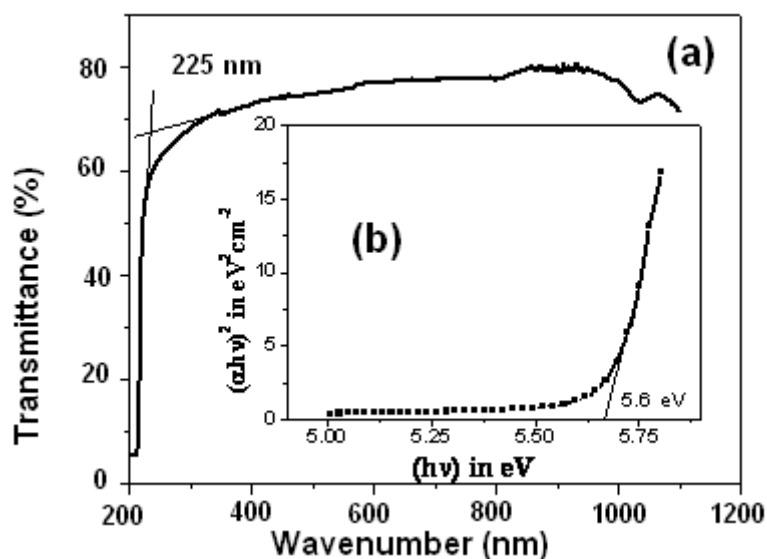


Fig. 4 (a) Optical transmittance spectrum of GuSL crystal. **(b)** Plot of $(\alpha h\nu)^2$ vs $h\nu$ for GuSL crystal.

“The second harmonic generation (SHG) has close correlation with the nonlinear electrical susceptibility. In centrosymmetric molecules, the action of the inversion centre reverses the sign of the electric transition dipole moments and possible to obtain SHG [16]”. The SHG efficiency of GuSL was measured by Kurtz and Perry powder technique [17]. A Q-switched Nd: YAG laser ($\lambda = 1064 \text{ nm}$) with a pulse duration of 10 ns and frequency repetition of 10 Hz was passed through the powder sample. The second harmonic signal of 32 mV was obtained for an input energy of 31 mJ/pulse, while the standard potassium dihydrogen phosphate (KDP) crystalline powder gave a SHG signal of 23 mV for the same input energy. From this, it is clear that the SHG efficiency of GuSL is 1.4 times that of KDP crystal.

3.4. Dielectric constant studies

The dielectric properties are correlated with electro-optic properties of the crystals. The sample of 2 mm thickness was used for the analysis of dielectric measurements for various frequencies and temperature using a HIOKI 3532-50 LCR HITESTER. The dielectric constant (ϵ_r) was calculated by $\epsilon_r = C t / A \epsilon_0$, where ϵ_0 is the permittivity of the free space, t is the thickness of the crystal. Figure 5(a) shows the plot between the calculated dielectric constant with respect to frequency for different temperatures of GuSL crystal. From the spectrum it is clear that the dielectric constant has higher value at lower frequencies and almost constant at higher frequencies (beyond 100 kHz). The magnitude of dielectric constant depends on degree of polarization and the charge displacement in crystals. The decrease in dielectric constant at the higher frequencies is attributed to the

absence of space charge polarization near the grain boundary interface [18, 19]. “The errors in these measurements are uses of parallel pate capacitor approximation and imperfect parallelness of sample surfaces”. For a material to be potential candidate for NLO applications, dielectric loss ($\tan \delta$) must be kept as low as possible. Figure 5(b) shows the variation of dielectric loss as a function of frequency. From the graph, it is evident that the grown GuSL crystal exhibit very low dielectric loss at high frequencies and can be used for NLO applications effectively [20].

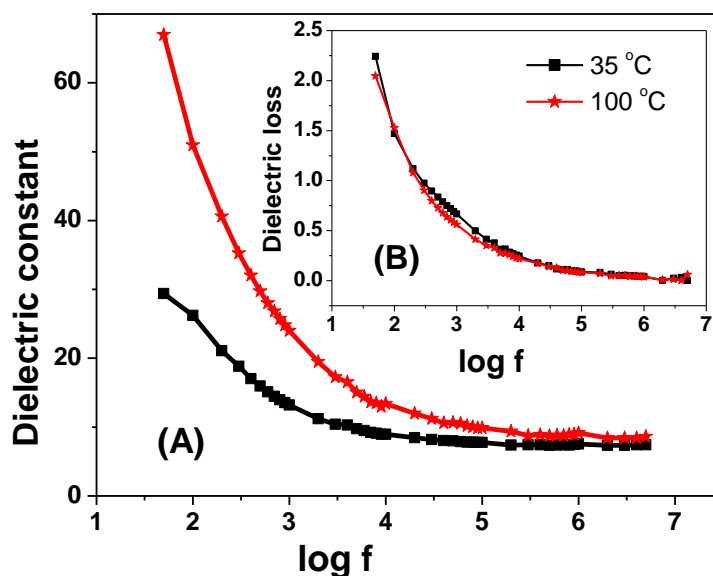


Fig. 5 (a) Variation of dielectric constant with frequency of GuSL crystal.
(b) Variation of dielectric loss with frequency of GuSL crystal.

4. Conclusion

The organic material GuSL was synthesized and “good” quality crystal was grown by slow evaporation technique at room temperature. The unit cell parameters have been assessed by single crystal X-ray diffraction technique. The spectroscopic analyses reveal all the functional groups and the mode of vibrations of the grown GuSL crystal. The grown crystal has a wide transparency window from 225 to 1100 nm thus confirming the suitability of this material for optical applications. The second harmonic generation efficiency of GuSL crystal was found to be 1.4 times that of standard material KDP. The grown crystal exhibits low dielectric constant and low dielectric loss. Hence GuSL single crystal can act as a promising material for NLO applications and it can be used for the fabrication of electro-optic devices.

Reference

- [1] Bosshard Ch, Bosch M, Liakatas I, Jager M, Gunter P. Springer series in Optical Science, Berline, Heideberg, New York **72** (2000), P. 163.
- [2] Zyss J, Nicoud JF, Coquillay M, J. Chem Phys. **81** (1984) 4160.
- [3] M. Ravi, P. Gangopadhyay, D.N. Rao, S. Cohen, I. Aganat, T.P. Radhakrishnan, Chem. Mater. **10** (1998) 2371.
- [4] M. Drozd, Spectrochimica Acta Part A **65** (2006) 1069.
- [5] W. Krumbe, S. Haussühl, R. Fröhlich, Zeitschrift fur Kristallographie 187 (1989) 309.
- [6] "Z. Machova, I. Nemeč, K. Teubner, P. Nemeč, P. Vanek, Z. Micka, J. Mole. Struc. **832** (2007) 101.
- [7] V. Siva shanker, R. Siddeswaran, T. Bharthasarathi, and P. Murugakoothan, J. Cryst. Growth. **311**(2009) 2709.
- [8] T. Arumanayagam, P. Murugakoothan. Mater. Lett. **65**, (2011) 2748.
- [9] T. Arumanayagam, P. Murugakoothan. J. Cryst. Growth **362** (2013) 304.
- [10] M. Fleck, E. Tillmanns and S. Haussühl, Zeit. für Krist. **215** (2000) 105.
- [11] X.M. Yang, D.A. Tryk, K. Hashimoto and, A. Fujishima, J. Phys. Chem. B **102** (1998) 4933.
- [12] S. Natarajan, G. P. Chitra, S. A. Martin Britto Dhas, and S. Athimoolam, Cryst. Res. Technol., **43** (2008) 713.
- [13] H.A. Petrosyan, "H.A.Karapetyan", A.M. Petrosyan, J. Molecular Structure **794** (2006) 160.
- [14] J.C. Tauc. et al., Optical Properties of Solids (Amsterdam: North-Holland) 1972, p.372.
- [15] Fahrettin Yakuphanoglu, Hilmi Erten, Opt. Appl. **35** (2005) 969.
- [16] E.W. Meijer, E.E. Havinga, G.L.J.A. Rikken, Phys. Revi. Lett. **65** (1990) 37.
- [17] S. K. Kurtz and T. T. Perry, J. Appl. Phys. **39** (1968) 3798.
- [18] P. Mythili, T. Kanagasekaran, S. Stella Mary, D. Kanjilal and R. Gopalakrishnan, Nucle. Instr. Meth. Phys. Res.B **266** (2008) 1737.
- [19] K.V. Rao, A. Smakula, J. Appl. Phys. **36** (1965) 2031.
- [20] D. Balasubramanian, P. Murugakoothan, R. Jayavel, J. Cryst. Growth, **312** (2010) 1855.

Studies on Growth and Optical Properties of an Organic NLO Crystal: Guanidinium 3-Nitrobenzoate

A. Suvitha^{1,2} and P. Murugakoothan*²

¹ Dept. of Physics, Anna Adarsh College for Women, Chennai – 600 040, India.

² PG and Research Dept. of Physics, Pachaiyappa's College, Chennai – 600 030, India.

Abstract

Single crystal of Guanidinium 3-Nitrobenzoate, an organic nonlinear optical material, was grown by the slow evaporation technique. The grown crystal was subjected to various studies to analyze its characteristics. Unit cell parameters of the grown crystals have been obtained using single crystal X-ray diffraction study. The lattice parameter values of Gu-3NB are, $a = 7.358 \text{ \AA}$, $b = 10.091 \text{ \AA}$, $c = 13.630 \text{ \AA}$. The mode of vibration of different molecular groups present in Gu-3NB was identified by Fourier transform infrared spectral analysis. The range and percentage of optical transmission was ascertained by recording UV-vis-NIR spectrum. The transmittance of Gu-3NB was used to calculate the refractive index (n), the extinction coefficient (k) and reflectance (R). The optical band gap of Gu-3NB is 3.94 eV with direct transition. Single-shot surface laser damage threshold of Gu-3NB estimated using an Nd:YAG laser of wavelength 1064 nm was found to be 3.84 GW/cm² and the results will be discussed in detail.

Keywords: Single crystal growth, Optical properties, Band gap energy, Refractive index.

1. Introduction

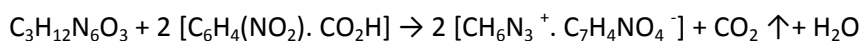
Among nonlinear optical crystals, organic salts occupy an intermediate position between molecular organic compounds with covalent bonds and inorganic compounds with mainly ionic bonds [1]. The ability of guanidium ion, $[\text{C}(\text{NH}_2)_3]^+$ in making hydrogen bonds and its unique planar shape has been recognized by Terao et al [2]. Further, guanidine is a strong Lewis base and the guanidinium cation may be easily anchored onto numerous inorganic and organic anions and polyanions, largely because of the presence of six potential

* Corresponding author

donor sites for hydrogen-bonding interactions. Thus the guanidine compounds are potential materials for nonlinear optical applications. Presently organic NLO crystal Gu-3NB has been grown by slow evaporation technique and the grown crystal is subjected to optical studies.

2 Growth Procedure

The pure guanidinium 3-nitrobenzoate has been synthesized from aqueous solution containing guanidine carbonate (Himedia) and 3-nitrobenzoic acid (Merck) in 1:2 stoichiometric ratio by slow evaporation technique at room temperature and the reaction is as follows



The synthesized Gu-3NB was recrystallized for several times to improve its purity. The Gu-3NB crystals were grown from the saturated solution. The seed crystals were obtained in a period of 3 days using slow evaporation method. To grow bulk crystal, the supersaturated solution of Gu-3NB was kept in a constant temperature bath with controller accuracy of ± 0.01 K at 40°C. The seed crystal of Gu-3NB obtained by slow evaporation method, as shown in Fig. 1(a) was suspended in the solution. The temperature of the bath was reduced at the rate of 0.05 K per day. Good transparent single crystal of Gu-3NB was obtained over a typical growth period of 23 days. Crystal of dimension 35x15x8 mm³ grown from aqueous solution by temperature-lowering method is shown in Fig 1(b).



Fig. 1 Gu-3NB crystal grown from methanol by (a) slow evaporation method and (b) slow cooling method.

3. Characterization

3.1. X-ray diffraction analysis

The grown crystal was subjected to single crystal X-ray diffraction (SXRD) study at room temperature using ENRAF NONIUS CAD4 single crystal X-ray diffractometer with MoK α radiation ($\lambda = 0.7170 \text{ \AA}$). It is observed that the title compound belongs to orthorhombic crystal system with noncentrosymmetric space group P2₁2₁2₁. The unit cell parameters obtained are $a = 7.358 \text{ \AA}$, $b = 10.091 \text{ \AA}$, $c = 13.63 \text{ \AA}$ and the volume of the material is found to be 1012.3 \AA^3 . The obtained lattice parameter values are in good agreement with the reported literature values [3].

3.2. FTIR studies

Infrared spectroscopy is an important tool to gather information about the structure of a compound, organic functional groups and the purity of a compound. The molecular vibrations of the organic functional groups due to absorption of infrared radiation are interpreted using Fourier transform infrared (FTIR) spectrum. The FTIR spectrum for Gu-3NB was recorded using the PERKIN ELMER spectrophotometer by KBr pellet method in the wavenumbers range from 4000 to 400 cm^{-1} . The FTIR absorption spectrum of Gu-3NB is shown in Fig. 3.

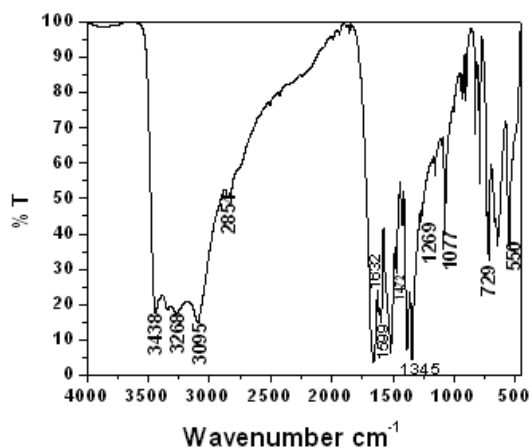


Fig. 2. FTIR spectrum of Gu-3NB crystal

The intense band in the high-energy region shows the NH stretching vibrations at 3438, 3338 and 3268 cm^{-1} . The peak at 3095 is due to aromatic ring carbon hydrogen stretching. The peak is broadened due to H₂ bonding of NH₂ groups. The C=O stretching vibration of carboxylate occur at 1632 cm^{-1} . The peaks at 1599, 1519 and 1472 cm^{-1} are due to aromatic skeletal vibrations. The symmetric and asymmetric stretching vibrations of NO₂ groups occur at 1519 and 1345 cm^{-1} . The groups of peaks below 1000 cm^{-1} are due to CH bending vibrations. Hence the spectrum carries vibrations due to guanidine carbonate and 3-nitrobenzoate.

3.3. Optical studies

The optical transmission range, transparency cut-off and absorbance band are the most important optical parameters for laser frequency conversion applications. A crystal of thickness 2 mm has been used for UV-vis-NIR spectral study and the spectrum obtained is shown in Fig. 3. The Gu-3NB crystal is optically transparent in the entire visible region with 80% transmittance and lower cut-off wavelength of 265 nm.

The measured transmittance (T) is used to calculate the absorption coefficient (α) using the formula,

$$\alpha = \frac{2.303 \log\left(\frac{1}{T}\right)}{t} \quad (1)$$

where t is the thickness of the crystal.

The optical band gap (E_g) is evaluated from the transmission spectra. The optical absorption coefficient (α) near the absorption edge is given by [4].

$$\alpha h\nu = A(h\nu - E_g)^{\frac{1}{2}} \quad (2)$$

where A is a constant, E_g the optical band gap, h the Planck's constant and ν the frequency of the incident photon. The Tauc's graph [5] plotted between $(\alpha h\nu)^2$ with the photon energy ($h\nu$) at room temperature, shown in Fig. 4, exhibits a linear behavior that can be considered as the evidence of direct transition. The optical band gap (E_g) of Gu-3NB crystal is found to be 4.17eV.

Extinction coefficient is the fraction of light lost due to scattering and absorption per unit distance in a participating medium. In electromagnetic terms, the extinction coefficient can be explained as the decay or damping of the amplitude of the incident electric and magnetic fields.

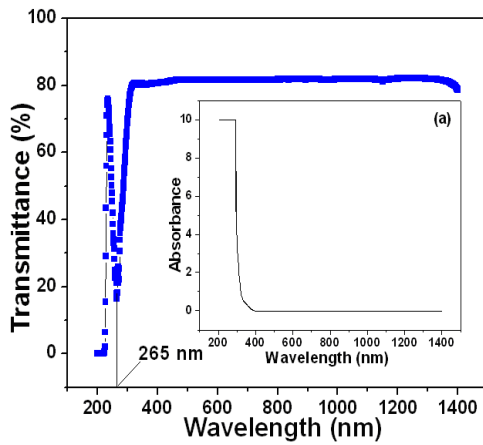


Fig. 3. UV-vis-NIR spectrum of Gu-3NB

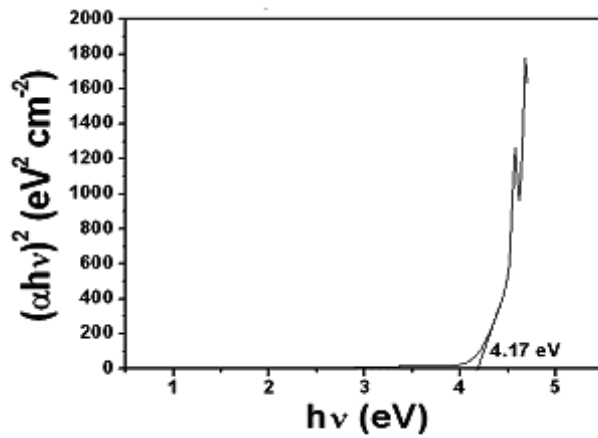


Fig.4. Plot of photon energy ($h\nu$) vs. $(\alpha h\nu)^2$

The extinction coefficient (k) obtained from the following equation is plotted against wavelength and is shown in Fig. 5.

$$k = \frac{\lambda\alpha}{4\pi} \quad (3)$$

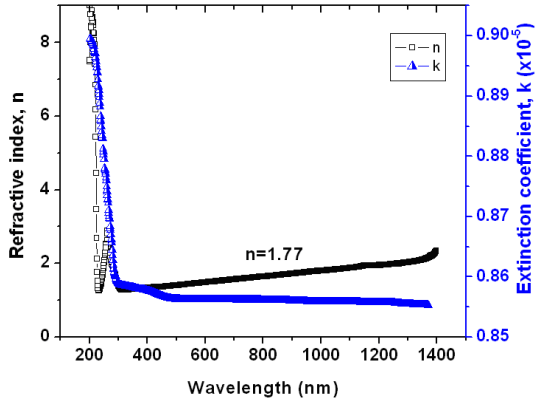


Fig. 5 Response of Refractive index (n) and Extinction Coefficient (k) against wavelength.

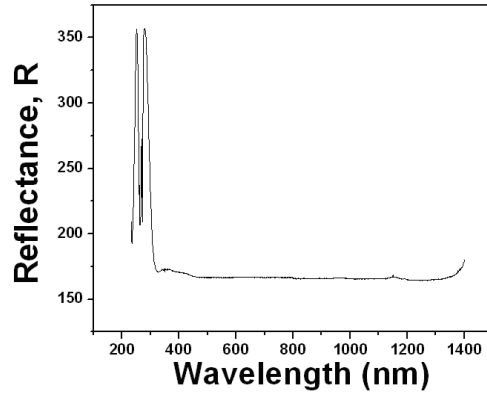


Fig. 6. Plot of Reflectance R vs. Wavelength.

The transmittance (T) is given by the following relation [6]

$$T = \frac{(1-R)^2 \exp(-\alpha t)}{1-R^2 \exp(-2\alpha t)} \quad (4)$$

The reflectance R in terms of the absorption coefficient(α) can be obtained from the equation [7]

$$R = \frac{\exp(-\alpha t) \pm \sqrt{\exp(-\alpha t)T - \exp(-3\alpha t)T + \exp(-2\alpha t)T^2}}{\exp(-\alpha t) + \exp(-2\alpha t)T} \quad (5)$$

The refractive index(n) can be determined from reflectance data using the following relation [8]

$$n = \frac{-(R+1) \pm 2\sqrt{R}}{R-1} \quad (6)$$

The wavelength dependence of 'n' and 'R' for Gu-3NB crystal in the range 250-1400 nm are shown in Fig. 5 and Fig. 6 respectively. Initially the refractive index decreases with increasing wavelength, and then becomes constant. The refractive index and extinction coefficient for grown Gu-3NB crystal in the visible region is found to be 1.77 and 8.56×10^{-6} respectively.

Kurtz and Perry technique [9] was used to investigate SHG of the grown crystal. A high intense beam of Nd:YAG laser ($\lambda = 1064$ nm) was directed into the powder sample. The SHG efficiency was confirmed from the

output of green light emission ($\lambda = 532$ nm). The SHG efficiency of Gu-3NB crystal is 45% of that of pure KDP crystal.

3.4. Laser damage threshold studies

Laser damage threshold is an important material parameter, the knowledge of which is essential for using the crystal as an NLO element in various applications. The damage thresholds depend on many factors like pulse duration, focal spot geometry, sample quality, experimental technique employed, etc. In this study, the selected surface of the Gu-3NB single crystals was polished with fine 4000 μ m polishing sheet in order to form the uniform surface quality. The single shot surface damage threshold of Gu-3NB was determined using Q-switched Nd-YAG laser of wavelength 1064 nm with a pulse width of 20 ns and 19 Hz repetition rate. The single-shot surface laser damage threshold is determined to be 3.84 GW/cm². The laser damage threshold value obtained for Gu-3NB is moderately good from the device point of view.

4. Conclusion

Optical quality single crystal of organic Gu-3NB has been grown using solution growth technique. The cell parameter values show that the Gu-3NB single crystal belongs to orthorhombic system. Optical studies show that the crystal has wide transmission range with UV cut-off wavelength at 265 nm. The optical band gap (E_g), absorption coefficient (α), extinction coefficient (k), refractive index (n), reflectance (R) have been calculated as a function of wavelength. The studies on the NLO property confirmed the second harmonic conversion efficiency of the crystal is 45% of that of pure KDP crystal. The laser damage threshold of this material is found to be 3.84 GW/cm². The promising growth and properties of Gu-3NB crystal nominate it as a potential material for photonics, electro-optic and SHG applications.

References

- [1] J.P. Nicoud, R.J. Twieg, in: D.S. Chemla, J. Zyss (Eds), "Nonlinear Optical Properties of Organic Molecules and Crystals" (Vol 1, Academic Press 1987)
- [2] Hiromitsu Terao, Thorsten M. Geising, Hideta Ishihara, Yoshihiro Furukawa and B. Thimme Gowda, *Acta Cryst.* M503. E65 (2009).
- [3] G. Smith and U.D. Wermuth, Guanidinium 3-nitrobenzoate, *Acta Cryst.* (2010). E66, o1946.
- [4] A. Ashour, N. El-Kadry, S.A. Mahmud, *Thin Solid Films* 269 (1995) 117-120.
- [5] J. Tauc, R. Grigorovici, A. Vanacu, Optical Properties and Electronic Structure of Amorphous Germanium. *Phys. Status Solidi* 15 (1966) 627–637.
- [6] J. I. Pankove, *Optical Processes in Semiconductors*, (Prentice-Hall, New York, 1971), p. 88.
- [7] V. Gupta, A. Mansingh, Influence of postdeposition annealing on the structural and optical properties of sputtered zinc oxide film, *J. Appl. Phys.* 80(2) (1996) 1063-1073.
- [8] M.A. Omar, *Elementary Solid State Physics*, Addison-Wesley Publishing Company, Reading, MA, 1975.
- [9] Kurtz S.K, Perry T.T, A powder technique for the evaluation of nonlinear optical materials *J. Appl. Phys.* 39 (1968) 3798 - 3813.

Effect of Thickness on the Band Gap of Selenium Thin Films

M.Pandiaraman⁺, N.Soundararajan*

+ Department of Physics, Nehru Memorial College, Puthanampatti, Trichy

*Thin Film lab, School of Physics, Madurai Kamaraj University, Madurai-625 021

+Email: pandiaraman@gmail.com

Abstract

The selenium films of thickness between 60nm and 150nm were thermally evaporated on glass substrates at vacuum better than 10^{-5} mbar. From the XRD studies, selenium films are found to exhibit hexagonal structure with [100] orientation and the particle size of the selenium film is found to be 48nm. The transmittance spectra of the selenium films have been recorded and analyzed to determine the optical band gap of selenium films of different thickness.

Key Words : Selenium Thin Film, XRD

INTRODUCTION

In recent years, semiconducting thin films are of considerable interest in the field of science and technology [1,-5]. Selenium is a semiconducting Group-VI element, with wide band gap. Selenium with trigonal structure exhibits band gap of 1.76eV; Selenium with monoclinic structure exhibits band gap of 1.8eV, but the amorphous selenium exhibits band gap of 2.05eV [6]. This structural dependence of band gap of selenium initiates us to study the optical band gap of selenium thin films and the effect of thickness on the band gap of selenium.

EXPERIMENTAL TECHNIQUE

The selenium thin films of thickness between 60nm and 150nm were prepared by thermal evaporation technique on well cleaned glass substrates (1cm X 3cm) at a deposition rate of 1.0nm/sec at a vacuum better than 10^{-5} mbar. The thickness and the deposition rate of the selenium films were monitored using a quartz crystal thickness monitor during deposition.

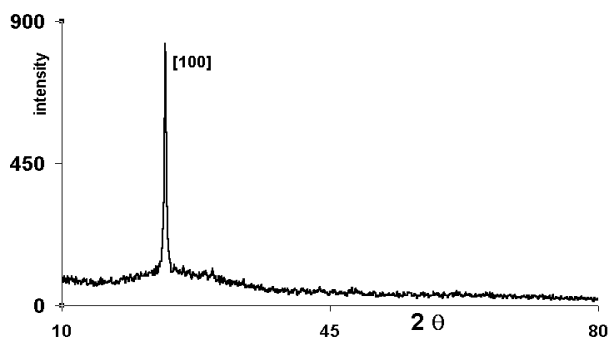


Figure 1: XRD spectra of selenium film

The XRD patterns of the selenium films have been recorded. The XRD of selenium film of thickness 147nm is shown in fig (1). The transmittance spectra of the selenium films were recorded using UV-Vis spectrophotometer in the wavelength range between 300nm and 850nm. The transmittance spectrum of selenium thin film of thickness 147nm is shown in fig (2).

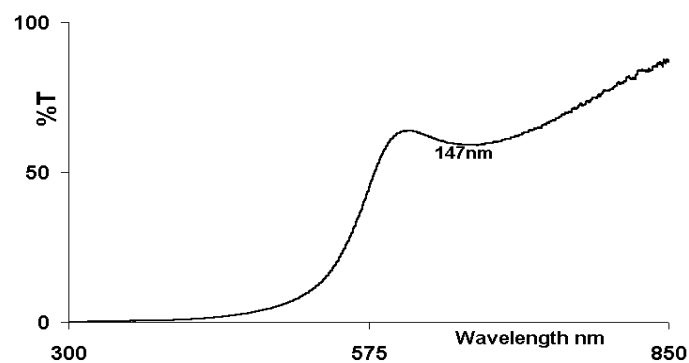


Figure 2: Transmittance (%) of selenium film of thickness 147nm

RESULTS AND DISCUSSION

Selenium is a Group VI element; it has two vacant orbitals for bonding to neighbour atoms [7]. The bonding in selenium takes place in two distinct ways. In monoclinic selenium, closed eight membered rings are formed. These atoms are arranged parallel to one another in the crystal. But the atoms link to form spiral chains of several hundred atoms long in hexagonal and vitreous form. In hexagonal form, these line-up's are parallel to one another along c axis, But in the vitreous form, these line-up's are short range order upto 10Å. The XRD pattern shows a peak at 23.7° with the orientation [100] for the hexagonal structure of selenium.

The absence of broad hump around 20° in the XRD indicates the selenium films are crystalline. The presence of the lone peak at 23.7° indicates the presence of long chain of selenium atoms in the hexagonal structure in selenium films [4]. Using Debye-scherrer relation the particle size of the selenium films was found to be 48nm.

As seen in fig (2) the transmittance of selenium film of thickness 147nm, increases with the increase in wavelength upto 600nm and then saturates upto 850nm. Similar spectra are obtained for different thickness of selenium films. The transmittance is found to decrease with the increase in thickness of the films. Using the transmittance data, the absorption coefficient (α) is determined using the well known relation [8,-10]

$$T = e^{-\alpha t} \quad (1)$$

From the α value we confirmed that the selenium films exhibit direct band gap with as α value greater than 10^4 cm^{-1} . Using the absorption coefficient spectra of the selenium films, we have determined the optical band gap using the relation [11,12]

$$\alpha h\nu = A(h\nu - E_g)^2 \quad (2)$$

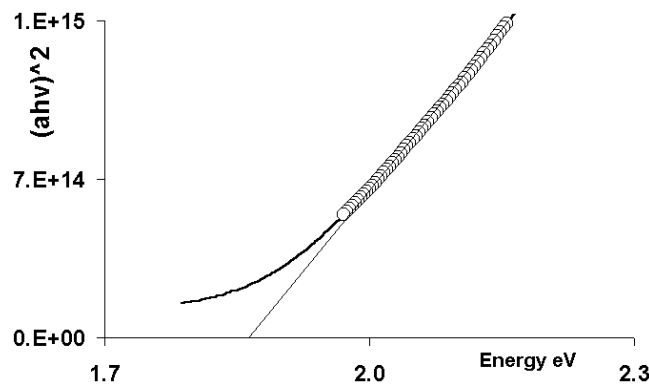


Figure 3: Dependence of $(\alpha h\nu)^2$ on the energy eV

The optical band gap of 147nm selenium film has been determined to be 1.8eV as shown in fig (3). Similarly the band gaps of other selenium films are determined and plotted as function of thickness of selenium thin films as shown in fig (4). The value of the band gap, 1.8eV also confirms the films are crystalline.

Generally the band gap of thin films vary because of the following reasons (i) the increase in the band gap is due to the size of grains in a polycrystalline film, (ii) the decrease in the band gap due to the large density of dislocations as a function of film thickness [5]. The determined value of selenium film is about 1.8eV. It is independent of film thickness. Since the observed band gap of selenium thin film is almost independent of thickness, it is apparent that both effects may be approximately equal.

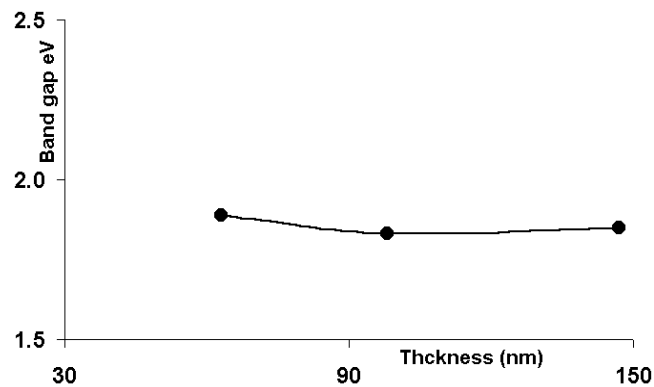


Figure 4: Dependence of the band gap of selenium film on the inverse of thickness

CONCLUSION

The selenium films of different thickness were prepared by thermal evaporation technique. From the XRD studies we concluded that the prepared selenium films exhibits hexagonal structure with the optical band gap of 1.8eV. The band gap of selenium thin film is found to be independent of the thickness of the films.

ACKNOWLEDGEMENT

Dr.M.Pandiaraman, thanks the UGC for providing RGNJRF fellowship, we thank the UGC-DRS scheme for providing facilities in our thin film lab, school of physics, Madurai Kamaraj University.

REFERENCES

1. Biljana Pejova, Ivan Grozdanov, Applied surface science **177** (2001) 152.
2. P.Gnanadurai, N.Soundararajan, C.E.Sooriamorthy: Vacuum, **67** (2002) 275
3. H.P.D. Lanyon, Physical Review **130** (1963) 134
4. M. Ferhat, J. Nagao, J. Appl. Phys. 88, 813 (2000)
5. R. Xu, A. Husmann, T.F. Rosenbaum, M.L. Saboungi, J.E. Enderby, P.B. Littlewood, Nature 57, 390 (1997)
6. R.Roy, V.S.Choudary, M.K.Patra, Journal of Optoelectronics and Advanced Materials **8** (2006) 1352
7. I.Ivan, S.Kokenyesi, A.Csik, Chalcogenide letters **4** (2007) 115.
8. V.Damodara Das, D.Karunakaran, J.Appl.Phys, **54** (1983) 5252.
9. Vincent Leon, Yang Ren, Marie-Louise Saboungi J. Appl. Phys. **103** 0161051 (2008)
10. Richard Dalven and Robert Gill, J. Appl. Phys. **38** 753 (1967)
11. M. Pandiaraman, N. Soundararajan, C.Vijayan, Journal of Ovonic Research 7, No. 1 (2011) 21
12. M. Pandiaraman, N. Soundararajan, C.Vijayan, C.Kumar and R.Ganesan, Journal of Ovonic Research Vol. **6**, No. 6, (2010) 285

Non Linear Effects on Phonon Polariton Modes in Ferroelectric Superlattices

K.S. Joseph Wilson and V. Revathy

Department of Physics, Arul Anandar College (Autonomous) Karumathur
Madurai, INDIA - 625 514.

Email- wilsonpra@yahoo.co.in

Abstract

The control of optical properties of matter has been one of the principle goals in recent years research. Recently, Non Linear effects modify several optical properties of crystals. In the present work, we discuss the phonon polariton modes in Ferro electric Superlattices and also we explore the possibilities of non linear effects of phonon polariton modes in Superlattices system. The various modes in polariton dispersion are analysed in detail. The presence of gap mode shows the propagation of electromagnetic radiation which may be exploited in optical communications.

Keywords: Phonon polariton; photonic gap; LiNbO₃ and LiTaO₃; nonlinear

Introduction

Electromagnetic radiation passing through condensed matter is coupled with the various excitations like phonons, magnons, plasmons, excitons etc. and exhibit polariton behavior [1-3]. Superlattices (SLs) are artificially fabricated crystals of alternate layers of different materials. . Recently there has been an increased interest in polaritons in infinite and finite Superlattices.. Though the spatial dispersion in a bulk material has very little effect on the polariton modes, the zone folding in a superlattice system makes the spatial dispersion an important effect for calculating the phonon-polariton modes[13]. The study of phonon-polariton modes, in SLs, has been a topic of great interest for over the two decades [4,5]. Recently, there has been an interest in the behavior of polaritons in left handed materials [6,7]. Photonic crystals, which prohibit the propagation of light for frequencies within a band gap, have enabled exciting new ways to control light and construct integrated optical devices. The effect of Non linear interaction plays a major role in all photonic devices.

Recently nonlinear effects on polaritons in isotropic crystals and uniaxial crystals were discussed[9,10]. The effect of nonlinear interactions cannot be ignored when the strength of the electric field is high. So, it is necessary to discuss their effects on the polaritons. The nonlinear effects introduce additional modes in the polaritonic gap. Here, the effect on nonlinear interactions of phonon polaritons in LiNbO₃/ LiTaO₃ superlattices is discussed. The various modes of polariton dispersion is analysed in detail.

Theory

The dependence of the frequency ω on the wave vector k of an electromagnetic wave in a crystal with a dielectric function $\varepsilon_1(\omega)$ is determined by a dispersion relation. For an infinite isotropic crystal, Maxwell's equations together with the constitutive relations lead to the polariton dispersion relation [11]

$$\frac{c^2 k^2}{\omega^2} = \varepsilon_1(\omega) = \varepsilon_\infty + \frac{(\varepsilon_s - \varepsilon_\infty)\omega_{TO}^2}{\omega_{TO}^2 - \omega^2} \quad (1)$$

where c is the velocity of light in vacuum, ε_s the static dielectric constant, ε_∞ the high frequency dielectric constant and ω_{TO} the transverse optical phonon frequency. There is a photonic gap between ω_{TO} and ω_{LO} within which no electromagnetic radiation can pass through. Recently it has been shown [10] that for noncentrosymmetric crystals, the dielectric function, is modified to

$$\varepsilon_i(\omega) = \varepsilon_1(\omega) + 4 \frac{f^2 b_{12}^4 E_0^2(\omega)}{(\omega^2 - \omega_{TO}^2)^4 \omega_{TO}^2 \varepsilon_0} \quad (2)$$

if nonlinear effects are included. Here i refers to A or B medium. In the above equations $b_{12} = b_{21} = \left[\frac{(\varepsilon_s - \varepsilon_\infty)}{4\pi} \right]^{1/2} \omega_{TO}$, $b_{11} = -\omega_{TO}^2$; $b_{22} = \frac{\varepsilon_\infty - 1}{4\pi}$; $f = \frac{\omega_{TO}^2}{d}$; and d is the lattice parameter[8]. All these parameters are available for the important materials like LiNbO_3 , and LiTaO_3 which are noncentrosymmetric crystals.

The study of excitations propagating in SL produces new results. Typically the thickness of an individual layer lies in the range 100-5000 Å. If one constituent, material A, always has thickness d_1 , and the second, material B, always has thickness d_2 , one has built a periodic structure known as a SL. In this work, assuming alternating layers of LiNbO_3 , and LiTaO_3 as A and B medium of thickness d_1 and d_2 stacked along the z -direction. Several authors[5,10] have derived the following dispersion relation for TM modes assuming the electromagnetic boundary conditions, namely, the electrostatic potentials and the electric displacement field perpendicular to each interface are continuous:

$$1 + \left(\frac{\varepsilon_B(\omega)\alpha_1}{\varepsilon_A(\omega)\alpha_2} \right)^2 + 2 \left(\frac{\varepsilon_B(\omega)\alpha_1}{\varepsilon_A(\omega)\alpha_2} \right) \left(\frac{\cosh(\alpha_1 d_1) \cosh(\alpha_2 d_2) - \cos(qL)}{\sinh(\alpha_1 d_1) \sinh(\alpha_2 d_2)} \right) = 0 \quad (3)$$

For the semiconductor SL ($\mu_v = 1$) consisting of alternating layers of materials A and B. Here,

$L = d_1 + d_2$ is the SL period and q is the component of the wave vector along the SL.

$$\alpha_1^2 = k_x^2 - \frac{\omega^2}{c^2} \epsilon_i$$

Where k_x is the component of the wave vector in the X-direction for TM modes

Results and discussion

The behavior of polaritons of LiNbO₃ / LiTaO₃ superlattice is studied. The dispersion relation given in Eq. (3) for the SL including nonlinear effect is solved numerically and the results are plotted for various cases. The numerical values of the physical parameters used in the calculations are easily available for the materials LiNbO₃ and LiTaO₃ [12] .

In Fig.1, we have shown the dispersion relation for the case $d_1 = d_2 = 100 \text{ \AA}$ with the Electric field $E = 1 \times 10^6 \text{ v/m}$ and the behavior of phonon polaritons at Brillouin zone edge ($q = \frac{\pi}{L}$) is discussed. We get eight modes. The top and bottom modes exhibit the behavior of the well known bulk modes of LiNbO₃, and LiTaO₃ while the middle modes approaches the surface mode frequencies. The top two modes are in the order of 10^{16} Hz , as suggested by the literature [14] in the case of LiNbO₃, and LiTaO₃, which were not shown in the figure and mode multiplicity occurs at frequencies 46.11 THz. In Fig.2, we consider the case of the behavior of phonon polaritons at $q = \frac{\pi}{4L}$ for the case $d_1 = d_2 = 100 \text{ \AA}$ with the Electric field $E = 1 \times 10^6 \text{ v/m}$. Here, we get eight modes. The top mode is in the order of 10^{16} Hz . It is not shown in the figure and for the other mode multiplicity occurs at frequencies 26.7 THz.

Fig.3 explains the behaviour of phonon polariton in LiNbO₃/LiTaO₃ superlattice at $q = \frac{\pi}{8L}$. The frequencies of the surface modes gets shifted to the higher values. The main significance of this case is that mode multiplicity do not occur. All the other behaviours are similar to the previous cases.

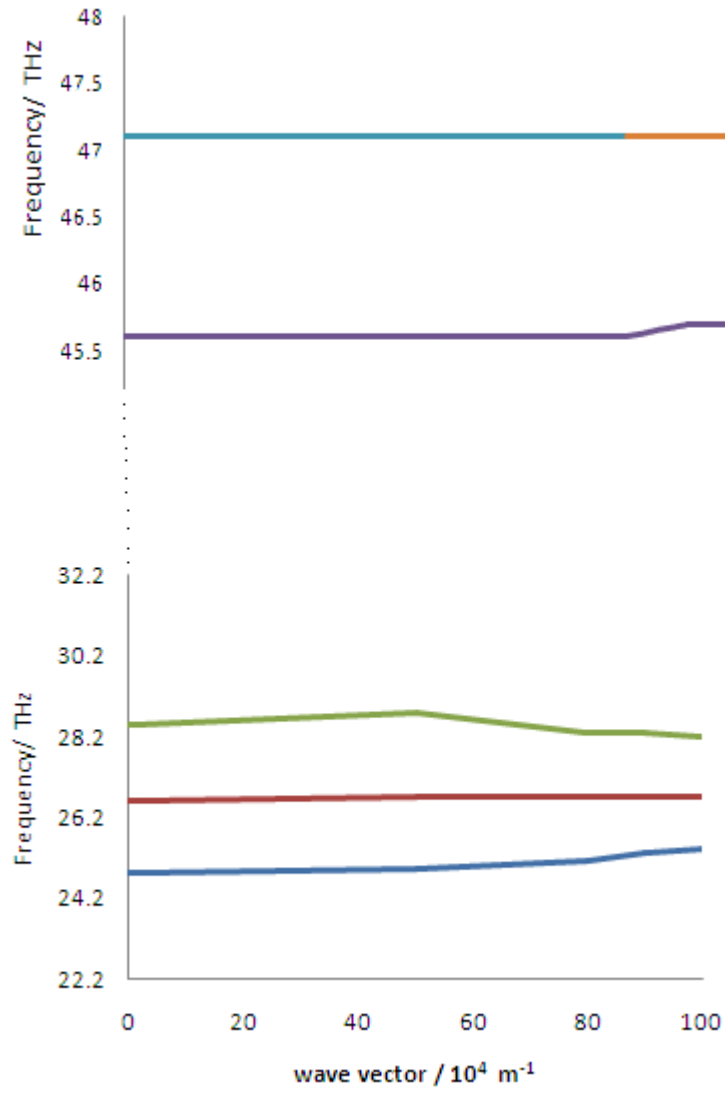


Fig 1. Polariton dispersion in ferroelectric superlattice for $d_1=100 \text{ \AA}$ and $d_2=100 \text{ \AA}$, at $q = \pi/L$

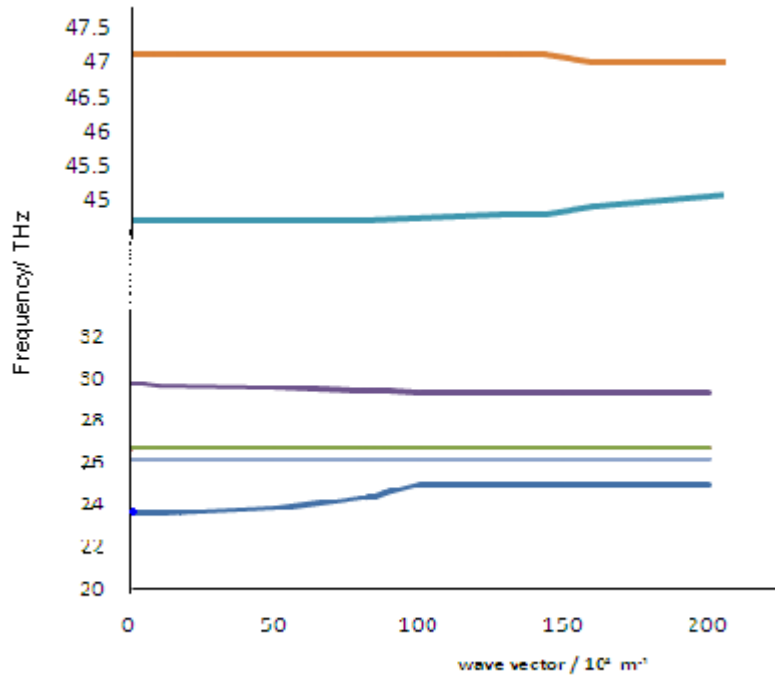


Fig 2. Polariton dispersion in ferroelectric superlattice for $d_1=100 \text{ \AA}$ and $d_2=100 \text{ \AA}$, at $q = \pi/4L$

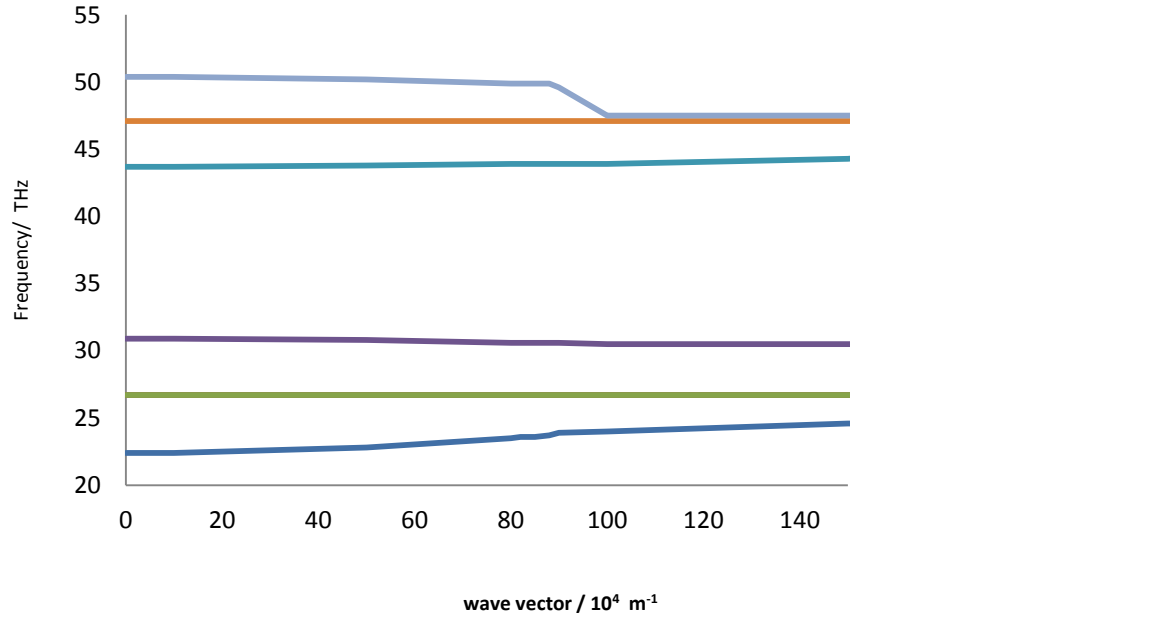


Fig 3. Polariton dispersion in ferroelectric superlattice for $d_1=100 \text{ \AA}$ and $d_2=100 \text{ \AA}$, at $q = \pi/8L$

Conclusion

Several Optical properties of the crystal can be modified due nonlinear interactions. Here the effect of nonlinear interactions on phonon polariton is analysed in detail. The various modes in the photonic band gap is the new feature due to nonlinearity. The presence of gap modes shows the propagation of electromagnetic radiation, which may be exploited in several modern application especially in optical communications.

Acknowledgement

We gratefully acknowledge University Grants Commission, India (Ref: No.F. 41-977/2012(SR)), for the Financial Support of this work.

REFERENCES

1. D.L.Mills and E.Burstein, Rep. Prog. Phys. **37**, 817 (1974).
2. R.F.Wallis in Interaction of Radiation with condensed matter, Volume 1, p.163
International Atomic Energy Agency, (Vienna 1977).
3. F.Bassani, Polaritons in Thin Films and Nanostructures, edited by V.M.Agranovich
and G.F.Bassani, Elsevier, Amsterdam (2003).
4. R.E.Camley, T.S.Rahman and D.L.Mills, Phys. Rev. B **27**, 261 (1983).
5. J.Barnas, Solid State Commun. **61**, 405 (1987).
6. R.Ruppin, Phys. Lett., A **277**, 61 (2000),
7. D.R.Smith et al., Phys. Rev. Lett., **84**, 4184 (2000).
8. R.W. Boyd, Nonlinear Optics (Academic Press, Newyork,2003)
9. J.S.Niu et al., Chinese Physics **10**, 836 (2001).
10. J.S.Niu et al., Chinese Physics **11**, 144 (2002).
11. C. Kittel, Introduction to solid state Physics, 7th edn. (Wiley, Singapore,1996)
12. Landolt-Bornstein: Numerical data and Functional Relationships in Science and
Technology, New Series, Vol.11 (Springer-Verlag,Berlin,1979).
13. Hanyou Chu and Yia-Chung Chang, Phys. Rev. B **38**,17 (1988)
14. K.S.J. Wilson and K. Navaneethakrishnan Mod. Phy. Lett. B19, 425 (2005)

Crystal and Molecular Structure of Diethyl 5-[(4-Chlorophenyl) Sulfinyl]-4-[(4-Chlorophenyl) Sulfinyl] Methyl-6-Hydroxy-2-(4-Methylphenyl)-3,6-Cyclohexadiene-1,3-Dicarboxylate

J. Suresh ^{1*}, P.S. Harikrishnan ², R. Vishnu Priya ¹, R. Nagalakshmi ¹

¹ Department of Physics, The Madura College (Autonomous), Madurai – 625 011.

² Department of Chemistry, The Madura College (Autonomous), Madurai – 625 011.

The title compound $C_{32}H_{30}O_9S_2Cl_4$, crystallizes in Triclinic system with $P\bar{1}$ space group and the unit cell parameters are : $a = 9.7057(7)\text{\AA}$, $b = 11.3020(8)\text{\AA}$, $c = 16.5423(11)$ and $\alpha = 70.339(1)^\circ$, $\beta = 82.234(1)^\circ$, $\gamma = 78.502(1)^\circ$ $V = 1669.94(7)\text{\AA}^3$ and $Z = 2$. The final R-factor is 7.3 %. The asymmetric unit comprises two molecules. Two types of intermolecular C-H...O hydrogen bonds generating graph set motifs $R_2^2(8)$ and $R_2^2(10)$ stabilize the structure. In addition to the intermolecular interactions large number of intra-molecular C-H...O and a C-H... π interaction exist in the structure.

Key Word: Molecular Structure, Triclinic System, Hydrogen bond

Introduction

Cyclohexanes are either prepared from natural sources or entirely *via* synthetic routes. The reason for their preparation is a variety of medical effects. The molecules provide anticonvulsant, antimalarial, antiinflammatory and cardiovascular effects [1]. Cyclohexanes are also important intermediates for many biologically active compounds [2, 3]. A number of their derivatives have fungicidal and antitumor activities [4]. Taking into consideration of these aspects, and in order to obtain a detailed information on the molecular structure in the solid state, the X-ray study of the title compound has been carried out.

Experimental

A mixture of ethyl-3-oxo-4-(arylsulfinyl)butanoate(0.577 g; 2 mmol) and aromatic aldehyde (0.106 g; 1 mmol) was dissolved in minimum amount of ethanol. To this, ammonium acetate (0.077g; 1mmol) was added and refluxed in a water bath for 1h.. The mixture was cooled and poured into water, extracted with dichloromethane, washed with a solution of sodium metabisulphate and brine, dried with anhydrous sodium sulfate and the solvent evaporated under reduced pressure. The resultant oil is purified in flash column using pet ether-ethyl acetate (1:1) mixture to give the desired product.

* Corresponding author

The chemical diagram of the compound is shown in Figure 1.

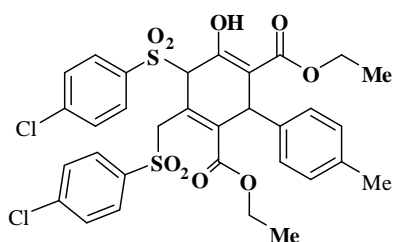


Fig. 1 Chemical diagram of the molecule

Data collection

Colourless crystal of dimension 0.18 x 0.16 x 0.11 mm was chosen for the intensity data collection on a Bruker SMART APEX diffractometer and graphite monochromated MoK α radiation ($\lambda = 0.71073 \text{ \AA}$) at 293 (2) K. Data collected with ω scan. Systematic extinction confirmed the lattice to be centric with space group P -1 with Z = 2. Least square refinement of 1025 reflections revealed the lattice parameters as $a = 9.7057(7) \text{ \AA}$, $b = 11.3020(8) \text{ \AA}$, $c = 16.5423(11)$ and $\alpha = 70.339(1)^\circ$, $\beta = 82.234(1)^\circ$, $\gamma = 78.502(1)^\circ$. The details of crystal data, parameters used for data collection and reliability factor are summarized in Table 1. Crystal structure was solved by direct method using the program SHELXS 97 [5] and refined by full matrix least squares with program SHELXL97 [5] to an R value of 0.073. All the non-hydrogen atoms were refined anisotropically while the hydrogen atoms, all found in ΔF map were refined with isotropic thermal parameters. The ORTEP drawing was performed with ORTEP3 program [6] and that of molecular packing with MERCURY[7].

Table 1 Summary of crystal data, data collection and refinement

Empirical formula	C ₃₂ H ₃₀ Cl ₂ O ₉ S ₂
Formula weight	693.58
Temperature	293(2) K
Wavelength	0.71073 Å
Crystal system, space group	Triclinic, P -1
Unit cell dimensions	a = 9.7057(7) Å alpha = 70.3390(10)° b = 11.3020(8) Å beta = 82.2340(10)° c = 16.5423(11) Å gamma = 78.5020(10)°
Volume	1669.9(2) Å ³
Z, Calculated density	2, 1.379 Mg/m ³
Absorption coefficient	0.371 mm ⁻¹
F(000)	720
Crystal size	0.18 x 0.16 x 0.11 mm ³
Theta range for data collection	1.31 to 27.99°
Limiting indices	-12<=h<=12, -14<=k<=14, -20<=l<=21
Reflections collected / unique	19319 / 7627 [R(int) = 0.0288]
Completeness to theta	94.80%
Refinement method	Full-matrix least-squares on F ²
Data / restraints / parameters	7627 / 0 / 410
Goodness-of-fit on F ²	1.132
Final R indices [I>2sigma(I)]	R1 = 0.0730, wR2 = 0.1673
R indices (all data)	R1 = 0.0966, wR2 = 0.1835
Largest diff. peak and hole	0.514 and -0.380 e.Å ⁻³

Table 2 Atomic coordinates (X 10⁴) and equivalent isotropic displacement parameters (Å² X 10³) for non-hydrogen atoms

Atom	x	y	z	U(eq)
C(61)	1158(3)	5159(3)	1588(2)	47(1)
C(62)	-156(3)	7597(3)	1506(2)	46(1)
C(63)	-440(3)	8384(3)	695(2)	59(1)
C(64)	-1747(4)	9149(3)	553(3)	68(1)
C(65)	-2741(4)	9075(3)	1223(3)	67(1)
C(66)	-2474(4)	8291(4)	2037(3)	76(1)
C(67)	-1159(3)	7534(3)	2182(2)	62(1)
O(1)	5664(2)	3402(2)	454(1)	51(1)
O(2)	3081(2)	1939(2)	630(1)	51(1)
O(3)	1017(2)	3661(2)	479(1)	51(1)
O(4)	2480(2)	7120(2)	986(2)	73(1)
O(5)	1822(3)	6370(2)	2544(2)	74(1)
O(6)	7496(2)	1880(2)	1456(2)	70(1)
O(7)	6948(3)	1354(2)	2873(2)	79(1)
O(8)	531(3)	3563(3)	3361(2)	94(1)
O(9)	2511(3)	3356(3)	3975(2)	82(1)
S(1)	2519(1)	3270(1)	371(1)	39(1)
S(2)	1499(1)	6601(1)	1681(1)	51(1)
Cl(1)	-4388(1)	9979(1)	1039(1)	110(1)
Cl(2)	4095(2)	5471(1)	-3556(1)	102(1)
C(55)	2528(4)	5486(3)	-2087(2)	59(1)
C(56)	2201(3)	5026(3)	-1219(2)	47(1)

Atom	x	y	z	U(eq)
C(1)	2766(3)	3367(3)	2546(2)	47(1)
C(2)	4102(3)	2392(3)	2738(2)	48(1)
C(3)	5147(3)	2523(3)	1964(2)	46(1)
C(4)	4802(3)	3255(2)	1171(2)	41(1)
C(5)	3367(3)	4011(2)	980(2)	39(1)
C(6)	2430(3)	4119(3)	1761(2)	42(1)
C(7)	1793(4)	3448(3)	3325(2)	66(1)
C(8)	1670(7)	3506(8)	4740(3)	144(3)
C(9)	2558(10)	3550(10)	5314(4)	210(4)
C(21)	3740(3)	1043(3)	3137(2)	52(1)
C(22)	4148(5)	283(4)	3929(3)	90(1)
C(23)	3820(6)	-941(4)	4282(3)	106(2)
C(24)	3091(5)	-1436(4)	3864(2)	78(1)
C(25)	2692(5)	-670(4)	3074(3)	85(1)
C(26)	3005(5)	549(4)	2715(2)	76(1)
C(27)	2724(7)	-2763(4)	4254(3)	117(2)
C(31)	6632(3)	1890(3)	2058(3)	57(1)
C(32)	8428(5)	772(5)	3000(4)	114(2)
C(33)	8728(7)	595(9)	3841(5)	196(4)
C(51)	3043(3)	3948(3)	-726(2)	41(1)
C(52)	4232(3)	3356(3)	-1097(2)	52(1)
C(53)	4566(3)	3842(4)	-1965(2)	62(1)
C(54)	3704(4)	4884(3)	-2454(2)	59(1)

Table 3 Torsion Angle (°)

Atoms	Angle
C(6)-C(1)-C(2)-C(3)	10.6(4)
C(1)-C(2)-C(3)-C(4)	-11.9(4)
C(2)-C(3)-C(4)-C(5)	0.5(4)
C(3)-C(4)-C(5)-C(6)	12.6(4)
C(2)-C(1)-C(6)-C(5)	2.3(4)
C(4)-C(5)-C(6)-C(1)	-13.9(4)

Results and discussion

The atomic coordinates of the non-hydrogen atoms and their equivalent isotropic displacement factors are presented in Table 2. The selected torsion angles are listed in Table 3. Inter molecular hydrogen bond geometry are listed in Table 4. Figure 2 shows the ORTEP plot drawn at 30 % probability displacement and the atom-numbering scheme. The asymmetric unit comprises two crystallographically independent molecules. The cyclohexadiene ring adopts boat conformation with atoms C2 and C5 deviating by 0.137 (2) Å and 0.158 (2) Å respectively from the least-squares plane defined by atoms C1/C3/C4/C6. The dihedral angle between the two adjacent (4-chlorophenyl)sulfinyl rings [(C51-C56) and (C62-C67)] is 14.54 (3)°. The C51-S1 bond 1.764(2) Å is shorter than C5-S1 bond 1.860(2) Å which may be due to the conjugation of S1 with the chlorophenyl group. Similarly C31-O7 is (1.329 Å) is longer than C31-O6 (1.213 Å) and considerably shorter than the C32-O7 (1.468 Å).

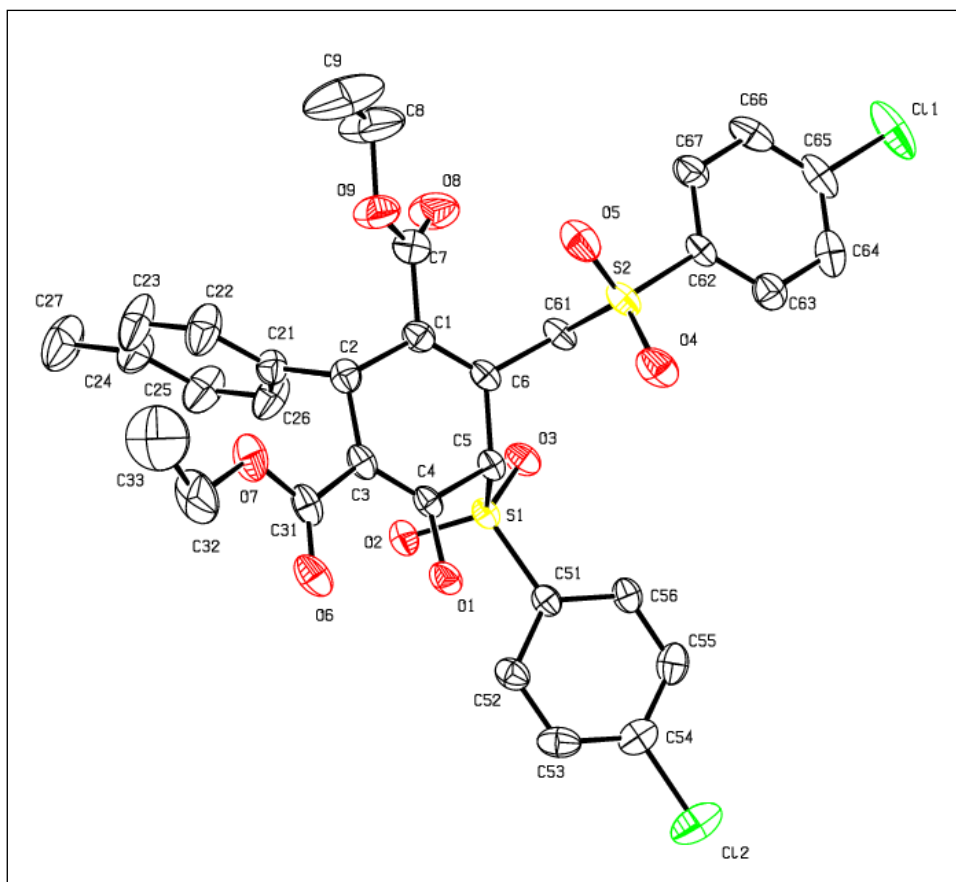


Fig. 2 ORTEP diagram with ellipsoids at the 30% probability level. H-atoms are omitted for clarity

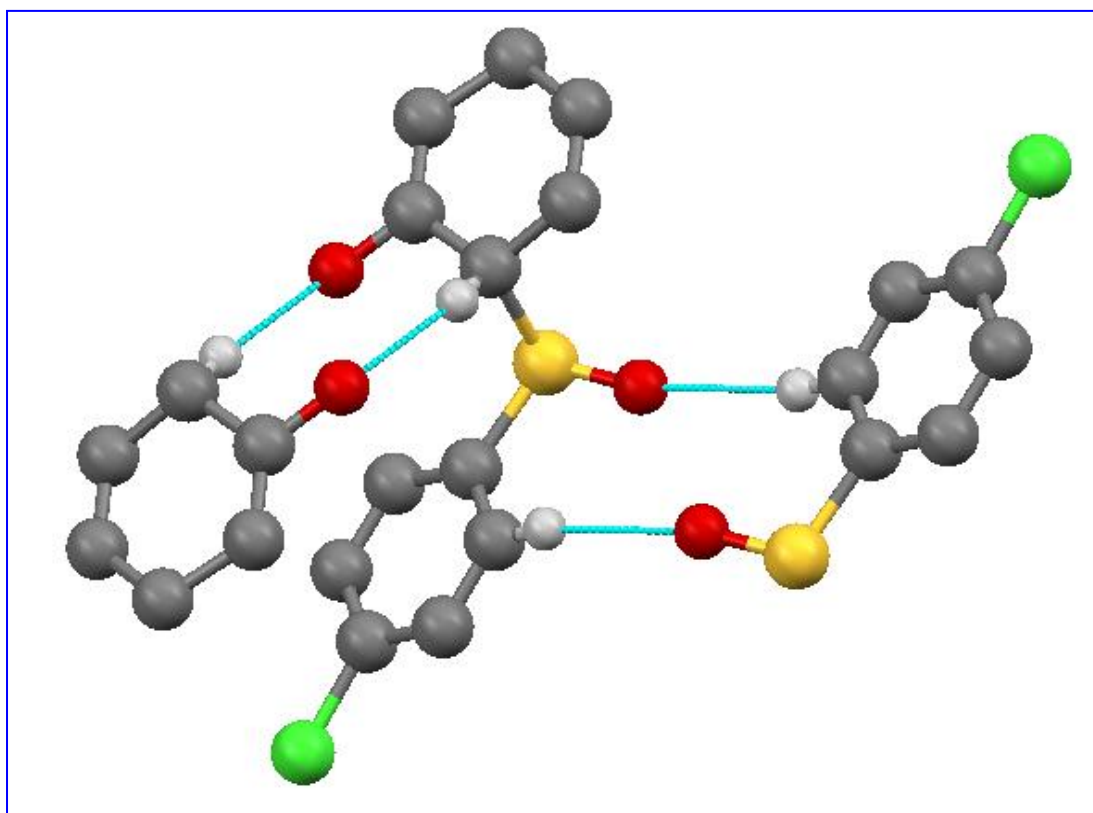


Fig. 3 Ring motifs $R_2^2(8)$ and $R_2^2(10)$

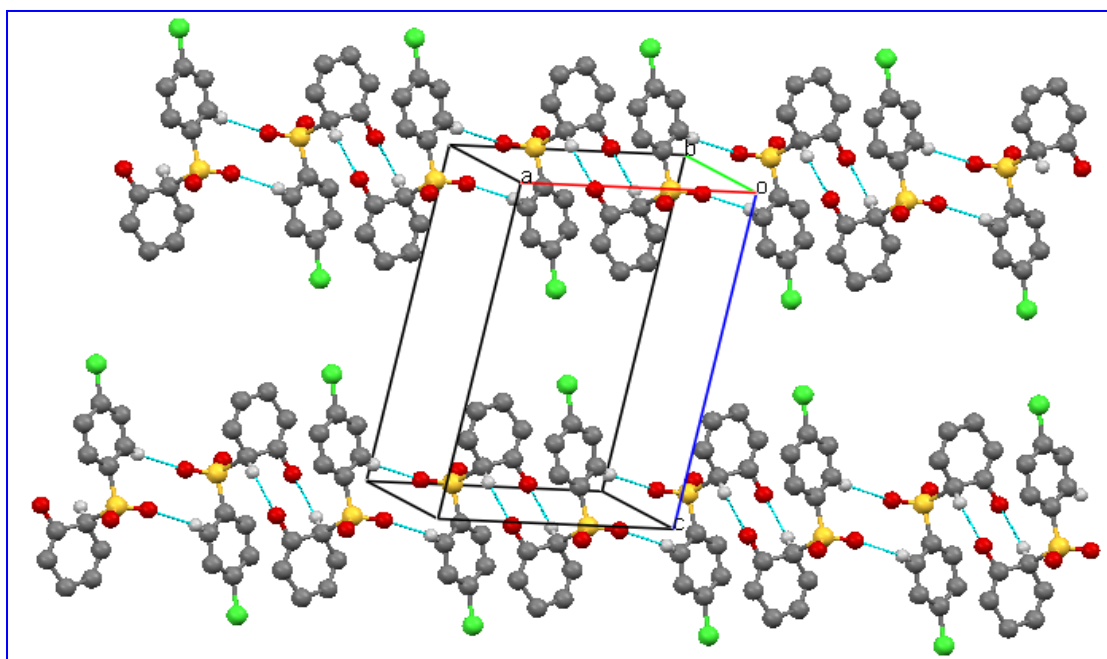


Fig. 4 Packing diagram

The crystal structure is stabilized by weak C-H...O interactions generating graph set motifs $R_2^2(8)$ and $R_2^2(10)$ (Table 4 ; Fig. 3). These motifs form linear infinite chain running along the a-axis. These chains do not have marked C-H...O interactions between them, however there are van der Waals interactions between them (Fig. 4).

Table 4 Hydrogen bonds [\AA and $^\circ$]

D-H...A	d(D-H)	d(H...A)	d(D...A)	<(DHA)
C(5)-H(5)...O(1) ⁱ	0.98	2.35	3.299(3)	163
C(56)-H(56)...O(3) ⁱⁱ	0.93	2.53	3.435(4)	166
C(2)-H(2)...O(9)	0.98	2.42	2.781(4)	101
O(1)-H(1)...O(6)	0.82	1.85	2.555(3)	143
C(26)-H(26)...O(2)	0.93	2.42	3.272(4)	153
C(56)-H(56)...O(3)	0.93	2.59	2.917(4)	102
C(61)-H(61A)...O(8)	0.97	2.26	2.936(4)	126
C(61)-H(61B)...O(3)	0.97	2.3	2.915(3)	120
C(63)-H(63)...O(4)	0.93	2.57	2.932(4)	104
C(26)-H(26)... Cg(1)	0.93	2.78	3.124(5)	103

Symmetry transformations used to generate equivalent atoms:

(i) $1-x, 1-y, -z$ (ii) $-x, 1-y, -z$ (iii) Cg(1) refers to C(1)-C(6) ring centroid

Acknowledgements : P.S. Harikrishnan thanks I.I.C.T. Hyderabad for their help in the data collection. J. Suresh thanks DST for the FIST support.

References :

- [1] Eddington, N. D., Cox, D. S., Roberts, R. R., Stables, J. P., Powell, C. B. & Scott, A. R. (2000). *Curr. Med. Chem.* **7**, 417-436.
- [2] Padmavathi, V., Reddy, B. J. M., Balaiah, A., Reddy, K. V. & Reddy, D. B. (2000). *Molecules*, **5**, 1281-1286.
- [3] Padmavathi, V., Sharmila, K., Reddy, A. S. & Reddy, D. B. (2001). *Indian J. Chem. Sect. B*, **40**, 11-14.
- [4] Li, J. Y. & Strobel, G. A. (2001). *Phytochemistry*, **57**, 261-265.
- [5] Sheldrick, G. M. (2008). *Acta Cryst. A* **64**, 112-122.
- [6] Farrugia, L. J. Ortep-3 for Windows: *J. Appl. Cryst.* (1997), **30**, 565.
- [7] Mercury CSD 2.0 - New Features for the Visualization and Investigation of Crystal Structures
Macrae, C.F., Bruno, I.J., Chisholm, J.A., Edgington, P.R., McCabe, P. E. Pidcock, E., Rodriguez-Monge, L., Taylor, R., van de Streek, J and Wood, P.A. *J. Appl. Cryst.*, **41**, 466-470, 2008

Solution of a Conjecture on Skolem Mean Graph of stars $K_{1,1} \cup K_{1,1} \cup K_{1,m} \cup K_{1,n}$

V. Balaji^a, D. S. T. Ramesh^b and V. Maheswari^c

^aDepartment of Mathematics, Sacred Heart College, Tirupattur-635 601, India

^bDepartment of Mathematics, Margoschis College, Nazareth-628617, India

^cDepartment of Mathematics, Manonmanian Sundaranar university, Tirunelveli-627012, India

Abstract

In this paper, we prove the conjecture that the four star $K_{1,1} \cup K_{1,1} \cup K_{1,m} \cup K_{1,n}$ is a skolem mean graph if $|m-n| < 7$ for $m = 1, 2, 3, 4, \dots$ and $1 \leq m < n$.

Keywords: Skolem mean graph and star. AMS(MOS) Subject Classification 05C78

1. INTRODUCTION

All graphs in this paper are finite, simple and undirected. Terms not defined here are used in the sense of Harary [6]. In [1], skolem mean labeling was focused an assignment of label to the vertices $x \in V$ with distinct elements $f(x)$ from $1, 2, \dots, p$ in such a way that when the edge

$e = uv$ is labeled with $\frac{f(u) + f(v)}{2}$ if $f(u) + f(v)$ is even and $\frac{f(u) + f(v) + 1}{2}$ if $f(u) + f(v)$ is odd then the

edges get distinct labels from the set $\{2, 3, \dots, p\}$ and it was proved that any path is a skolem mean graph, if $m \geq 4$, $K_{1,m}$ is not a skolem mean graph and the two stars $K_{1,m} \cup K_{1,n}$ is a skolem mean graph if and only if $|m-n| \leq 4$. In [2], it was proved that the three star $K_{1,\ell} \cup K_{1,m} \cup K_{1,n}$ is a skolem mean graph if $|m-n| = 4 + \ell$ for $\ell = 1, 2, 3, \dots$; $m = 1, 2, 3, \dots$; $n = \ell + m + 4$ and $\ell \leq m < n$; the three star $K_{1,\ell} \cup K_{1,m} \cup K_{1,n}$ is not a skolem mean graph if $|m-n| > 4 + \ell$ for $\ell = 1, 2, 3, \dots$; $m = 1, 2, 3, \dots$; $n \geq \ell + m + 5$ and $\ell \leq m < n$; the four star $K_{1,\ell} \cup K_{1,\ell} \cup K_{1,m} \cup K_{1,n}$ is a skolem mean graph if $|m-n| = 4 + 2\ell$ for $\ell = 2, 3, 4, \dots$; $m = 2, 3, 4, \dots$;

$n = 2\ell + m + 4$ and $\ell \leq m < n$; the four star $K_{1,\ell} \cup K_{1,\ell} \cup K_{1,m} \cup K_{1,n}$ is not a skolem mean graph if $|m-n| > 4 + 2\ell$ for $\ell = 2, 3, 4, \dots$; $m = 2, 3, 4, \dots$; $n \geq 2\ell + m + 5$ and $\ell \leq m < n$; the four star $K_{1,1} \cup K_{1,1} \cup K_{1,m} \cup K_{1,n}$ is a skolem mean graph if $|m-n| = 7$ for $m = 1, 2, 3, \dots$; $n = m + 7$ and $1 \leq m < n$ and the four star $K_{1,1} \cup K_{1,1} \cup K_{1,m} \cup K_{1,n}$ is not a skolem mean graph if $|m-n| > 7$ for $m = 1, 2, 3, \dots$; $n \geq m + 8$ and $1 \leq m < n$. In [4], the condition for a graph to be skolem mean is that $p \geq q + 1$. In [3], We proved a conjecture that the three stars $K_{1,\ell} \cup K_{1,m} \cup K_{1,n}$ is a skolem mean graph if $|m-n| < 4 + \ell$ for $\ell = 1, 2, 3, \dots$; $m = 1, 2, 3, \dots$ and $\ell \leq m < n$. In [5], We proved a conjecture if $\ell \leq m < n$, the

four star $K_{1,\ell} \cup K_{1,\ell} \cup K_{1,m} \cup K_{1,n}$ is a skolem mean graph if $|m-n| < 4 + 2\ell$ for $\ell = 2, 3, 4, \dots$; $m = 2, 3, 4, \dots$.

2. MAIN THEOREMS

Definition 2.1.0 The four star is the disjoint union of $K_{1,a}, K_{1,b}, K_{1,c}$ and $K_{1,d}$. It is denoted by $K_{1,a} \cup K_{1,b} \cup K_{1,c} \cup K_{1,d}$.

Theorem 2.1.1 If $1 \leq m < n$, the four star $K_{1,1} \cup K_{1,1} \cup K_{1,m} \cup K_{1,n}$ is a skolem mean graph if $|m-n| < 7$ for $m = 1, 2, 3, 4, \dots$.

Proof:

Case : 1 Consider the graph $G = K_{1,1} \cup K_{1,1} \cup K_{1,m} \cup K_{1,n}$.

Let $1 \leq m < n$ where $n = m+6$ for $m = 1, 2, 3, 4, \dots$. Let us take the case that $|m-n| < 7$ for $m = 1, 2, 3, 4, \dots$. We have to prove that G is a skolem mean graph.

Therefore, the graph $G = K_{1,1} \cup K_{1,1} \cup K_{1,m} \cup K_{1,n}$ where $n = m + 6$ for $m = 1, 2, 3, 4, \dots$.

Let $\{u, u_1\}, \{v, v_1\}, \{w\} \cup \{w_k: 1 \leq k \leq m\}$ and $\{x\} \cup \{x_h: 1 \leq h \leq n\}$ be the vertices of G . Then G has $m + n + 6$ vertices and $m + n + 2$ edges.

We have $V(G) = \{u, v, w, x\} \cup \{u_1\} \cup \{v_1\} \cup \{w_k: 1 \leq k \leq m\} \cup \{x_h: 1 \leq h \leq n\}$.

The required vertex labeling $f: V(G) \rightarrow \{1, 2, 3, 4, \dots, m + n + 6\}$ is defined as follows:

$$f(u) = 1; f(v) = 2; f(w) = 4; f(x) = m + n + 5;$$

$$f(u_1) = 8;$$

$$f(v_1) = 6;$$

$$f(w_k) = 2k + 8 \text{ for } 1 \leq k \leq m;$$

$$f(x_h) = 2h + 1 \text{ for } 1 \leq h \leq n - 2;$$

$$f(x_{n-1}) = m + n + 4 \text{ and}$$

$$f(x_n) = m + n + 6$$

The corresponding edge labels are as follows:

The edge label of uu_1 is 5; vv_1 is 4; ww_k is $k + 6$ for $1 \leq k \leq m$ and xx_h is $\frac{2h+m+n+6}{2}$ for $1 \leq$

$h \leq n - 2$; the edge label of xx_{n-1} is $m + n + 5$ and the edge label of xx_n is $m + n + 6$.

Hence the induced edge labels of G are distinct.

Hence the graph G is a skolem mean graph.

Case : 2 Consider the graph $G = K_{1,1} \cup K_{1,1} \cup K_{1,m} \cup K_{1,n}$.

Let $1 \leq m < n$ where $n = m+5$ for $m = 1, 2, 3, 4, \dots$. Let us take the case that $|m-n| < 7$ for $m = 1, 2, 3, 4, \dots$. We have to prove that G is a skolem mean graph.

Therefore, the graph $G = K_{1,1} \cup K_{1,1} \cup K_{1,m} \cup K_{1,n}$ where $n = m + 5$ for $m = 1, 2, 3, 4, \dots$.

Let $\{u, u_1\}, \{v, v_1\}, \{w\} \cup \{w_k: 1 \leq k \leq m\}$ and $\{x\} \cup \{x_h: 1 \leq h \leq n\}$ be the vertices of G . Then G has $m + n + 6$ vertices and $m + n + 2$ edges.

We have $V(G) = \{u, v, w, x\} \cup \{u_1\} \cup \{v_1\} \cup \{w_k: 1 \leq k \leq m\} \cup \{x_h: 1 \leq h \leq n\}$.

The required vertex labeling $f: V(G) \rightarrow \{1, 2, 3, 4, \dots, m + n + 6\}$ is defined as follows:

$$f(u) = 1; f(v) = 2; f(w) = 5; f(x) = m + n + 5;$$

$$f(u_1) = 3;$$

$$f(v_1) = 7;$$

$$f(w_k) = 2k + 7 \text{ for } 1 \leq k \leq m;$$

$$f(x_h) = 2h + 2 \text{ for } 1 \leq h \leq n - 2;$$

$$f(x_{n-1}) = m + n + 4 \text{ and}$$

$$f(x_n) = m + n + 6$$

The corresponding edge labels are as follows:

The edge label of uu_1 is 2; vv_1 is 5; ww_k is $k + 5$ for $1 \leq k \leq m$ and xx_h is $\frac{2h+m+n+7}{2}$ for $1 \leq$

$h \leq n - 2$; the edge label of xx_{n-1} is $m + n + 4$ and the edge label of xx_n is $m + n + 6$.

Hence the induced edge labels of G are distinct.

Hence the graph G is a skolem mean graph.

Case : 3 Consider the graph $G = K_{1,1} \cup K_{1,1} \cup K_{1,m} \cup K_{1,n}$.

Let $1 \leq m < n$ where $n = m+4$ for $m = 1, 2, 3, 4, \dots$. Let us take the case that $|m-n| < 7$ for $m = 1, 2, 3, 4, \dots$. We have to prove that G is a skolem mean graph.

Therefore, the graph $G = K_{1,1} \cup K_{1,1} \cup K_{1,m} \cup K_{1,n}$ where $n = m + 4$ for $m = 1, 2, 3, 4, \dots$.

Let $\{u, u_1\}, \{v, v_1\}, \{w\} \cup \{w_k: 1 \leq k \leq m\}$ and $\{x\} \cup \{x_h: 1 \leq h \leq n\}$ be the vertices of G . Then G has $m + n + 6$ vertices and $m + n + 2$ edges.

We have $V(G) = \{u, v, w, x\} \cup \{u_1\} \cup \{v_1\} \cup \{w_k: 1 \leq k \leq m\} \cup \{x_h: 1 \leq h \leq n\}$.

The required vertex labeling $f: V(G) \rightarrow \{1, 2, 3, 4, \dots, m + n + 6\}$ is defined as follows:

$$f(u) = 1; f(v) = 3; f(w) = 6; f(x) = m + n + 5;$$

$$f(u_1) = 2;$$

$$f(v_1) = 4;$$

$$f(w_k) = 2k + 6 \text{ for } 1 \leq k \leq m;$$

$$f(x_h) = 2h + 3 \text{ for } 1 \leq h \leq n - 2;$$

$$f(x_{n-1}) = m + n + 4 \text{ and}$$

$$f(x_n) = m + n + 6$$

The corresponding edge labels are as follows:

$$\text{The edge label of } uu_1 \text{ is } 2; vv_1 \text{ is } 4; ww_k \text{ is } k + 6 \text{ for } 1 \leq k \leq m \text{ and } xx_n \text{ is } \frac{2h+m+n+8}{2} \text{ for } 1 \leq$$

$h \leq n - 2$; the edge label of xx_{n-1} is $m + n + 5$ and the edge label of xx_n is $m + n + 6$.

Hence the induced edge labels of G are distinct.

Hence the graph G is a skolem mean graph.

Case : 4 Consider the graph $G = K_{1,1} \cup K_{1,1} \cup K_{1,m} \cup K_{1,n}$.

Let $1 \leq m < n$ where $n = m+3$ for $m = 1, 2, 3, 4, \dots$. Let us take the case that $|m-n| < 7$ for $m = 1, 2, 3, 4, \dots$. We have to prove that G is a skolem mean graph. Therefore, the graph $G = K_{1,1} \cup K_{1,1} \cup K_{1,m} \cup K_{1,n}$ where $n = m + 3$ for $m = 1, 2, 3, 4, \dots$.

Let $\{u, u_1\}, \{v, v_1\}, \{w\} \cup \{w_k: 1 \leq k \leq m\}$ and $\{x\} \cup \{x_h: 1 \leq h \leq n\}$ be the vertices of G . Then G has $m + n + 6$ vertices and $m + n + 2$ edges.

$$\text{We have } V(G) = \{u, v, w, x\} \cup \{u_1\} \cup \{v_1\} \cup \{w_k: 1 \leq k \leq m\} \cup \{x_h: 1 \leq h \leq n\}.$$

The required vertex labeling $f: V(G) \rightarrow \{1, 2, 3, 4, \dots, m + n + 6\}$ is defined as follows:

$$f(u) = 1; f(v) = 3; f(w) = 5; f(x) = m + n + 5;$$

$$f(u_1) = 2;$$

$$f(v_1) = 4;$$

$$f(w_k) = 2k + 5 \text{ for } 1 \leq k \leq m;$$

$$f(x_h) = 2h + 4 \text{ for } 1 \leq h \leq n - 2;$$

$$f(x_{n-1}) = m + n + 4 \text{ and}$$

$$f(x_n) = m + n + 6$$

The corresponding edge labels are as follows:

$$\text{The edge label of } uu_1 \text{ is } 2; vv_1 \text{ is } 4; ww_k \text{ is } k + 5 \text{ for } 1 \leq k \leq m \text{ and } xx_n \text{ is } \frac{2h+m+n+9}{2} \text{ for } 1 \leq$$

$h \leq n - 2$; the edge label of xx_{n-1} is $m + n + 5$ and the edge label of xx_n is

$m + n + 6$.

Hence the induced edge labels of G are distinct.

Hence the graph G is a skolem mean graph.

Case 5: Consider the graph $G = K_{1,1} \cup K_{1,1} \cup K_{1,m} \cup K_{1,n}$.

Let $1 \leq m < n$ where $n = m+2$ for $m = 1, 2, 3, 4, \dots$. Let us take the case that $|m-n| < 7$ for $m = 1, 2, 3, 4, \dots$. We have to prove that G is a skolem mean graph. Therefore, the graph

$G = K_{1,1} \cup K_{1,1} \cup K_{1,m} \cup K_{1,n}$ where $n = m + 2$ for $m = 1, 2, 3, 4, \dots$.

Let $\{u, u_1\}, \{v, v_1\}, \{w\} \cup \{w_k: 1 \leq k \leq m\}$ and $\{x\} \cup \{x_h: 1 \leq h \leq n\}$ be the vertices of G . Then G has $m + n + 6$ vertices and $m + n + 2$ edges.

We have $V(G) = \{u, v, w, x\} \cup \{u_1\} \cup \{v_1\} \cup \{w_k: 1 \leq k \leq m\} \cup \{x_h: 1 \leq h \leq n\}$.

The required vertex labeling $f: V(G) \rightarrow \{1, 2, 3, 4, \dots, m + n + 6\}$ is defined as follows:

$$f(u) = 1; f(v) = 3; f(w) = 5; f(x) = m + n + 5;$$

$$f(u_1) = 2;$$

$$f(v_1) = 4;$$

$$f(w_k) = 2k + 4 \text{ for } 1 \leq k \leq m;$$

$$f(x_h) = 2h + 5 \text{ for } 1 \leq h \leq n - 2;$$

$$f(x_{n-1}) = m + n + 4 \text{ and}$$

$$f(x_n) = m + n + 6$$

The corresponding edge labels are as follows:

The edge label of uu_1 is 2; vv_1 is 4; ww_k is $k + 5$ for $1 \leq k \leq m$ and xx_h is $\frac{2h+m+n+10}{2}$ for 1

$\leq h \leq n - 2$; the edge label of xx_{n-1} is $m + n + 5$ and the edge label of xx_n is $m + n + 6$.

Hence the induced edge labels of G are distinct.

Hence the graph G is a skolem mean graph.

Case 6: Consider the graph $G = K_{1,1} \cup K_{1,1} \cup K_{1,m} \cup K_{1,n}$.

Let $1 \leq m < n$ where $n = m + 1$ for $m = 1, 2, 3, 4, \dots$. Let us take the case that $|m-n| < 7$ for $m = 1, 2, 3, 4, \dots$. We have to prove that G is a skolem mean graph.

Therefore, the graph $G = K_{1,1} \cup K_{1,1} \cup K_{1,m} \cup K_{1,n}$ where $n = m + 1$ for $m = 1, 2, 3, 4, \dots$.

Let $\{u, u_1\}, \{v, v_1\}, \{w\} \cup \{w_k: 1 \leq k \leq m\}$ and $\{x\} \cup \{x_h: 1 \leq h \leq n\}$ be the vertices of G . Then G has $m + n + 6$ vertices and $m + n + 2$ edges.

We have $V(G) = \{u, v, w, x\} \cup \{u_1\} \cup \{v_1\} \cup \{w_k: 1 \leq k \leq m\} \cup \{x_h: 1 \leq h \leq n\}$.

The required vertex labeling $f: V(G) \rightarrow \{1, 2, 3, 4, \dots, m + n + 6\}$ is defined as follows:

$$f(u) = 1; f(v) = 3; f(w) = 6; f(x) = m + n + 5;$$

$$f(u_1) = 2;$$

$$f(v_1) = 4;$$

$$f(w_k) = 2k + 3 \text{ for } 1 \leq k \leq m;$$

$$f(x_h) = 2h + 6 \text{ for } 1 \leq h \leq n - 2;$$

$$f(x_{n-1}) = m + n + 4 \text{ and}$$

$$f(x_n) = m + n + 6$$

The corresponding edge labels are as follows:

The edge label of uu_1 is 2; vv_1 is 4; ww_k is $k + 5$ for $1 \leq k \leq m$ and xx_h is $\frac{2h + m + n + 11}{2}$ for 1

$\leq h \leq n - 2$; the edge label of xx_{n-1} is $m + n + 5$ and the edge label of xx_n is $m + n + 6$.

Hence the induced edge labels of G are distinct.

Hence the graph G is a skolem mean graph.

References

[1] V. Balaji, D. S. T. Ramesh and A. Subramanian, Skolem Mean Labeling, Bulletin of Pure and Applied Sciences, vol. 26E No. 2, 2007, 245 – 248.

[2] V. Balaji, D. S. T. Ramesh and A. Subramanian, Some Results On Skolem Mean Graphs, Bulletin of Pure and Applied Sciences, vol. 27E No. 1, 2008, 67 – 74.

[3] V. Balaji, Solution of a Conjecture on Skolem Mean Graph of stars $K_{1,\ell} \cup K_{1,m} \cup K_{1,n}$ International Journal of Mathematical Combinatorics, vol.4, 2011, 115 – 117.

[4] J. A. Gallian, A Dynamic Survey of Graph Labeling, The Electronic Journal of combinatorics 16(2009), # DS6.

[5] V. Balaji, D. S. T. Ramesh and V. Maheswari, Solution of a Conjecture on Skolem Mean Graph of stars $K_{1,\ell} \cup K_{1,\ell} \cup K_{1,m} \cup K_{1,n}$, International Journal of Science & Engineering Research, vol.3, issue 11 November 2012, 125 – 128.

[6] F. Harary, Graph Theory, Addison – Wesley, Reading Mars., (1972).

A Dynamic Approach of Generalized Difference Operator to n -Multiple Series

G.Britto Antony Xavier*, H.Nasira Begum, S.U.Vasantha Kumar and B.Govindan
Department of Mathematics, Sacred Heart College, Tirupattur - 635601, Vellore District.

Abstract:

We investigate a numerical and a closed form solutions of the n^{th} - kind generalized difference equation $\prod_{i=1}^n \Delta_{\ell_i} v(k) = u(k)$, $\ell_i > 0$ with useful tool $\prod_{i=1}^n \Delta_{\ell_i}^{-1} u(k)$ for finding the values of various n -multiple series by iteration method in the field of numerical analysis. We also provide the suitable numerical examples to illustrate our main result.

Key words: Closed form solution, Difference operator, Generalized difference equation, Numerical solution.

AMS Subject classification: 39A70, 47B39, 39A10.

1. Introduction:

In 1989, Miller and Ross introduced the discrete analogue of the Riemann-Liouville fractional derivative and proved some properties of the fractional difference operator [12]. In the general fractional h -difference Riemann-Liouville operator mentioned in [2, 14], the presence of the h parameter is particularly interesting from the numerical point of view, because when h tends to zero the solutions of the fractional difference equations can be seen as approximations to the solutions of corresponding Riemann-Liouville fractional differential equation [2, 3].

The formulae for sums and partial sums of the n^{th} powers of an arithmetic progression, the sums and partial sums of the products of n consecutive terms of an arithmetic progression and the sums and partial sums of an arithmetic-geometric progression using the generalized difference operators of the first, second and n^{th} kinds and their inverses had been derived in ([4], [9], [10], [11]).

In the existing literature of Mathematics, there are formulas available for finding the value of single series but there is no formula to find the value of n -multiple series given as

$$\prod_{t=1}^n \left[\frac{k - \sum_{s=n+2-t}^n r_s \ell_s}{\sum_{r_{n+1-t}=1}^{\ell_{n+1-t}} u(k - \sum_{i=1}^n r_i \ell_i) \right] \tag{1}$$

In this paper, we derive the numerical and closed form solutions of the higher kind linear generalized difference equation by iteration method using power set notation and obtain the value of n -multiple series as given in (1).

2. Preliminaries:

Before stating and proving our results, we present some notations, basic definitions and preliminary results which will be used in the subsequent discussions. Let $\ell_i > 0$, $k \in [0, \infty)$,

$$j = k - \left\lfloor \frac{k}{\ell_i} \right\rfloor \ell_i \text{ where } \left\lfloor \frac{k}{\ell_i} \right\rfloor \text{ denotes the integer part of } \frac{k}{\ell_i}, \mathbf{N}_{\ell_i}(j) = \{j, \ell_i + j, 2\ell_i + j, \dots\},$$

$\mathbf{N}_1(j) = \mathbf{N}(j)$ and c_j is a constant for all $k \in \mathbf{N}_{\ell_i}(j)$. For $m \in \mathbf{N}(1)$, we denote

$$\Delta_{[\ell_1, \ell_n]}^{-1} u(k) = \Delta_{\ell_1}^{-1} (\Delta_{\ell_2}^{-1} (\dots (\Delta_{\ell_n}^{-1} u(k)))) \quad \Delta_{[\ell_{1_{m_1}}, \ell_{m_{i+1}}]}^{-1} u(k) = \Delta_{\ell_1 + m_i}^{-1} (\Delta_{\ell_2 + m_i}^{-1} (\dots (\Delta_{\ell_{m_{i+1}}}^{-1} u(k)))).$$

Definition 2.1.1 [4] Let $u(k)$ be a real valued function on $[0, \infty)$. Then the generalised difference operator denoted by Δ_{ℓ} is defined as

$$\Delta_{\ell} u(k) = u(k + \ell) - u(k). \quad (2)$$

Definition 2.2. [10] Let $L = \{\ell_1, \ell_2, \dots, \ell_n\}$ be a non empty set of real numbers. The generalized difference operator of the n^{th} -kind, denoted as Δ_L for the function $u(k)$, $k \in [0, \infty)$ is defined as

$$\Delta_L u(k) = \sum_{r=0}^n (-1)^{n-r} \left\{ \sum_{A \in \wp = \cup r(L)} u \left(k + \sum_{\ell \in A} \ell \right) \right\}. \quad (3)$$

Note that $\Delta_L = \Delta_{\ell_1} \Delta_{\ell_2} \dots \Delta_{\ell_n}$.

Definition 2.3. [10] The inverse of the generalized difference operator of the n^{th} kind denoted by Δ_L^{-1} is defined as if $\Delta_L v(k) = u(k)$, then

$$v(k) = \Delta_L^{-1} u(k) + c_{(n-1)j} \frac{k_{\ell_{n-1}}^{(n-1)}}{(n-1)! \ell_{n-1}^{n-1}} + c_{(n-2)j} \frac{k_{\ell_{n-2}}^{(n-2)}}{(n-2)! \ell_{n-2}^{n-2}} + \dots + c_{2j} \frac{k_{\ell_2}^{(2)}}{(2)! \ell_2^2} + c_{1j} \frac{k}{\ell_1} + c_{0j}, \quad (4)$$

where c_{ij} , for $i = 0, 1, 2, \dots, (n-1)$ are constants. In general $\Delta_L^{-m} = \Delta_L^{-1} (\Delta_L^{-(m-1)})$.

Lemma 2.4.4 [4] Let s_q^n and S_q^n are the Stirling numbers of the first and second kinds respectively and $k_{\ell}^{(n)} = k(k-\ell)(k-2\ell) \dots (k-(n-1)\ell)$, $s_0^0 = S_0^0 = 1$ and $s_q^0 = S_q^0 = 0 = s_0^q = S_0^q$ if $q \neq 0$. Then,

$$k_{\ell}^{(n)} = \sum_{q=0}^n s_q^n \ell^{n-q} k^q, \quad k^n = \sum_{q=0}^n S_q^n \ell^{n-q} k_{\ell}^{(q)} \text{ and } \Delta_{\ell}^{-1} k_{\ell}^{(n)} = \frac{k_{\ell}^{(n+1)}}{(n+1)\ell} \quad (5)$$

Theorem 2.5.5 [4] Let $k \in [\ell, \infty)$, $\ell \in (0, \infty)$. Then,

$$\Delta_{\ell}^{-1} u(k) \Big|_j^k = \sum_{r=1}^{\lfloor \frac{k}{\ell} \rfloor} u(k - r\ell). \quad (6)$$

is a numerical solution of the equation $\Delta_{\ell} v(k) = u(k)$.

Theorem 2.6. 6 For the difference equation $\prod_{i=1}^n \Delta_{\ell_i} v(k) = k^{(0)}$, we have a closed form solution as

$$\Delta_{[\ell_1, \ell_n]}^{-1} k^{(0)} = \sum_{r_3=1}^2 \sum_{q_3=1}^{r_3} s_{r_3}^2 s_{q_3}^{r_3} \ell_2^{2-r_3} \ell_3^{r_3-q_3} \prod_{p=4}^n \sum_{r_p=1}^{1+q_{p-1}} s_{r_p}^{1+q_{p-1}} \sum_{q_p=1}^{r_p} s_{q_p}^{1+q_{p-1}} \ell_p^{1+q_{p-1}-r_p} \ell_p^{r_p-q_p} \quad (7)$$

$$\frac{k_{\ell_n}^{(1+q_n)}}{2\ell_1 \ell_2 \prod_{p=3}^n \ell_p (1+q_p)}, \quad n \geq 3$$

Proof. The proof follows from (2.4) and applying $\Delta_{\ell_1}^{-1}, \Delta_{\ell_2}^{-1}, \dots, \Delta_{\ell_n}^{-1}$ on $k^{(0)}$

3. Main Results and Applications

In this section we derive a numerical-closed form solution of equation (3) by dynamical approach and provide a example to illustrate our main results.

Theorem 3.1. 7 Let $u(k)$ be defined on $[0, \infty)$, $\ell \in (0, \infty)$ and $\ell_{i+1} \geq \ell_i$, $i = 1, 2, \dots$. Then, for $k \in [n\ell_n, \infty)$

$$\text{Let } \Delta_{[\ell_1, \ell_n]}^{-1} u(k) \Big|_{j_{\ell_1, n}^k} = \Delta_{\ell_n}^{-1} (\Delta_{\ell_{n-1}}^{-1} (\dots \Delta_{\ell_1}^{-1} u(k) \Big|_{j_{\ell_1}^k} \Big|_{j_{\ell_2}^k} \Big|_{j_{\ell_n}^k}) \dots \Big|_{j_{\ell_n}^k} \quad (8)$$

then

$$U_n(k) = \Delta_{[\ell_1, \ell_n]}^{-1} u(k) \Big|_{j_{\ell_1, n}^k} = \Delta_{[\ell_1, \ell_n]}^{-1} u(k) + \sum_{t=1}^n (-1)^t \sum_{\{m_1, m_2, \dots, m_t\} \in (J_n)} \Delta_{[\ell_1, \ell_{m_1}]}^{-1} u(j_{\ell_{m_1}}(k)) \prod_{i=1}^t \Delta_{[\ell_{1+m_i}, \ell_{m_{i+1}}]}^{-1} (j_{\ell_{m_{i+1}}}(k))^{(0)} \Delta_{[\ell_{1+m_t}, \ell_n]}^{-1} k^{(0)} \quad (9)$$

where $\Delta_{[\ell_{1+m_t}, \ell_n]}^{-1} k^{(0)}$ is obtained from theorem 2.9 and $\Delta_{[\ell_{1+m_i}, \ell_{m_{i+1}}]}^{-1} (j_{\ell_{m_{i+1}}}(k))^{(0)}$ is obtained from corollary 2.11.

Proof. From (4) and taking limit $j_{\ell_1}(k)$ to k , we find

$$\Delta_{\ell_1}^{-1}u(k)|_{j_{\ell_1}}^k = \Delta_{\ell_1}^{-1}u(k) - \Delta_{\ell_1}^{-1}u(k)|_{j_{\ell_1}}(k) \quad (10)$$

Again using (4) and taking limit $j_{\ell_2}(k)$ to k , we get

$$\begin{aligned} \Delta_{\ell_1\ell_2}^{-1}u(k)|_{j_{\ell_1}}^k|_{j_{\ell_2}}^k &= \Delta_{\ell_1\ell_2}^{-1}u(k) - \Delta_{\ell_1}^{-1}u(k)|_{j_{\ell_1}}(k) \Delta_{\ell_2}^{-1}k_{\ell_2}^{(0)} - \Delta_{\ell_1\ell_2}^{-1}u(k)|_{j_{\ell_2}}(k) \\ &+ \Delta_{\ell_1}^{-1}u(k)|_{j_{\ell_1}}(k) \Delta_{\ell_2}^{-1}k_{\ell_2}^{(0)}|_{j_{\ell_2}}(k) \end{aligned}$$

Applying equation (4) for $(n-1)$ times, we obtain the result.

Theorem 3.2. 8 Let $u(k)$ be real valued functions and $k \in [n\ell_n, \infty)$. Then,

$$\Delta_L^{-1}u(k)|_{j_{\ell_1}}^k|_{j_n}^k = \sum_{r_n=1}^{r_n^*} \sum_{r_{n-1}=1}^{r_{n-1}^*} \cdots \sum_{r_1=1}^{r_1^*} u(k - r_n\ell_n - r_{n-1}\ell_{n-1} - \cdots - r_2\ell_2 - r_1\ell_1) \quad (11)$$

where

$$r_n^* = \left\lfloor \frac{k}{\ell_n} \right\rfloor, r_{n-1}^* = \left\lfloor \frac{k - r_n\ell_n}{\ell_{n-1}} \right\rfloor, \dots, r_1^* = \left\lfloor \frac{k - r_n\ell_n - \cdots - r_2\ell_2}{\ell_1} \right\rfloor. \quad (12)$$

Proof. From (6), we find

$$\Delta_{\ell_1}^{-1}u(k)|_{j_{\ell_1}}^k = \sum_{r_1=1}^{\left\lfloor \frac{k}{\ell_1} \right\rfloor} u(k - r_1\ell_1). \quad (13)$$

Taking $\Delta_{\ell_2}^{-1}$ on both sides of (13) and again applying (6), we obtain

$$\Delta_{\ell_2}^{-1}(\Delta_{\ell_1}^{-1}u(k)|_{j_{\ell_1}}^k)|_{j_{\ell_2}}^k = \sum_{r_2=1}^{\left\lfloor \frac{k}{\ell_2} \right\rfloor} \sum_{r_1=1}^{\left\lfloor \frac{k - r_2\ell_2}{\ell_1} \right\rfloor} u(k - r_2\ell_2 - r_1\ell_1).$$

Continuing this process $(n-1)$ times and applying (6) we get the desired result.

Theorem 3.3. 9 Let $u(k)$ be real valued functions and $k \in [n\ell_n, \infty)$. Then,

$$\Delta_{[\ell_1, \ell_n]}^{-1} u(k) \Big|_{j_{1,n}(k)}^k = \Delta_{[\ell_1, \ell_n]}^{-1} u(k) + \sum_{t=1}^n (-1)^t \sum_{\{m_1, m_2, \dots, m_t\} \in t(J_n)} \Delta_{[\ell_1, \ell_{m_1}]}^{-1} u(j_{\ell_{m_1}}(k))$$

$$\prod_{i=1}^t \Delta_{[\ell_{1+m_i}, \ell_{m_{i+1}}]}^{-1} (j_{\ell_{m_{i+1}}}(k))^{(0)} \Delta_{[\ell_{1+m_t}, \ell_n]}^{-1} k^{(0)} \quad (14)$$

$$-(u_{1.2.3 \dots n} + u_{2.3 \dots n} + \dots + u_{n-1.n}).$$

where r_p^* , $p = 1, 2, \dots, n$ is defined in (11).

Proof. The proof follows by equating (9) and (11).

Theorem 3.4. 10 Let $k \in [n\ell, \infty)$, $\ell_i \geq \ell_{i-1}$ and $a \neq 1$. If

$$F_{\ell_n}^{(m)}(k) = \Delta_{\ell_n}^{-1} \Delta_{\ell_{n-1}}^{-1} \dots \Delta_{\ell_1}^{-1} (k_{\ell_1}^{(m)} a^k), \quad (15)$$

then

$$\sum_{r_n=1}^{r_n^*} \sum_{r_{n-1}=1}^{r_{n-1}^*} \dots \sum_{r_1=1}^{r_1^*} (k - r_n \ell_n - r_{n-1} \ell_{n-1} - \dots - r_2 \ell_2 - r_1 \ell_1)_{\ell_1}^{(m)} a^{k - r_n \ell_n - r_{n-1} \ell_{n-1} - \dots - r_2 \ell_2 - r_1 \ell_1}$$

$$= F_{\ell_n}^{(m)}(k) - F_{\ell_n}^{(m)}(j_{\ell_n}(k)) - \{F_{1.2 \dots n} + F_{2.3 \dots n} + \dots + F_{(n-1).n}\} \quad (16)$$

where r_p^* , $p = 1, 2, \dots, n$ is defined in (12),

$$F_{i.(i-1) \dots (n-1).n} = \sum_{r_n=1}^{r_n^*} \sum_{r_{n-1}=1}^{r_{n-1}^*} \dots \sum_{r_{i+1}=1}^{r_{i+1}^*} F_{\ell_i}^{(m)}(j_{i r_{i+1} r_{i+2} \dots r_n}(k)) \text{ and}$$

$$j_{i r_{i+1} r_{i+2} \dots r_n}(k) = (k - r_n \ell_n - \dots - r_{i+1} \ell_{i+1}) - \left[\frac{k - r_n \ell_n - \dots - r_{i+1} \ell_{i+1}}{\ell_i} \right] \ell_i,$$

for $i = 1.2 \dots (n-1)$.

Proof. From (6), we find

$$\Delta_{\ell_1}^{-1} k_{\ell_1}^{(m)} a^k \Big|_{j_{\ell_1}(k)}^k = \sum_{r_1=1}^{\left\lceil \frac{k}{\ell_1} \right\rceil} (k - r_1 \ell_1)_{\ell_1}^{(m)} a^{k - r_1 \ell_1} = F_{\ell_1}^{(m)}(k) - F_{\ell_1}^{(m)}(j_{\ell_1}(k)) \quad (17)$$

where $F_{\ell_1}^{(m)}(k) = \Delta_{\ell_1}^{-1} k_{\ell_1}^{(m)} a^k = \sum_{r=0}^m \frac{(-\ell_1)^r m C_r r! k_{\ell_1}^{(m-r)} a^{k+r\ell_1}}{(a^{\ell_1} - 1)^{r+1}}$.

Applying $\Delta_{\ell_2}^{-1}$ on both sides of (17) and using striling number of first and second kind, we get

$$\begin{aligned} \Delta_{\ell_2}^{-1} \Delta_{\ell_1}^{-1} k_{\ell_1}^{(m)} a^k \Big|_{j_{\ell_1}(k)}^k \Big|_{j_{\ell_2}(k)}^k &= \left[\begin{matrix} k \\ \ell_2 \end{matrix} \right] \left[\begin{matrix} k - r_2 \ell_2 \\ \ell_1 \end{matrix} \right] (k - r_2 \ell_2 - r_1 \ell_1)_{\ell_1}^{(m)} a^{k - r_2 \ell_2 - r_1 \ell_1} \\ &= F_{\ell_2}^{(m)}(k) - F_{\ell_2}^{(m)}(j_{\ell_2}(k)) - F_{1,2} \end{aligned} \quad (18)$$

where $F_{\ell_2}^{(m)}(k) = \Delta_{\ell_2}^{-1} \left(\Delta_{\ell_1}^{-1} F_{\ell_1}^{(m)} a^k \right)$, $F_{1,2} = \sum_{r_2=1}^{\left[\frac{k}{\ell_2} \right]} F_{\ell_1}^{(m)}(j_{\ell_1 r_2}(k))$ with

$$j_{\ell_1 r_2}(k) = (k - r_2 \ell_2) - \left[\frac{k - r_2 \ell_2}{\ell_1} \right] \ell_1.$$

Again applying $\Delta_{\ell_3}^{-1}$ on both sides of (18) and using the striling numbers of the first and second kind, we obtain

$$\begin{aligned} \Delta_{\ell_3}^{-1} \Delta_{\ell_2}^{-1} \Delta_{\ell_1}^{-1} k_{\ell_1}^{(m)} a^k \Big|_{j_{\ell_1}(k)}^k \Big|_{j_{\ell_2}(k)}^k \Big|_{j_{\ell_3}(k)}^k &= \left[\begin{matrix} k \\ \ell_3 \end{matrix} \right] \left[\begin{matrix} k - r_3 \ell_3 \\ \ell_2 \end{matrix} \right] \left[\begin{matrix} k - r_3 \ell_3 - r_2 \ell_2 \\ \ell_1 \end{matrix} \right] (k - r_3 \ell_3 - r_2 \ell_2 - r_1 \ell_1)_{\ell_1}^{(m)} \\ a^{k - r_3 \ell_3 - r_2 \ell_2 - r_1 \ell_1} &= F_{\ell_3}^{(m)}(k) - F_{\ell_3}^{(m)}(j_{\ell_3}(k)) - [F_{1,2,3} + F_{2,3}] \end{aligned} \quad (19)$$

where $F_{\ell_3}^{(m)}(k) = \Delta_{\ell_3}^{-1} \Delta_{\ell_2}^{-1} \left(\Delta_{\ell_1}^{-1} k_{\ell_1}^{(m)} a^k \right)$, $F_{1,2,3} = \sum_{r_3=1}^{\left[\frac{k}{\ell_3} \right]} \left[\begin{matrix} k - r_3 \ell_3 \\ \ell_2 \end{matrix} \right] F_{\ell_1}^{(m)}(j_{\ell_1 r_3}(k))$,

$$j_{\ell_1 r_2 r_3}(k) = (k - r_3 \ell_3 - r_2 \ell_2) - \left[\frac{k - r_3 \ell_3 - r_2 \ell_2}{\ell_1} \right] \ell_1, \quad F_{2,3} = \sum_{r_2=1}^{\left[\frac{k}{\ell_2} \right]} F_{\ell_2}^{(m)}(j_{\ell_2 r_3}(k)) \text{ and}$$

$$j_{\ell_2 r_3}(k) = (k - r_3 \ell_3) - \left\lfloor \frac{k - r_3 \ell_3}{\ell_2} \right\rfloor \ell_2.$$

The proof follows by continuing this process $(n-1)$ times and from the equations (17), (18) and (19).

Corollary 3.5. 11 *If $\ell_2 \geq \ell_1$ and $k \in [2\ell_2, \infty)$, then,*

$$\sum_{r_2=1}^{\left\lfloor \frac{k}{\ell_2} \right\rfloor} \sum_{r_1=1}^{\left\lfloor \frac{k - r_2 \ell_2}{\ell_1} \right\rfloor} (k - r_2 \ell_2 - r_1 \ell_1)_{\ell_1}^{(m)} a^{k - r_2 \ell_2 - r_1 \ell_1} = F_{\ell_2}^{(m)}(k) - F_{\ell_2}^{(m)}(j_{\ell_2}(k)) - F_{1,2}, \quad (20)$$

$$\text{where } F_{1,2} = \sum_{r_2=1}^{\left\lfloor \frac{k}{\ell_2} \right\rfloor} F_{\ell_1}^{(m)}(j_{\ell_1 r_2}(k)) \text{ with } j_{\ell_1 r_2}(k) = (k - r_2 \ell_2) - \left\lfloor \frac{k - r_2 \ell_2}{\ell_1} \right\rfloor \ell_1.$$

Proof. The proof follows by substituting $n = 2$ in (16).

Example 3.6. 12 *When $m = 3$, we obtain*

$$\sum_{r_2=1}^{\left\lfloor \frac{k}{\ell_2} \right\rfloor} \sum_{r_1=1}^{\left\lfloor \frac{k - r_2 \ell_2}{\ell_1} \right\rfloor} (k - r_2 \ell_2 - r_1 \ell_1)_{\ell_1}^{(3)} a^{k - r_2 \ell_2 - r_1 \ell_1} = F_{\ell_2}^{(3)}(k) - F_{\ell_2}^{(3)}(j_{\ell_2}(k)) - F_{1,2}, \quad (21)$$

$$\begin{aligned} \text{where } F_{\ell_2}^{(3)}(k) &= \frac{k_{\ell_2}^{(3)} a^k}{\prod_{i=1}^2 (a^{\ell_i} - 1)} - \sum_{i=1}^2 \left\{ \frac{3 \ell_i k_{\ell_2}^{(2)} a^{k+\ell_i}}{(a^{\ell_i} - 1)^2 \prod_{\substack{j=1 \\ j \neq i}}^2 (a^{\ell_j} - 1)} - \frac{3! \ell_i^2 k_{\ell_2}^{(1)} a^{k+2\ell_i}}{(a^{\ell_i} - 1)^3 \prod_{\substack{j=1 \\ j \neq i}}^2 (a^{\ell_j} - 1)} \right. \\ &+ \left. \frac{3! \ell_i^3 a^{k+3\ell_i}}{(a^{\ell_i} - 1)^4 \prod_{\substack{j=1 \\ j \neq i}}^2 (a^{\ell_j} - 1)} \right\} + \sum_{i < j}^2 \left\{ \frac{3! \ell_i \ell_j k_{\ell_j}^{(1)} a^{k+\ell_i+\ell_j}}{\prod_{j=1}^2 (a^{\ell_j} - 1)^2} - \frac{3! \ell_i^2 \ell_j a^{k+2\ell_i+\ell_j}}{(a^{\ell_i} - 1)^3 \prod_{\substack{j=1 \\ j \neq i}}^2 (a^{\ell_j} - 1)^2} \right. \end{aligned}$$

$$\frac{3! \ell_i \ell_j^2 a^{k+\ell_i+2\ell_j}}{(a^{\ell_i}-1)^2 \prod_{\substack{j=1 \\ j \neq i}}^2 (a^{\ell_j}-1)^3} \} + \frac{(3\ell_2-3\ell_1)}{(a^{\ell_1}-1)} \Delta_{\ell_2}^{-1}(k_{\ell_2}^{(2)} a^k)$$

$$+ \left[\frac{\ell_2^2-3\ell_1\ell_2+2\ell_1^2}{(a^{\ell_1}-1)} - \frac{(3\ell_2-3\ell_1)\ell_1 a^{\ell_1}}{(a^{\ell_1}-1)^2} \right]$$

$$\Delta_{\ell_2}^{-1} k_{\ell_1}^{(1)} a^k - \Delta_{\ell_1}^{-1} k_{\ell_1}^{(3)} a^k \Big|_{j_1} \frac{k_{\ell_2}^{(1)}}{\ell_2}$$

When $k = 24$, $a = 2$, $\ell_1 = 5$, $\ell_2 = 6$, $j_{\ell_1}(k) = 4$ and $j_{\ell_2}(k) = 0$, we get

$$F_6^{(3)}(24) = 2538879.194, \quad F_6^{(3)}(0) = -2.031085702,$$

$$F_{1,2} = \sum_{r_2=1}^4 F_5^{(3)}(j_{\ell_1 r_2}(k)) = F_5^{(3)}(3) + F_5^{(3)}(2) + F_5^{(3)}(1) + F_5^{(3)}(0) = 41.2325697 \text{ and hence}$$

$$\left[\frac{24}{6} \right] \left[\frac{24-6r_2}{5} \right] \sum_{r_2=1}^4 \sum_{r_1=1}^5 (24-6r_2-5r_1)^{(3)} 2^{(21-6r_2-5r_1)} = 2538840.$$

Corollary 3.7.13 Let $k \in [3\ell_3, \infty)$, $\ell_3 \geq \ell_2 \geq \ell_1$, then,

$$\left[\frac{k}{\ell_3} \right] \left[\frac{k-r_3\ell_3}{\ell_2} \right] \left[\frac{k-r_3\ell_3-r_2\ell_2}{\ell_1} \right] (k-r_3\ell_3-r_2\ell_2-r_1\ell_1)_{\ell_1}^{(m)} a^{k-r_3\ell_3-r_2\ell_2-r_1\ell_1}$$

$$= F_{\ell_3}^{(m)}(k) - F_{\ell_3}^{(m)}(j_{\ell_3}(k)) - \{F_{1,2,3} + F_{2,3}\} \quad (22)$$

$$\text{where } F_{1,2,3} = \sum_{r_3=1}^{\left[\frac{k}{\ell_3} \right]} \sum_{r_2=1}^{\left[\frac{k-r_3\ell_3}{\ell_2} \right]} F_{\ell_1}^{(m)}(j_{\ell_1 r_2 r_3}(k)), \quad j_{\ell_1 r_2 r_3}(k) = (k-r_3\ell_3-r_2\ell_2) - \left[\frac{k-r_3\ell_3-r_2\ell_2}{\ell_1} \right] \ell_1,$$

$$F_{2,3} = \sum_{r_3=1}^{\left[\frac{k}{\ell_3} \right]} F_{\ell_2}^{(m)}(j_{\ell_2 r_3}(k)) \text{ and } j_{\ell_2 r_3}(k) = (k-r_3\ell_3) - \left[\frac{k-r_3\ell_3}{\ell_2} \right] \ell_2$$

Proof. The proof follows by substituting $n = 3$ in (16).

Example 3.8. 14 Put $m = 2$ in (22), we find

$$\left[\begin{array}{c} k \\ \ell_3 \end{array} \right] \left[\begin{array}{c} k - r_3 \ell_3 \\ \ell_2 \end{array} \right] \left[\begin{array}{c} k - r_3 \ell_3 - r_2 \ell_2 \\ \ell_1 \end{array} \right] (k - r_3 \ell_3 - r_2 \ell_2 - r_1 \ell_1)_{\ell_1}^{(2)} a^{k - r_2 \ell_2 - r_2 \ell_2 - r_1 \ell_1}$$

$$= F_{\ell_3}^{(2)}(k) - F_{\ell_3}^{(2)}(j_{\ell_3}(k)) - \{F_{1,2,3} + F_{2,3}\} \quad (23)$$

where $F_{\ell_3}^{(2)}(k) = \frac{k_{\ell_3}^{(2)} a^k}{\prod_{i=1}^3 (a^{\ell_i} - 1)} - \sum_{i=1}^3 \left\{ \frac{2\ell_i k_{\ell_3}^{(1)} a^{k+\ell_i}}{(a^{\ell_i} - 1)^2 \prod_{\substack{j=1 \\ j \neq i}}^3 (a^{\ell_j} - 1)} - \frac{2\ell_i^2 a^{k+2\ell_i}}{(a^{\ell_i} - 1)^3 \prod_{\substack{j=1 \\ j \neq i}}^3 (a^{\ell_j} - 1)} \right\}$

$$+ \sum_{i < j}^3 \frac{2\ell_i \ell_j a^{k+\ell_i+\ell_j}}{(a^{\ell_i} - 1)^2 (a^{\ell_j} - 1)^2 \prod_{\substack{s=1 \\ s \neq i, j}}^3 (a^{\ell_s} - 1)} + \sum_{i=1}^2 \frac{(\ell_{i+1} - \ell_i)}{\prod_{j=1}^2 (a^{\ell_j} - 1)} \Delta_{\ell_3}^{-1} k_{\ell_3}^{(1)} a^k$$

$$- \frac{(\ell_2 - \ell_1) \ell_2 a^{k+\ell_2}}{(a^{\ell_2} - 1) \prod_{j=1}^3 (a^{\ell_j} - 1)} - \Delta_{\ell_1}^{-1} \left(k_{\ell_1}^{(2)} a^k \right) |_{j_1} \frac{k_{\ell_3}^{(2)}}{2\ell_3} - \Delta_{\ell_1, \ell_2}^{-1} k_{\ell_1}^{(2)} a^k |_{j_1} |_{j_2} \frac{k_{\ell_3}^{(1)}}{\ell_3}.$$

When $k = 21$, $\ell_1 = 2$, $\ell_2 = 4$, $\ell_3 = 6$, $j_{\ell_1}(k) = 1$, $j_{\ell_2}(k) = 1$, $j_{\ell_3}(k) = 3$, we get,

$$F_6^{(2)}(21) = 37760.51493, \quad F_6^{(2)}(3) = 0.8829695017,$$

$$F_{1,2,3} = \sum_{r_3=1}^{\left\lfloor \frac{21}{6} \right\rfloor} \sum_{r_2=1}^{\left\lfloor \frac{21-6r_3}{4} \right\rfloor} F_2^{(2)}(j_{\ell_1 r_2 r_3}(k)) = 5F_2^{(2)}(1) = 0,$$

$$F_{2,3} = \sum_{r_2=1}^{\left\lfloor \frac{21}{4} \right\rfloor} F_4^{(2)}(j_{\ell_1 r_2}(k)) = 2F_4^{(2)}(3) + F_4^{(2)}(1) = -0.3679999873$$

$$\sum_{r_3=1}^{\left\lfloor \frac{21}{6} \right\rfloor} \sum_{r_2=1}^{\left\lfloor \frac{21-6r_3}{4} \right\rfloor} \sum_{r_1=1}^{\left\lfloor \frac{21-6r_3-4r_2}{2} \right\rfloor} (21-6r_3-4r_2-2r_1)_2^{(2)} 2^{21-6r_3-4r_2-2r_1} = 37760.$$

Remark 3.9. 15 Replacing $k_{\ell_n}^{(m)} a^k$ by $k_{\ell_n}^{(m)} a^{-k}$ in (16), we obtain the new type of series namely

$$\begin{aligned} & \sum_{r_n=1}^{r_n^*} \sum_{r_{n-1}=1}^{r_{n-1}^*} \cdots \sum_{r_1=1}^{r_1^*} (k - r_n \ell_n - r_{n-1} \ell_{n-1} - \cdots - r_2 \ell_2 - r_1 \ell_1)_{\ell_1}^{(m)} a^{-(k - r_n \ell_n - r_{n-1} \ell_{n-1} - \cdots - r_2 \ell_2 - r_1 \ell_1)} \\ & = F_{\ell_n}^{(m)}(k) - F_{\ell_n}^{(m)}(j_{\ell_n}(k)) - \{F_{1,2 \cdots n} + F_{2,3 \cdots n} + \cdots + F_{(n-1),n}\} \end{aligned} \quad (24)$$

when $m = 3$, $n = 2$, $k = 13$, $\ell_1 = 4$, $\ell_2 = 6$, $a = 2$, $j_{\ell_1}(k) = 1$ and $j_{\ell_2}(k) = 1$, we obtain

$$F_6^{(3)}(13) = 22.2141097, F_6^{(3)}(1) = 11.9967097 \text{ and } F_{1,2} = 8.3424.$$

Hence

$$\sum_{r_2=1}^{\left\lfloor \frac{13}{6} \right\rfloor} \sum_{r_1=1}^{\left\lfloor \frac{13-6r_2}{4} \right\rfloor} (13-6r_2-4r_1)_4^{(3)} \times 2^{-(13-6r_2-4r_1)} = F_6^{(3)}(13) + F_6^{(3)}(1) - F_{1,2} = \frac{15}{8}.$$

Theorem 3.10. 16 For the positive integer m and n

$$\begin{aligned} & \sum_{r_n=1}^{r_n^*} \sum_{r_{n-1}=1}^{r_{n-1}^*} \cdots \sum_{r_1=1}^{r_1^*} (k - r_n \ell_n - r_{n-1} \ell_{n-1} - \cdots - r_2 \ell_2 - r_1 \ell_1)^m a^{k - r_n \ell_n - r_{n-1} \ell_{n-1} - \cdots - r_2 \ell_2 - r_1 \ell_1} \\ & = F_{\ell_n}^m(k) - F_{\ell_n}^m(j_{\ell_n}(k)) - \{F_{1,2 \cdots n} + F_{2,3 \cdots n} + \cdots + F_{(n-1),n}\} \end{aligned} \quad (25)$$

where $r_n^* = \left[\frac{k}{\ell_n} \right]$, $r_{n-1}^* = \left[\frac{k - r_n \ell_n}{\ell_{n-1}} \right]$, \dots , $r_1^* = \left[\frac{k - r_n \ell_n \cdots r_2 \ell_2}{\ell_1} \right]$

$$F_{i,(i-1)\cdots(n-1),n} = \sum_{r_n=1}^{r_n^*} \sum_{r_{n-1}=1}^{r_{n-1}^*} \cdots \sum_{r_{i+1}=1}^{r_{i+1}^*} F_{\ell_i}^m(j_{\ell_i}^{i r_{i+1} r_{i+2} \cdots r_n}(k)) \text{ and}$$

$$j_{\ell_i}^{i r_{i+1} r_{i+2} \cdots r_n}(k) = (k - r_n \ell_n - \cdots - r_{i+1} \ell_{i+1}) - \left[\frac{k - r_n \ell_n - \cdots - r_{i+1} \ell_{i+1}}{\ell_i} \right] \ell_i \text{ for}$$

$i = 1, 2, \dots, (n-1)$ and $F_{\ell_n}^m(k) = \sum_{r=1}^m s_r^m \ell_n^{m-r} F_{\ell_n}^{(r)}(k)$, $F_{\ell_n}^{(r)}(k)$ is obtained from (15).

Proof. The proof follows from (2.4) and Theorem 3.4.

Corollary 3.11. 17 If $\ell_2 \geq \ell_1$ and $k \in [2\ell_2, \infty)$, then,

$$\sum_{r_2=1}^{\left[\frac{k}{\ell_2} \right]} \sum_{r_1=1}^{\left[\frac{k - r_2 \ell_2}{\ell_1} \right]} (k - r_2 \ell_2 - r_1 \ell_1)^m a^{k - r_2 \ell_2 - r_1 \ell_1} = F_{\ell_2}^m(k) - F_{\ell_2}^m(j_{\ell_2}(k)) - F_{1,2}, \quad (26)$$

$$\text{where } F_{1,2} = \sum_{r_2=1}^{\left[\frac{k}{\ell_2} \right]} F_{\ell_1}^m(j_{\ell_1 r_2}(k)) \text{ with } j_{\ell_1 r_2}(k) = (k - r_2 \ell_2) - \left[\frac{k - r_2 \ell_2}{\ell_1} \right] \ell_1$$

Example 3.12. 18 when $m = 3$, we obtain

$$\sum_{r_2=1}^{\left[\frac{k}{\ell_2} \right]} \sum_{r_1=1}^{\left[\frac{k - r_2 \ell_2}{\ell_1} \right]} (k - r_2 \ell_2 - r_1 \ell_1)^3 a^{k - r_2 \ell_2 - r_1 \ell_1} = F_{\ell_2}^3(k) - F_{\ell_2}^3(j_{\ell_2}(k)) - F_{1,2}, \quad (27)$$

$$\text{where } F_{\ell_2}^3(k) = \sum_{i=1}^3 \frac{S_i^3 \ell_1^{3-i} k_{\ell_2}^{(i)} a^k}{\prod_{j=1}^i (a^{\ell_j} - 1)} - \sum_{i=1}^2 \left\{ \frac{S_1^3 \ell_1^2 \ell_i a^{k+\ell_i}}{(a^{\ell_i} - 1)^2 \prod_{\substack{j=1 \\ j \neq i}}^2 (a^{\ell_j} - 1)} + \frac{S_2^3 \ell_1 2 \ell_i k_{\ell_2}^{(1)} a^{k+\ell_i}}{(a^{\ell_i} - 1)^2 \prod_{\substack{j=1 \\ j \neq i}}^2 (a^{\ell_j} - 1)} \right\}$$

$$\begin{aligned}
& + \frac{S_3^3 3! k_{\ell_2}^{(2)} a^{k+\ell_i}}{(a^{\ell_i} - 1)^2 \prod_{\substack{j=1 \\ j \neq i}}^2 (a^{\ell_j} - 1)} - \frac{S_2^3 \ell_1 2 \ell_2^2 a^{k+2\ell_i}}{(a^{\ell_i} - 1)^3 \prod_{\substack{j=1 \\ j \neq i}}^2 (a^{\ell_j} - 1)} - \frac{S_3^3 3! \ell_i^2 k_{\ell_2}^{(1)} a^{k+2\ell_i}}{(a^{\ell_i} - 1)^3 \prod_{\substack{j=1 \\ j \neq i}}^2 (a^{\ell_j} - 1)} + \\
& \frac{S_3^3 3! \ell_i^3 a^{k+3\ell_i}}{(a^{\ell_i} - 1)^4 \prod_{\substack{j=1 \\ j \neq i}}^2 (a^{\ell_j} - 1)} \left. + \sum_{i=0}^1 \frac{S_2^3 \ell_1^{1-i} 2 \ell_1 \ell_2 k_{\ell_2}^{(i)} a^{k+\ell_1+\ell_2}}{\prod_{j=1}^2 (a^{\ell_j} - 1)^2} - \left\{ S_2^3 \ell_1 \left(\frac{2 \ell_2^2 a^{k+\ell_1+2\ell_2}}{(a^{\ell_1} - 1)^2 (a^{\ell_2} - 1)^3} \right. \right. \right. \\
& \left. \left. \left. + \frac{2 \ell_1 \ell_2 a^{k+2\ell_1+\ell_2}}{(a^{\ell_1} - 1)^3 (a^{\ell_2} - 1)^2} \right) \right\} + \frac{S_2^3 \ell_1 (\ell_2 - \ell_1) a^{\ell_1}}{(a^{\ell_1} - 1)^2} \Delta_{\ell_2}^{-1}(k_{\ell_2}^{(1)} a^k) + \frac{S_3^3 3 (\ell_2 - \ell_1)}{(a^{\ell_1} - 1)} \Delta_{\ell_2}^{-1}(k_{\ell_1}^{(2)} a^k) \\
& + S_3^3 \left[\frac{\ell_2^2 - 3 \ell_1 \ell_2 + 2 \ell_1^2}{(a^{\ell_1} - 1)} - \frac{3 \ell_1 (\ell_2 - \ell_1) a^{\ell_1}}{(a^{\ell_1} - 1)^2} \right] \Delta_{\ell_2}^{-1}(k_{\ell_1}^{(1)} a^k) - \sum_{i=1}^3 S_i^3 \ell_1^{3-i} \Delta_{\ell_1}^{-1}(k_{\ell_1}^{(i)} a^k) \Big|_{j_1} \frac{k_{\ell_2}^{(1)}}{\ell_2}.
\end{aligned}$$

When $k = 9$, $\ell_1 = 2$, $\ell_2 = 3$, $a = 2$, $j_{\ell_1}(k) = 1$ and $j_{\ell_2}(k) = 0$, we obtain

$$\begin{aligned}
F_3^3(9) &= 1043.688983, \quad F_3^3(0) = -14.16286424, \quad F_{1,2} = \sum_{r_2=1}^3 F_2^3(j_{\ell_1 r_2}(k)) = 2F_2^3(0) + F_2^3(1) = \\
& -0.1481481481 \text{ and hence } \sum_{r_2=1}^{\left\lfloor \frac{9}{3} \right\rfloor} \sum_{r_1=1}^{\left\lfloor \frac{9-3r_2}{2} \right\rfloor} (9-3r_2-2r_1)^3 2^{9-3r_2-2r_1} = 1058.
\end{aligned}$$

Corollary 3.13. 19 Let $k \in [3\ell_3, \infty)$, $\ell_3 \geq \ell_2 \geq \ell_1$ then,

$$\begin{aligned}
& \left[\frac{k}{\ell_3} \right] \left[\frac{k-r_3 \ell_3}{\ell_2} \right] \left[\frac{k-r_3 \ell_3 - r_2 \ell_2}{\ell_1} \right] \\
& \sum_{r_3=1}^{\left\lfloor \frac{k}{\ell_3} \right\rfloor} \sum_{r_2=1}^{\left\lfloor \frac{k-r_3 \ell_3}{\ell_2} \right\rfloor} \sum_{r_1=1}^{\left\lfloor \frac{k-r_3 \ell_3 - r_2 \ell_2}{\ell_1} \right\rfloor} (k-r_3 \ell_3 - r_2 \ell_2 - r_1 \ell_1)^m a^{k-r_3 \ell_3 - r_2 \ell_2 - r_1 \ell_1} \\
& = F_{\ell_3}^m(k) - F_{\ell_3}^m(j_{\ell_3}(k)) - \{F_{1,2,3} + F_{2,3}\} \tag{28}
\end{aligned}$$

$$\text{where } F_{1,2,3} = \sum_{r_3=1}^{\left\lfloor \frac{k}{\ell_3} \right\rfloor} \sum_{r_2=1}^{\left\lfloor \frac{k-r_3 \ell_3}{\ell_2} \right\rfloor} F_{\ell_1}^m(j_{\ell_1 r_2 r_3}(k)), \quad j_{\ell_1 r_2 r_3}(k) = (k-r_3 \ell_3 - r_2 \ell_2) - \left[\frac{k-r_3 \ell_3 - r_2 \ell_2}{\ell_1} \right] \ell_1,$$

$$F_{2,3} = \sum_{r_3=1}^{\left\lfloor \frac{k}{\ell_3} \right\rfloor} F_{\ell_2}^m(j_{\ell_2 r_3}(k)) \text{ and } j_{\ell_2 r_3}(k) = (k - r_3 \ell_3) - \left\lfloor \frac{k - r_3 \ell_3}{\ell_2} \right\rfloor \ell_2$$

Example 3.14. 20 Putting $m = 2$ in (28) we get,

$$\begin{aligned} & \sum_{r_3=1}^{\left\lfloor \frac{k}{\ell_3} \right\rfloor} \sum_{r_2=1}^{\left\lfloor \frac{k - r_3 \ell_3}{\ell_2} \right\rfloor} \sum_{r_1=1}^{\left\lfloor \frac{k - r_3 \ell_3 - r_2 \ell_2}{\ell_1} \right\rfloor} (k - r_3 \ell_3 - r_2 \ell_2 - r_1 \ell_1)^2 a^{k - r_3 \ell_3 - r_2 \ell_2 - r_1 \ell_1} \\ & = F_{\ell_3}^2(k) - F_{\ell_3}^2(j_{\ell_3}(k)) - \{F_{1,2,3} + F_{2,3}\} \end{aligned} \quad (29)$$

where

$$\begin{aligned} F_{\ell_3}^2(k) &= \sum_{i=1}^2 \frac{S_i^2 \ell_1^{2-i} k_{\ell_3}^{(i)} a^k}{\prod_{j=1}^3 (a^{\ell_j} - 1)} - \sum_{i=1}^3 \left\{ \frac{S_1^2 \ell_1 \ell_i a^{k+\ell_i}}{(a^{\ell_i} - 1)^2 \prod_{\substack{j=1 \\ j \neq i}}^3 (a^{\ell_j} - 1)} + \frac{S_2^2 2 \ell_i k_{\ell_3}^{(1)} a^{k+\ell_i}}{(a^{\ell_i} - 1)^2 \prod_{\substack{j=1 \\ j \neq i}}^3 (a^{\ell_j} - 1)} \right. \\ & \left. - \frac{S_2^2 2 \ell_i a^{k+2\ell_i}}{(a^{\ell_i} - 1)^3 \prod_{\substack{j=1 \\ j \neq i}}^3 (a^{\ell_j} - 1)} \right\} + \sum_{i=2}^3 \frac{S_2^2 (\ell_i - \ell_{i-1}) \Delta_{\ell_3}^{-1} (k_{\ell_3}^{(1)} a^k) +}{\prod_{j=1}^3 (a^{\ell_j} - 1)} \\ & \sum_{\substack{i=1 \\ i < j}}^3 \frac{S_2^2 2 \ell_i \ell_j a^{k+\ell_i+\ell_j}}{(a^{\ell_i} - 1)^2 (a^{\ell_j} - 1)^2 \prod_{\substack{t=1 \\ t \neq i, j}}^3 (a^{\ell_t} - 1)} - \frac{S_2^2 (\ell_2 - \ell_1) \ell_2 a^{k+\ell_2}}{(a^{\ell_1} - 1) (a^{\ell_2} - 1)^2 (a^{\ell_3} - 1)} \\ & \sum_{j=1}^2 S_j^2 \ell_1^{2-j} \Delta_{\ell_1}^{-1} (k_{\ell_1}^{(j)} a^k) \Big|_{j_1} \frac{k_{\ell_3}^{(2)}}{2 \ell_2 \ell_3} = \sum_{j=1}^2 S_j^2 \ell_1^{2-j} \Delta_{\ell_1, \ell_2}^{-1} k_{\ell_1}^{(j)} a^k \Big|_{j_1} \Big|_{j_2} \frac{k_{\ell_3}^{(1)}}{\ell_3} \end{aligned}$$

In Particular when $k = 19$, $\ell_1 = 3$, $\ell_2 = 6$, $\ell_3 = 9$, $a = 2$, $j_{\ell_1}(k) = 1$, $j_{\ell_2}(k) = 1$ and $j_{\ell_3}(k) = 1$, we get

$$F_9^2(19) = 1.950132999, F_9^2(1) = 0.1600094733,$$

$$F_{1.2.3} = \sum_{r_3=1}^{\left\lfloor \frac{19}{9} \right\rfloor} \left\lfloor \frac{19-9r_3}{6} \right\rfloor F_3^2(j_{\ell_{1r_2r_3}}(k)) = F_3^2(1) = 0,$$

$$F_{2.3} = \sum_{r_2=1}^{\left\lfloor \frac{19}{6} \right\rfloor} F_6^2(j_{\ell_{2r_3}}(k)) = F_6^2(4) + F_6^2(1) = -0.2098765432$$

and hence

$$\sum_{r_3=1}^{\left\lfloor \frac{19}{9} \right\rfloor} \left\lfloor \frac{19-9r_3}{6} \right\rfloor \left\lfloor \frac{19-9r_3-6r_2}{3} \right\rfloor (19-9r_3-6r_2-3r_1)^2 2^{(19-9r_3-6r_2-3r_1)} = 2.$$

Remark 3.15. 21 Replacing $k^m a^k$ by $k^m a^{-k}$ in (25), we obtain the new type of series namely

$$\begin{aligned} & \sum_{r_n=1}^{r_n^*} \sum_{r_{n-1}=1}^{r_{n-1}^*} \cdots \sum_{r_1=1}^{r_1^*} (k - r_n \ell_n - r_{n-1} \ell_{n-1} - \cdots - r_2 \ell_2 - r_1 \ell_1)^m a^{-(k - r_n \ell_n - r_{n-1} \ell_{n-1} - \cdots - r_2 \ell_2 - r_1 \ell_1)} \\ & = F_{\ell_n}^m(k) - F_{\ell_n}^m(j_{\ell_n}(k)) - \{F_{1.2 \cdots n} + F_{2.3 \cdots n} + \cdots + F_{(n-1).n}\} \end{aligned} \quad (30)$$

When $n = 3$, $m = 1$, $k = 17$, $\ell_1 = 2$, $\ell_2 = 4$, $\ell_3 = 6$, $a = 2$, $j_{\ell_1}(k) = 1$, $j_{\ell_2}(k) = 1$ and $j_{\ell_3}(k) = 5$, we obtain

$F_6^1(17) = -0.3538407029$, $F_6^1(5) = -1.765090703$, $F_{1.2.3} = 0$ and $F_{2.3} = -0.12$ and hence

$$\frac{5}{32} + \frac{3}{8} + \frac{1}{2} + \frac{1}{2} = -0.3538407029 + 1.765090703 + 0.12 = \frac{49}{32}.$$

References:

- [1] R.P Agarwal, *Difference Equations and Inequalities*, Marcel Dekker, New York, 2000.
- [2] N.R.O.Bastos, R.A.C.Ferreira, D.F.M.Torres, *Discrete-time fractional variational problems*, Signal Process. 91 (2011), no. 3, 513-524. arXiv:1005.0252.
- [3] G.S.F.Frederico, D.F.M.Torres, *A formulation of Noether's theorem for fractional problems of the calculus of variations*, J. Math. Anal. Appl. 334 (2007), no. 2, 834-846. arXiv:math/0701187.
- [4] M.Maria Susai Manuel, G.Britto Antony Xavier and E.Thandapani, *Theory of Generalized Difference Operator and Its Applications*, Far East Journal of Mathematical Sciences, 20(2) (2006), 163 - 171.
- [5] M.Maria Susai Manuel, G.Britto Antony Xavier and E.Thandapani, *Qualitative Properties of Solutions of Certain Class of Difference Equations*, Far East Journal of Mathematical Sciences, 23(3) (2006), 295-304.
- [6] M.Maria Susai Manuel, G.Britto Antony Xavier and E.Thandapani, *Generalized Bernoulli Polynomials Through Weighted Pochhammer Symbols*, Far East Journal of Applied Mathematics, 26(3) (2007), 321-333.
- [7] M. Maria Susai Manuel, A. George Maria Selvam and G. Britto Antony Xavier, *On the solutions and applications of some class of generalized difference equations*, Far East Journal of Applied Mathematics 28(2)(2007), 223-241.
- [8] M.Maria Susai Manuel and G.Britto Antony Xavier, *Recessive, Dominant and Spiral Behaviours of Solutions of Certain Class of Generalized Difference Equations*, International Journal of Differential Equations and Applications, 10(4) (2007), 423-433.
- [9] M.Maria Susai Manuel, G.Britto Antony Xavier and V.Chandrasekar, *Generalized Difference Operator of the Second Kind and Its Application to Number Theory*, International Journal of Pure and Applied Mathematics, 47(1) (2008), 127-140.
- [10] M.Maria Susai Manuel, G.Britto Antony Xavier and V.Chandrasekar, *Theory and Application of the Generalized Difference Operator of the n^{th} Kind (Part - I)*, Demonstratio Mathematica, 45(1) (2012), 95 - 106.
- [11] M.Maria Susai Manuel, G.Britto Antony Xavier and V.Chandrasekar, *Some Applications of the Generalized Difference Operator of the n^{th} Kind*, Far East Journal of Applied Mathematics, 66(2) (2012), 107 - 126.

- [12] K.S.Miller,B.Ross ,*Fractional difference calculus, in "Univalent functions,fractional calculus, and the applications (Koriyama, 1988)"*, 139-152, Horwood, Chichester, 1989.
- [13] Ronald E.Mickens, *Difference Equations*, Van Nostrand Reinhold Company, New York, 1990.
- [14] Ruta.C.Ferreira and Delfim F.M.Jorres,*Fractional h -Difference equations arising from the Calculus of variations*, Journal of Applicable Analysis and Discrete Mathematics, (2011).

Application of K Means Clustering Algorithm for Password Authentication through Keystroke Biometrics

Nisha Raj Nair

Assistant Professor (Department of Computer Applications), Don Bosco College, Panaji, Goa-403001.

E-mail:Nisha_nair112000@yahoo.com

ABSTRACT

Password Authentication is the most inseparable part of any system developed. But in today's world this type of security is not a fool proof system. Therefore comes the need to add an extra layer of security to the existing password authentication system. The security can be enhanced by validating the user not only by his password but also by the way he is typing it.

The typing rhythm of the users are captured and validated using the k means clustering algorithm. The research focuses on having a study in between the use of the various distance metrics in the k means clustering algorithm for the purpose of keystroke biometrics.

Keywords: *password authentication, k means clustering algorithm, distance metrics.*

1.0 Introduction

Biometrics are automated systems to recognize a person using some physiological or a behavioral characteristics. Throughout history various forms of biometrics have been used to identify a person. Among the features measured have been face, fingerprints, hand geometry, handwriting, iris, retinal, vein, and voice. There are two major forms of biometrics: those based on physiological attributes and those based on behavioral attributes. Physiological biometrics integrates a measurement of some physiological feature such as fingerprints, retinal blood vessel patterns and iris patterns into an automated authentication schema. Behavioral biometrics on the other hand extract and integrate information about human behavior such as variations in our speech pattern, gait, signature and the way we type into the authentication schema[2].

Keystroke dynamics is a method for identifying the individuality of a given sequence of characters entered through a traditional computer keyboard. Researchers focused on the keystroke pattern, in terms of keyboard duration and keyboard latency. Evidence from preliminary studies indicated that when two individuals entered the same login details, their typing patterns would be sufficiently unique as to provide a characteristic signature that could be used to differentiate one from the other [3][4].

1.1 Cluster Analysis

Cluster analysis are important techniques that partition objects that have many attributes into meaningful disjoint groups so that the objects in each group are more similar to each other in the values of their attributes than they are to objects in other groups. The aim of cluster analysis is exploratory, to find if data naturally falls into meaningful groups with small within-group variation and large between group variation. It is possible to define cluster analysis as an optimization problem in which a given function consisting of within cluster similarity and between cluster dissimilarity needs to be optimized [1].

K means is the simplest and most popular clustering method that is easy to implement. The method is called K means since each of the K clusters is represented by the mean of the objects within the cluster. It is also called centroid method since at each step the centroid point of each cluster is assumed to be known and each of the remaining points are located to the cluster whose centroid is closest to it [9].

Most cluster analysis methods are based on measuring similarity between objects by computing the distance between each pair. There are number of methods for computing distance in a multidimensional environment like the Euclidean, Manhattan, Canberra, Chebyshev, Minkowski etc.

1.2 K MEANS CLUSTERING FOR KEY STROKE BIOMETRICS

In this research work the k means clustering algorithm has been used for authenticating the user through his typing rhythms. Each users typing rhythm can be viewed as a cluster of measurements that can be differentiated from the clusters of the other users. Each of these clusters is represented by cluster identities which consist of the centroid and the distance measure for that cluster. During the process of validating the keystroke latencies captures at the time of log in are compared with the centroids of the clusters with their distance measures. If the measurements falls in that cluster the user is valid else not.

1.2.1 Problem Statement Given a set of keystroke latencies L for the username and password in attempts. Identify the k clusters where each cluster C has a set of cluster identity and distance measure

Algorithm for identifying the clusters

Input: L , a set of keystroke latencies for username and password.

Output: K clusters with the optimum cluster criterion function.

Method:

Step 1: Input an initial partition with k clusters

Step 2: Calculate the centroids of their respective clusters and distance from centroid using the particular metric being considered.

Step 3: With every set of keystroke latency, generate a new partition by assigning each latency to a cluster based on an allocation function. A point is allocated to the cluster if it is closer to the centroid of the cluster.

Step 4: Recalculate cluster centroids and distance metrics.

Step 5: Repeat step 3 and 4 for N set of keystroke latencies.

Step 6: Generate a standard cluster criterion consisting of centroids and distance metric separated by suitable delimiter for each key stroke latency.

The above algorithms were applied with the 5 distance metrics i.e Euclidean distance, Squared Euclidean distance, Manhattan or City Block, Canberra distance and Chebyshev distance metric.

Once the clusters are formed, each cluster is represented using cluster identities, which are the centroids for that cluster. Along with it, the distance metrics is also calculated and stored for the cluster.

At the time of validation, the new keystroke latencies are compared with these centroids using the distance measures.

Algorithm for validating user

Input: Keystroke latencies for a string of m username and password captured during log in, K clusters with their cluster identities and distance measures for various metrics.

Output: True if user is valid else false.

Method:

Step 1: Accept m-1 keystroke latency for username of length m.

Step 2: Using the distance metric from the cluster criterion function, identify if the latency is close to the respective centroid.

Step 3: Repeat step 1 and 2 for each keystroke latency.

Step 4: If each key stroke latency falls in the cluster repeat steps 1 to 3 for password of user else return False.

Step 5: If keystroke latencies for both username and password falls in respective clusters then return true else return False.

2.0 Experimental Setup

2.1 Data Collection

The data required to generate pattern for keystroke biometrics was obtained through an enrollment process. The enrollment phase involves the user typing the username and the password a couple of times. An application was created for this purpose. The users were asked to run the application on their computer and the application in the background logged their keystrokes. These keystroke latencies were all preprocessed with appropriate delimiters.

A set of 10 users in different age groups were asked to perform the enrollment process in three phases. These users were from different backgrounds. Some were those who were computer experts, regularly logging into their email accounts and had a very good hand on the computer. Some were clerical personnel, who made bare minimum use of the computer. The other set of users were students who were moderate users of the computer.

In the first phase the users typed the password 10 times to obtain the preprocessed enrollment data. The clusters were formed with their respective centroids and distance metrics. The users were then asked to log in. Also a set of users were asked to imitate the others and the acceptance rate and rejection rates were noted.

During the next 2 phases the users were asked to simply log in wherein if the user is a valid user, his login keystroke latencies were included in the enrollment data. For each phase, when the new keystroke latencies are included in the group which was derived from the enrollment process, the respective data from the top was omitted. The clusters were formed again with their respective centroids and distance metrics. Keystroke Biometrics is based on behavioral attributes like the state of mind of the user, his mood etc. His typing rhythm could change depending on these behavioral factors. The process of recomputing the centroids and distance metrics in three phases was done basically with this problem in mind.

The above process was accomplished over a period of 20 days after which, the final set of clusters with the centroids were created. Some days out of these 20, which were chosen for capturing the keystroke latency, were those days when the users were under high work pressure or in different mood.

2.2 Pattern Recognition

The raw data was obtained from the enrollment phase. The K means algorithm was applied to this data. The number of clusters i.e. k was decided. During the enrollment phase, each time the user types the username and the password, his keystrokes are logged. The k means clustering algorithm recalculates the new centroids and the distance metrics. The centroid is nothing but the mean of all the consecutive keystroke latencies. The distance metrics i.e. Euclidean, Squared Euclidean, Manhattan, Chebyshev, Canberra are evaluated. The centroids and the distance metrics are grouped together to form a pattern representing the respective cluster.

2.3 User Verification

For classifying the users, the authorized users were asked to log in to the application. The users were validated and the False Rejection Rate (FRR) was calculated. Also some imposters were told the username and passwords of the other users and asked to log in. They were validated and the False Acceptance Rate (FAR) was recorded. Other imposters were told the username and password and also shown the way they were typed and were asked to log in. The FAR was recorded again.

2.4 Software/Simulator Tool

The software used for this experiment was created on the Microsoft's .Net platform. A GUI was created for the user to enter the username and password while registration and login. Finally the k means algorithm was used to get the results. The results were later compared using a spreadsheet application.

3.0 Results

Clusters were formed from the enrollment data collected from the user. Each of these clusters, are represented using cluster identities that consists of the centroid for that cluster. A distance metric is also defined for each of the cluster to define the distance within which an object can fall to be a part of the cluster. Two sets of users were asked to login. One set were the authorized users and the others were the imposters who knew the password and tried to imitate the

typing style. The False Rejection Rate (FRR) and the False Acceptance Rate (FAR) for each of the distance metrics were noted.

The following graph shows the FAR and FRR for the various distance metrics. The data was collected from 10 users some days after the enrollment process. Most of the users were in a very relaxed and comfortable mood while trying to log in.

The Euclidean distance shows an FRR of 10% and a FAR of 20% whereas the Squared Euclidean which is not at all desirable shows 100% FAR and 0% FRR.

The Manhattan shows a high FAR of 40% and FRR of 0%. The Canberra which is considered to be quite strict shows a FRR of 80% and FAR of 0%. The Chebyshev metrics shows FRR of 20% and FAR of 20%.

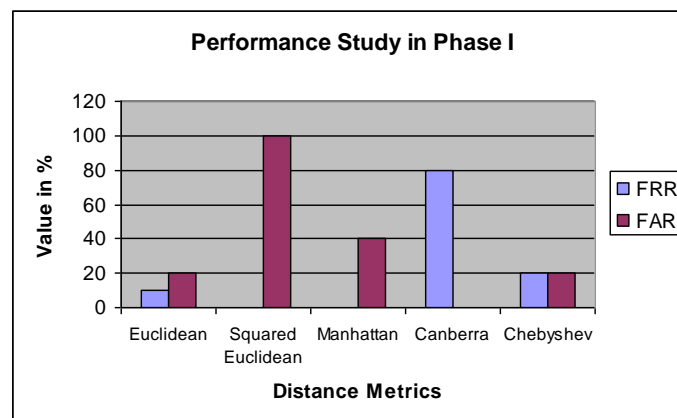


Figure 1: Performance of different distance metrics at the end of phase I

The second set of data collected was under extreme circumstances. The objective of this type of data collection was to show how the results are affected due to the behavior of the users. The users were asked to log in to the system at a time when they were very busy or in between some very urgent work where their mind would not be as quite and calm as in the earlier phase. Like the clerical staff were asked to log in, in between their important cash transactions with customers. Some users who were teachers were asked to log in, in between their lectures as also the students. This exercise helped us capture the mood of the user and we were successful in showing how the results are affected due to this. The following figure depicts the same.

Only the FRR was noted in this case, as the objective of this exercise was to show the effect of the behavior of the user on his typing rhythm. As we can see the all the distance metrics have shown an increase in the FRR. Canberra shows an FRR of 100% with Chebyshev being next with a FRR

of 75%. The FRR for Euclidean distance has also risen by 40% and Manhattan distance shows a rise in FRR by 25%.

With this we can see how the behavior of the user will affect his typing rhythm and number of valid users who are not accepted increases.

The phase II of the experiment was conducted after a long gap of about 10-12 days. This was done to observe whether the typing rhythms change as time passes. And it was observed that the typing rhythm change, not only with the present mood of the user but also as time passes. This is depicted in fig 4.4. There was an increase in the FRR for all distance metrics.

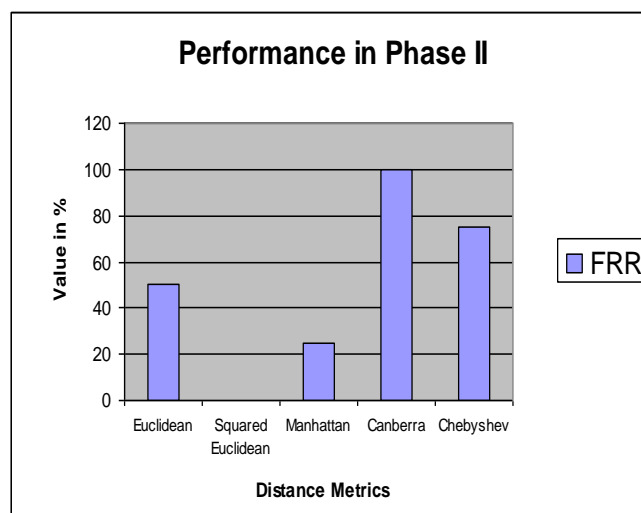


Figure 2: Performance of distance metrics with data collected in Phase II

4.0 Incremental K Means Clustering For Keystroke Biometrics

As we have seen in Fig. 2, we can say that the technology of keystroke biometrics does change as the behavior of the user changes over a period of time. It was one of the goals of this research to overcome this problem. For this we used an incremental k means clustering technique which was implemented in the following way: Once the enrollment process is over and the clusters for the users are formed, we also record the login timings of the user for the next 3 – 4 (which could be modified) login attempts. These login attempts are at a considerable interval. On each of these login attempts, the cluster is again formed and the cluster identities with distance measures are recomputed. But this time the data for computing the centroids change. The first set of data from the enrollment data i.e. keystroke latencies collected during attempt 1 during enrollment, is removed and the recent keystroke latencies collected during login is included in the set. Now, the

centroid and distance measures are recomputed with the new data set. This is continued with the next 2 login attempts and the first 2 data sets of enrollment data.

The technique was proposed with the idea of, incorporating that slight change in typing rhythm that could occur as time passes, in the calculation of centroid and distance measures. The technique has shown a good improvement in the FRR values and makes the study of distance metrics even more clear.

4.1 Results

The performance of the different distance metrics were noted after the implementation of the incremental k means clustering for keystroke biometrics. The users were asked to log in to the system, when they were in a different mental situation. The FAR and FRR for the users were noted and is depicted in the following diagram.

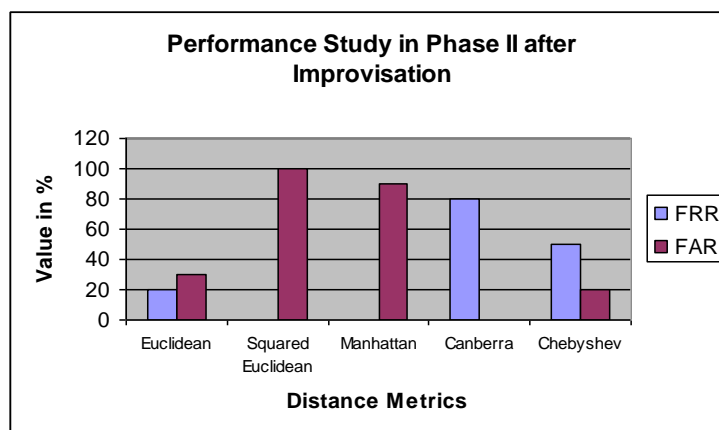


Figure 3: Performance of distance metrics in Phase III for Incremental K means clustering.

The figure above shows the FRR and FAR for the different distance metrics collected in Phase III of the experiment. Phase III, is basically intended towards applying the incremental k means clustering. The authorized users were asked to log in. Along with them imposters, who were told the password and also shown the style in which the password was typed by the authorized user, tried to log in. The results shown were quite positive as compared to phase I and II. Due to this technique, the FRR values have reduced for most of the distance metrics. Euclidean distance shows a FRR of 20% with an FAR of 30%. There is no considerable change in the values for Squared Euclidean and Manhattan distance. Canberra distance shows a FRR of 80% with FAR of 0%. Finally Chebyshev distance shows a FRR of 50% with FAR of 20%.

5.0 Conclusion

The research was aimed at comparing and categorizing these distance metrics as per the users of the system. After conducting this experiment keeping all aspects in mind, it can be observed that the Chebyshev Distance that shows moderate values for FRR and FAR can be used in biometric systems targeted for users who do have a good hand on the keyboard. These users could be programmers, data entry operators etc. who do frequently use the keyboard. They could use it to protect their source code and data from imposters. Canberra distance which gives a value only between 0 and 1 can be used in systems which need to be highly secure. User of such system need to have their typing rhythm accurate, each time he tries to log in. Squared Euclidean and Manhattan distance do not show results that can be appreciated for the purpose of user authentication. They could be used in the earlier stages, when the user has just started using the application, till his typing rhythm stabilizes and he gets comfortable with the keyboard. Later it could be shifted to another distance metric.

Lastly, Euclidean distance which does show quite moderate values for FRR and FAR proves to be the method that is best suited for applications that need to be authenticated using keystroke biometrics. It could be used in applications that cover a general population including people from wide areas.

The research also concentrated on improvising the k means clustering technique to consider the behavioral aspect of the user while he tries to log in. We tried to make the system dynamic, wherein the users log in timings after his enrollment process was over, were also considered in the clustering process. This technique has shown a good result from which we can conclude that it can be in keystroke biometric enabled password authenticating systems which use k means clustering algorithm.

REFERENCES

- [1]. G.K.Gupta, "Introduction to Data Mining with Case Studies".
- [2]. Bhaskar Rao, Media Arts and Technology. "Continuous Keystroke Biometric System". A Project Paper submitted to University of California, Santa Barbara, and September 2005.
- [3]. Cheng Soon Ong and Weng Kin Lai, "Enhanced Password Authentication Through Typing Biometrics With The K-Means Clustering Algorithm" at World Automation Congress Seventh International Symposium on Manufacturing with Applications, Maui, Hawaii, June 11-16, 2000
- [4]. Clara Eusebi, Cosmin Gilga, Deepa John, Andre Maisonave Seidenberg School of CSIS, ace University 1 Martine Ave, White Plains, NY, 10606, USA, "A Data Mining Study of Mouse Movement, Stylometry, and Keystroke Biometric Data"
- [5]. Dr. Bhavani Thuraisingham, the University of Texas at Dallas, "Data and Applications Security Developments and Directions"
- [6]. Edmond Lau, Xia Liu, Chen Xiao, Xia Yu, Massachusetts Institute of Technology, "Enhanced User Authentication through Keystroke Biometrics"
- [7]. Fabian Monrose, Courant Institute of Mathematical Sciences, New York University, New York, NY., Aviel D. Rubin, AT&T Labs - Research, Florham Park, NJ, "Keystroke Dynamics as a Biometric for Authentication"
- [8]. Hussien, Bleha, McLaren (1989) 'An application of fuzzy algorithms in a computer access security system', Pattern recognition letters.
- [9]. Kardi Teknomo, PhD - K-Means Clustering Tutorial [<http://people.revoledu.com/kardi/tutorial/kMean>]

A Local Monitoring Approach with Scheduling in Wireless Sensor Networks

K.J Eldho

Department of Computer Science, Don Bosco College, Sulthan Bathery, eldhorvs@gmail.com

ABSTRACT

To monitor critical events in infrastructure less area such as fire detection in forest, gas monitoring in coal mines sensor network has been employed .To prolong the network lifetime, some sleep scheduling methods are used .The sensor network can be divided into number of groups based on some criteria, each group consists of a node capable of monitoring its group is called local monitoring node. When a critical event occurs the alarm message and event information is transmitted to the concerned local monitoring node and that is again transmitted to the center node through one channel. That is again transmitted to the entire network through another channel with the help of local monitoring node; level by level offset based wakeup pattern is designed for transmission. The broadcasting delay is $3D+2L$, where D -number of hop of nodes to the center node, L -length of sleeping duty cycle.

Key Word: Wireless Sensor Networks, Local monitoring Approach, Sleep Scheduling, and Transmission Delay

I. INTRODUCTION

A wireless sensor network consists of battery powered wireless devices ,that are capable of monitoring environmental conditions such as temperature, noise etc.,and critical events such as forest fire ,gas leakage etc., Due to a wide diversity of WSN application requirements, however, a general-purpose WSN design cannot fulfill the needs of all applications. Many network parameters such as sensing range, transmission range, and node density have to be carefully considered at the network design stage, according to specific applications. Sleep scheduling methodology is implemented to make the sensor nodes to work for long time without recharging the batteries. This may cause transmission delay because, the nodes in the network should wait until the receive nodes are active and ready to receive the event information .In critical event monitoring,most of the time only small number of packets need to be transmitted ,so the transmission delay is an important issue. Level by level offset schedule was proposed.(i.e.) the packet from node a to node c can be sent through node b with minimum delay. In this paper we propose Local

Monitoring approach, which is introduced to minimize the broadcasting delay?

II. EXISTING WORK

- When a critical event occurs, an alarm and event information is transmitted along one of the traffic path to a center node
- Then it is immediately broadcast by that center node along another path to all nodes in the network.

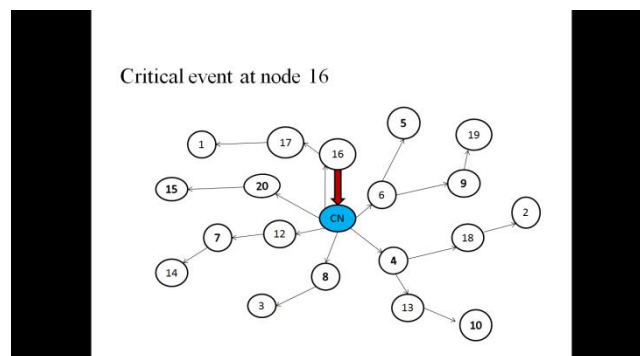


Fig 1. Packet transmission to center node

It may cause transmission delay because the entire sensor network is depends on the single center node; It also implements sleep scheduling where the energy consumption is also comparatively high.

III. PROBLEM DESCRIPTION

The critical event information should be transmitted to the entire sensor network. Each node is capable of detecting a critical event and generating an alarm message. The alarm message and event information should be transmitted to the entire network with less transmission delay. Also analyze the energy consumption of sensor nodes with the proposed scheme in WSN. Since the energy consumption is mainly due to the idle listening when there is no critical event most of the time, it is reasonable for us to approximatively calculate the energy consumption according to the length of wake-up duration in a duty cycle. To reduce the broadcasting delay and energy Consumption in the existing system with the help of Local Monitoring Approach.

IV. PROPOSED WORK

To reduce the broadcasting delay the proposed method include two paths

1).Any node that detects critical event sends alarm and event information to the center node through local monitoring node along determined path according to level by level offset schedule.

2).The center node transmits the alarm and event information through local monitoring node to the entire network along another determined path according to level by level offset schedule. The traffic paths from nodes to the center node through local monitoring node are uplink and the traffic path from the center node through local monitoring node to other node is downlink.

To minimize the delay,

- 1).Breadth first search is implemented for uplink.
- 2).Colored connected dominant set is implemented for downlink.

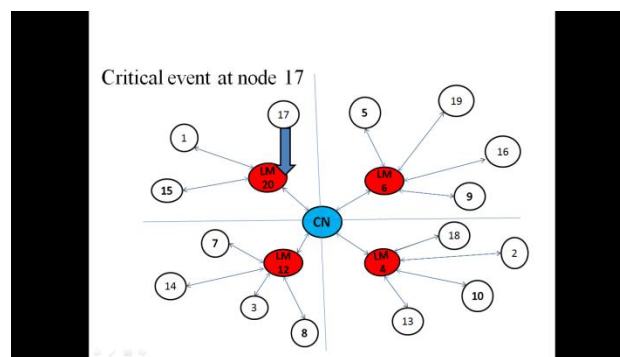


Fig 2.Packet transmission to center node

A.SLEEP SCHEDULING

It is introduced to minimize the energy consumption, making all nodes to sleep; sensor nodes are equipped with passive event detection capabilities that allow a node to detect an event even when its wireless communication module is in sleep mode. When sensor node detects the event the radio module is immediately woken up and is ready to send an alarm message.

B. LOCAL MONITORING APPROACH

Local monitoring is a collaborative detection strategy where a node monitors the control traffic going in and out of its neighbors. Many techniques have been introduced that use the framework of local monitoring to achieve specific tasks such as intrusion detection, building

trust and reputation among nodes, protecting against control and data traffic attacks, and building secure routing protocols. Though local monitoring has been demonstrated as a powerful technique for enhancing security of WSNs, it results in a high energy cost since it requires the monitoring nodes to be constantly awake to oversee network activity.

In local monitoring approach, sensor nodes are divided into number of groups based on some criteria. Each group consists of local monitoring nodes. All the nodes in the group belong to the local monitoring node. The local monitoring nodes are under the control of the center node. When a node in group detects a critical event, It is immediately transmitted to the local monitoring node from there the alarm message and event information is transmitted to the center node through one channel, Again the alarm message and event information is transmitted to all the other nodes in the network through other channel, This is known as level by level offset schedule.(i.e)the two possible traffic path is made. The node just needs to be awake for T time ,where T is the minimum time needed by a node to transmit alarm packet.

The nodes are maintain in three states to establish Sleep wake scheduling which are

Active state-Node in routing process

Ideal state-Node which are in ready state

Sleeping state-Node which is in slow sleeping state by reducing its transmission range wake up once get the wake signal from authorized node

C. WAKEUP PATTERNS

After the nodes are initiated and the path is established, the wakeup patterns are required for sensor nodes to wakeup and receive alarm packet to achieve minimum delay for both of the two traffic paths.

Two level by level offset schedules:-

1).Sensor nodes use BFS wakeup level by level scheduling according to the distance to center node.

2).Sensor nodes use CCDS wakeup level by level scheduling according to the distance to all other nodes.

Hence, when an alarm packet is originated it is forwarded to the center node along a path in the BFS, then the center node immediately broadcasts it along the paths in the CCDS.

Time slots should be arranged at different positions, so that two traffic paths can work separately.

Time slot assignment:-

1).All nodes obtain slots for uplink traffic according to hops and sequence number of duty cycle.

2). All nodes obtain slots for downlink traffic according to hops and sequence number of duty cycle

V. METHODOLOGY

Distributed network has multiple nodes and services messages, and each node is a shared resource, many decisions must be made

A. ROUTING

There may be multiple paths from the source to the destination. Therefore, message routing is an important topic. The main performance measures affected by the routing scheme are throughput (quantity of service) and average packet delay (quality of service). Routing schemes should also be avoided for both deadlock and live lock. Routing methods can be fixed (i.e. pre-planned), adaptive, centralized, distributed, broadcast, etc. Perhaps the simplest routing scheme is the token ring. Here, a simple topology and a straightforward fixed protocol result in very good reliability and precomputable Quos. A token passes continuously around a ring topology. When a node desires to transmit, it captures the token and attaches the message. As the token passes, the destination reads the header, and captures the message. In some schemes, it attaches a 'message received' signal to the token, which is then received by the original source node. Then, the token is released and can accept further messages. The token ring is a completely decentralized scheme that effectively uses TDMA. Though this scheme is very reliable, one can see that it results in a waste of network capacity. The token must pass once around the ring for each message. Therefore, there are various modifications of this scheme, including using several tokens, etc.

Fixed routing schemes often use Routing Tables that dictate the next node to be routed to, given the current message location and the destination node. Routing tables can be very large for large networks, and cannot take into account real-time effects such as failed links, nodes with backed up queues, or congested links.

Adaptive routing schemes depend on the current network status and can take into account various performance measures, including cost of transmission over a given link, congestion of a given link, reliability of a path, and time of transmission. They can also account for link or node failures.

B. SENSOR NETWORK SETUP

To contribute to a more systematic understanding and treatment of sensor deployment issues, the existing literature on deployment experience and present a classification of common problems encountered during deployment of sensor networks. A wireless network

that is temporarily installed alongside the actual sensor network during the deployment process.

Parameters considered during sensor network formation

- **Transmission range:** nodes communication depends under transmission range which is placed nearly close to each other thus gets better link.
- **Local information system:** Nodes must be grouped under specific feature like battery power, processing capability, bandwidth, memory etc. so according to those, nodes are partitioned using driver methods.
- **Mobility:** Mobility refers the node movement procedure so need to consider the mobility options with limitation in maximum and minimum speed.

According to the critical event monitoring process, sensor network formed under local information system with sleep wake scheduling mechanisms

VI. ROUTING PROTOCOL DESIGN

A routing protocol is a protocol that specifies how routers communicate with each other, disseminating information that enables them to select routes between any two nodes on a computer network, the choice of the route being done by routing algorithms. Each router has a prior knowledge only of networks attached to it directly. A routing protocol shares this information first among immediate neighbors, and then throughout the network. This way, routers gain knowledge of the topology of the network. Design a Routing protocol named as ELMP (Energy aware local monitoring protocol), which is going to implement in OSI layer that need to get and deliver the messages from other layers for that make some more changes in supported layers. The routing protocol is implemented in the layered architecture of the GloMoSim simulator.

To configure some attributes which is supported to execute the routing protocols like Number of nodes, Mobility, Mac protocol, Simulation time, Band width, Transmission range etc... by setting these kinds of attributes the routing protocol can be executed with layers interaction.

C. PERFORMANCE EVALUATIONS

The following are the parameters for performance evaluations

- **Packet arrival rate:** The ratio of the number of received data packets to the number of total data packets sent by the source.
- **Average end-to-end delay:** The average time elapsed for delivering a data packet within a successful transmission.
- **Communication overhead:** The average number of transmitted control bytes per second, including both the data packet header and the control packets.
- **Energy consumption:** The energy consumption for the entire network, including transmission energy consumption for both the data and control packets.

D. SIMULATION

GloMoSim is a scalable simulation library for wireless network Systems built using the Parsec simulation environment. GloMoSim has been designed and built with the primary goal of simulating very large network models that can scale up to a million nodes using parallel simulation to significantly reduce execution times of the simulation model. As most network systems adopt a layered approach similar to the OSI seven layer network architecture. Simple APIs are defined between different similar simulation layers. This allows the rapid integration of models developed at different layers by different people. GloMoSim is designed using a layered approach with standard APIs between layers. The layered design benefits from the features of modular development, such that the layers as well as the protocols and models at different layers are treated as independent modules and can be modified or replaced without affecting other layers. The modular design allows people to develop and implement new protocols at different layers such that the design conforms with the standard API used between the layers.

E. RESULTS

The proposed technique has been simulated and results are shown in the figure 3-5.

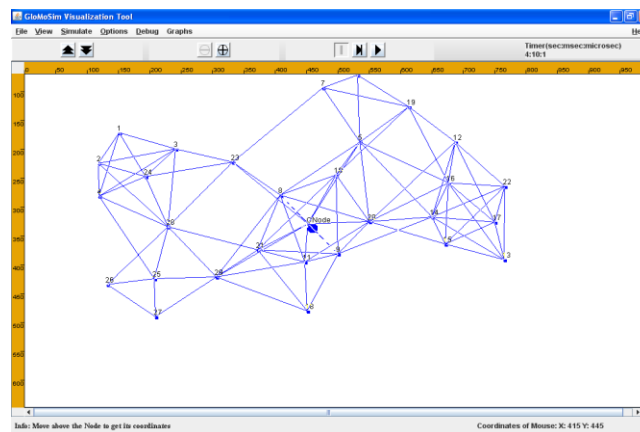


Fig 3. Framework Structure for Routing

Nodes connected each other (blue lines) in terms of neighbor extraction and initialization of center node (CN). The above screen describes about the framework structure for routing with respect to center node. Blue line presents the possible connectivity among the nodes towards the center nodes through neighbor nodes i.e. multichip routing.

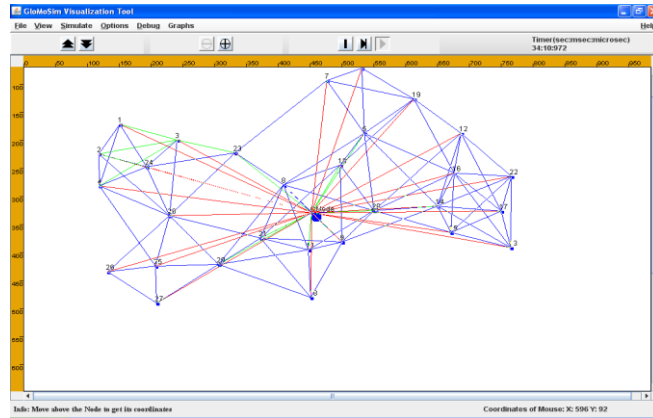


Fig 4. Routing structure of routing protocol

Above figure describes about the routing structure of routing protocol. This structure explains about the nodes placement according to the center node monitoring area. So Red color line - Center node makes possible connection path with each nodes. Green color line – Path establishment through multiple normal nodes (Multichip routing path) towards the center node for forwarding alarm packet via the path.

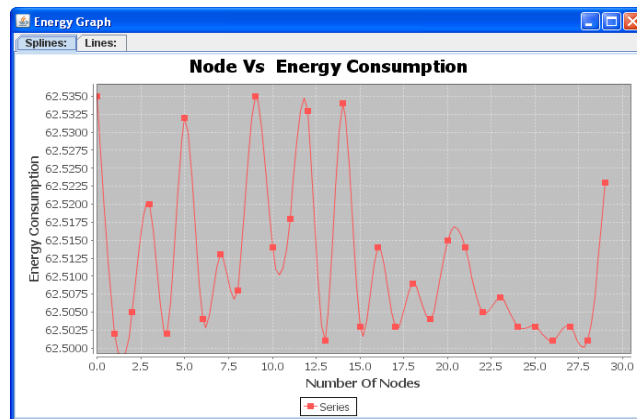


Fig 5. Energy Consumption

This graph represents the energy consumption mega watt hour performance metric for routing protocol. Consider x axis as no of nodes and y axis as energy consumption according to the values plot the graph and at average energy consumption occur in range of 62.5. The less energy consumption with the comparison of nodes of multichip is the attractive of our proposed work by using the routing protocol. Thus we reduced the energy consumption.

VII. CONCLUSION

The proposed scheme could essentially decrease the delay of alarm broadcasting from any node in WSN. Presented the mechanisms of monitoring a wireless sensor networks, for the following reasons: topology control (connectivity and the coverage), and the security in wireless sensor networks. Theoretical analysis and conducted simulations will show that the broadcasting delay and the energy consumption of the proposed scheme is much lower than that of existing methods. Finally, it will demonstrate the effectiveness of the approach and algorithms with satisfactory results obtained through simulation.

REFERENCES

- [1] Peng Guo, Tao Jiang and Kui Zhang, "Sleep Scheduling for Critical Event Monitoring in Wireless Sensor networks", *Wireless networks*, VOL. 23, NO. 2, FEB 2012
- [2] N. Bouabdallah, M.E. Rivero-Angeles, and B. Sericola, "Continuous Monitoring Using Event-Driven Reporting for Cluster-Based Wireless Sensor Networks," *IEEE Trans. Vehicular Technology*, vol. 58, no. 7, pp. 3460-3479, Sept. 2009.
- [3] M.I. Brownfield, K. Mehrjoo, A.S. Fayez, and N.J. Davis IV., "Wireless Sensor Network Energy-Adaptive Mac Protocol," *Proc. Third IEEE Consumer Comm. and Networking Conf.*, pp. 778-782, Jan. 2006.
- [4] T. Zheng, S. Radhakrishnan, and V. Sarangan, "PMAC: An Adaptive Energy-Efficient MAC Protocol for Wireless Sensor Networks," *Proc. 19th IEEE Int'l Parallel and Distributed Processing Symp.*, pp. 224-231, Apr. 2005.
- [5] S.C. Ergen and P. Varaiya, "TDMA Scheduling Algorithms for Wireless Sensor Networks," *Wireless Networks*, vol. 16, no. 4, pp. 985-997, 2010.
- [6] G. Lu, B. Krishnamachari, and C. Raghavendra, "An Adaptive Energy-Efficient and Low-Latency MAC for Data Gathering in Wireless Sensor Networks," *Proc. 18th IEEE Int'l Parallel and Distributed Processing Symp.*, pp. 224-230, Apr. 2004.
- [7] A. Keshavarzian, H. Lee, and L. Venkatraman, "Wakeup Scheduling in Wireless Sensor Networks," *Proc. Seventh ACM Int'l Conf. Mobile Ad Hoc Networking and Computing*, pp. 322-333, May 2006.
- [8] G. Lu, N. Sadagopan, B. Krishnamachari, and A. Goel, "Delay Efficient Sleep Scheduling in Wireless Sensor Networks," *Proc. 24th IEEE Int'l Conf. Computer Comm.*, pp. 2470-2481, Mar. 2005.
- [9] N.A. Vasanthi and S.A., "Energy Efficient Sleep Schedule for Achieving Minimum Latency in Query Based Sensor Networks," *Proc. IEEE Int'l Conf. Sensor Networks, Ubiquitous, and Trustworthy Computing*, pp. 214-219, June 2006.
- [10] N.A. Vasanthi and S. Annadurai, "AWS: Asynchronous Wakeup Schedule to Minimize Latency in Wireless Sensor Networks," *Proc. IEEE Int'l Conf. Sensor Networks, Ubiquitous, and Trustworthy Computing*, pp. 144-151, June 2006.
- [11] Y. Sun, O. Gurewitz, S. Du, L. Tang, and D.B. Johnson, "ADB: An Efficient Multihop Broadcast Protocol Based on Asynchronous Duty-Cycling in Wireless Sensor Networks," *Proc. Seventh ACM Conf. Embedded Networked Sensor Systems*, pp. 43-56, Nov. 2009.

- [12] Y. Sun, S. Du, O. Gurewitz, and D.B. Johnson, "DW-MAC: A Low Latency, Energy Efficient Demand-Wakeup MAC Protocol for Wireless Sensor Networks," Proc. Ninth ACM Int'l Conf. Mobile Ad Hoc Networking and Computing, pp. 53-62, 2008.
- [13] S.C.-H. Huang, P.-J. Wan, X. Jia, H. Du, and W. Shang, "Minimum-Latency Broadcast Scheduling in Wireless Ad Hoc Networks," Proc. 26th IEEE Int'l Conf. Computer Comm., pp. 733- 739, May 2007.
- [14] J. Silva, J. Shamberger, M.J. Ammer, C. Guo, S. Li, R. Shah, T. Tuan, M. Sheets, J.M. Rabaey, B. Nikolic, A. Sangiovanni- Vincentelli, and P. Wright, "Design Methodology for Picoradio Networks," Proc. Conf. Design Automation and Test in Europe, pp. 314-323, 2001.
- [15] Y. Huang and W. Lee, "A Cooperative Intrusion Detection System for Ad Hoc Networks," Proc. First ACM Workshop Security of Ad Hoc and Sensor Networks, pp. 135-147, 2003.

Synthesis, Spectroscopic Characterization of Manganese and Vanadium Substituted Keggin-type Heteropolymolybdates

T. Jeyabalan*, U. Anto Maria Jeraldin

APRC, Department of Chemistry, Sacred Heart College (autonomous), Tirupattur-635601.

Abstract:

The Mn-substituted heteropolymolybdates $K_6[V^V Mn^{IV} Mo_{10} PO_{40}] \cdot 3H_2O$ (HPM1) and $K_7[Mn^{IV} Mo_{11} PO_{40}] \cdot 4H_2O$ (HPM2) were synthesized and characterized. The IR results confirm the framework of polyoxometalates. The EPR investigations indicate the delocalisation of the unpaired electron of Mn(IV) due to the substitution in HPM1 and HPM2. The optical absorption and E_g was extracted from DRS.

Keywords: Heteropolymolybdates, Infrared spectra(IR), Electron paramagnetic Resonance(EPR), Diffused Reflectance Spectral(DRS).

Introduction:

The chemistry of Keggin type heteropolyanions of Molybdenum and Tungsten has received much attention because of the application of these compounds in several fields such as analytical chemistry¹, catalysis^{2,3}, material science⁴ and biochemistry^{5,6}. They have stimulated many current research activities because of their chemical properties such as redox potentials, acidities, and solubilities in various media can be finely tuned by choosing constituent elements and counter cations⁷. Particularly, the interest in the catalysis of metal-substituted polyoxometalates, which are synthesized by the substitution of metal cations into the vacant site(s) of lacunary polyoxometalates as “structural motifs”, has been growing because of the rich diversity of lacunary polyoxometalates, ranging from monovacant to hexavacant anions⁷. Polyoxometalates (POMs) of various classes are very interesting compounds with unusual behaviour: they are good catalysts, superionic proton conductors, compounds with photoconductive and magnetic characteristics and biochemical active species⁸⁻¹³. Polyoxometalates consist of a polyhedral cage structure or framework bearing negative charge, which is balanced by cations that are external to the cage, and may also contain centrally located heteroatom surrounded by the cage framework.

Generally, suitable heteroatoms like phosphorus, antimony, silicon, and boron. The framework of polyoxometalates typically comprises a plurality of metal atoms (addenda), which can be the same or different, bonded to oxygen atoms. The framework metal is

* Corresponding author

generally limited to a few elements such as Tungsten, Molybdenum, Vanadium, Niobium and Tantalum. In this paper the preparation, spectral characterization of two manganese substituted heteropolymolybdates, namely $K_6[V^V Mn^{IV} Mo_{10} PO_{40}] \cdot 3H_2O$ and $K_7[Mn^{IV} Mo_{11} PO_{40}] \cdot 4H_2O$ have been discussed.

Experimental:

All chemicals were of analar grade and were used as received. All reagents were purchased from Merck.

Synthesis of $K_6[V^V Mn^{IV} Mo_{10} PO_{40}] \cdot 3H_2O$:

$NaH_2PO_4 \cdot 2H_2O$ (0.22g, 14mmol) was added to a solution of $(NH_4)_6Mo_7O_{24} \cdot 4H_2O$ (3.7g, 30mmol) in H_2O ($3cm^3$), followed by the addition of $MnSO_4$ (0.045g, 2.7mmol) and a pinch of $K_2S_2O_8$. To the resulting mixture, NH_4VO_3 (0.0315g, 2.7mmol) in H_2O ($1cm^3$) was added dropwise with stirring. The mixture was boiled under reflux for 20 min and filtered. To the clear filtrate, 1g of solid KCl was added with stirring. The solid which separated was collected and recrystallized from hot water. (Found: V, 2.5; Mn, 2.71; Mo, 47.38; P, 1.53, H_2O , 2.67; $K_6[V^V Mn^{IV} Mo_{10} PO_{40}] \cdot 3H_2O$ Calculated: V, 2.6; Mn, 2.83; Mo, 48.50; P, 1.61, H_2O , 2.79.)

Synthesis of $K_7[Mn^{IV} Mo_{11} PO_{40}] \cdot 4H_2O$:

$NaH_2PO_4 \cdot 2H_2O$ (2.42g, 14mmol) was added to a solution of $(NH_4)_6Mo_7O_{24} \cdot 4H_2O$ (4.07g, 30mmol) in H_2O ($4.5cm^3$), followed by the addition of $MnSO_4$ (0.22g, 2.7mmol) and a pinch of $K_2S_2O_8$. The mixture was boiled under reflux for 20 min and filtered. To the clear filtrate, 1.5g of solid KCl was added with stirring. The solid which separated was collected and recrystallized from hot water. (Found: Mn, 2.54; Mo, 48.84; P, 1.43, H_2O , 3.33; $K_7[Mn^{IV} Mo_{11} PO_{40}] \cdot 4H_2O$ Calculated: Mn, 2.68; Mo, 49.30; P, 1.52, H_2O , 3.41.)

Analytical Measurements:

The Mo^{VI} was estimated by gravimetry after precipitating as the Oxinate¹⁴. Phosphorus was estimated by gravimetry after precipitating as magnesium pyrophosphate¹⁴. Vanadium was estimated by spectrophotometry as the citrate complex¹⁵. Infrared (IR) spectra were recorded on KBR pellets using a Bruker alpha model spectrophotometer. The powder EPR spectra were recorded at 300K with 100 kHz field

modulation. The Diffused Reflectance Spectra (DRS) were recorded using Cary100 UV-Visible spectrophotometer to estimate the band gap energy.

Results and discussion:

Infrared Spectral Studies:

The vibrational spectra of Keggin type heteropolymolybdates are sensitive to the substitution of Molybdenum (VI) by lower oxidation state transition ions such as Vanadium (V), Manganese (IV) etc. Hence IR spectra are extensively used for characterization of heteropolymolybdates. For Keggin anion four characteristic modes of vibrations are observed at 1067 cm^{-1} , 975 cm^{-1} , 870 cm^{-1} and 810 cm^{-1} which correspond to $\nu_{\text{sym}}(\text{M-O}_t)$, $\nu_{\text{asym}}(\text{M-O}_b\text{-M})$, $\nu_{\text{sym}}(\text{M-O}_c\text{-M})$ and $\nu_{\text{asym}}(\text{M-O}_c\text{-M})$. IR spectra confirm the presence of (M-O_t) , $(\text{M-O}_b\text{-M})$, $(\text{M-O}_c\text{-M})$ (Where $\text{M} = \text{W}$ or Mo). The terminal oxygen has double bond character and hence it gives peak at higher wave number region. hence it gives peak at higher wave number region.

The IR spectral data of $\text{K}_6[\text{V}^{\text{V}}\text{Mn}^{\text{IV}}\text{Mo}_{10}\text{PO}_{40}]\cdot 3\text{H}_2\text{O}$ (HPM1) and $\text{K}_7[\text{Mn}^{\text{IV}}\text{Mo}_{11}\text{PO}_{40}]\cdot 4\text{H}_2\text{O}$ (HPM2) are given in table 1:

Table 1: IR Spectral values of the samples

HPM1 (cm^{-1})HPM2(cm^{-1})Tentative	Assignment
1460	1411 ν (Mo-OH)
1038	1033 $\nu_{\text{sym}}(\text{Mo-O}_t)$
954	937 $\nu_{\text{asym}}(\text{Mo-O}_b\text{-Mo})$
738	722 $\nu_{\text{sym}}(\text{Mo-O}_c\text{-Mo})$
616	572 $\nu_{\text{asym}}(\text{Mo-O}_c\text{-Mo})$

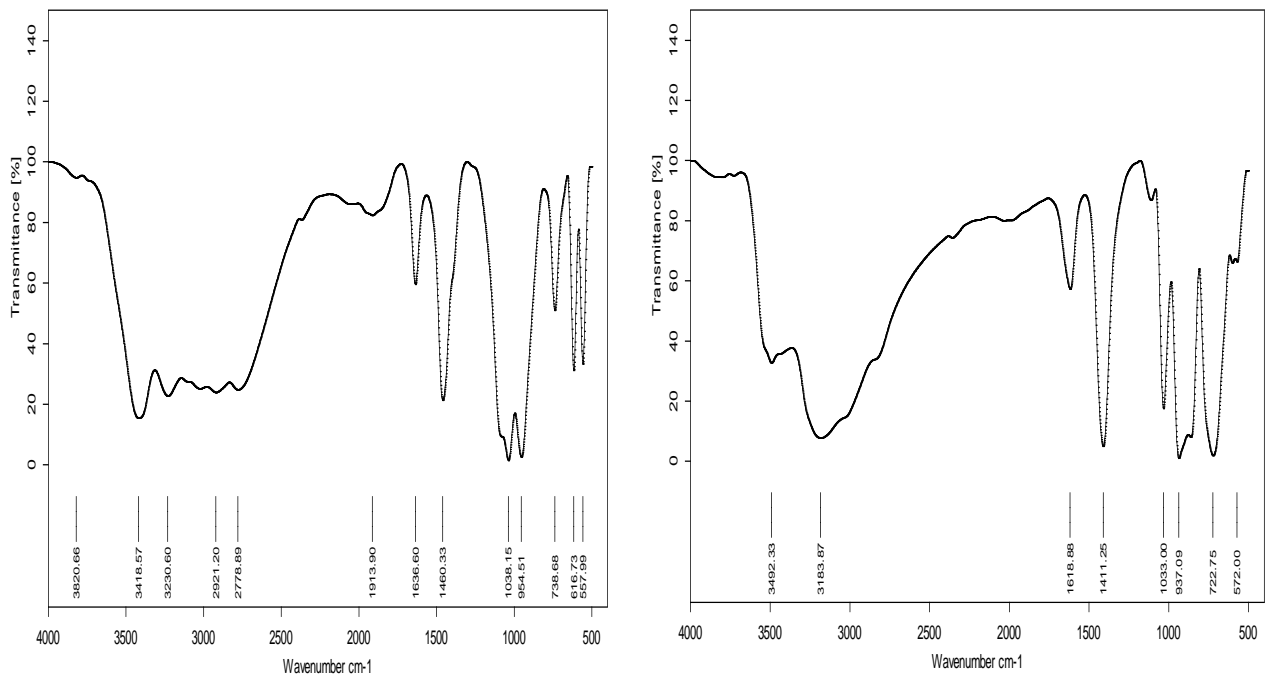


Fig 1. The IR spectrum of HPM1 Fig.2 The IR spectrum of HPM2

EPR Spectral Studies:

The powder EPR spectra of samples were recorded at 300K with 100 kHz field modulation. The EPR spectra of $K_6[V^V Mn^{IV} Mo_{10} PO_{40}] \cdot 3H_2O$ (HPM1) and $K_7[Mn^{IV} Mo_{11} PO_{40}] \cdot 4H_2O$ (HPM2) are in the figure 4 and 5. The g value derived from the spectra are given in the table 2.

Table 2: EPR Spectral values of the samples

Compound	g value
$K_6[V^V Mn^{IV} Mo_{10} PO_{40}] \cdot 3H_2O$	2.032
$K_7[Mn^{IV} Mo_{11} PO_{40}] \cdot 4H_2O$	2.026

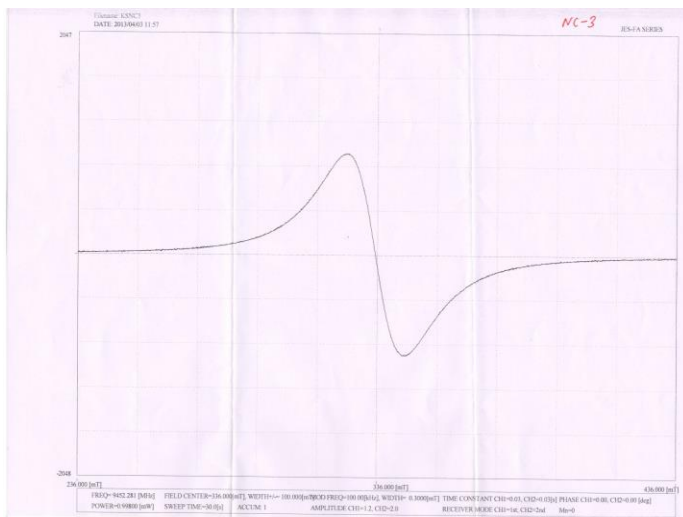


Fig 3. EPR spectrum of HPM1



Fig 4. EPR spectrum of HPM2

Optical Spectral Studies:

Diffused Reflectance Spectroscopy (DRS):

Diffused Reflectance Spectroscopy (DRS) is a more convenient technique to characterize the powder materials than UV-visible spectroscopy, since it takes advantage of the enhanced scattering phenomenon in powder materials. Moreover the effects of light scattering in the absorption spectra of powder samples dispersed in liquid media can be avoided by using DRS¹⁶.

Diffused Reflectance Spectral studies in the UV- visible region were carried out to investigate the band gap energy (E_g) of samples HPM1 and HPM2. These spectra are shown in figure 5 and 6. In order to assign the band gap with certainty, the diffused reflectance (R) of the sample were transformed using Kubelka-Munk function $F(R)$. The definition of Kubelka-Munk function^{17,18} is enumerated as follows:

$$F(R) = (1-R^2)$$

2R

Where R is the diffused reflectance factor.

The E_g of the sample was obtained by plotting of between $[F(R)E]^2$ versus energy of the incident light and extrapolating the linear region to the zero. The E_g value of sample HPM1 is about 6.10 eV(203nm) and sample HPM2 is about 6.19 eV(200nm). In the UV range, the electronic spectra of HPAs having Keggin structure exhibit two intense absorption bands at about 200 and 260 nm, attributed to the transition $M-O_t$, $M-O_b$ and $M-O_c$ respectively¹⁹. From this we conclude that for both the compounds HPM1 and HPM2, the two peak positions were considerably blue shifted.

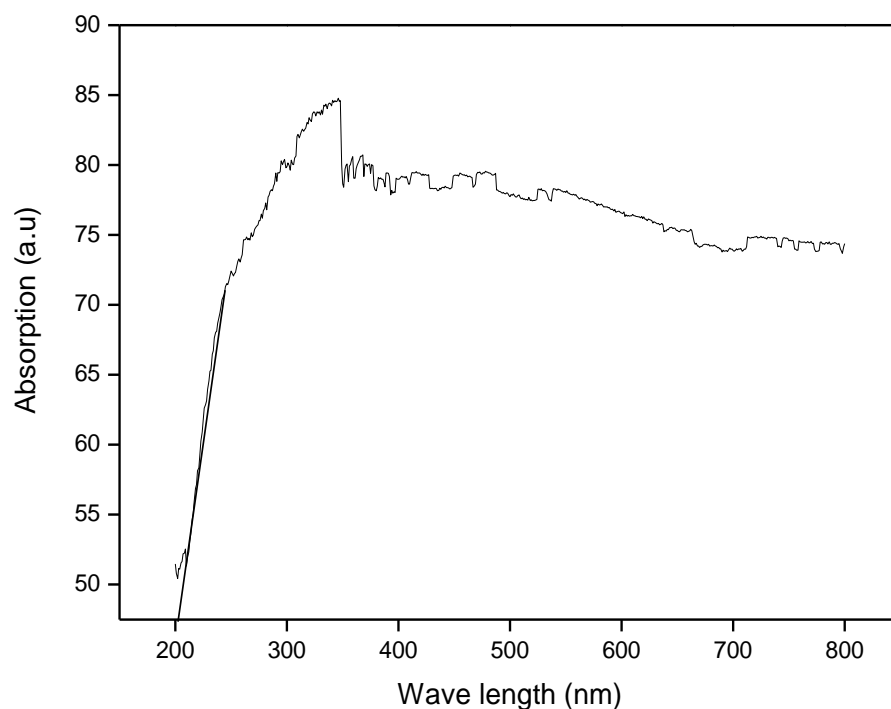


Fig.5 DRS of HPM1

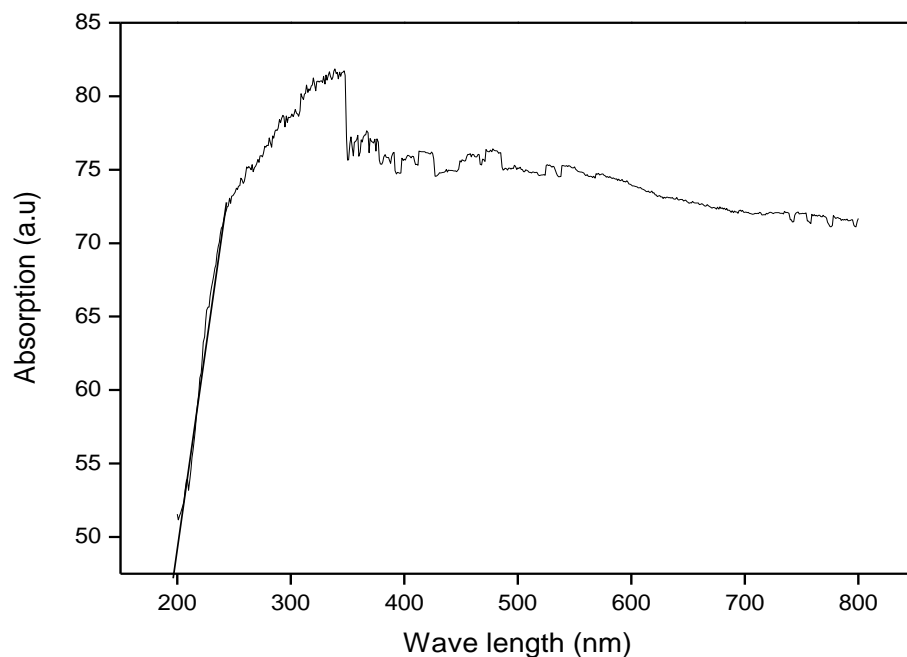


Fig 6. DRS of HPM2

Conclusion

The Mn-substituted heteropolymolybdates HPM1 and HPM2 were successfully synthesized. Diffused Reflectance Spectra indicated maximum absorption at 203nm (6.10eV) and 200 nm (6.19eV). The framework of synthesized HPM1 and HPM2 were characterized spectroscopically.

Acknowledgements:

The authors duly acknowledge the APRC, Sacred Heart College, Tirupattur, India for providing research facilities. We thank School of Chemistry, Bharathidasan University, Trichy for recording EPR. We thank the Environmental Technology Division, (CLRI),Adiyar, Chennai for recording DRS.

References

1. G. A. Perker, *Analytical Chemistry of Molybdenum*, Springer, New York, 1983.
2. M. Misono, *Catal, Rev. Sci. Eng.*, 29, 269,1987.

3. A. Mylonas and E. Papaconstantinou, *J. Mol. Catal.*, 92, 261, 1994.
4. H. Sung, H. So and W. K. Paik, *Electrochim. Acta*, 39, 645, 1994.
5. E. G. Demasterand R. A. Mitchell, *Biochem. Arch.*, 3, 301, 1987.
6. T. Yamase, M. Fujita and K. Fukushima, *Inorg. Chem. Acta*, 151, 15, 1988.
7. Hill, C. L.; Prosser-McCartha, C. M. *Coord. Chem. Rev* 143, 407, 1995.
8. M. T. Pope, *Heteropoly and IsopolyOxometalates*, Springer-Verlag, Berlin, 1983.
9. M. T. Pope, A. Muller, *Polyoxometalates: From Platonic Solids to Anti-Retroviral Activity*, Kluwer Academic Publishers, Dordrecht, 1994
10. M. T. Pope, A. Muller, *Polyoxometalates Chemistry, Fromopologyvia Self-Assembly to Applications*, Kluwer Academic Publishers, Dordrecht, 2001
11. U. Mio., Ph. Colomban, A. Novak, *J. Mol. Struct.* 218, 123, 1990.
12. U. B. Mio., M. R. Todoroviš , M. Davidoviš , Ph. Colomban, I. Holclajtner–Antunoviš , *Solid State Ionics* 176, 2837, 2005.
13. J. T. Rhule, C. L. Hill, D. A. Judd, R. F. Schinazi, *Chem. Rev.* 98, 327, 1998.
14. A. I. Vogel, *A Textbook of Quantitative Inorganic Analysis*, III Edit., Longman, London, 1969.
15. D. P. Smith and M. T. Pope, *Anal. Chem.*, 40, 1906, 1968.
16. Jong Dae Han and SeongIhl Woo, *Korean J. of Chem. Eng.* 8(4), 235-239, 1991.
17. L. C. Nehru, V. Swaminathan, and C. Sanjeeviraja, *Powder Technol.* 226, 29, 2012.
18. N. Serpone, D. lawless, and R. Khairutdinov, *J. Phys. Chem.* 99, 16646, 1995.
19. J. Liu, W. J. Mei, *Antivir. Res.* 62, 65, 2004.

Mixed Convection in Two-Sided Lid-Driven Differentially Heated Square Cavity Using Nanofluid

Nitesh Mittal¹, A Satheesh^{1*}, D. Santhosh Kumar²

¹School of Mechanical and Building Sciences, VIT University, Vellore-632014, Tamilnadu.

²Senior Engineer, Bharath Heavy Electricals Limited, Trichy, Tamilnadu

ABSTRACT

In the present work, a steady-state two-dimensional mixed convection in a vertical two-sided lid-driven differentially heated square cavity filled with water base nanofluid containing various volume fractions of Cu and Al₂O₃ is investigated numerically. The left and right moving walls are maintained at different constant temperatures while top and bottom walls are thermally insulated. Two cases are considered depending upon the direction of vertical moving walls. The numerical approach is based on the finite volume technique with a staggered grid arrangement. The SIMPLE algorithm is used for handling the pressure velocity coupling. Pertinent parameters such as Richardson number, Prandtl number, Grashof number and solid volume fraction are used to investigate the significance of fluid flow and heat transfer effects. Numerical results show the inclusion of nanoparticles in the base fluid has produced an augmentation of the heat transfer coefficient, which has been found to increase appreciably with an increase of particles volume concentration. Detailed results are presented in the form of streamlines, isotherms and average Nusselt numbers.

Keywords: Nanofluid, Mixed convection, two-sided lid-driven, Finite volume method

1. INTRODUCTION

Nanofluids are created by dispersing nanometer-sized particles (<100 nm) in a base fluid such as water, ethylene glycol or propylene glycol. Use of high thermal conductivity metallic nanoparticles (e.g., copper, aluminum, silver and silicon) increases the thermal conductivity of such mixtures, thus enhancing their overall energy transport capability [1]. Nanofluids have attracted attention as a new generation of heat transfer fluids in building heating, in heat exchangers, in plants and in automotive cooling applications, because of their excellent thermal performance. Various benefits of the application of nanofluids include: improved heat transfer, heat transfer system size reduction, minimal clogging, micro channel cooling and miniaturization of systems [2]. Therefore, research is underway to apply nanofluids in environments where higher heat flux is encountered and the conventional fluid is not capable of achieving the desired heat transfer. Xuan *et al.* [3] have examined the transport properties of nanofluid and have expressed that thermal dispersion, which takes place due to the random movement of particles, takes a major role in increasing the heat transfer rate between the fluid and the wall. This requires a thermal dispersion coefficient, which is still unknown. Brownian motion of the particles, ballistic phonon transport through the particles and nanoparticles clustering can also be the possible reason for this enhancement [4]. Das *et al.* [5] has observed that the thermal conductivity for nanofluid increases with increasing temperature. They have also observed the stability of Al₂O₃-water and Cu-water nanofluid. Experiments

* Corresponding author

on heat transfer due to natural convection with nanofluid have been studied by Putra *et al.* [6] and Wen and Ding [7]. They have observed that heat transfer decreases with increase in concentration of nanoparticles. The viscosity of this nanofluid increases rapidly with the inclusion of nanoparticles as shear rate decreases.

Khanafer *et al.* [8] numerically investigated the heat transfer behavior of nanofluids in a two dimensional horizontal enclosure. The nanofluids were assumed to be in single phase, in thermal equilibrium and without velocity slip between base fluid and particle. They found that the suspended nanoparticles substantially increase the heat transfer rate for any given Grashof number. More recently, Tiwari and Das [9] investigated numerically heat transfer augmentation in a lid-driven cavity filled with nanofluids. They found that the nanoparticles when immersed in a fluid are capable of increasing the heat transfer capacity of base fluid. As solid volume fraction increases, the effect is more pronounced. Koo and Kleinstreuer [10] discussed the effects of Brownian, thermo-phoretic and osmo-phoretic motions on the effective thermal conductivities. They found that the role of Brownian motion is much more important than the thermo-phoretic and osmo-phoretic motions. They suggested that a high-Prandtl number base fluid and a high aspect ratio channel should be used for better heat transfer performance. Furthermore, the particle interaction can be neglected when the nanofluid concentration is low ($< 0.5\%$). Maiga *et al.* [11] presented a mathematical formulation and numerical method to determine the forced convective heat transfer and wall shear stress for the laminar and turbulent regions of water- Al_2O_3 and ethylene glycol- Al_2O_3 flowing inside a uniformly heated tube. The solid-liquid mixture takes a single-phase behaviour into account, so the slip velocity between the phases was neglected. Furthermore, the local thermal equilibrium of the mixture and symmetry in flow were considered. Recently, Jou and Tzeng [12] used Khanafer's model to analyze heat transfer performance of nanofluids inside an enclosure taking into account the solid particle dispersion. More applications and good understanding of the subject is given in the recent articles [13–21].

As diverse industrials including microelectronics, transportation, and manufacturing become more advanced, cooling technology is one of the most important challenges. For example chemical vapor deposition instruments (CVD) [22], furnace engineering [23], solar energy collectors [24], phase change material [25], non-Newtonian chemical processes [26, 27], and domains are affected by electromagnetic fields [28, 29]. On the other hand, fluid flow and heat transfer in a cavity filled by pure fluid which is driven by buoyancy and shear have been studied extensively in literature [30–32]. The most usage of the mixed convection flow with lid-driven effect is to include the cooling of the electronic devices, lubrication technologies, drying technologies, etc.

Motivated by the investigations mentioned above, the purpose of the present work is to investigate the mixed convection flows of Cu-water and Al_2O_3 – water nanofluid in a differentially heated square cavity in a vertical moving lid whose horizontal walls are kept adiabatic and stationary.

2. MATHEMATICAL MODELING

Consider a steady-state two-dimensional square cavity filled with nanofluid of height H as shown in Fig.1. It is assumed that the left wall is moving upward vertical direction at a constant speed u_o and is maintained at constant temperature T_c . The right wall is maintained

at constant temperature T_h ($T_h > T_c$). Two different cases were considered as shown in Fig.1. In Case1, the right wall is moving upward and in Case2, the right wall is moving downward.

The horizontal walls are considered to be adiabatic and stationary. The nanofluid in the enclosure is Newtonian, incompressible and laminar. The nanoparticles are assumed to have uniform shape and size. Also, it is assumed that both the fluid phase and nanoparticles are in thermal equilibrium state and they flow at the same velocity. The physical properties of the nanofluid are considered to be constant except the density variation in the body force term of the momentum equation which is satisfied by the Boussinesq's approximation. Under the above assumptions, the system of equations governing the two dimensional motion of the nanofluid is:

$$\frac{\partial u}{\partial x} + \frac{\partial v}{\partial y} = 0$$

(1)

$$u \frac{\partial u}{\partial x} + v \frac{\partial u}{\partial y} = -\frac{1}{\rho_{nf}} \frac{\partial p}{\partial x} + \frac{\mu_{nf}}{\rho_{nf}} \left[\frac{\partial^2 u}{\partial x^2} + \frac{\partial^2 u}{\partial y^2} \right]$$

(2)

$$u \frac{\partial v}{\partial x} + v \frac{\partial v}{\partial y} = -\frac{1}{\rho_{nf}} \frac{\partial p}{\partial y} + \frac{\mu_{nf}}{\rho_{nf}} \left[\frac{\partial^2 v}{\partial x^2} + \frac{\partial^2 v}{\partial y^2} \right] + \frac{1}{\rho_{nf}} [\chi \rho_s \beta_s + (1 - \chi) \rho_{nf} \beta_f] g(\theta - \theta_c)$$

(3)

$$u \frac{\partial \theta}{\partial x} + v \frac{\partial \theta}{\partial y} = \alpha_{nf} \left[\frac{\partial^2 \theta}{\partial x^2} + \frac{\partial^2 \theta}{\partial y^2} \right] \quad (4)$$

Where

$$\alpha_{nf} = \frac{k_{nf}}{\rho_{nf} C_{p_{nf}}}$$

(5)

And the effective viscosity as given by Brinkman[33]

$$\mu_{nf} = \frac{\mu_f}{(1 - \chi)^{2.5}}$$

(6)

The effective density of fluid at reference temperature is

$$\rho_{nf} = (1 - \chi) \rho_f + \chi \rho_s$$

(7)

And the heat capacitance of the nanofluid is

$$(\rho Cp)_{nf} = (1 - \chi)(\rho Cp)_f + \chi(\rho Cp)_s$$

(8)

As given by Xuan and Li [1]. The effective thermal conductivity of solid-liquid mixture was introduced by Wasap [34] and is given by

$$\frac{k_{nf}}{k_f} = \frac{(k_s + 2k_f) - 2\chi(k_f - k_s)}{(k_s + 2k_f) + \chi(k_f - k_s)}$$

(9)

This equation is applicable for the two-phase mixture containing micro-sized particles. In the absence of any convenient formula, the calculation of effective thermal conductivity can be obtained from the above equation. Introducing the following dimensionless variables and parameters:

$$X = \frac{x}{H}, Y = \frac{y}{H}, U = \frac{u}{u_0}, V = \frac{v}{u_0}, T = \frac{\theta - \theta_c}{\theta_h - \theta_c},$$

$$Gr = \frac{g\beta\Delta\theta H^3}{\nu_f^2}, Re = \frac{u_0 H}{\nu_f}, Pr = \frac{\nu_f}{\alpha_f}, P = \frac{p}{\rho u_0^2}$$

After dropping out the asterisks, the dimensionless governing equations can be written as follows

$$\frac{\partial U}{\partial X} + \frac{\partial V}{\partial Y} = 0$$

(10)

$$U \frac{\partial U}{\partial X} + V \frac{\partial U}{\partial Y} = -\frac{\rho_f}{\rho_{nf}} \frac{\partial P}{\partial X} + \frac{1}{Re} \frac{\nu_{nf}}{\nu_f} \left[\frac{\partial^2 U}{\partial X^2} + \frac{\partial^2 U}{\partial Y^2} \right]$$

(11)

$$U \frac{\partial V}{\partial X} + V \frac{\partial V}{\partial Y} = -\frac{\rho_f}{\rho_{nf}} \frac{\partial P}{\partial Y} + \frac{1}{\text{Re}} \frac{v_{nf}}{v_f} \left[\frac{\partial^2 V}{\partial X^2} + \frac{\partial^2 V}{\partial Y^2} \right] + \frac{[\chi \rho_s \beta_s + (1-\chi) \rho_{nf} \beta_f] Ri T}{\rho_{nf} \beta_f}$$

(12)

$$U \frac{\partial T}{\partial X} + V \frac{\partial T}{\partial Y} = \frac{\alpha_{nf}}{\alpha_f} \frac{1}{\text{Pr Re}} \left[\frac{\partial^2 T}{\partial X^2} + \frac{\partial^2 T}{\partial Y^2} \right]$$

(13)

The dimensionless boundary conditions, used to solve equations are given as:

$$U = 0, V = 0, \partial T / \partial Y = 0 \quad (Y = 0, 1)$$

$$U = 0, V = 1, T = 0 \quad (X = 0)$$

$$U = 0, V = -1 \text{ (Case 1) and } V = 1 \text{ (Case 2), } T = 0 \quad (X = 1)$$

The average Nusselt number can be expressed as

$$\overline{Nu} = -\frac{k_{nf}}{k_f} \int_0^1 \frac{\partial T}{\partial y} \partial x$$

(14)

3. SOLUTION METHODOLOGY

Numerical solutions to the governing equations are secured by employing the finite volume computational procedure using staggered grid arrangement with the SIMPLE algorithm as given in Patankar [35]. The convective terms in the interior points are discretized by using the deferred QUICK scheme [36] and central difference scheme was used adjacent to the boundaries. The resulting algebraic equations are solved by using tridiagonal matrix (TDMA) algorithm. The pseudo-transient approach is followed for the numerical solution as it is useful for situation in which the governing equations give rise to stability problems, e.g., buoyant flows [37]. Euclidean norm of the residual is taken as convergence criteria for each dependent variable in the entire row field [38]. The iteration is carried out until the normalized residuals of the mass, momentum and temperature equation become less than 10^{-8} .

4. RESULTS AND DISCUSSION

4.1 Grid independence and code validation

To test and access the grid independence solutions, numerical experiments were performed for various grid sizes viz. 41×41 , 61×61 , 91×91 , and 131×131 choosing extreme values

of Richardson number ($Ri=1$), Grashof number ($Gr=10^4$) and volume fraction ($\chi=0.1$). The u -velocity in the horizontal mid-plane, v -velocity in the vertical mid-plane, and temperature in the horizontal mid-plane are shown in Fig.2, for all grid sizes. It is observed that the curves overlap with each other for all grid sizes. Hence, a grid size of 131×131 is chosen for further computations, considering both the accuracy and the computational time involved.

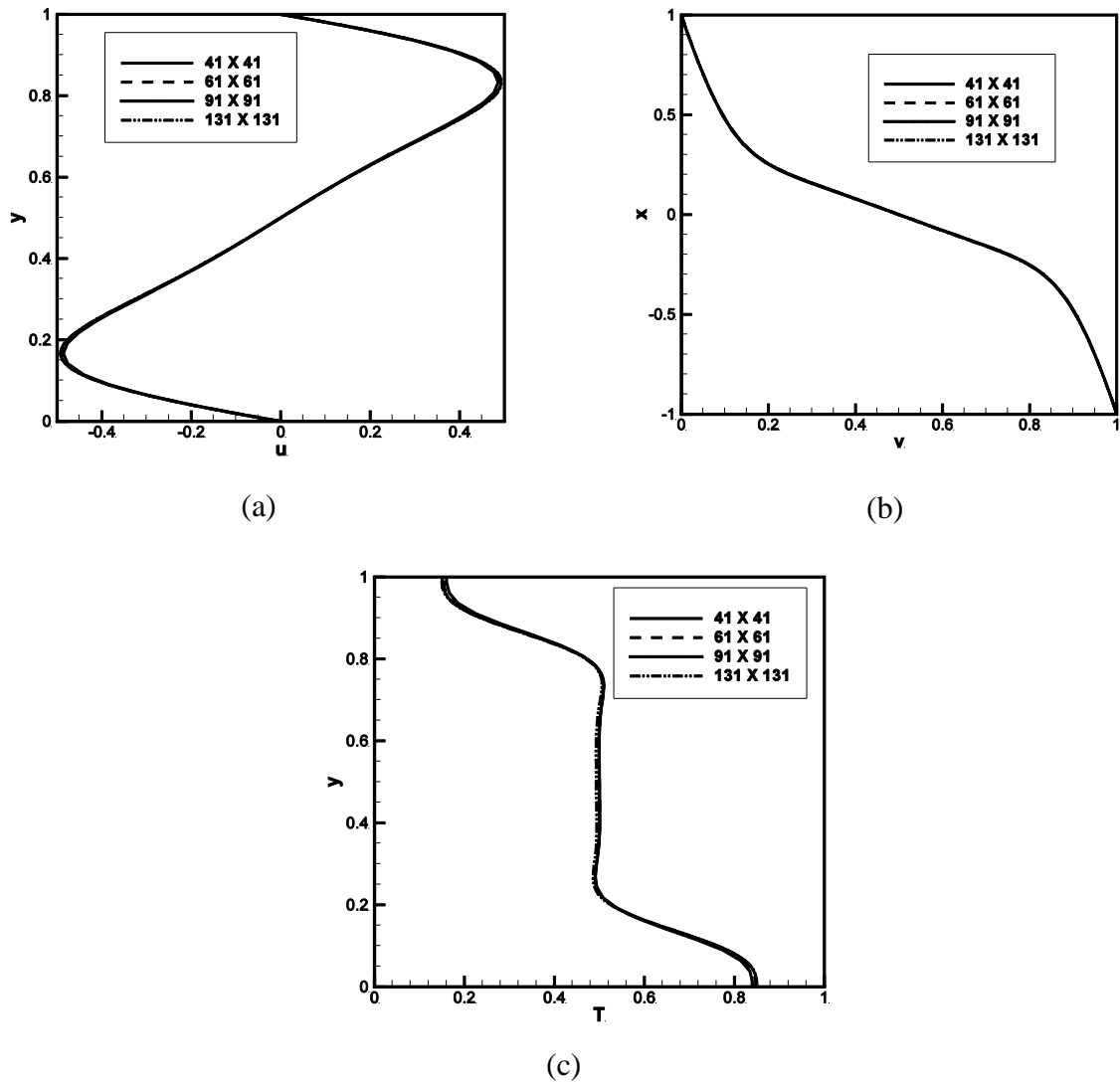


Fig.2. Grid-independence study (a) horizontal velocity along vertical centre line, (b) vertical velocity along horizontal centre line and (c) temperature profile along vertical centre line for $Ri=1$, $Gr=10^4$ and $\chi=0\%$

To validate the present code, computations were performed for natural convection in a square cavity for various Rayleigh numbers and the streamlines and isotherm patterns were depicted in Fig.3. These patterns bear very close resemblance with those obtained by De Vahl Davis [39] and Kalita *et al.*[40].

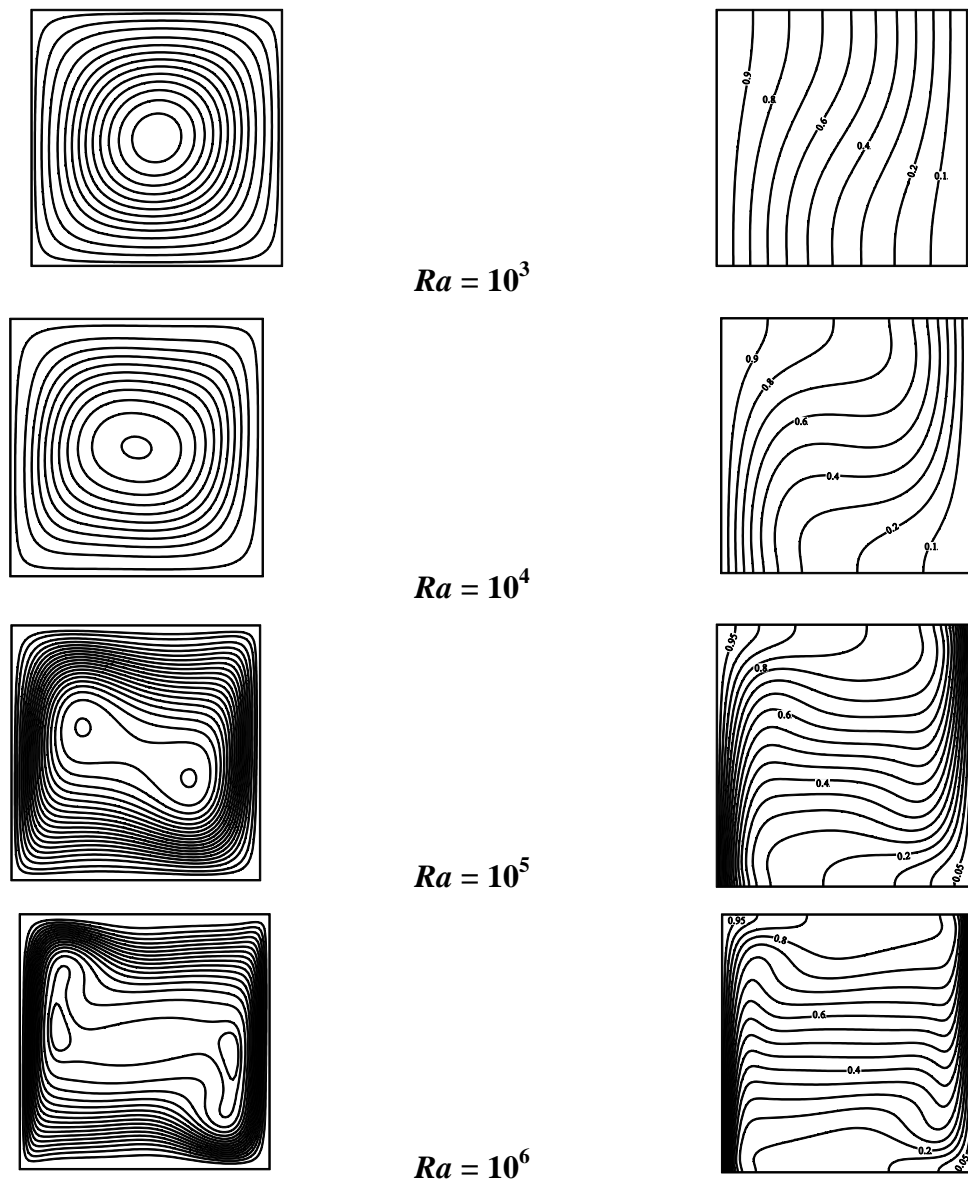


Fig.3. Streamlines (left column) and isotherms (right column) for various Rayleigh numbers for natural convection in a square cavity

The predicted average Nusselt number on the hot wall are compared with those given by De Vahl Davis[39] and Nithiarasu *et al.* [41] for various Rayleigh numbers (Table 1). The results of the present study agree well with those of earlier investigators over the entire range of Rayleigh numbers, thus leading credibility to the present code and numerical method.

Table1. Comparison of average Nusselt number for different Rayleigh number

Ra	Average Nusselt Number		
	De Vahl Davis [27]	Nithiarasu <i>et al.</i> [29]	Present Result

10^3	1.116	1.127	1.117
10^4	2.238	2.245	2.246
10^5	4.509	4.521	4.530
10^6	8.817	8.800	8.822

Mixed convection flow in a two-sided lid-driven square cavity using Cu and Al₂O₃ nanoparticles along with the water as the base fluid are examined. The governing parameters such as Richardson number and Grashof number are fixed to 1 and 10⁴ respectively, while the solid volume fraction (χ), which characterizes the relative importance of enhancement of heat transfer inside the cavity, is investigated for 0, 5 and 10%. The working fluids are chosen as water-Cu and water-Al₂O₃ nanofluid with Prandtl number (Pr) 7.01. The thermo-physical properties of the fluid and solid phase were given by Khanfer *et al.* [8]. Two-sided lid-driven cavity is analyzed according to the direction of moving plate in two cases shown in Fig1. and the results are discussed in the subsequent sections.

Case1

In this case, the vertical left wall is moving upward and the vertical right wall is moving downward which is shown in the Fig.1 (a). It is to be noted that the sliding lids induce a clockwise fluid motion, whereas the buoyancy force tries to rotate the fluid in the counter-clockwise direction. Streamlines (on the left column) and isotherms (on the rights column) for $Ri = 1$ and $Gr = 10^4$ for water-Cu and water-Al₂O₃ are shown in Fig. 4 & 5. As it is seen from Fig.4 & 5, the recirculation is clockwise and some perturbations are seen in streamlines in the upper right and lower left corners due to impingement of fluid to the horizontal wall. In case1, for water-Cu and water-Al₂O₃ nanofluids, the effect of nanoparticles on streamlines and isotherms is not much. Thus the streamlines and isotherms show a similar trend for the range of χ from 0% to 10%.

Fig10(a, b) and 8(a, b). depicts the effects of solid volume fraction χ , on the vertical velocity component at the enclosure mid-section v ($y=0.5$) and local Nusselt number along the cold wall for water-Cu and water-Al₂O₃ nanofluid, respectively. The results show that, in general, the upward flow and downward flow are symmetric with respect to the centre of the cavity. Moreover for water-Cu nanofluid, as the solid volume fraction increases, the vertical velocity component increases, whereas, it takes an opposite behavior when the length along the x-direction increases. But in case of water-Al₂O₃ nanofluid, not much change in the centerline vertical velocity component has been observed with the increment in solid volume fraction. Regarding the local Nusselt number along the cold wall, increasing the concentration of nanoparticles in the base fluid results in an increase in the rate of heat transfer along the cold all (Fig.8(a,B))

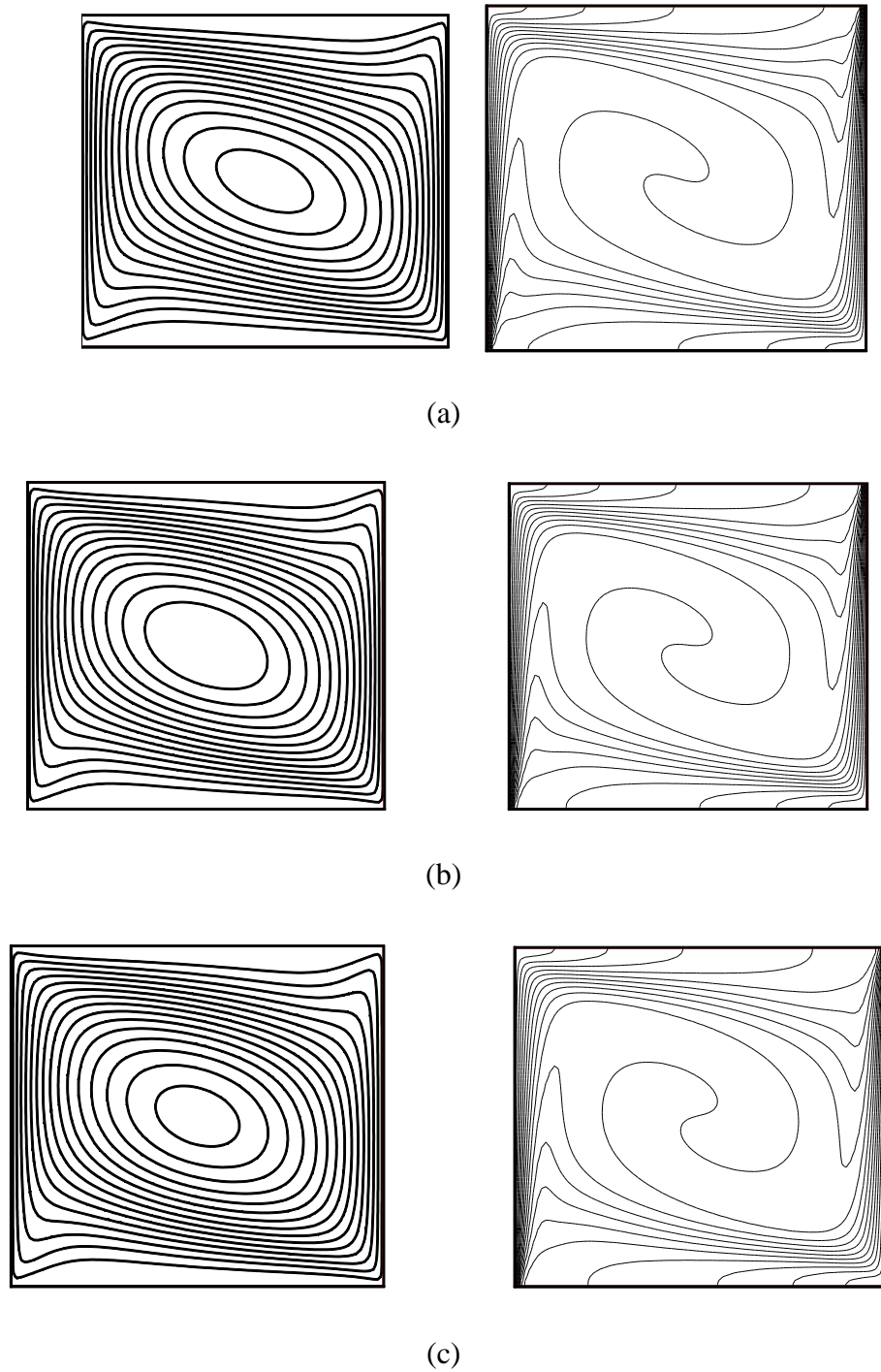
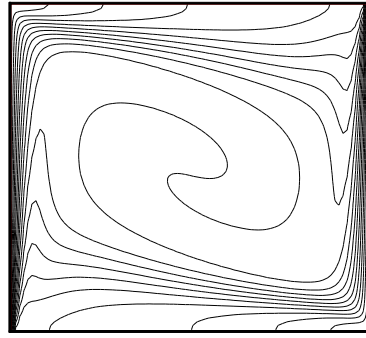
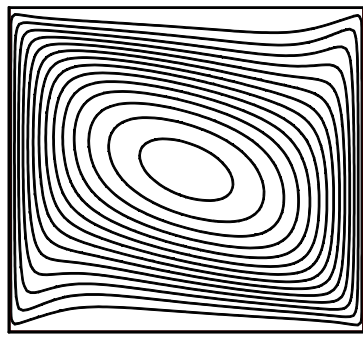
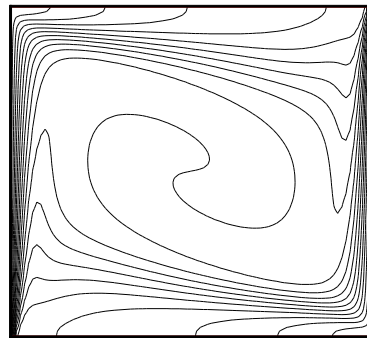
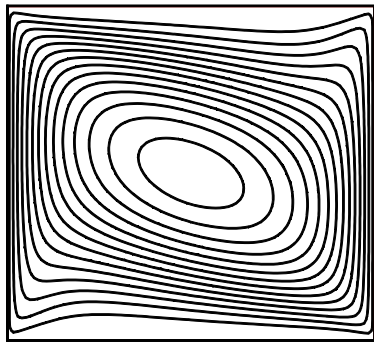


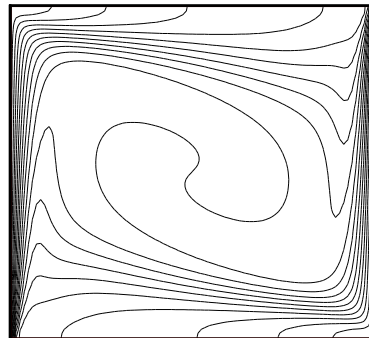
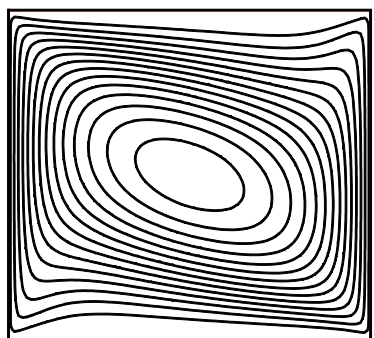
Fig.4. Streamlines (on the left) and isotherm (on the right) patterns at $Ri=1$, $Gr=10^4$ for Case 1 for Cu nanoparticles (a) $\chi = 0\%$, (b) $\chi = 5\%$ and (c) $\chi = 10\%$



(a)



(b)



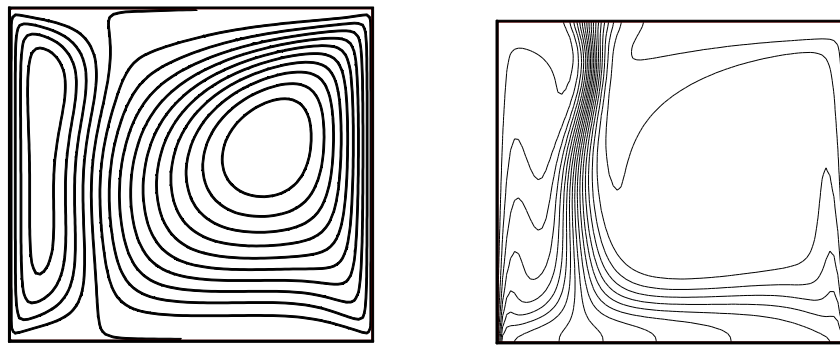
(c)

Fig.5. Streamlines (on the left) and isotherm (on the right) patterns at $Ri=1$, $Gr=10^4$ for Case 1 for Al_2O_3 nanoparticles (a) $\chi = 0\%$, (b) $\chi = 5\%$ and (c) $\chi = 10\%$

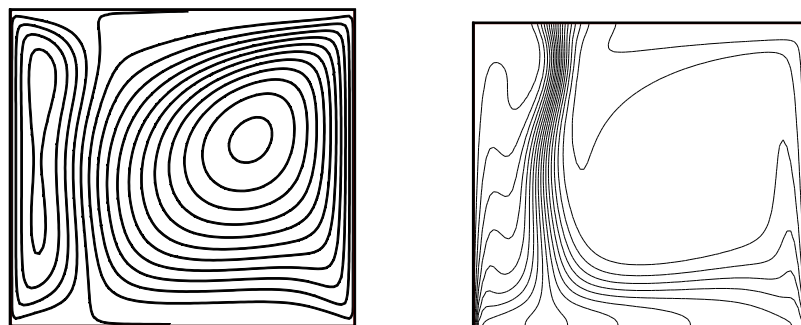
Case2

In this case both vertical walls move upward in which both buoyancy force and force due to the sliding right wall rotates the fluid in the counter-clockwise direction and the left sliding wall tries to rotate the fluid in clockwise direction as shown in Fig.1. Therefore, we should expect that main circulation will be on the right side of the cavity. Streamlines (on the left column) and isotherms (on the right column) at $Ri=1$ and $Gr=10^4$ using water-Cu and water- Al_2O_3 nanofluids are presented in Fig.6 & 7, for various solid volume fractions. Since $Ri = 1$, both buoyancy and shear force produce an equal impact in the flow and heat transfer pattern. However, at the right vertical plane, both natural convection and forced convection rotates the fluid in counter clockwise direction and at the left vertical plane only forced convection which rotates the fluid in clockwise direction. As a result, the vorticity generated on the right wall grows larger and occupy the cavity more than the vorticity generated on the left. In Fig.6 & 7, the vorticity on the right grows further with its geometric centre shifting upwards. In this case (Case2) also, like in Case1, not much effect of solid volume fraction of nanoparticles on streamlines and isotherms is observed. Thus the streamlines and isotherms show a similar trend for the range of χ from 0% to 10%.

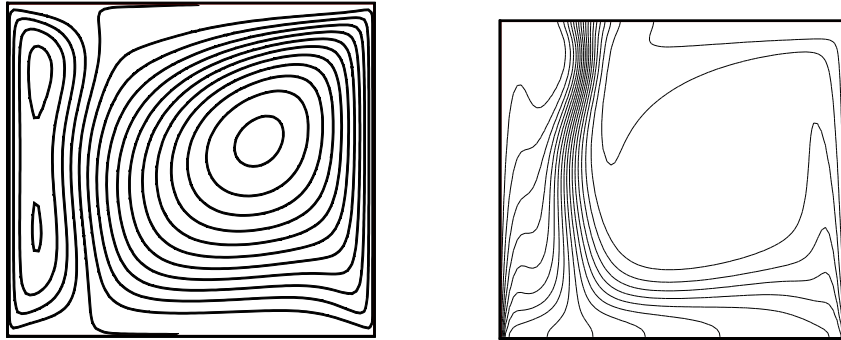
Fig 10(c, d) and 8(c. d), displays the effects of solid volume fraction χ , on the vertical velocity component at the enclosure mid-section v ($y=0.5$) and local Nusselt number along the cold wall for water-Cu and water- Al_2O_3 nanofluid, respectively. The results show that, in general, the upward flow and the downward flow is not symmetric with respect to the centre of the cavity.



(a)

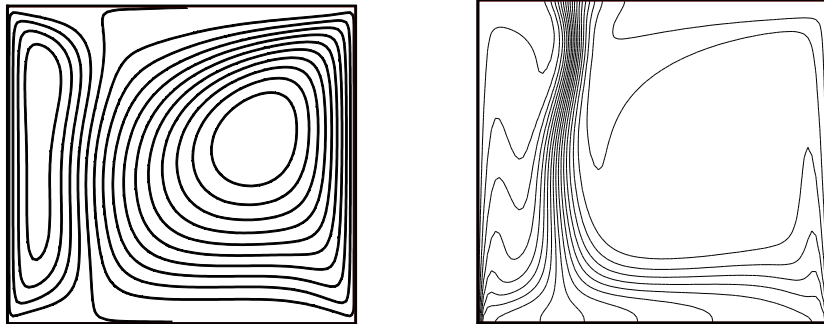


(b)

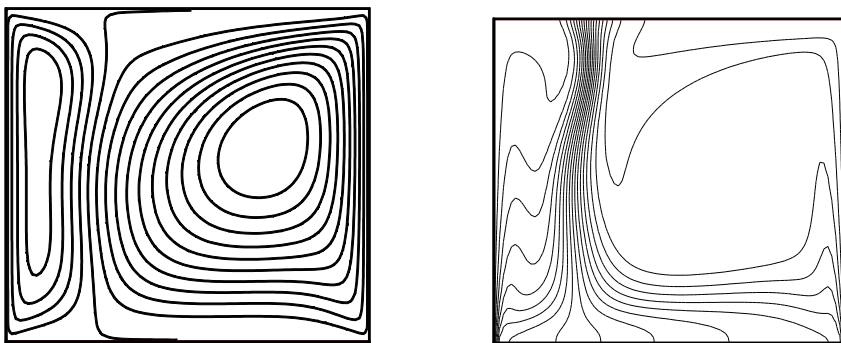


(c)

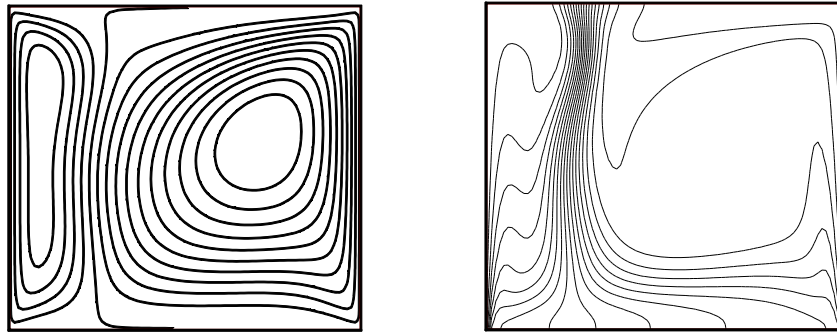
Fig.6. Streamlines (on the left) and isotherm (on the right) patterns at $Ri=1$, $Gr=10^4$ for Case 2 for Cu nanoparticles (a) $\chi = 0\%$, (b) $\chi = 5\%$ and (c) $\chi = 10\%$



(a)



(b)



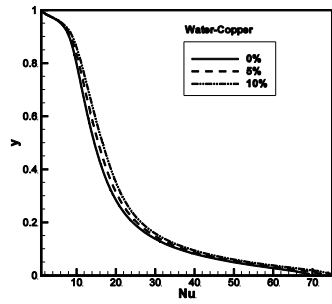
(c)

Fig.7. Streamlines (on the left) and isotherm (on the right) patterns at $Ri=1$, $Gr=10^4$ for Case 2 for Al_2O_3 nanoparticles (a) $\chi = 0\%$, (b) $\chi = 5\%$ and (c) $\chi = 10\%$

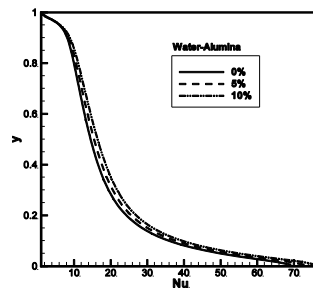
Moreover for water-Cu nanofluid, as the solid volume fraction increases, the vertical velocity component decreases, whereas, it takes an opposite behavior when the length along the x-direction increases till $x=0.8$ and after that it again starts decreasing. But in case of water- Al_2O_3 nanofluid, not much change in the centerline vertical velocity component has been observed with the increment in solid volume fraction. The local Nusselt number along the cold wall, increasing the concentration of nanoparticles in the base fluid results in an increase in the rate of heat transfer along the cold wall (Fig. 8 (c, d)).

Overall heat transfer

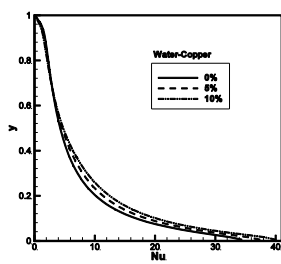
Finally, the average Nusselt number for two cases and different solid volume fraction (χ), for water-Cu and water- Al_2O_3 nanofluids are calculated using Eq.14 and presented in Fig.9 and Table2. It is observed that large values of average Nusselt number is obtained by adding alumina (Al_2O_3) nanoparticles in Case1, whereas; by adding copper (Cu) nanoparticles this gives small values of average Nusselt numbers. But in Case2, the results obtained are different from Case1. In this case (Case2), the average Nusselt number values for copper (Cu) nanoparticles are higher than the Alumina (Al_2O_3) nanoparticles. In general, the average nusselt number values in case1 are higher than in Case2. On the other hand, the average Nusselt number increases by increasing solid volume fraction in both the cases. All these characteristics are presented in Fig.9 and Table2, with the referenced case $Ri=1$, $Gr=10^4$ and $Pr=7.01$.



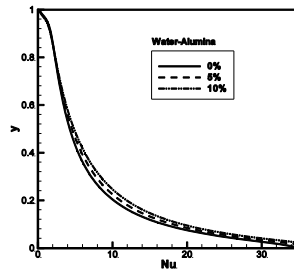
(a)



(b)

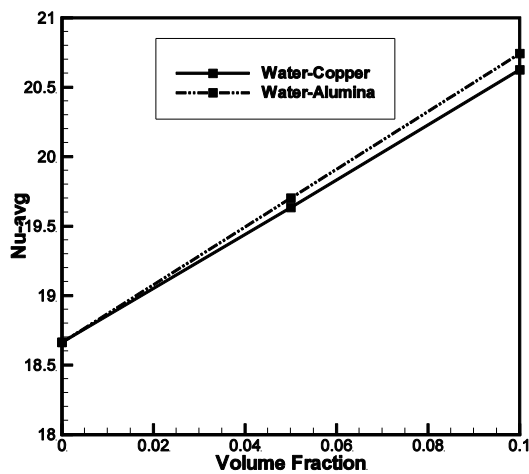


(c)

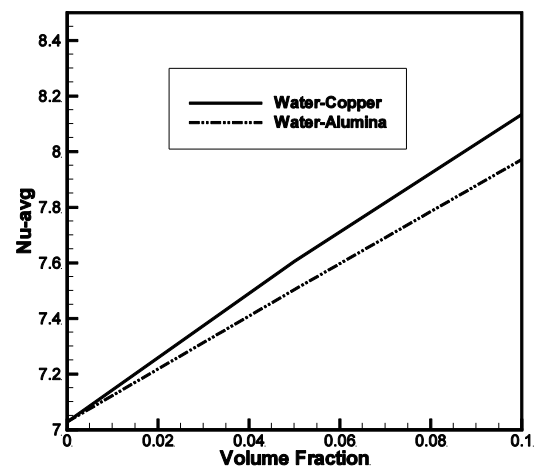


(d)

Fig.8. Variation of local Nusselt number (Nu) on the hot wall for various χ at $Ri=1$, $Gr=10^4$ for (a) Cu nanoparticles (Case1), (b) Al_2O_3 nanoparticles (Case1), (c) Cu nanoparticles (Case2) and (d) Al_2O_3 nanoparticles (Case2)



(a)

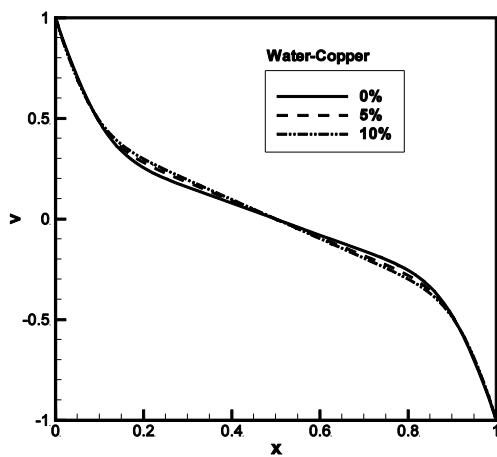


(b)

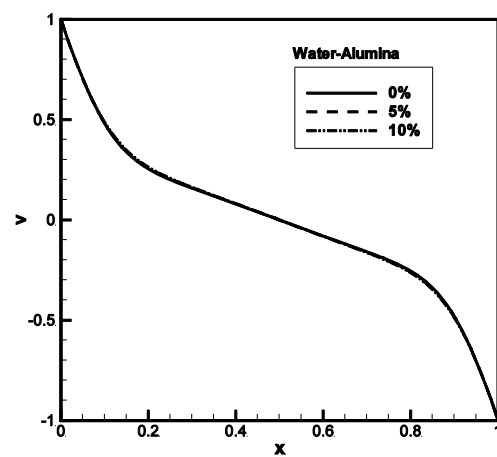
Fig.9. Average Nusselt number variation for various solid volume fractions at $Ri=1$, $Gr=10^4$ (a) for Case1 and (b) for Case2

Table2. Average Nusselt numbers for different volume fraction

Nu-avg ($Ri=1$, $Gr=10^4$ and $Pr=7.01$)				
Volume Fraction (χ)	Case 1		Case 2	
	Copper (Cu)	Alumina (Al_2O_3)	Copper (Cu)	Alumina (Al_2O_3)
0.0	18.664	18.663	7.028	7.028
0.05	19.634	19.702	7.606	7.504
0.1	20.625	20.743	8.137	7.972



(a)



(b)

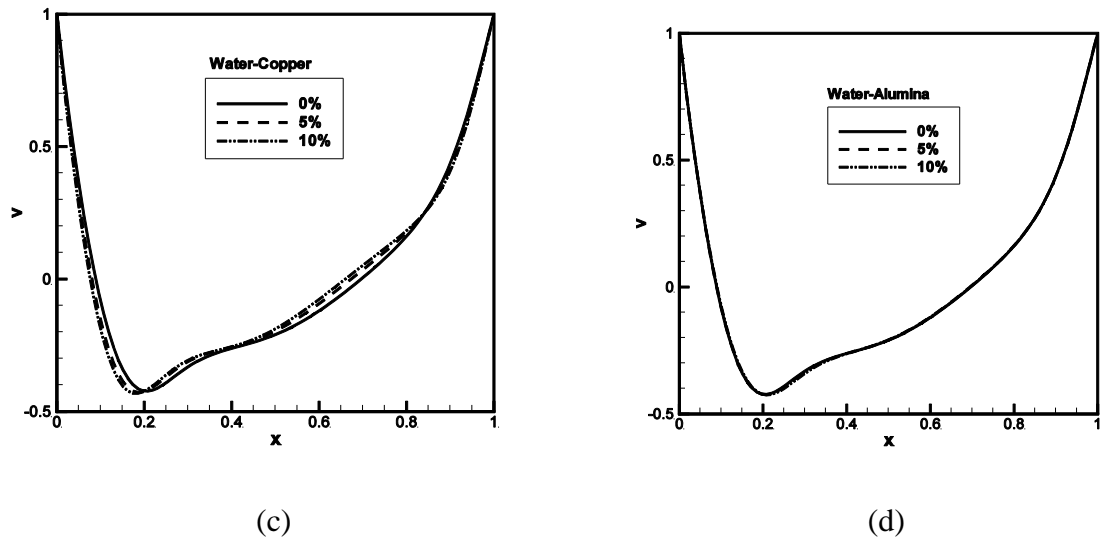


Fig.10. Vertical velocity profile along horizontal centerline at $Ri=1$, $Gr=10^4$ for (a) and (b) Case1, (c) and (d) Case2

Conclusion

In the present paper, a numerical simulation of mixed convection flows in a differentially heated square lid-driven cavity using water-Cu and water- Al_2O_3 was studied. The study has been performed for two different cases characterized by the direction of movement of vertical walls. The governing parameter is solid volume fraction of the nanoparticles, which characterizes the enhancement of heat transfer through mixed convection inside the cavity. Graphical and tabular results for various parametric conditions were presented and discussed. From this investigation, we can draw the following conclusions:

- I. Adding nanoparticles to the base fluid increases the thermal conductivity and hence the heat transfer.
- II. By adding alumina (Al_2O_3) nanoparticles to the base fluid, this gives large values of average Nusselt number. On the contrary, by adding copper (Cu) nanoparticles to the base fluid, this gives small values of average Nusselt number for Case1. But in Case2, average Nusselt number value obtained by the addition of Copper (Cu) nanoparticles to the base fluid is higher than that of alumina (Al_2O_3) nanoparticles.
- III. The heat transfer in the Case1 (when both vertical walls move in the opposite direction) is higher than the Case2 (when both vertical walls move upward). Hence the average Nusselt number is greater for Case1 than Case2.
- IV. Though the presence of nanoparticles in the fluid does not show appreciable effects on the flow field for both cases. However, there is an increase of average Nusselt number.
- V. Increasing in solid volume fraction leads to decrease both of activity of the fluid motion and fluid temperature however, it leads to increase the corresponding average Nusselt number.

Nomenclature: C_p - Specific heat at constant pressure, KJ/kgK, H - Enclosure height, I - x-direction grid point, J - y-direction grid point, Nu -Local Nusselt number, \overline{Nu} - Average Nusselt number, Pr - Prandtl number, Gr -Grashof number, p -pressure, Re -Reynolds number, Ri -Richardson number (Gr/Re^2), k -thermal conductivity, T -dimensional temperature, T_h -dimensional temperature of hot fluid, T_c -dimensional temperature of cold fluid, u - horizontal wall velocity, v - vertical wall velocity, U , V -dimensionless velocity components along (x,y) axes, x , y - cartesian co-ordinates, X , Y dimensionless cartesian co-ordinates, P - dimensionless pressure, g - gravitational acceleration.

Greek symbols: α -effective thermal diffusivity, β - fluid thermal expansion coefficient, θ - dimensionless temperature, $(T-T_c/T_h-T_c)$, μ - effective dynamic viscosity, ν - effective kinematic viscosity (μ/ρ), ρ -density, k - permeability of the porous medium, χ - solid volume fraction

Subscripts: nf - nanofluid, f - fluid, s - solid

References

1. Y. Xuan, Q. Li, Journal of Heat Transfer vol. 125, pp.151–155, 2003.
2. S. Choi, ASME Publications, vol.66, pp.99–105, 1995.
3. Y. Xuan, K. Yu, Q. Li, Progress in Computational Fluid Dynamics, vol.5, pp.13–19, 2005.
4. P. Keblinski, S.R. Phillpot, S.U.S. Choi, J.A. International Journal of Heat and Mass Transfer vol. 45, pp.855–863, 2002.
5. S.K. Das, N. Putra, P. Thiesen, W. Roetzel, Journal of Heat Transfer, vol.125, pp.567–574, 2003.
6. N. Putra, W. Roetzel, S.K. Das, Heat and Mass Transfer vol.39, pp.775–784, 2003.
7. D. Wen, Y. Ding, , IEEE Transport Nanotechnology, vol.5, pp.220–227, 2006.
8. Khanafer, K., Vafai, K., Lightstone, M., Int. J. Heat Mass Transfer, vol.46, pp.3639–3653, 2003.
9. Tiwari, R.K., Das M.K., Int. J. Heat Mass Transfer, vol.50, pp.2002- 2018, 2007.
10. Koo, J., Kleinstreuer, C. Laminar nanofluid flow in microheat-sinks, Int. J. Heat Mass Transfer, vol.48, pp.2652-2661, 2005.
11. Maiga, S.E.B., Nguyen, C.T., Galanis, N., Roy, G. Super lattices Microstructures, vol.35, pp.543-557, 2004.
12. Jou R-Y., Tzeng S-C. Int. Comm. Heat Mass Transfer, vol.33, pp.727-736, 2006.
13. S. Kumar, S.K. Prasad, J. Banerjee, Applied Mathematical Modeling, vol.34, pp.573–592, 2010.
14. F. Talebi, A.H. Mahmoudi, M. Shahi, International Communications in Heat and Mass Transfer, vol.37, pp.79–90, 2010.
15. S.M. Aminossadatia, B. Ghasemi, European Journal of Mechanics B/Fluid, vol.28, pp.630–640, 2009.
16. H.F. Oztop, E. Abu-Nada, International Journal of Heat and Fluid Flow, vol.29, pp.1326–1336, 2008.
17. D. Wen, Y. Ding, International Journal of Heat and Fluid Flow vol. 26, pp.855–864, 2005.
18. A.K. Santra, S. Sen, N. Chakraborty, Journal of Enhanced Heat Transfer, vol.15 pp.273–287, 2008.
19. C.J. Ho, M.W. Chen, Z.W. Li, International Journal of Heat and Mass Transfer, vol.51, pp.4506–4516, 2008.
20. K.S. Hwang, J.H. Lee, S.P. Jang, International Journal of Heat and Mass Transfer, vol.50, pp. 4003–4010, 2007.

21. E. Abu-Nada, Z. Masoud, H. Oztop, A. Campo, *International Journal of Thermal Sciences*, vol. 49, pp.479–491, 2010.
22. P.O. Iwanik, W.K.S. Chiu, *Numerical Heat Transfer A- Application*, vol. 43, no.3, pp. 221–237, 2003.
23. K.O. Lim, K.S. Lee, T.H. Song, *Numerical Heat Transfer A- Application*, vol. 36, no.3, pp.309–325, 1999.
24. S. Singh, M.A.R. Sharif, *Numerical Heat Transfer A- Application*, vol. 44, no. 3, pp. 233–253, 2003.
25. F.L. Tan, S.F. Hosseinizadeh, J.M. Khodadadi, Liwu Fan, *International Journal of Heat and Mass Transfer*, vol.19–20, pp.4105–4116, 2009.
26. P.M. Patil, P.S. Kulkarni, *International Journal of Thermal Science*, vol. 47, no.8, pp.1043–1054, 2008.
27. M. Lamsaadi, M. Naimi, M. Hasnaoui, M. Mamou, *Numerical Heat Transfer A- Application*, vol. 49, no.10, pp. 969–990, 2006.
28. L.K. Saha, M.A. Hossain, R.S.R. Gorla, *International Journal of Thermal Science*, vol.46, no.8, pp. 790–801, 2007.
29. Y.Y. Yang, H.B. Zhang, J.B. Hull, *Numerical Heat Transfer A-Application*, vol. 46, no. 5, pp. 453–471, 2004.

30. T.-H.Hsu, P.-T.Hsu, C.-K. Chen, *International Communications in Heat and Mass Transfer*, vol.22, pp.189–200, 1995.
31. S.G. Rubin, P.K. Khosla, *Journal of Computational Physics*, vol.24, pp. 217–244, 1977.
32. U. Ghia, K.N. Ghia, C.T. Shin, *Journal of Computational Physics*, vol.48, pp. 387–411, 1982.
33. Brinkman, H.C. *The Journal of Chemical Physics*, vol 20, no. 4, pp. 571-581, 1952.
34. Wasap, F.J. *Trans. Tech.: Berlin* 1977.
35. S.V. Patankar, *Numerical Heat Transfer and Fluid Flow*, Hemisphere, New York, 1980.
36. T. Hayase, J. A. C. Humphrey, and R. Greif, *J. Comp. Phys.*, vol. 98, pp. 108–118, 1990.
37. H. K. Versteeg and W. Malalasekera, *An Introduction to Computational Fluid Dynamics, The Finite Volume Method*, Longman, England, UK, 1996.
38. J. P. Van Doormaal and G. D. Raithby, *Numerical Heat Transfer; Part A*, vol.7, pp. 147–163, 1984.
39. G. De Vahl Davis, *Int. Journal for Numerical Methods in Fluids*, vol. 3, pp. 249-264, 1984.
40. Kalita J.C., Dalal D.C. and Dass A.K.(2001). *Phys. Rev. E* 64, 066703, 1-13.
41. P. Nithiarasu, K. N. Seetharamu, and T. Sundararajan, *Inter. J. Heat and Mass Transfer*, vol. 40, pp. 3955–3967, 1997.

An $M/G/1//N$ Gated Vacation Queueing System with Markov Regenerative Approach

R. Jayaraman

Department of Mathematics, P.S.R. Rengasamy College of Engineering for Women, Sivakasi, India.

Abstract

In this paper, we present a Markov Regenerative approach to the $M/G/1$ queueing system with server vacations under a gated discipline. We consider the case of a system with a finite population. We have obtained closed form analytical expressions for the local and global kernels of the system. Simple numerical examples have been given to illustrate the usefulness of the representation given.

Keywords: Markov Regenerative Process, Gated vacation scheme, Evaluation of performance measures.

1 Introduction:

Let us consider an industry where several types of products are manufactured. Each type of product goes through a quality testing process and then finally queues up at a counter where a final seal is affixed testifying to the quality of the product. After attending to the products of one particular type, the supervisor may turn his attention to the products of another type. As far as the first type of product is concerned, the server has proceeded on a vacation. When he returns back to the inspection of the products of the first type, he finds a certain number, say R units awaiting him. He only serves these R units before proceeding to the products of another type. Subsequent units which arrive when he is servicing these R units join the queue, but they are gated off. These units will have to wait until the server returns from a second so-called vacation. This is a typical example of a queueing system with a gated vacation scheme.

Queueing systems with server vacations are used in the study of production, manufacturing and communication and computer networks. Doshi[1] has provided a survey of the available results on vacation queueing systems and has also provided several examples of queueing situations with vacations. We have widely studied the different contexts in literature and refer the reader to Doshi [2], Takagi[6, 7] and Tian and Zhang [9] for details on various vacations systems and further references. Also, we have gone through Langaris et al.[3]and Zhang et al.[8].

The gated service scheme is a non exhaustive type of vacation scheme. Here, the server finds a random number, say R customers. Any further arrivals are gated off, i.e, they have to wait

until the server goes back for his next vacation and returns. Such a vacation scheme has been fairly extensively discussed in the book by Takagi[5].

In this paper, we present a Markov Regenerative approach to the study of the $M/G/1//N$ queueing systems with server vacations under a gated scheme. The explicit closed form expressions provided for the local and global kernels can be efficiently utilized in deriving the transient and the steady state probabilities of the system.

The rest of the paper is organized as follows. In section 2, we present the main features of the Markov Regenerative Processes. In section 3, we analyze the $M/G/1//N$ queueing system using the theory of Markov Regenerative Processes. In section 4, we take up simple numerical examples to illustrate the usefulness of the theory developed in section 3. In section 5, we present a few concluding remarks.

2 Markov Regenerative Processes

A Regenerative Stochastic process has the characteristic property that there exists a sequence of regeneration time points at which the process probabilistically restarts. The essence of regeneration is that the evolution of the process between any two successive regeneration time points is a probabilistic replica of the process between any two other successive regeneration time points. In the presence of mild regularity conditions, the regenerative structure guarantees the existence of a limiting or a steady state distribution, provided that the expected time between regeneration time points is finite. The behavior of a regeneration process between any pair of successive regeneration time points helps to determine the limiting distribution of the process.

Definition 1: A Markov Regeneration Process(MRGP) is a continuous time, discrete state stochastic process with an embedded sequence of Regeneration Time Points(RTPs) T_n at which the process enjoys the Markov property.

Because of the memoryless property of the MRGP at the RTPs, the analysis of a MRGP can be split into independent subproblems, wherein, the subordinated process between any two consecutive RTPs is examined. The probability functions required for the analysis of a MRGP are commonly referred to as the global and local kernels. They are defined as follows. If $\{M(t): t \geq 0\}$ is a MRGP with an embedded sequence of RTPs T_n and a state space, the global kernel is given by

$$K_{ij}(t) = Pr\{M(T_1+) = j, T_1 \leq t / M(0) = i\} \quad (2.1)$$

Here $M(T_1+)$ refers to the state of the system immediately after the end of the first regeneration cycle at the time epoch T_1 . $M(0)$ is the initial state at the beginning of the cycle and $i, j \in \Omega$.

The local kernel is given by the expression

$$E_{ij}(t) = Pr\{M(t) = j, T_1 > t/M(0) = i\} \quad (2.2)$$

If $V_{ij}(t) = Pr\{M(t) = j/M(0) = i\}$, then $V_{ij}(t)$ is given by the renewal equation

$$V_{ij}(t) = E_{ij}(t) + \sum_{k \in \Omega} \int_0^t V_{kj}(t-x) dK_{ik}(x). \quad (2.3)$$

In order to obtain the steady state probabilities of the MRGP, we need to obtain the steady state probabilities of the embedded Markov chain(EMC) at the RTPs. These are obtained as the solution of

$$v = vP, \text{ where } P = K(\infty)$$

$K(\infty)$ is the matrix whose i, j^{th} entry is $K_{ij}(\infty)$. After calculating $v = (v_1, v_2, \dots)$, we compute

$$\alpha_{ij} = \int_0^\infty E_{ij}(t) dt.$$

$$\text{Define } \mu_j = \sum_{k \in \Omega} \alpha_{jk}.$$

The steady state probabilities P_j of the MRGP are given by the

$$P_j = \lim_{t \rightarrow \infty} Pr\{M(t) = j/M(0) = i\} = \frac{\sum_{k \in \Omega} \alpha_{kj} v_k}{\sum_{k \in \Omega} \mu_k v_k} \quad (2.4)$$

3 Markov Regenerative analysis of the M/G/1//N vacation queueing system under a gated vacation scheme

In this section, we consider the analysis of a $M/G/1//N$ queueing system with server vacations under a gated scheme.

The arrivals to the system are in accordance with a Poisson process with a parameter λ . The service times of the individual customers are assumed to be identically independently distributed random variables with a distribution function $B(t)$. The Laplace Stieltjes transform of the distribution is given by

$$\beta(s) = \int_0^\infty e^{-sx} dB(x), \quad \text{Re}(s) > 0$$

The expected service time of a customer in the system is given by

$$-\beta'(0) = \mu$$

We assume that the system has a single service facility. Whenever the server returns back from a vacation, he decides to complete the service of only those customers who are present in the system at the time of his re-entry into the system. The customers who arrive during the course of the service of the customers already waiting, have to wait until the server goes away on a vacation again

and comes back after that vacation. This type of vacation scheme is known as a gated vacation scheme.

In this section, we consider the case where the source population of the system is finite, say N . We assume that initially, the system starts with the server not being available and with j customers in the system. After the completion of the j services the server proceeds on a vacation. The duration of the server vacation is assumed to be exponentially distributed with a parameter γ . After the completion of the vacation, the server returns back to the system and finds a certain number of customers, say k customers awaiting service. He starts servicing them one by one. However, any customer who arrives after his return to the system is not serviced. These customers will have to wait while the server goes back for a vacation for a second time. The state of the system at any instant of time can be represented by the vector $(C(t), X(t), Y(t))$ where

$C(t)$ = The state of the server at any instant of time t ,

$$\text{where } C(t) = \begin{cases} 0, & \text{if the server is idle} \\ 1, & \text{if the server is busy} \end{cases}$$

$X(t)$ = Number of customers awaiting service in the system.

$Y(t)$ = Number of customers who arrive

after the return of the server from a vacation.

When the server goes back for the next vacation $X(t)$ becomes 0. At this instant of time we transfer the value of $Y(t)$ to $X(t)$ and put $Y(t)=0$.

Therefore, $Y(t) = 0$ whenever $C(t) = 0$. So, the state space of this system is therefore given by

$$\Omega = \{(0, r, 0) : 0 \leq r \leq N\} \cup \{(1, r, s) : 1 \leq r \leq N, 0 \leq s \leq N - r\}$$

The stochastic process $(C(t), X(t), Y(t))$ can be made into a Markov Regenerative Process by defining the regeneration time points T_n as follows:

1. Define $T_0 = 0$.

2. If, at the n^{th} regeneration point T_n , the process is in the state $(0, r, 0)$, the server is not available for service in the system. The next regeneration time point T_{n+1} is defined as the instant of time at which the next state change occurs. This could be due to the arrival of a fresh customer to the system or due to the return of the server back from his vacation.

3. If at the n^{th} regeneration point T_n , the process is in the state $(1, r, s)$ with $1 \leq r \leq N$ and $0 \leq s \leq N - r$, the server is available for service. The next regeneration time point T_{n+1} is therefore defined as the instant of time at which a service completion occurs.

In this case, the process in between the two regeneration time points T_n, T_{n+1} is a Markov process with a state space

$$\Omega(1, r, s) = \{(1, r, s') : s \leq s' \leq N - r\}$$

The infinitesimal generator of this subordinated process is a square matrix $Q = [q_{ij}]$ of order $N - r - s + 1$. Its entries are as follows.

For $1 \leq i \leq N - r - s$

$$q_{i,j} = 0 \quad \text{for } j \neq i, i + 1$$

$$q_{i,i} = -[N - (r + s + i - 1)]\lambda$$

$$q_{i,i+1} = [N - (r + s + i - 1)]\lambda$$

The $N - r - s + 1_{th}$ row is a zero row.

Arranging the states of the system in a lexicographic order, we can take the state space Ω as follows:

$$\Omega = \{i : 1 \leq i \leq \frac{(N+1)(N+2)}{2}\}$$

where the state $(1, k, s)$ corresponds to $kN + s + 2 - \frac{k^2 - 3k + 2}{2}$ with $1 \leq k \leq N, 0 \leq s \leq N - k$.

In order to obtain the transient and steady state solution of the queueing system, we have to obtain the expressions for the local and global kernels of the Markov Regenerative process.

The behavior of a subordinated process inside a regeneration cycle beginning in one of the states i with $i \geq N + 2$ is characterized by the following theorem.

Theorem.1: In an $M/G/1//N$ queueing system with vacations under a gated scheme, the subordinated process inside a regeneration cycle beginning in the state $i = kN + s + 2 - \frac{k^2 - 3k + 2}{2}$ for some $1 \leq k \leq N$ and some $0 \leq s \leq N - k$, is a pure birth process with a state space

$$\Omega(i) = \{j : j = i + s' - s \quad \text{with } s \leq s' \leq N - k\}$$

If P_{ij} = probability of the process being in the state j having started in the state i , then

$$P_{ii}(t) = e^{-(N-(k+s))\lambda t} \tag{3.1}$$

$$P_{ij}(t) = \frac{(N-(k+s))(N-(k+s+1))\dots(N-(k+s'-1))}{(s'-s)!} e^{-(N-(k+s))\lambda t} (e^{\lambda t} - 1)^{s'-s} \quad (3.2)$$

Proof: When the regeneration cycle begins in the state $i = kN + s + 2 - \frac{k^2-3k+2}{2}$, the server is available for service, $X(t) = k, Y(t) = s$.

Here $1 \leq k \leq N$ and $0 \leq s \leq N - k$. The cycle ends with the completion of one service. Thus, the only state changes inside a regeneration cycle are due to the arrival of new customers for service. These customers will not however be served until the server goes away for his next vacation and returns. Thus, the only state changes can be due to an increase in the value of $Y(t)$ from s upto a maximum of $N - k$. The arrival process has been assumed to be a Poisson process with a parameter λ . Therefore, the subordinated process inside the regeneration cycle can only be a pure birth process. The probabilities are given by equation (3.1) and (3.2).

The above theorem allows us to determine the local and global kernels of the system.

Theorem.2: The expressions for the local kernel $E_{ij}(t)$ of the $M/G/1//N$ queueing system with a gated vacation scheme are given by the following expressions.

(a) When the regeneration cycle begins in the state i with $1 \leq i \leq N + 1$,

$$E_{ij}(t) = 0, j \neq i \quad (3.3)$$

$$E_{ii}(t) = e^{-[(N-(i-1))\lambda + \gamma]t} \quad (3.4)$$

(b) When the regeneration cycle begins in one of the states

$$i = kN + s + 2 - \frac{k^2-3k+2}{2} \text{ with } 1 \leq k \leq N, 0 \leq s \leq N - k$$

$$E_{ij}(t) = 0 \text{ for } j \neq i + s' - s \text{ with } s \leq s' \leq N - k \quad (3.5)$$

$$E_{ii}(t) = e^{-[N-(k+s)]\lambda t} (1 - B(t)) \quad (3.6)$$

For $j = i + s' - s$ with $s < s' \leq N - k$,

$$E_{ij}(t) = \frac{(N-(k+s))(N-(k+s+1))\dots(N-(k+s'-1))}{(s'-s)!} e^{-[N-(k+s)]\lambda t} (e^{\lambda t} - 1)^{s'-s} (1 - B(t)) \quad (3.7)$$

Proof:

a) When the regeneration cycle begins in the state i with $1 \leq i \leq N+1$ there are $i - 1$ customers awaiting service and the service cannot be performed because of the absence of the server from the system. The cycle therefore ends with the next change of state. Hence there are no state changes inside the regeneration cycle. Therefore, equation(3.3) follows.

The next change of state could be either due to an arrival of a customer into the system or due to the return of the server back from his vacation.

The arrival process has been assumed to be a Poisson process with a parameter λ and the duration of the server vacation is exponentially distributed with a parameter γ . Therefore equation (3.4) follows.

(b) When the regeneration cycle begins in a state $i = kN + s + 2 - \frac{k^2 - 3k + 2}{2}$ with $1 \leq k \leq N$ and $0 \leq s \leq N - k$

$$C(0) = 1, X(0) = k, Y(0) = s.$$

The regeneration cycle ends with the completion of a service.

The only state changes inside the regeneration cycle could be due to the arrival of customers into the system. These arrivals will increase the value of $Y(t)$. Thus the state i can change to a state $j = i + s' - s$ where $s \leq s' \leq N - k$. Therefore equation(3.5) as follows.

For $j = i + s' - s$ with $s \leq s' \leq N - k$,

$$E_{ij}(t) = p_{ij}(t)(1 - B(t))$$

Therefore equations (3.6) and (3.7) follows

The expressions for the global kernel of the system are given by the following theorem.

Theorem.3: The global kernel of the M/G/1//N queueing system with a gated vacation scheme are as given below.

(a)When the regeneration cycle begins in one of the states i with

$$1 \leq i \leq N + 1,$$

$$K_{ij}(t) = 0 \quad \text{for } j \neq i + 1, (i - 1)N - \frac{i^2 - 5i + 2}{2} \quad (3.8)$$

$$K_{i,i+1}(t) = \frac{(N-(i-1))\lambda}{(N-i+1)\lambda+\gamma} [1 - e^{-[(N-i+1)\lambda+\gamma]t}] \quad (3.9)$$

$$\text{For } j = (i - 1)N - \frac{i^2 - 5i + 2}{2}$$

$$K_{ij}(t) = \frac{\gamma}{(N-i+1)\lambda+\gamma} [1 - e^{-[(N-i+1)\lambda+\gamma]t}] \quad (3.10)$$

(b) When the regeneration cycle begins in one of the states $i = kN + s + 2 - \frac{k^2 - 3k + 2}{2}$ with $1 \leq k \leq N$ and $0 \leq s \leq N - k$,

$$K_{i,j}(t) = 0 \quad \text{for } j \neq i + s' - s - N + k - 2 \quad \text{with } s \leq s' \leq N - k \quad (3.11)$$

For $j = i + s' - s - N - k - 2$ with $s < s' \leq N - k$,

$$K_{i,j}(t) = \frac{(N-(k+s))(N-(k+s+1)) \cdots (N-(k+s'-1))}{(s'-s)!} \int_0^t (e^{\lambda x} - 1)^{s'-s} e^{-(N-(k+s))\lambda x} dB(x) \quad (3.12)$$

For $j = i + k - N - 2$

$$K_{i,j}(t) = \int_0^t e^{-(N-(k+s))\lambda x} dB(x) \quad (3.13)$$

Proof: (a) When the regeneration cycle begins in the state i with $1 \leq i \leq N + 1$, the server is not available in the system. The regeneration cycle ends with the next change of state. If this occurs because of an arrival into the system the state i becomes $i+1$. If the server returns back from his vacation, the state i changes to $(i - 1)N + 2 - \frac{(i-1)^2 - 3(i-1) + 2}{2} = (i - 1)N - \frac{i^2 - 5i + 2}{2}$

Therefore equations (3.8),(3.9),(3.10) follow.

(b) When the regeneration cycle begins in the state $i = kN + s + 2 - \frac{k^2 - 3k + 2}{2}$ with $1 \leq k \leq N$, $0 \leq s \leq N - k$, then $C(0) = 1, X(0) = k, Y(0) = s$.

The regeneration cycle ends with the completion of a service. Let us assume that this service completion occurs at an instant of time lying between x and $x + dx$ where $0 \leq x \leq t$. Let us assume that at the epoch of service completion, the state of the system has changed because of the arrival of $s' - s$ customers into the system. After the service completion, there will be $k - 1$ customers who have to be necessarily served before the server proceeds on his next vacation. The number of gated customers will increase to s' . The system will therefore be in the state $(k - 1)N + s' + 2 - \frac{(k-1)^2 - 3(k-1) + 2}{2} = i + k + s' - N - s - 2$

Therefore equation(3.11) follows.

$$\text{For } j = i + k - N - 2, K_{i,j}(t) = \int_0^t P_{ii}(x) dB(x)$$

Therefore equation(3.12) follows.

For $j = i + k + s' - s - N - 2$ with $s < s' \leq N - k$

$K_{ij}(t) = \int_0^t P_{i,i+s'-s} dB(x)$. Therefore equation(3.13) as follows.

The expressions of the local and global kernels can be used to obtain the transient probabilities. The formula given in equation(2.4) can be used to determine the steady state probabilities P_n , $1 \leq n \leq \frac{(N+1)(N+2)}{2}$ of the system. Since we assume that the system has a finite population, it can be assumed to be ergodic. Some useful performance measures which have been derived for numerical examples in section 4 are as follows.

$$\begin{aligned} \lambda_{eff} &= \text{Effective arrival rate} \\ &= \text{Number of arrivals per unit time} \\ &= \lambda \left[\sum_{i=1}^{N+1} (N-i+1)P_i + \sum_{k=1}^N \sum_{s=0}^{N-k} (N-(k+s))P_{kN+s+2-\frac{k^2-3k+2}{2}} \right] \end{aligned}$$

$$\begin{aligned} L_s &= \text{Expected number of customers in the system} \\ &= \left[\sum_{r=1}^{N+1} (r-1)P_r + \sum_{k=1}^N \sum_{s=0}^{N-k} (k+s)P_{kN+s+2-\frac{k^2-3k+2}{2}} \right] \end{aligned}$$

$$\begin{aligned} W_s &= \text{Mean response time} \\ &= \text{Expected waiting time in the system} \\ &= \frac{L_s}{\lambda_{eff}} \text{ (By Little's formula)} \end{aligned}$$

$$\begin{aligned} \mu_v &= \text{Expected number of vacations per unit time} \\ &= \gamma \sum_{r=1}^{N+1} P_r \end{aligned}$$

$$\begin{aligned} W_t &= \text{Expected busy time of the server in an} \\ &\text{interval of time length } t \text{ units} \\ &= t \sum_{k=1}^N \sum_{s=0}^{N-k} P_{kN+s+2-\frac{k^2-3k+2}{2}} \end{aligned}$$

In the next section, we will take up simple examples to illustrate the applicability of the results given in this section.

4 Numerical Examples

In this section, we present two numerical examples to illustrate as to how the theory developed in the previous section can be used to obtain useful performance measures for the vacation queueing system considered in section 3.

Example 1:

In this example, we take up the case of the $M/G/1/3$ queueing system. In this model, the server takes vacations under a gated vacation scheme. The state space of the process $(C(t), X(t), Y(t))$ consists of the following ten elements.

$$M_i = (0, i, 0), \text{ for } i = 0, 1, 2, 3.$$

$$M_i = (1, 1, i - 4), \text{ for } i = 4, 5, 6.$$

$$M_i = (1, 2, i - 7), \text{ for } i = 7, 8$$

$$M_9 = (1, 3, 0)$$

We shall use the letter i to denote the state M_i .

In table 1, we give the values of the steady state probabilities. We have used a deterministic service time distribution with an expected service time μ . For these values of μ and γ , the minimum probability corresponds to the state M_0 and the maximum probability corresponds to the state M_3 .

Table 1: Steady state probabilities for the $M/G/1/3$ queueing systems with the gated service discipline

$$\lambda = 1.0$$

		$\gamma = \frac{1}{3}$
P_n	$\mu=1.5$	$\mu = 1.6$
0	0.000596	0.000426
1	0.016275	0.014005
2	0.102630	0.099131
3	0.307891	0.297394
4	0.017084	0.015038

5	0.104288	0.104163
6	0.092025	0.099748
7	0.106307	0.105489
8	0.098953	0.105991
9	0.153945	0.158610

Example 2:

In this example, we have calculated some performance measures of the queueing system considered in example 1. We have considered 3 types of service time distributions namely, the deterministic distribution, the three phase Erlang distribution and the hyper exponential distribution. In all the three cases, we have taken the same value for the expected service time μ of the server. Table 2 gives the values of the performance measures of the system. We have taken $\lambda = 1.0$ and $\gamma = 1/3$.

Table 2: Performance measures of the $M/G/1/3$ vacation queueing systems with the gated service discipline

Type	Distribution	W_s	μ_v	W_t
	Deterministic	7.54143	0.14246	3.43563
$\mu = 1.5$	Three Phase Erlang	7.85325	0.14338	3.41908
	Hyper Exponential	8.55134	0.14545	3.38175
	Deterministic	7.78066	0.136986	3.53425
$\mu = 1.6$	Three Phase Erlang	8.10507	0.13789	3.51790
	Hyper exponential	8.83110	0.13995	3.51790
	Deterministic	8.02507	0.13191	3.62553
$\mu = 1.7$	Three Phase	8.36062	0.13280	3.62553

	Erlang			
	Hyper exponential	9.11274	0.13484	3.60949

From table 2, we see that the mean response time is minimum for the deterministic distribution and a maximum for the hyper exponential distribution for the same value of μ . The expected busy period of the server W_t therefore maximum for the deterministic distribution and minimum for the hyper exponential distribution. In all the three cases, it is seen that as the expected service time μ increases, the mean response time W_s and the expected busy period of the server W_t both increase.

5 Concluding Remarks

In this paper, we have used the theory of Markov Regenerative Processes to analyse the $M/G/1/3$ queueing system with server vacations under a gated vacation scheme. We have taken up a system with a finite population. However, not many results are available for models with a finite system population. Also, a lot of work remains to be done regarding the transient behaviour of such queueing systems.

In our future work, we hope to use our approach to the queueing systems to obtain the stochastic decomposition of these models. We also hope to derive analytical expressions for the waiting time distribution of a customer in the system and expressions for the busy period of the server.

References

- [1] Doshi, B.T., *Queueing system with vacations-a survey*, Queueing Systems, **1**, 29-66, 1986.
- [2] Doshi, B.T., *Single server queues with vacations*, in: H. Takagi (Ed.), *Stochastic Analysis of Computer and Communication Systems*, Elsevier Science Publishers B.V. (North-Holland), Amsterdam, 217-265, 1990.
- [3] Langaris, C. and Katsaros, A., *An M/G/l Queue with finite population and gated service discipline*, Journal of the Operations Research, **40**(1), 133-139, 1997.
- [4] J. Medhi., *Stochastic Models in queueing theory*, Second Edition, Academic press, 2002.
- [5] Takagi, H., *A survey of queueing analysis of polling models*, ACM computing surveys (CSUR), **20**(1), 5-28, 1988.
- [6] Takagi, H., *Queueing Analysis - A foundation of Performance Evaluation*, vol. 1, Elsevier Science Publishers B.V., 1991.
- [7] Takagi, H., *Queueing Analysis - A foundation of Performance Evaluation*, vol. 3, Elsevier Science Publishers B.V., 1993.
- [8] Zhang, Y., and Yue. D. and Yue. w., *Analysis of an M/M/1/N Queue with Balking, Reneging and Server Vacations*, International Symposium on OR and Its Applications, 37-47, 2005.
- [9] Tian, N. and Zhang, Z. G., *Vacation Queueing Models -Theory and Applications*, Springer Science, 2006.

Enhanced Information Retrieval and Storage of RDF Graph in Clouds

Pramod Mathew Jacob¹ and S. Jagadeesan²

¹Software Engineering and ²Computer Science and Engineering
SRM University, Chennai, India

Abstract— Cloud computing is an emerging paradigm in IT and data processing organizations. User can store and access data at remote locations using clouds. Challenges faced by cloud service providers is to maintain huge quantities of heterogenous data for providing efficient information retrieval. Solutions are to implement scalability and enhance query efficiency. In cloud computing semantic web technologies are used to present data in standardized way so that data can be retrieved and understood by both human and machine. Prominent standard includes Resource Description Framework (RDF) and SPARQL protocol and RDF Query language (SPARQL). RDF is the standard for storing & representing data and SPARQL is a query language to retrieve data from RDF store. But the drawbacks in this system is that we cannot achieve scalability as well as the response time is also slow. A distributed system can be built to overcome scalability and performance problems using distributed databases which uses relational schema for storing RDF data. Disadvantage is that they may not perform well for RDF data since they are sets of triples.

So we go for a new system architecture which consists of 2 components : Data preprocessing component and query processing component. Data processing component convert the RDF/XML to N-Triples using N-Triple converter. Predicate Split(PS) component takes the N- Triples data and splits into predicate files which are then fed to Predicate Object Split(POS) component which splits predicate files into smaller files based on type of objects. Map reduce framework takes the SPARQL query from the user and passes it to Input Selector & Plan Generator. It selects the input files by using the proposed algorithm which performs the needed map reduce jobs and passes information to Join Executer Component. The proposed system will improve the scalability and better query efficiency than any other methodologies that are used for retrieving RDF data. The proposed system will perform the above said functions with optimal time and cost bounds which is beneficial for cloud service providers to provide better facility to their users.

1. INTRODUCTION

Semantic web and Cloud computing is an emerging paradigm in the IT and data processing communities. Enterprises utilize cloud computing service to outsource data maintenance, which can result in significant financial benefits. Businesses store and access data at remote locations in the “cloud.” As the popularity of cloud computing grows, the service providers face ever increasing challenges. They have to maintain huge quantities of heterogenous data while providing efficient information retrieval. Thus, the key emphasis for cloud computing solutions is scalability and query efficiency. Semantic web technologies are being developed to present data in standardized way such that such data can be retrieved and understood by both human and machine. Historically, webpages are published in plain html files which are not suitable for reasoning. Instead, the machine treats these html files as a bag of keywords. Researchers are developing Semantic web technologies that have been standardized to address such inadequacies. The most prominent standards are

Resource Description Framework¹ (RDF) and SPARQL Protocol and RDF Query Language² (SPARQL). RDF is the standard for storing and representing data and SPARQL is a query language to retrieve data from an RDF store. Cloud Computing systems can utilize the power of these Semantic web technologies to provide the user with capability to efficiently store and retrieve data for data intensive applications. Semantic web technologies could be especially useful for maintaining data in the cloud. Semantic web technologies provide the ability to specify and query heterogeneous data in a standardized manner. Moreover, via Web Ontology Language (OWL) ontologies, different schemas, classes, data types, and relationships can be specified without sacrificing the standard RDF/SPARQL interface.

Our contributions are as follows:

1. We design a storage scheme to store RDF data in Hadoop distributed file system (HDFS).
2. We propose an algorithm that is guaranteed to provide a query plan whose cost is bounded by the log of the total number of variables in the given SPARQL query. It uses summary statistics for estimating join selectivity to break ties.
3. We build a framework which is highly scalable and fault tolerant and supports data intensive query processing.
4. We demonstrate that our approach performs better than Jena for all queries and BigOWLIM and RDF-3X for complex queries having large result sets. The remainder of this paper is organized as follows: in Section 2, we investigate related work. In Section 3, we discuss our system architecture. In Section 4, we discuss how we answer an SPARQL query. In Section 5, we present the results of our experiments. Finally, in Section 6, we draw some conclusions and discuss areas we have identified for improvement in the future.

2. RELATED WORK

MapReduce, though a programming paradigm, is rapidly being adopted by researchers. This technology is becoming increasingly popular in the community which handles large amounts of data. It is the most promising technology to solve the performance issues researchers are facing in Cloud Computing. In [1], Abadi discusses how MapReduce can satisfy most of the requirements to build an ideal Cloud DBMS. Researchers and enterprises are using MapReduce technology for web indexing, searches, and data mining. In this section, we will first investigate research related to MapReduce. Next, we will discuss works related to the semantic web. Google uses MapReduce for web indexing, data storage, and social networking. Yahoo! uses MapReduce extensively in its data analysis tasks. IBM has successfully experimented with a scale-up scale-out search framework using MapReduce technology. In a recent work, they have reported how they integrated Hadoop and System R. Teradata did a similar work by integrating Hadoop with a parallel DBMS. Researchers have used MapReduce to scale up classifiers for mining petabytes of data. They have worked on data distribution and partitioning for data mining, and have applied three data mining algorithms to test the performance. Data mining algorithms are being rewritten in different forms to take advantage of MapReduce technology. Researchers rewrite well-known machine learning algorithms to take advantage of multicore machines by leveraging MapReduce programming paradigm. Another area

where this technology is successfully being used is simulation. In [4], researchers reported an interesting idea of combining MapReduce with existing relational database techniques. These works differ from our research in that we use MapReduce for semantic web technologies. Our focus is on developing a scalable solution for storing RDF data and retrieving them by SPARQL queries.

In the semantic web arena, there has not been much work done with MapReduce technology. We have found two related projects: BioMANTA¹¹ project and Scalable, High-Performance, Robust and Distributed (SHARD).¹² BioMANTA proposes extensions to RDF Molecules and implements a MapReduce-based Molecule store. They use MapReduce to answer the queries. They have queried a maximum of four million triples. Our work differs in the following ways: first, we have queried one billion triples. Second, we have devised a storage schema which is tailored to improve query execution performance for RDF data. We store RDF triples in files based on the predicate of the triple and the type of the object. Finally, we also have an algorithm to determine a query processing plan whose cost is bounded by the log of the total number of variables in the given SPARQL query. By using this, we can determine the input files of a job and the order in which they should be run. To the best of our knowledge, we are the first ones to come up with a storage schema for RDF data using flat files in HDFS, and a MapReduce job determination algorithm to answer an SPARQL query. As our experiments show it does not perform well when there is no bound object in a query. However, the performance of our framework is not affected in such a case. RDF-3X is considered the fastest existing semantic web repository. In other words, it has the fastest query times. RDF-3X uses histograms, summary statistics, and query optimization to enable high performance semantic web queries. As a result, RDF-3X is generally able to outperform any other solution for queries with bound objects and aggregate queries. However, RDF-3X's performance degrades exponentially for unbound queries, and queries with even simple joins if the selectivity factor is low. This becomes increasingly relevant for inference queries, which generally require unions of subqueries with unbound objects. Our experiments show that RDF-3X is not only slower for such queries, it often aborts and cannot complete the query. For example, consider the simple query "Select all students." This query in LUBM requires us to select all graduate students, select all undergraduate students, and union the results together. However, there are a very large number of results in this union. While both subqueries complete easily, the union will abort in RDF-3X for LUBM (30,000) with 3.3 billion triples. RDF Knowledge Base (RDFKB) is a semantic web repository using a relational database schema built upon bit vectors. RDFKB achieves better query performance than RDF-3X or vertical partitioning. However, RDFKB aims to provide knowledge base functions such as inference forward chaining, uncertainty reasoning, and ontology alignment. RDFKB prioritizes these goals ahead of scalability. RDFKB is

not able to load LUBM (30,000) with three billion triples, so it

cannot compete with our solution for scalability. Hexastore and BitMat [5] are main memory data structures optimized for RDF indexing. These solutions may achieve exceptional performance on hot runs, but they are not optimized for cold runs from persistent storage. Furthermore, their scalability is directly associated with the quantity of main memory RAM available. These products are not available for testing and evaluation. In our previous works we proposed a greedy and an exhaustive search algorithm to generate a query processing plan. However, the exhaustive search algorithm was expensive and the greedy one was not bounded and its theoretical complexity was not defined. In this paper, we present a new greedy algorithm with an upper bound. Also, we did observe

scenarios in which our old greedy algorithm failed to generate the optimal plan. The new algorithm is able to obtain the optimal plan in each of these cases. Furthermore, in our prior research, we were limited to text files with minimal partitioning and indexing. We now utilize dictionary encoding to increase performance. We have also now done comparison evaluation with more alternative repositories.

3. PROPOSED SYSTEM ARCHITECTURE

Our architecture consists of two components. The upper part of Fig. 1 depicts the data preprocessing component and the lower part shows the query answering one. We have three subcomponents for data generation and preprocessing. We convert RDF/XML¹³ to N-Triples¹⁴ serialization format using our N-Triples Converter component. The Predicate Split (PS) component takes the Ntriples data and splits it into predicate files. The predicate files are then fed into the Predicate Object Split (POS) component which splits the predicate files into smaller files based on the type of objects. These steps are described in Sections 3.2, 3.3, and 3.4. Our MapReduce framework has three subcomponents in it. It takes the SPARQL query from the user and passes it to the Input Selector (see Section 4.1) and Plan Generator. This component selects the input files, by using our algorithm described in Section 4.3, decides how many MapReduce jobs are needed, and passes the information to the Join Executer component which runs the jobs using MapReduce framework. It then relays the query answer from Hadoop to the user.

For our experiments, we use the LUBM [2] data set. It is a benchmark data set designed to enable researchers to evaluate a semantic web repository's performance [4]. The LUBM data generator generates data in RDF/XML serialization format. This format is not suitable for our purpose because we store data in HDFS as flat files and so to retrieve even a single triple, we would need to parse the entire file.

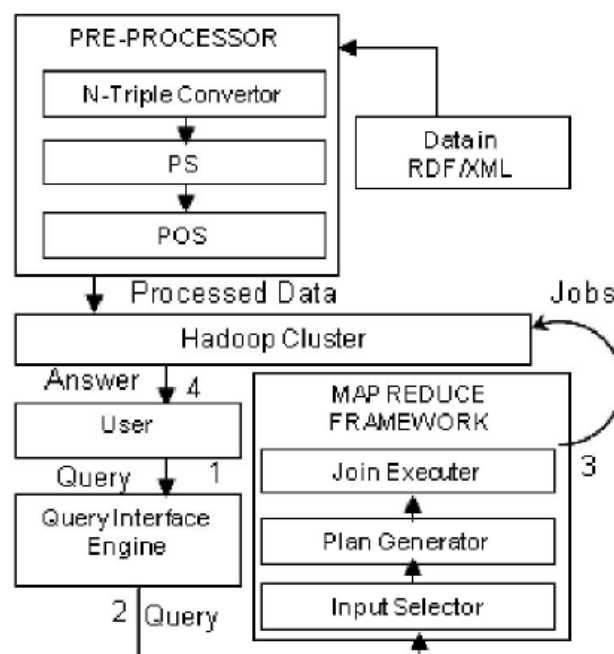


Fig 1. The System Architecture

3.1 Data Generation and Storage

Therefore, we convert the data to N-Triples to store the data, because with that format, we have a complete RDF triple (Subject, Predicate, and Object) in one line of a file, which is very convenient to use with MapReduce jobs. The processing steps to go through to get the data into our intended format are described in following sections.

3.2 File Organization

We do not store the data in a single file because, in Hadoop and MapReduce Framework, a file is the smallest unit of input to a MapReduce job and, in the absence of caching, a file is always read from the disk. If we have all the data in one file, the whole file will be input to jobs for each query. Instead, we divide the data into multiple smaller files. The splitting is done in two steps which we discuss in the following sections.

3.3 Predicate Split

In the first step, we divide the data according to the predicates. This division immediately enables us to cut down the search space for any SPARQL query which does not have a variable¹⁵ predicate. For such a query, we can just pick a file for each predicate and run the query on those files only. For simplicity, we name the files with predicates, e.g., all the triples containing a predicate `p1:pred` go into a file named `p1-pred`. However, in case we have a variable predicate in a triple pattern¹⁶ and if we cannot determine the type of the object, we have to consider all files. If we can determine the type of the object, then we consider all files having that type of object. We discuss more on this in Section 4.1. In real-world RDF data sets, the number of distinct predicates is in general not a large number [3]. However, there are data sets having many predicates. Our system performance does not vary in such a case because we just select files related to the predicates specified in a SPARQL query.

3.4 Predicate Object Split

In the next step, we work with the explicit type information in the `rdf_type` file. The predicate `rdf:type` is used in RDF to denote that a resource is an instance of a class. The `rdf_type` file is first divided into as many files as the number of distinct objects the `rdf:type` predicate has. Then it is splitted to objects.

4. MAPREDUCE FRAMEWORK

In this section, we discuss how we answer SPARQL queries in our MapReduce framework component. Section 4.1 discusses our algorithm to select input files for answering the query. Section 4.2 talks about cost estimation needed to generate a plan to answer an SPARQL query. It introduces few terms which we use in the following discussions. Section 4.2.1 discusses the ideal model we should follow to estimate the cost of a plan. Section 4.2.2 introduces the heuristics-based model we use in practice. Section 4.3 presents our heuristics-based greedy algorithm to generate a query plan which uses the cost model introduced in Section 4.2.2. We face tie situations in order to generate a plan in some cases and Section 4.4 talks about how we handle these special cases. Section 4.5 shows how we implement a join in a Hadoop MapReduce job by working through an example query.

4.1 Input Files Selection

Before determining the jobs, we select the files that need to be inputted to the jobs. We have some query rewriting capability which we apply at this step of query processing. We take the query submitted by the user and iterate over the triple patterns. We may encounter the following cases:

1. In a triple pattern, if the predicate is variable, we select all the files as input to the jobs and terminate the iteration.

2. If the predicate is `rdf:type` and the object is concrete, we select the type file having that particular type. For example, for LUBM query 9 (Listing 1), we could select file `type_Student` as part of the input set. However, this brings up an interesting scenario. In our data set, there is actually no file named `type_Student` because `Student` class is not a leaf in the

ontology tree. In this case, we consult the LUBM ontology,¹⁷ part of which is shown in Fig. 2, to determine the correct set of input files. We add the files `type_GraduateStudent`, `type_UndergraduateStudent`, and `type_ResearchAssistant` as `GraduateStudent`, `UndergraduateStudent`, and `ResearchAssistant` are the leaves of the subtree rooted at node `Student`.

3. If the predicate is `rdf:type` and the object is variable, then if the type of the variable is defined by another triple pattern, we select the type file having that particular type. Otherwise, we select all type files.

4. If the predicate is not `rdf:type` and the object is variable, then we need to determine if the type of the object is specified by another triple pattern in the query. In this case, we can rewrite the query eliminate some joins. For example, in LUBM Query 9 (Listing 1), the type of `Y` is specified as `Faculty` and `Z` as `Course` and these variables are used as objects in last three triple patterns. If we choose files `advisor_Lecturer`, `advisor_PostDoc`, `advisor_FullProfessor`, `advisor_AssociateProfessor`, `advisor_AssistantProfessor`, and `advisor_VisitingProfessor` as part of the input set, then the triple pattern in line 2 becomes unnecessary. Similarly, triple pattern in line 3 becomes unnecessary if files `takesCourse_Course` and `takesCourse_GraduateCourse` are chosen. Hence, we get the rewritten query shown in Listing 2. However, if the type of the

object is not specified, then we select all files for that predicate.

5. If the predicate is not `rdf:type` and the object is concrete, then we select all files for that predicate

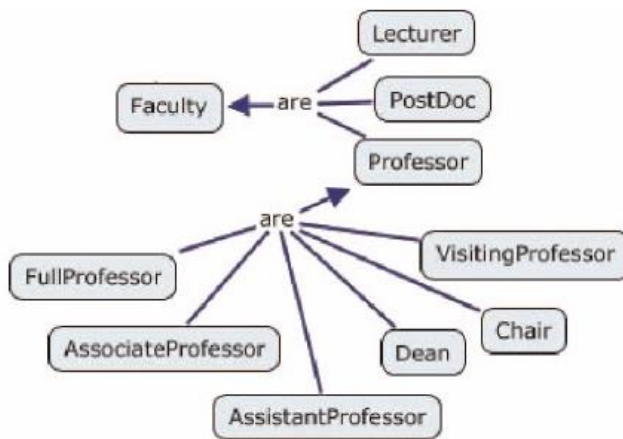


Fig 2. Partial LUBM ontology

4.5 MapReduce Join Execution

In this section, we discuss how we implement the joins needed to answer SPARQL queries using MapReduce framework of Hadoop. Algorithm 1 determines the number of jobs required to answer a query. It returns an ordered set of jobs. Each job has associated input information. The Job Handler component of our MapReduce framework runs the jobs in the sequence they appear in the ordered set. The output file of one job is the input of the next. The output file of the last job has the answer to the query. Listing 7 shows LUBM Query 2, which we will use to illustrate the way we do a join using map and reduce methods. The query has six triple patterns and nine joins between them on the variables X, Y, and Z. Our input selection algorithm selects files `type_GraduateStudent`, `type_University`, `type_Department`, all files having the prefix `memberOf`, all files having the prefix `subOrganizationOf`, and all files having the prefix `undergraduateDegreeFrom` as the input to the jobs needed to answer the query.

Listing 7. LUBM Query 2

```
SELECT ?X, ?Y, ?Z WHERE {  
  
?X rdf:type ub:GraduateStudent.  
  
?Y rdf:type ub:University.  
  
?Z rdf:type ub:Department.  
  
?X ub:memberOf ?Z.  
  
?Z ub:subOrganizationOf ?Y.  
  
?X ub:undergraduateDegreeFrom ?Y}
```


The query plan has two jobs. In job 1, triple patterns of lines 2, 5, and 7 are joined on X and triple patterns of lines 3 and 6 are joined on Y. In job 2, triple pattern of line 4 is joined with the outputs of previous two joins on Z and also the join outputs of job 1 are joined on Y. The input files of job 1 are type_GraduateStudent, type_University, all files having the prefix memberOf, all files having the prefix subOrganizationOf, and all files having the prefix underGraduateDegreeFrom. In the map phase, we first tokenize the input value which is actually a line of the input file. Then, we check the input file name and, if input is from type_GraduateStudent, we output a key-value pair having the subject URI prefixed with X# the key and a flag string GS# as the value. The value serves as a flag to indicate that the key is of type GraduateStudent. The subject URI is the first token returned by the tokenizer. Similarly, for input from file type_University output a key-value pair having the subject URI prefixed with Y# the key and a flag string U# as the value. If the input from any file has the prefix memberOf, we retrieve the subject and object from the input line by the tokenizer and output a key-value pair having the subject URI prefixed with X# the key and the object value prefixed with MO# as the value. For input from files having the prefix subOrganizationOf, we output key-value pairs making the object prefixed with Y# the key and the subject prefixed with SO# the value. For input from files having the prefix underGraduateDegreeFrom, we output key-value pairs making

the subject URI prefixed with X# the key and the object value prefixed with UDF# the value. Hence, we make either the subject or the object a map output key based on which we are joining. This is the reason why the object is made the key for the triples from files having the prefix subOrganizationOf because the joining variable Y is an object in the triple pattern in line 6. For all other inputs, the subject is made the key because the joining variables X and Y are subjects in the triple patterns in lines 2, 3, 5, and 7. In the reduce phase, Hadoop groups all the values for a single key and for each key provides the key and an iterator to the values collection. Looking at the prefix, we can immediately tell if it is a value for X or Y because of the prefixes we used. In either case, we output a key-value pair using the same key and concatenating all the values to make a string value. So, after this reduce phase, join on X is complete and on Y is partially complete. The input files of job 2 are type_Department file and the output file of job 1, job1.out. Like the map phase of job 1, in the map phase of job 2, we also tokenize the input value which is actually a line of the input file. Then, we check the input file name and, if input is from type_Department, we output a key-value pair having the subject URI

prefixed with Z# the key and a flag string D# as the value. If the input is from job1.out, we find the value having the prefix Z#. We make this value the output key and concatenate rest of the values to make a string and make it the output value. Basically, we make the Z# values the keys to join on Z. In the reduce phase, we know that the key is the value for Z. The values collection has two types of strings. One has X values, which are URIs for graduate students and also Y values from which they got their undergraduate degree. The Z value, i.e., the key, may or may not be a subOrganizationOf the Y value. The other types of strings have only Y values which are universities and of which the Z value is a suborganization. We iterate over the values collection and then join the two types of tuples on Y values. From the join output, we find the result tuples which have values for X, Y, and Z.

5 RESULTS

In this section, we first present the benchmark data sets with which we experimented. Next, we present the alternative repositories we evaluated for comparison. Then, we detail our experimental setup. Finally, we present our evaluation results.

5.1 Data Sets

In our experiments with SPARQL query processing, we use two synthetic data sets: LUBM and SP2B. The LUBM data set generates data about universities by using an ontology.²⁰ It has 14 standard queries. Some of the queries require inference to answer. The LUBM data set is very good for both inference and scalability testing. For all LUBM data sets, we used the default seed. The SP2B data set is good for scalability testing with complex queries and data access patterns. It has 16 queries most of which have complex structures.

5.2 Baseline Frameworks

We compared our framework with RDF-3X [29], Jena,²¹ and BigOWLIM.²² RDF-3X is considered the fastest semantic web framework with persistent storage. Jena is an open source framework for semantic web data. It has several models which can be used to store and retrieve RDF data. We chose Jena's in-memory and SDB models to compare our framework with. As the name suggests, the in-memory model stores the data in main memory and does not persist data. The SDB model is a persistent model and can use many off-the-shelf database management systems. We used MySQL database as SDB's backend in our experiments. BigOWLIM is a proprietary framework which is the state-of-the-art significantly fast framework for semantic web data. It can act both as a persistent and nonpersistent storage. All of these frameworks run in a single machine setup.

5.3 Experimental Setup

5.3.1 Hardware

We have a 10-node Hadoop cluster which we use for our framework. Each of the nodes has the following configuration: Pentium IV 2.80 GHz processor, 4 GB main memory, and 640 GB disk space. We ran Jena, RDF-3X, and BigOWLIM frameworks on a powerful single machine having 2.80 GHz quad core processor, 8 GB main memory, and 1 TB disk space.

5.3.2 Software

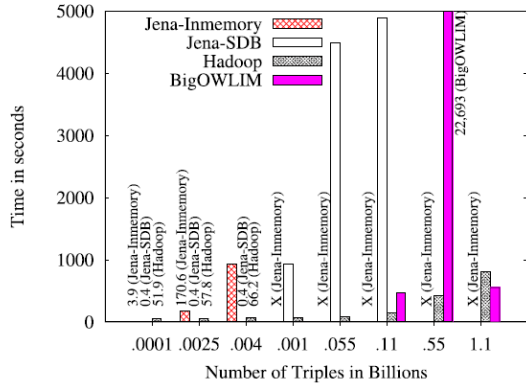
We used hadoop-0.20.1 for our framework. We compared our framework with Jena-2.5.7 which used MySQL 14.12 for its SDB model. We used BigOWLIM version 3.2.6. For RDF-3X, we utilized version 0.3.5 of the source code.

Table 1. Comparison with RDF-3x

Comparison with RDF-3X

	LUBM-10,000		LUBM-20,000		LUBM-30,000	
	RDF-3X	HadoopRDF	RDF-3X	HadoopRDF	RDF-3X	HadoopRDF
Query 1	0.373	248.3	0.219	418.523	0.412	591
Query 2	1240.21	801.9	3518.485	924.437	FAILED	1315.2
Query 4	0.856	1430.2	0.445	2259.768	1.160	3405.6
Query 9	225.54	1663.4	FAILED	3206.439	FAILED	4693.8
Query 12	0.298	204.4	0.825	307.715	1.254	425.4
Query 13	380.731	325.4	480.758	462.307	1287	697.2

Fig 3. Response time of LUBM query



6 CONCLUSIONS and FUTURE WORKS

We have presented a framework capable of handling enormous amount of RDF data.. The framework is highly scalable. To increase capacity of our system, all that needs to be done is to add new nodes to the Hadoop cluster. We have proposed a schema to store RDF data, an algorithm to determine a query processing plan, whose worst case is bounded, to answer an SPARQL query and a simplified cost model to be used by the algorithm. Our experiments demonstrate that our system is highly scalable. If we increase the data volume, the delay introduced to answer a query does not increase proportionally. The results indicate that for very large data sets (over one billion triples), HadoopRDF is preferable and more efficient if the query includes low selectivity joins or significant inference. Other solutions may be more efficient if the query includes bound objects which produce high selectivity. In the future, we would like to extend the work in few directions. First, we will investigate more sophisticated query model. We will cache statistics for the most frequent queries and use dynamic programming to exploit the statistics. Second, we will evaluate the impact of the number of reducers, the only parameter of a Hadoop job specifiable by user, on the query runtimes. Third, we will investigate indexing opportunities and further usage of

binary formats. Finally, we will handle more complex SPARQL patterns, e.g., queries having OPTIONAL blocks.

ACKNOWLEDGMENTS

We thank M. Murali for his useful comments on earlier drafts of this paper.

References

- [1] D.J. Abadi, "Data Management in the Cloud: Limitations and Opportunities," *IEEE Data Eng. Bull.*, vol. 32, no. 1, pp. 3-12, Mar. 2009.
- [2] D.J. Abadi, A. Marcus, S.R. Madden, and K. Hollenbach, "SWStore: A Vertically Partitioned DBMS for Semantic Web Data Management," *VLDB J.*, vol. 18, no. 2, pp. 385-406, Apr. 2009.
- [3] D.J. Abadi, A. Marcus, S.R. Madden, and K. Hollenbach, "Scalable Semantic Web Data Management Using Vertical Partitioning," *Proc. 33rd Int'l Conf. Very Large Data Bases*, 2007.
- [4] A. Abouzeid, K. Bajda-Pawlikowski, D.J. Abadi, A. Silberschatz, and A. Rasin, "HadoopDB: An Architectural Hybrid of MapReduce and DBMS Technologies for Analytical Workloads," *Proc. VLDB Endowment*, vol. 2, pp. 922-933, 2009.
- [5] F. Chang, J. Dean, S. Ghemawat, W.C. Hsieh, D.A. Wallach, M. Burrows, T. Chandra, A. Fikes, and R.E. Gruber, "Bigtable: A Distributed Storage System for Structured Data," *Proc. Seventh USENIX Symp. Operating System Design and Implementation*, Nov.2006
- [6] Mohammad Farhan Husain, James McGlothlin, Mohammad Mehedy Masud, Latifur R. Khan, and Bhavani Thuraisingham, "Heuristics-Based Query Processing for Large RDF Graphs Using Cloud Computing" September 2011
- [7] L. Ding, T. Finin, Y. Peng, P.P. da Silva, and D.L. McGuinness, "Tracking RDF Graph Provenance Using RDF Molecules," *Proc.Fourth Int'l Semantic Web Conf.*, 2005.
- [8] R. Elmasri and B. Navathe, *Fundamentals of Database Systems*.Pearson Education, 1994.
- [9] L. Sidirourgos, R. Goncalves, M. Kersten, N. Nes, and S. Manegold, "Column-Store Support for RDF Data Management:Not All Swans Are White," *Proc. VLDB Endowment*, vol. 1, no. 2,pp. 1553-1563, Aug. 2008.
- [10] Y. Guo and J. Heflin, "A Scalable Approach for Partitioning OWL Knowledge Bases," *Proc. Second Int'l Workshop Scalable Semantic Web Knowledge Base Systems*, 2006.

Residential Water Consumption

- *A Urban Perspective*

K. Sathyamurthi

Madras School of Social Work, Chennai-8

ABSTRACT

Water is extremely important for developing nations, such as India. Water is a basic resource which supports economic growth and maintains daily life. India has only four percent of the world's fresh water to meet the demands of 17 per cent of the world's people. Tamil Nadu is the third and the most urbanized state in the country. Chennai city, one of the major metropolises of India, is situated at the northern coastal edge of the State of Tamil Nadu. Urban Residential area is a land use in which housing predominates, as opposed to industrial and commercial areas. Housing may vary significantly between, and through, residential areas. These include single family housing, multi-family residential, or mobile homes. Henry h. Zhang, David f. Brown (2004) in their empirical study on urban residential water use provides first-hand information regarding urban household water use and consumption patterns, household amenities and facilities household water use habits and behavior, household water perception, household environmental attitudes, and household capacity and willingness to respond to water conservation policy in the Chinese context. This study aims at describing the residential water usage in urban area; descriptive research design was used in this study. Researcher collected the data through non probability purposive sampling method from four different residential areas in Chennai namely Anna Nagar, Besant Nagar, Kodambakkam, and Villivakkam. The findings of the study are; more than (76.7%) of the respondents are unaware of their household water usage. It is surprising to understand that none the respondents are aware of have the water measurement system in their household in urban areas.

Key Words: *Residential Water, Consumption, Urban, Urban Residential area and water usage*

Introduction

Little is known about residential water use in developing economy, especially that in Indian context. One reason may be that most of the developing economy is in the transition states. Swiftly changed demand pattern usually makes the study very difficult. Water is the elixir of life, a precious gift of nature to mankind and millions of other species living on the earth. Water resources comprising of surface water (river and lakes), ground water and marine and coastal waters, support all living things including human beings. Though water is available in the universe in huge quantity in the order of 1400×10^6 km³, only 3 per cent of the water in the universe is fresh water. Among the fresh waters, only about 5 per cent of them or 0.15 per cent of the total world waters are readily available for beneficial use. The total water resources available in India are 1850 km³, which is roughly 4 per cent of the world's fresh water resources. Large numbers of households in cities around the developing world do not have access to one of the most basic of human needs – a safe and reliable supply of drinking water.

According to the UN estimates, the total amount of water on earth is about 1400 million cubic kilometer which is enough to cover the earth with a layer of 3000 meters depth. However the fresh water constitutes a very small proportion of this enormous quantity. About 2.7 per cent of the total water available on the earth is fresh water of which about 75.2 per cent lies frozen in Polar Regions and another 22.6 per cent is present as ground water. The rest is available in lakes, rivers, atmosphere, moisture, soil and vegetation. What is effectively available for consumption and other uses is a small proportion of the quantity available in rivers, lakes and ground water.

The crisis about water resources development and management thus arises because most of the water is not available for use and secondly it is characterized by its highly uneven spatial distribution. Accordingly, the importance of water has been recognized and greater emphasis is being laid on its economic use and better management. Water also regulates the temperature of the planet and cycles essential nutrients through the land, air, and all living things. The flow of water through the atmosphere, biosphere, lithosphere, and hydrosphere is called the hydrologic, or water, cycle. Thus, water is both the most abundant natural resource on our planet and a fundamental element of life whose preciousness requires diligent management.

Water is extremely important for developing nations, such as India. Water is a basic resource which supports economic growth and maintains daily life. India has only seven percent of the world's fresh water to meet the demands of 17 per cent of the world's people.

(Pacific Institute, 2011). India needs to be able to use water in a sustainable way and this presents the country with a big challenge. Tamil Nadu is the third and the most urbanized state in the country. Chennai city, one of the major metropolises of India, is situated at the northern coastal edge of the State of Tamil Nadu. The water requirement for the Chennai area have been assumed at the rate of 90 lpcd, when most of the growth takes place, both the quality and quantity of water are already under pressure and the increase in population may push the resources to scarcity. Water resource management in India is going to be vitally important to sustain the needs of one billion population of India.

Human needs are growing rapidly and the need for water is also growing. The main source of water supply is no doubt rainfall, but the rainfall in Tamil Nadu the rainfall is not uniform either spatially or temporally. Availability of water determines the location of human activities. All agricultural operations need water. Tamil Nadu accounts for 4 percent of the land area and 6 per cent of the population, but only 3 per cent of the water resources of the country. Most of Tamil Nadu is located in the rain shadow region of the Western Ghats and hence receives limited rainfall from the south-west monsoon. Although population growth has slowed down, Tamil Nadu is urbanizing rapidly. Consequently, the domestic water requirements are projected to increase by more than 50 per Cent. Water quality is also becoming a serious concern due to pollution by industrial effluents, sewage, etc. and also due to naturally occurring phenomena. The Government of Tamil Nadu has indicated that water security, i.e. provision of drinking water to the people will be the highest priority of the government.

Background of the Study

Chennai is a particularly water-scarce city. In fact, it has the lowest water availability per capita of any large metropolitan area in India. Ensuring an adequate water supply isn't only an issue for large urban centers. It's also a vital concern of the growing populations of cities. The main sources of public water supply in the city are the three reservoirs - Poondi, Redhills and Cholavaram - with an aggregate storage capacity of 175 MCM. Even when the reservoirs are not full, they get inflows from intermittent rains, which are then drawn. On the other hand, losses due to evaporation from the reservoirs result in the effective availability being lower than the storage. The other major resource is groundwater from the well fields in the Araniar-Kortaliyar basin and the southern coastal aquifer, and a large number of wells and tube wells spread all across the city. Groundwater levels within the city also fell and

brackish water began to appear even in localities which earlier had good quality groundwater sources.

During dry periods, the public utility can provide residents of the city with only 100 liters of water a day, or less .In Chennai there is a public water delivery system, but during dry periods running water may be available only a couple of hours a day, or not at all, and for many people that means filling buckets or pans from an outside water tap or pump, and carrying it home. Other options include drawing water from private wells, which can be poor quality and can also go dry during drought, or purchasing water from tanker trucks. People who are able to install storage tanks and sump pumps are able to weather the dry spells with less inconvenience. The cost and benefit factors that go into people's decisions on how to acquire the water they need, and the prospects for different methods of provision. This, combined with forecasting water availability through 2025 based on past conditions,

Residential Water Usage

It is estimated that 8 per cent of worldwide water use is for household purposes. These include drinking water, bathing, cooking, sanitation, and gardening. Basic household water requirements have been estimated that around 50 liters per person per day, excluding water for gardens. Drinking water is water that is of sufficiently high quality so that it can be consumed or used without risk of immediate or long term harm. Such water is commonly called potable water. In most developed countries, the water supplied to households, commerce and industry is all of drinking water standard even though only a very small proportion is actually consumed or used in food preparation. There is growing concern regarding the increasing stress on water resources caused by population growth, unsustainable consumption patterns and uncontrolled uses, both in urban and rural areas. Although despite the broad recognition of the central role of water in sustainable development, including in efforts to eradicate poverty, addressing the water needs of the poor through concerted global action has not been given enough priority. Provision of safe drinking water and sanitation services remains one of the most critical challenges humanity is facing today.

Urban Residential area is a land use in which housing predominates, as opposed to industrial and commercial areas. Housing may vary significantly between, and through, residential areas. These include single family housing, multi-family residential, or mobile

homes. Zoning for residential use may permit some services or work opportunities or may totally exclude business and industry. It may permit high density land use or only permit low density uses. Residential zoning usually includes a smaller FAR (floor area ratio) than business, commercial or industrial/manufacturing zoning. The area may be large or small.

The urban areas in cities and metropolitans are experiencing unbridled growth of population even at a rate of 40-50 per cent in a decade, outpacing the required rate of growth in infrastructure development in terms of housing, roads, transportation, Communication, power supply, water supply & sewerage systems, sanitation etc. to accommodate the population in a healthy environment. As a result, the backlog of providing adequate services is mounting, not to speak of the expected level of satisfaction, which could be a distant dream. To tide over the crisis, quantity of water supplied by the municipal bodies is reduced; and in extreme cases, water is supplied at alternate days or even at reduced frequency. Severe doses of disinfectants, like chlorine, used to protect/maintain the quality of water from bacteriological contamination during its journey from the water treatment site to the farthest consumer end, make the pipes and sanitary fittings vulnerable to corrosion and also contamination from their metallic constituents.

Urban Water Use

Even though the rate of urbanization in India is among the lowest in the world, the nation has more than 250 million city-dwellers. Experts predict that this number will rise even further, and by 2020, about 50 per cent of India's population will be living in cities. This is going to put further pressure on the already strained centralized water supply systems of urban areas. Urban water use is generally determined by population, its geographic location, and the percentage of water used in a community by residences, industry, government, and commercial enterprises. It also includes water that cannot be accounted for because of distribution system losses, fire protection, or unauthorized uses.

Urban water usage is unique in its fragmentation, in terms of both physical utilization of the resource and the institutional structures that govern its use. Municipal uses usually include residential plus industrial, commercial, and institutional (ICI). Each end use has distinct quality requirements, usage processes, disposal methods, and jurisdictional oversight and responsibilities. As a result, there is no cohesive approach to planning and policy that can formulate consistent and effective responses to urban water issues, in particular protracted

droughts. Increased urbanization, population growth and living standards have been major drivers in the increase of urban water use in the past century. The amount of urban water use depends on climate, level and efficiency of public supply services, patterns and habits of water use by the population, technological changes (for example, water saving technologies and use of alternative sources) and socioeconomic instruments. The connection of populations to water supply systems has also increased over recent decades, especially in southern countries. Urban water use is not evenly distributed over time as households and services tend to demand more water in hot and dry periods. Thus, gross urban water demands continue to grow because of significant population increases and the establishment of urban centers. Even with the implementation of aggressive water conservation programs, urban water demand is expected to grow in conjunction with increases in population.

Urban Residential Water Consumption

Man and water are closely related in a dualistic manner: on one hand water has great influence on man's welfare and social development, on the other man's activities greatly affects water as such. Comparing the present and future water needs with water availability, some world regions should be considered as truly water scarce at least during the next generation. Man's activities create water problems which tend to change with time and exhibit a regional pattern. Many problems can be avoided if advance impact studies were made more regularly for planned water-related activities and projects. The author ends by stressing that differences in climate, hydrology, culture and dominating water problems tend to complicate the important process of transfer of knowledge between temperate and tropical countries.

At the beginning of the 21st century many people face formidable challenges to meet increasing demand for water. However, there are significant pressures that make it difficult to meet these demands including inefficient agriculture, expanding urban areas, water pollution, and international conflict. The situation has led many in the international development community to point to a "global water crises." The urban water supply and sanitation sector in the country is suffering from inadequate levels of service, an increasing demand-supply gap, poor sanitary conditions and deteriorating financial and technical performance. According to Central Public Health Engineering Organization (CPHEEO) estimates, as on 31 March 2011, 76 per cent of urban population has access to a potable water supply. But this supply is highly erratic and unreliable. Transmission and distribution networks are old and poorly maintained, and generally of a poor quality. Consequently physical losses are typically

high, ranging from 25 to over 50 per cent. Low pressures and intermittent supplies allow back siphoning, which results in contamination of water in the distribution network. Water is typically available for only 2-8 hours a day in most Indian cities. The situation is even worse in summer when water is available only for a few minutes, sometimes not at all.

Human actions bring about water scarcity in three ways: through population growth, misuse and inequitable access. Population growth contributes to scarcity simply because the available water supply must be divided among more and more people. Every country has a more or less fixed amount of internal water resources, defined as the average annual flow of rivers and aquifers generated from precipitation. Overtime, this internal renewable supply must be divided among more and more people, eventually resulting in water scarcity. Thus the study will focus on the usage of water in Urban Residential areas which is the growing user of the scarce resource.

Significance of the Study

This paper aims at focusing on the how the socio-economic status and the housing environment are related to the consumption of water, analyze the relationship between water use and the socio-economic status of the people living in a particular area, focus on how the people in the particular area of study collects water and the source of water available for the people, the house hold behavior of using water as well as calculate the ways by which the people waste water and understand the pattern and the knowledge between water availability and the water usage and how the youth practice the water measuring in the urban youth households of Chennai

Literature Review

Residential water is used for household purposes, such as drinking, food preparation, bathing, washing clothes, flushing toilets, and watering lawns and gardens. In the guidelines for Drinking Water Quality, WHO defines residential water as being „water used for all usual domestic purposes including consumption, bathing and food preparation (WHO, 1993). Residential water use standards vary with climatic conditions, life style, culture, technology and economy. There is no fixed data to estimate the amount of water needed to maintain acceptable of minimum living standard (Zhang, 1999). A water use standard was identified about thirty years ago. In 1977, the United Nations determined the concept of a water use standard to meet people’s basic need for water.

... All people, whatever their stage of development and their social and economic Conditions, have the right to have access to drinking water in quantities and of a quality equal to their basic needs.(United Nations 1977)

This concept was further developed in the 1992 Earth Summit and in the 1997 UN General Assembly.

In developing and using water resources, priority has to be given to the satisfaction of basic needs and safeguarding of ecosystems. (United Nations 1992)

... it is essential for water planning to secure basic human and environmental needs for water... develop sustainable water strategies that address basic human needs, as well as the preservation of ecosystem.(United Nations 1997)

The new concept is more towards the environment and sustainable development. Water comes from the natural environment. So the usage of water needs to be planned to make sure that there is enough for current needs without damaging the environment. The U.S Agency for International Development, the World Bank and the World Health Organization recommend the „basic water requirement BWR (include drinking and sanitation needs) in the range from 20 to 40 l/p/c/d (Zhang, 1999). Gleick in 1996 estimated the basic water requirement at 50 l/p/c/d for meeting four household basic needs: drinking, sanitation, bathing and cooking. The basic water requirement is enough to keep our alive and healthy. Now many of people choose to purchase some liquid drinking water as bottled water, juices, milk, and soft drinks. Although many of us purchase the bottled drinking water, the household water consumption is till greater than the basic water requirement

Henry h. Zhang, David f. Brown (2004) in their empirical study on urban residential water use provides first-hand information regarding urban household water use and consumption patterns, household amenities and facilities household water use habits and behavior, household water perception, household environmental attitudes, and household capacity and willingness to respond to water conservation policy in the Chinese context. In a transition economy with a planned and highly regulated tradition, urban residential water use and consumption in Beijing and Tianjin shows certain variation from prior studies in both the developed and developing economies. Many important variables identified in prior studies, such as water price or income, do not have the expected impact on household water use and

consumption. A new set of variables has been found to be important in explaining the variation of household water use and consumption in Beijing and Tianjin. Rapid urbanization, along with improved housing and standards of living, has transformed domestic water use in Beijing and Tianjin.

Ajzen and Fishbein's (1980) theory of reasoned action is probably the best-known attitude-behaviour model. The theory of reasoned action builds on expectancy value theory to incorporate normative social influences on behavioural intention. It conceptualizes the linkages between beliefs, attitudes, perceived social norms and behaviours (see Figure 1). Kantola et al. (1982) and Kantola et al. (1983) used the Fishbein and Ajzen (1975) predecessor of the theory of reasoned action as a predictive model of human behaviour related to the environment. Kantola et al. (1982) found the Fishbein and Ajzen model useful for explaining intentions to conserve water; they found that most influence on intentions to conserve water was explained by subjective normative feelings (perceived peer pressure) and the exogenous variable age. The ability of evaluative beliefs to predict evaluative attitudes was low. A later study on the ability of persuasive communications with differing levels of intensity (severity) to influence water conservation did not support the dominant mediation role for subjective norms and evaluative attitude for predicting behavioural intention to conserve water (Kantola et al., 1983). Syme and Nancarrow (1992) tested aspects of the ability of Ajzen and Fishbein's model to explain the extent to participation in urban water planning. More recently, CSIRO's Australian Research Centre for Water in Society has improved the predictive ability of modified Ajzen and Fishbein type models specifically refined for predicting consumer responses to water supply systems and to aquifer recharge using recycled water (Porter et al., 2005; Po et al., 2005; Leviston et al. 2006). These models have been particularly useful for predicting behaviour when taking account of risks and other social elements associated with delivery of potable water

Social cognitive theory identifies human behaviour as a dynamic interaction of personal factors, behaviour, and the environment (Bandura 1986). Social cognitive theory accords a central role to cognitive, self-regulatory, and self-reflective processes in human adaptation and change. People are viewed as self-organizing, proactive, self-reflecting and self-regulating rather than as reactive organisms shaped by external forces (Pajares, 2002). As a consequence Social cognitive theory suggests that behaviour change is affected by

environmental influences, personal factors and attributes of the behaviour itself (Grizzell, 2005).

It is clear from this review that behavioural models describing voluntary behavioural change are, by their nature, complicated. This is because human behaviour is usually complicated and the consequence of the multiple factors influencing it, with many factors not easily controlled. It should also be clear that the multiple models contesting to be explicators of human behaviour reflect differential focus on different factors influencing conservation behaviour and reflect the fact that any one model is rarely a satisfactory, universal predictor of human behaviour. No single method works to facilitate behaviour change to reduce water consumption in all contexts internal and external to the individual. As a consequence, simplified approaches and simplifying assumptions are usually taken in seeking behavioural change to reduce water consumption. The focus is on relevant or key aspects of influence that can be used to influence behavioural change in household water consumption. Often, we focus on refining the elements of good communication strategies rather than attempting to respond to the more complex, deeper behavioural factors and influences that might be relevant to water use.

Objective of the Study

To study the demographic profile, socioeconomic status and housing environment of the respondents, to study the methods and ways and means of water collecting process in urban areas, to understand the pattern of water usage practices among urban residences and to study the knowledge of respondents about the water usage and water measurement system. The present study aims at describing the urban residential water usage; descriptive research design was used in this study. Researcher collected the data through non probability purposive sampling method from four different residential areas in Chennai namely Anna Nagar, Besant Nagar, Kodambakkam, and Villivakkam. The researcher conducted interviews from the heads of the family, in the above mentioned areas with the inclusion and exclusion criteria such as respondents should have been residing in the area for more than two years and people residing for less than a year were not included in the study. The respondent must be married and be living with family. Respondent must be within the age group of below 25 – above 65. After going through the Chennai Corporation list of households' researcher selected the sample of 138 from 1328 residences in four areas. Among the 1328 of households, researcher selected 138 respondents by using non probability purposive sampling method. A semi

structured Interview schedule was used for obtaining responses to a set of questions from the respondents or informants.

Analysis and Discussion

- Majority of the respondent (64.5%) belongs to the age category of 41 to 50 years.
- Majority (73%) of the respondents were Male and More than One fourth of the respondents were (27%) Female.
- More than one third (38.4%) of the respondents are dwelling in Single story independent house. One fifth (20.7%) of the respondents are dwelling in High rise buildings, one third (33 %) of the respondents are dwelling in the infill housing which is less than seven storied high rise buildings and eight per cent of them stayed in the courtyard.
- Less than half (41.7%) of the housing is owned by the respondents themselves and others live in rented house.
- Majority (82.3%) of the building condition is good and A vast Majority (80.0%) of the respondents have building which doesn't include Private Garden
- Majority (88.3%) of the respondents are having indoor tap water supply in their household. Others use either well or shared water supply for household water supply.
- Majority (88%) of the respondents collect water from indoor tap water supply for their all household purpose.
- Majority (88%) of the respondents do not drink tap water directly.
- Majority (63.3%) of the respondents use water supply from government and private sources for all the household use.
- Sixty four per cent of the respondents do not use the tap water for drinking purposes even though they consider the water purity to be good. Twenty eight per cent of the respondents have rated the purity of water as poor.
- Around two third of the respondents (64.2%) have rated the color of the water is good and they do not use it for drinking purposes. Only thirty per cent of the respondents feel that the color of the public water supply is poor.
- Fifty eight per cent respondents as rated the water taste as good but they do not use it for drinking purposes, one third (34 per cent) of the respondents have rated the colour of the water as poor.

- Little more than two fifth of the respondents (43.4%) have mentioned that the pressure is good but they do not use it for drinking purposes. 28.6% has rated the pressure as poor but they use it for drinking purpose.
- Sixty nine percent of the respondents use washing machines to laundry, twenty one percent uses both machine and hand to wash clothes and ten per cent washes by hand on daily and weekly basis. Seventy eight per cent of the respondents perform laundry with less than 15 items every day.
- Majority of the respondents (75.9%) maintain their water resources properly and their toilet cistern does not leak. Majority of the respondents (76.9%) maintain water resources properly and their taps do not have brown running water. Nearly two third (63.30%) of the respondents most frequently use shower for their personal hygiene.
- More than one third (33.3%) of the respondent spend Rs. 200 - 400 for water, every month and around one tenth (13.3%) of the respondent are unaware about their monthly expense for water.
- Almost all (100%) the respondents use water for drinking, cooking, laundering, bathing, toilet flushing purposes. One fifth (20%) of the respondents use water for watering plants, and little less than (32%) of the respondents use water for washing their cars.
- More than (76.7%) of the respondents are unaware of their household water usage.
- Majority (72.7%) of the respondents who live in a family size of more than five are unaware of their household drinking water consuming level.
- More than half (53.1%) of the respondents who live in a family size of less than five are unaware of their household drinking water consuming level.
- One third of the respondents do not know how much they pay for their water but their monthly expense on water falls under the category of Rs.201-400.
- With regard to the water pricing, two third (66.7%) of the respondents said that the water price is normal. One fifth (20.0%) of the respondents said that the pricing of water is too high and more than One tenth (13.3%) of the respondents are unaware of the current water rate.
- It is surprising to understand that none the respondents are aware of have the water measurement system in their household.
- Almost all (95%) of the respondents do not use the water saving measures in their house hold.

- Nearly half (48.3%) of the respondents wants to improve their water quality and nearly one eighth (12%) of the respondents want to improve their water maintenance of the household.
- Majority (80%) of the respondents not aware of any water conservation programmes.
- More than half (76.7%) of the respondents are willing to participate in the existing water system improvement program and little less than one fourth (23%) of the respondents are not willing to participate in programs to improve the existing water system.

Suggestion

Many of the respondents are not aware or they have not come across any water conservation programs by any organization. As most of the respondents are willing to participate and follow systems to improve water, the government and NGOs can train people on effective and simple water management practices. Through the Professionals working in Water and Professionally Qualified Social Workers can be utilized for Water budgeting system in the residential areas, which is being used now around the world. This water budgeting system can be extended to individual households of Chennai. This will enhance the civic responsibility of the consumers. None of the respondents have water management system in their household, the corporation and NGOs can train and introduce metering systems in households, where water users will know how much water is consumed by them usefully and how much water is wasted. The opinion of the public water supply is poor, though accepted by many of respondents that color and pressure of the water through public water supply is good. The image of the government service delivery should be enhanced so that many of them start using the public water supply.

Conclusion

India is fast becoming urbanized. Tamil nadu has already exceeded fifty percent of urbanization and is now an urban state. With urbanization, people have better access to education and other services and infrastructure. This also means we have exploited and become unaware of natural resources particularly, water. This study emphasizes the need to manage water as even the urban educated are not fully aware about water shortage and water management practices.

Reference

1. Boland, John J, Ben Dzieglewski, Duane D. Bauman, and Eva, M. Opitz. 1984. *Influence of price and rate structures on municipal and industrial water use*. Planning and Management Consultants, Ltd. Carbondale, Illinois.
2. Burke, J.J. 2002. Groundwater for irrigation: productivity gains and the need to manage hydro-environmental risk. In R. Llamas & E. Custodio, eds. *Intensive use of groundwater challenges and opportunities*, 478 pp. Abingdon, UK, Balkema.
3. Dziegielewski, Ben. 1998. Commercial and institutional water use and conservation in North American cities: analytical review of existing information. Planning and Management Consultants. Ltd. Carbondale Illinois
4. Falkenmark, Malin. 2000. Competing freshwater and ecological services in the river basin perspective: an expanded conceptual framework. *Water International*. 25 (2):172- 177.
5. Foster, Henry S. Jr. and Bruce R. Beattie. 1979. Urban residential demand for water in the United States. *Land Economics* 55 (1):43-58.
6. Gottlieb, M. 1963. Urban domestic demand for water: a Kansas case study. *Land Economics* 39 (3):204-210.
7. Griffin, Ronald. C. and C. Chang. 1990. Pretest analysis of water demand in thirty communities. *Water Resources Research* 3 (1):2251-2255.
8. Grafton, R.Q. et al. (2011), “Determinants of Residential Water Consumption: Evidence and Analysis from a 10-country Household Survey”, *Water Resources Research*, Vol. 47, No. W08537, doi:10.1029/2010WR009685.
9. Government Policy and Investment in Water Supply and Sanitation in India. Kataliha, K. P., Shelter, Vol. 5, No.1, HUDCO and HSMI, January 2002.
10. Hanemann, W. Michael. 1997. Determinants of urban water use. In *Urban Water Demand Management and Planning*, edited by D. F. Baumann, J. J. Boland and W. M. Hanemann: McGraw-Hill, Inc.
11. Hewitt, Julie A. and W. Michael Hanemann. 1995. A discrete/continuous choice approach to residential water demand under block rate pricing. *Land Economics*. 71 (2): 173-192.
12. Jackson, E., *1999 Residential Water Audits*, unpublished report, Utah State University Cooperative Extension Service, Salt Lake City, Utah, 2000
13. MIDS (1995). ‘Water Allocation and Management in the Chennai Metropolitan area.’ Madras Institute of Development Studies [cited in Ruet, Saravanan and Zérah 2002] <http://www.corpwatchindia.org/issues/PID.jsp?articleid=3623> [accessed 01/2004].
14. National Water Policy, 2002. Ministry of Water Resources, New Delhi, April 2002

15. Nieswiadomy, Michael L. 1992. Estimating urban residential water demand: effects of price structure, conservation and education. *Water Resources Research* 28,609-615.
16. Ward, M.B., J. O'Donohue and R.Q. Grafton (2011), "Prices versus Rationing of Urban Water: Is There an Equity-Efficiency Trade-off", *Centre for Water Economics, Environment, and Policy Working Paper*, ANU.

Work Motivation among the Primary School Teachers

M. Govindan

Department of Education, Annamalai University

Abstract

This study was designed to find the work motivation of the teachers working in primary schools. A random sample of 250 teachers working in Primary schools were selected. Work Motivation Questionnaire was used to collect the required information. The results of the study reveals that the teachers in general posses work motivation “to a great extent.” Further, there is a significant relationship exists between most of the dimensions of work motivation of teachers.

Key Words: Work motivation, Dependence, Organisational orientation, Work Group Relations, Psychological Work Incentives, Material Incentives, Job situation.

Work Motivation

Motivation is an umbrella term having a wide variety of meaning. It is the process which leads the individual to attempt to satisfy some need. Motivation is broadly considered as the process of arousing, sustaining, and regulating activity, a concept limited to some aspect such as the energetic of behavior or purposive regulation.

Miller(1978) defined motivation as “ an inner state of mind that energizes, activates a moves and that which directs or channels behaviour towards goals”.

Motivation X Skill = Ability

Situation X Attitude = Motivation

Ability X Motivation = Human performance

Human Performance X Physical effort = Teaching Performance

Teachers work motivation

Teaching is the noblest profession in the world. The teacher is nowadays considered as the powerful agent that can inculcate the democratic ideals of nationhood in children, future citizen of the nation. The teacher is the managers as well as director of the entire teaching-learning process. High achievements of the students, better school performance, molding the children into good citizens and exposing them in the arena of growing campervan are some of the major issues lying at the hand of the teacher. However, present

day teachers are themselves absorbed in innumerable pressures, tensions, worries about their own status and proper work conditions. So they are often diverted from their real aim and work mechanically and receive salaries. The teaching community is dissatisfied with the working conditions in schools, which has a significant bearing on the quality of teaching and the students' performance. (Waseem Ahmad khan,2007)

Need and importance of the study

Teacher occupy a key position in the whole gamut of education. Recent technological advancement have further enhanced the role of teachers in the lives of children. The teachers plays a crucial role in the learning process of the pupil. The terms 'motivation' and 'behaviour' are found to be closely associated as most behavior occurs as a result of motivation. Motivation seems apparently one of the important determinants of behavior. For an educational institution to be more effective, the motivational problems of stimulating both the decision to participate and the decision to produce at work need to be paid much attention. To put in a nutshell, an effective educational system can influence motivation by designing jobs in ways that consider teacher's need. To wed human action to achievement of educational objectives, we need to understand the concepts of motivation and behavior that are indeed important keys to manage people. These are all the rationale behind the investigator to study the work motivation of the teachers.

Objectives of the study

The following are the objectives of the study

1. To study the work motivation among the teachers working in primary schools.
2. To find if there is any significant difference between the male and female teachers attitude towards the following six dimensions of work motivation
 - a) Dependence
 - b) Organizational orientation
 - c) Work group relations
 - d) Psychological work incentives
 - e) Material incentives and
 - f) Job situation
3. To find if there is any significant difference between the rural and urban teachers attitude towards the six dimensions of work motivation.
4. To find if there is any significant difference between the married and unmarried teachers attitude towards the six dimensions of work motivation.

5. To find if there is any significant difference between the teachers of below 30 years and above 30 years of age attitude towards the six dimensions of work motivation.
6. To find if there is any significant difference among the teachers having the educational qualifications of D.T.Ed, Undergraduate, and Post graduate attitude towards the six dimensions of work motivation.
7. To find if there is any significant relationship exists in the teachers attitude between the six dimensions of work motivation.

Hypotheses of the study:

Based on the objectives of the study necessary hypotheses were formulated.

Method and Material:

Method:

Normative survey method was used for the present study.

Sample:

A random sample of 250 teachers working in 52 primary schools located in Cuddalore District of Tamilnadu was selected.

Instrument used:

Work Motivation Questionnaire (1988)-Constructed by Dr. K.G.Aggarwal was used to find the work motivation of the teachers. The Questionnaire consists of 26 items. These items have been categorized into six dimensions. The maximum score is 130 and the minimum score is 26.

Table 1

Sl. No.	Name of the Dimensions	Number of Corresponding items
1	Dependence	15, 16, 17, 18, 21, 22
2	Organizational Orientation	1, 8, 11, 12, 13
3	Work Group Relations	6, 14, 19, 20
4	Psychological Work incentives	23, 24, 25, 26
5	Material Incentives	2, 3, 4, 5
6	Job Situation	7, 9, 10

Statistical techniques applied:

Mean, Standard deviation, 't' test, 'F' test and Pearson product moment co-efficient correlation were used to analyze the collected data.

Descriptive Analysis:

Table - 2

Mean scores of the work motivation of teachers in each dimension

Sl. No.	Dimension	N	Mean	SD
1	Dependence	250	22.72	3028
2	Organizational Orientation	250	19.36	2.40
3	Work Group Relation	250	16.46	2.53
4	Psychological Work incentives	250	14.48	2.81
5	Material Incentives	250	10.55	2.28
6	Job Situation	250	12.27	2.08
	Over all work motivation	250	96.30	10.66

The obtained mean score on overall work motivation is 96.30. This can be interpreted as the teachers were having work motivation 'to a great extent'. The results of the table also reveals that the teachers were having work motivation 'to mostly great extent' of the Dependence, Organizational Orientation, Work Group Relations and Psychological Work Incentives dimensions. The teachers having work motivation 'to a some extent' and 'to a great extent' of Material Incentive and Job Situation dimensions respectively.

Differential Analysis

Table -3
Mean Difference of Teachers Work Motivation with respect to their Gender, Locality, Marital Status and their age group

Variables	Sub Samples	Dimensions																	
		Dependence			Organisational Orientation			Work Group Relations			Psychological Work Incentives			Material Incentives			Job Situation		
		M	SD	t	M	SD	t	M	SD	t	M	SD	t	M	SD	t	M	SD	t
Gender	Male	22.71	3.22	0.23 [#]	19.54	2.33	1.33 [#]	16.63	2.55	1.06 [#]	15.03	2.82	0.28 [#]	10.35	2.10	1.32 [#]	12.47	1.99	1.32 [#]
	Female	22.72	3.35		14.13	2.45		16.29	2.51		14.93	2.82		10.73	2.43		12.07	2.16	
Location	Urban	21.00	3.62	6.01 ^{**}	18.65	2.59	3.15 ^{**}	15.44	2.88	4.43 ^{**}	14.24	2.99	2.90 ^{**}	10.18	2.01	2.98 ^{**}	11.61	2.28	3.48 ^{**}
	Rural	23.58	2.73		19.67	2.23		16.96	2.17		15.34	2.66		10.73	2.38		12.59	1.90	
Marital Status	Married	23.24	3.18	3.30 ^{**}	19.50	2.24	1.29 [#]	16.79	2.50	2.82 ^{**}	14.78	2.97	1.30 [#]	10.31	2.41	2.17 [*]	12.42	2.04	1.64 [#]
	Unmarried	21.83	3.29		19.09	2.31		15.87	2.49		15.25	2.50		10.94	2.00		11.97	2.13	
Age Group	Below 30 years	22.25	3.41	4.85 ^{**}	19.22	2.44	1.27 [#]	16.22	2.57	2.80 ^{**}	14.88	2.89	0.93 [#]	10.64	2.30	1.37 [#]	12.04	2.15	3.35 ^{**}
	Above 30 years	24.30	2.16		19.67	2.24		17.26	2.24		15.26	2.51		10.17	2.20		13.01	1.65	

Not Significant

* Significant at 0.05 level

** Significant at 0.01 level

A close look at table 3, the male and female teachers do not differ significantly in all the dimensions of work motivation. The table also indicates that the urban and rural teachers differ significantly in all the dimensions of work motivation. Further, the married and unmarried teachers differ significantly in the Dependence, Work Group Relations, and material Incentives dimensions, but they do not differ significantly in the organizational orientation, Psychological work incentives and Job situation dimensions of work motivation. The table also indicates that the teachers of below 30 years and above 30 years of age groups differ significantly in the Dependence, Work Group Relations and Job situation dimensions and do not differ significantly in the organizational orientation, Psychological Work Incentives and Material Incentives dimensions of work motivation.

Table -4

ANOVA for Various Dimension of Work Motivation of the Teachers Based on Their Educational Qualification

Dimensions	Source of variance Variance	Sum of square	df	Mean square	'F' value	Level of Significance
Dependence	Between groups	99.47	2	49.73	4.75	0.01
	Within groups	2584.48	247	10.46		
	Total	2683.95	249			
Organizational Orientation	Between groups	15.41	2	7.70	1.33	N.S.
	Within groups	1424.36	247	5.76		
	Total	1439.77	249			
Work Groups Relations	Between groups	54.56	2	27.28	4.36	0.01
	Within groups	1545.53	247	6.25		
	Total	1600.10	249			
Psychological Work Incentives	Between groups	99.25	2	49.62	6.52	0.01
	Within groups	1877.64	247	7.60		
	Total	1976.90	249			
Material Incentives	Between groups	49.09	2	24.54	4.85	0.01
	Within groups	1248.73	247	5.05		
	Total	1297.82	249			
Job Situation	Between groups	31.99	2	15.99	3.74	0.05
	Within groups	1055.50	247	4.27		
	Total	1087.50	249			

The results of table 4 indicates that the teachers of D.T.Ed., Graduate, and Post graduate qualification differ significantly in all the dimensions of work motivation except the dimension of Organizational Orientation.

Correlation Analysis

Table – 5
Relationship between the Different Dimensions of Work Motivation of the Teachers

Dimensions	Depen dence	Organizational Orientation	Work group relation	Psycho- logical work incentives	Material incentives	Job situation
Dependence	-	0.43	0.56	0.50	0.04	0.56
Organizational Orientation	-	-	0.53	0.43	0.09	0.49
Work Group Relation	-	-	-	0.45	0.02	0.58
Psychological	-	-	-	-	0.14	0.50
Material	-	-	-	-	-	0.04
Job Situation	-	-	-	-	-	-

The results of the table reveals that there is a significant relationship between the Dependence and Organizational Orientations, Dependence and Work Group Relations, Dependence and Psychological Work Incentives, Dependence and Job Situations, Organizational Orientations and Work Group Relations, Organizational Orientation and Psychological work Incentives, organizational Orientations and Job Situation, Work Group relations and Psychological Work Incentives, Work Group Relations and Job situations, Psychological Work Incentives and Job situations, Dimensions of Work Motivation.

Findings of the study:

- The teachers working in primary schools of Cuddlore district in general posses work motivation ‘to a great extent’.
- The male and female teachers do not differ significantly in all the dimensions of work motivation.
- The teachers working in rural and urban primary schools differ significantly in all the dimensions of work motivation.
- The married and unmarried teachers differ significantly in the Dependences, Work Group Relations and Material Incentive Dimensions of work motivation. They do not differ significantly in the Organizational Orientation, Psychological Work Incentives and Job Situation Dimensions of work motivations.

- The teachers of below 30 years and above 30 years of age groups differ significantly in the Dependence, Work Group Relations, and Job Situation Dimensions of work motivation. They do not differ in the Organizational Orientation, Psychological Work Incentives and Material Incentive Dimensions of work motivation.
- Teachers having D.T.Ed., Graduate, and Post-graduate qualifications differ significantly in all the dimensions except the Organizational Orientation dimension of work motivation.
- There is a significant relationship exists between most of the dimensions of work motivation of teachers.

Conclusion:

The results of the study reveals that the teachers working in Primary schools posses work motivation “to a great extent”. The male and female teachers do not differ significantly in all the dimensions of work motivation. However, there is significant relationship exists between most of the dimensions of work motivation of teachers.

Educational Implications:

The teachers having work motivation “to a some extent” and “a great extent” of material incentive and job situation dimensions. In order to develop and retain excellent teachers, we will need to continue to adjust and redesign the organizational climate of our schools in such a way that both extrinsic and intrinsic teacher motivation is strengthened. To enhance the motivation, some novel approaches like micro-teaching techniques, workshops, seminars and discussions and so on may be adopted. Orientation and Refresher courses may be organized for capacity building of the teachers. Financial rewards may be given to the outstanding teachers.

References:

- Aggarwal, K.G.(1998) Work Motivation Questionnaire. National Psychological Corporation, Agra.
- Waseem Ahmad Khan.(2007) Teaching Motivation. Discovery Publishing House, New Delhi.

கைப்பொருளும் மெய்ப்பொருளும் : பொருள்வயிற் பிரிதல் அடிப்படையில் ஒரு விவாதம்

கி.பார்த்திபராஜா

தமிழ் முதுகலை மற்றும் ஆய்வுத்துறை, தூய நெஞ்சக் கல்லூரி, திருப்பத்தூர்.

முதலாக...

மனித குல வரலாற்றில் சொத்துடைமையின் தோற்றத்திலிருந்தே உலகளாவிய அளவில் பொருளியல் சிந்தனை உருவாக்கம் பெற்றது. தமிழ்ச் சமூகத்தைப் பொறுத்தவரை இனக்குழு வாழ்க்கையின் பங்கீட்டு உண்ணுமுறை, பொருளியல் குவிப்புக்கு இடமளிக்காமலேயே இருந்தது. இனக்குழு வாழ்க்கையின் அழிவும் பேரரசு உருவாக்கத்தின் தோற்றமும் கொடை, புகழ் முதலான விழுமியங்களைக் கட்டி எழுப்பின. கண வாழ்க்கை சிறிது சிறிதாகச் சிதைவற்றுத் தனிச் சொத்துடைமை வாழ்க்கை - அதாவது குடும்ப வாழ்க்கை - தோற்றம் பெற்றது.

பொருள் என்பது இக்காலகட்டத்தில் புதுப்பொருள் பெறுகிறது. பழந்தமிழ் இலக்கியங்களான சங்க இலக்கியங்களைப் பொறுத்தவரை, தமிழரின் பொருளியல் சிந்தனைகளுக்கு அகன்ற இடம் கொடுத்த இலக்கியப் பரப்பு எனல் பொருத்தமாகும்.

பொருள் என்ற கருத்துருவாக்கத்தோடு புதிய சிந்தனை மரபும் உடைமைக் கருத்தியலும் இணைவு பெறுகின்றன. அருள் பொருள் என்ற எதிர் முரண் கட்டமைக்கப்படும் அதே வேளையில் இரண்டையும் இணைவுபடுத்தும் முயற்சியும், பொருளைத் தேடுவதிலும் பார்க்க, அருளைத் தேடுதலே சிறந்தது என்ற கண்ணோட்டத்தை உருவாக்கும் முயற்சியும் தொடர்ச்சியாக நடைபெறுகிறது.

ஆனாலும் உடைமைச் சமூகம் பொருள் இன்றி இயங்க முடியாது. உற்பத்தி - வணிகம் - நுகர்தல் என்ற அளவில் சமூக அசைவியக்கம் நடைபெற்றாக வேண்டும். சமூகத்தின் பொதுநிலையினர் பொருளின் மீதான ஆசை கொள்வதும் அவ்வாசை மிகுவதும் சமூகத்தின் உடைமை வர்க்கத்தாரைத் தொந்தரவுபடுத்தும் ஒன்றாகும். அதாவது உழைக்கும் வர்க்கத்தார் உடைமையின் மீது ஆசை கொள்வது என்பது 'உடைமை வர்க்கத்தாரின் இருப்புக்கான சவாலாகும். எனவே பொருள் பற்றிய கட்டுமானங்களையும் விதிகளையும் உடைமை வர்க்கம் உருவாக்கி, அதைப்பரப்பவும் நிலை நிறுத்தவும் முயலும். எளிய குடிகள் பொருள் உற்பத்தி - வணிகம் - நுகர்வு ஆகியவற்றைக் கட்டுப்படுத்தும் உயர்குடி, அவ்வளவுகோலினைத் தங்களுக்கு இட்டுக்கொள்ள விரும்பாது. அவ்வளவுகோல்கள் அவர்களுக்குப் பொருந்தவும் பொருந்தாது. எல்லை அகற்சி, எதிரியின் வளத்தைச் சூறையாடுதல், உற்பத்திக் கட்டுமானங்களை நிர்மாணித்து நிலைத்த குடியினராக மக்களை மாற்றுதல் ஆகியவை உடைமைச் சமூகத்திற்கு அவசியமான ஒன்றாகவே இருக்கிறது.

எனவே பொருளியல் குறித்த சிந்தனையில் ஒரு எதிர் முரணைக் கட்டமைத்து அவற்றுக்கிடையே ஒரு தத்துவார்த்த ஊடாட்டத்தை நிகழ்த்துவதும் அதன்மேல் இலக்கியங்களை உருவாக்குவதும் இலக்கியக் கோட்பாடுகளை உருவாக்குவதும் உடைமைச் சமூகத்தின் இயல்பாகிவிடுகிறது.

பொருள் குறித்த சிந்தனைகள்:

பொருள் நிலையில்லாதது என்றும் எனவே பொருளைத் தேடுவதில் வாழ்க்கையை இழக்க வேண்டாம் என்பதும் அக இலக்கியங்களில் தலைவனைச் செல்வமுங்குவிக்க முயற்சிக்கும் தோழி வற்புறுத்திக் கூறுவது ஆகும். தலைவியைத் தேற்ற வரும் தோழி, 'புகழை விரும்புவனுடைய பொருள் போல உன் பசுலை அழியும்' (குறுந்.143) என்கிறாள். தமக்கென நீண்டகாலம் பொருளைப் பாதுகாத்தலில்லை என்று புறம் (163) பேசுகிறது. 'உண்டும் தின்றும் இரப்போர்க் கீந்தும் \ மகிழ்க வம்மோ மறப்போ ரோயே...' (புறம்.384) என்பது பொருளை அழித்துத் தீர வேண்டிய கட்டாயத்தைக் குறிப்பிடுகிறது. அவ்வாறின்றிப் பாதுகாக்கப்படும் பொருள் நிலைத்திருத்தல் இல்லை என்பது பெறப்படும்.

பொருளின் முக்கியத்துவத்தை வலியுறுத்தல்:

பொருள் என்பது நிலையில்லாதது என்ற கருத்துருவம் முன்வைக்கப்படும் அதே வேளையில், பொருளின் அவசியமும் வற்புறுத்தப்படுவதைச் சங்க இலக்கியங்களில் காணமுடிகிறது.

'இருள்படு நெஞ்சத்து இடும்பை தீர்க்கும்

அருள்நன்கு உடையர் ஆயினும், ஈதல்

பொருளில் லோர்க்கு அஃது இயை யாதுஆகுதல்

யானும் அறிவென் மன்னே... ' (அகம்.335)

அருள் உள்ளத்தை உடையராயினும் பொருள் இல்லாதார்க்கு ஈதல் இயலாது என்ற உண்மையினை மேற்குறித்த வரிகள் வெளிப்படுத்துகின்றன.

'ஈதலும் துய்த்தலும் இல்லோர்க்கு இல்லெனச் செய்வினை கைம்மிக எண்ணுதி' (குறுந்.63) என்ற குறுந்தொகைப் பாடலும் பொருள் இல்லோர், ஈதலையும் ஈதலால் வரும் இன்பத்தையும் அடைய முடியாது என்று குறிப்பிடுகிறது. எனவே பொருள் என்பது அறத்தையும் இன்பத்தையும் அடையவைக்கும் இணைப்புப் பாலமாக இருக்கிறது என்ற கருத்து வற்புறுத்தப்படுவதைக் காணமுடிகிறது.

பொருளைத் தேடாதவர்க்குப் புகழ், இன்பம், கொடை ஆகிய மூன்றும் இல்லை என்று குறிப்பிடுகிறது ஒரு நற்றிணைப் பாடல் (214). பரத்தை ஒருத்தி, இரவலர்க்கு ஈயாச் செல்வம் புகழாகப் பரவி வெளிப்படாது போல, என் நலன் வருந்துக' (அகம்.276) என்று வஞ்சினம் கூறுவதை அகநானூற்றில் காணமுடிகிறது.

எனவே பொருளின் இன்றியமையாமை பல்வேறு நிலைகளில் சங்க இலக்கியங்களில் வற்புறுத்தப்படுவது நோக்கத் தக்கது.

பொருளின் பயன்:

'அறன் கடைப்படாஅ வாழ்க்கையும் பிறன் கடைச் செலாஅச் செல்வமும் இரண்டும் பொருளின் ஆகும்' (அகம்.155) என்பது பொருளின் தலைமையை வலியுறுத்திச் சொல்லும் குரல் ஆகும்.

'அறம்தலைப் பிரியாது ஒழுகலும், சிறந்த

கேளிர் கேடுபல ஊன்றலும், நாளும்

வருந்தா உள்ளமொடு இருந்தோர்க்கு இல்' (அகம்.173) என்ற பாடலில் பொருள் சுற்றத்தாரின் துயர் துடைத்தல் குறிப்பிடப்படுகிறது.

'செறுவோர் செம்மல் வாட்டலும், சேர்ந்தோர்க்கு

உறும்இடத்து உவக்கும் உதவி ஆண்மையும்

இல்இருந்து அமைவோர்க்கு இல்' என்று (அகம்.231) தலைவன் பொருள் தேடிச் சென்றதாகக் குறிப்பிடப்படுகிறது. பகைவரின் செருக்கினை அடக்குவது பொருள் என்ற கருத்து இங்குக் கருத்தூன்றி நோக்கத்தக்கது.

'இரப்போர் ஏந்துகை நிறைய, புரப்போர் புலம்புஇல் உள்ளமொடு புதுவதந்து உவக்கும் அரும் பொருள் வேட்டம்' (அகம்.389) என்று இரப்போர்க்கு உதவுதற்குப் பொருள் பயன்படுதலையும், நண்பர்களுக்குச் செல்வம் பெருகவும் தலைவியின் தோள்கள் நல்ல அணிகலன்களைப் பூணவும் (நற்.286) பொருள் உதவும் என்று குறிப்பிடப்படுகிறது. அருள், பகையழித்தல், புணர்ச்சி பெறல் இவை யாவும் பொருளால் பெறலாம் என்று கலித்தொகை (11) குறிப்பிடுகிறது.

எனவே பொருளின் பயன் அறத்தைப் பெறுவது, கொடை, புகழ், புணர்ச்சி ஆகிய இன்பத்தைப் பெறுவது என்பதாக அமைவது சுட்டிக்காட்டப்பட்டுப் பொருள் தேடும் வேட்கை மிகுவிக்கப்படுகிறது.

பொருள் தேடும் நோக்கம்:

பொருள் தேடுவதற்கான நோக்கங்கள் சங்க இலக்கியங்களில் மிகவும் உயர்வாகவே எடுத்துரைக்கப்படுகின்றன. பொருளீட்டும் முயற்சி வெற்றாகப் பொருள் சேகரித்தல், வளம் பெறுதல், தன் குடும்பத்திற்கு ஊட்டமளித்தல் என்ற அளவில் மட்டும் அமைவதன்று என்பதும் அம்முயற்சிக்கு ஒரு சமூகநிலைப்பட்ட பின்னணி வழங்கப்படுவதும் கருதத்தக்கது. அதாவது பொருளீட்டும் முயற்சிக்கு ஒரு பொதுமை நோக்கம் கற்பிக்கப்படுகிறது. சங்க இலக்கியங்களைப் பொறுத்தவரை பொருளீட்டுவது என்பது இழிவான ஒன்றல்ல; மாறாக சமூகத்தின் பொதுக்கட்டுமானங்களுக்கு உதவுவதாகும்.

எனவே ஒரு வகையான தத்துவ நிலைப்பட்ட நிலையைப் பொருளீட்டும் முயற்சிக்குத் தர இலக்கியங்கள் முயன்றுள்ளமை வெளிப்படுகின்றது.

'பிறருக்கு என முயலும் பேரருள் நெஞ்சம்' (நற்.186) என்று பொருள் தேடும் உள்ளம் புகழ்ந்துரைக்கப்படுகிறது. பிறருக்கு ஈதல் வேண்டியே பொருள் தேடப்படுகிறது என்றுரைக்கிறது ஓர் அகநானூற்றுப் பாடல்(53). 'ஈதல் இன்பம் வெஃகி மேவரச் \ செய்பொருள் திறவராகி' (அகம்.69) என்றும் ஈயாமை இழிவு (கலி.1) என்றும் குறிப்பிடப்படுகிறது.

'பொருள் என்பது எல்லாக் காலத்திலும் மதிப்புடையதாக இருப்பினும், அதனை அறம் சார்ந்ததாகக் கூறும் கருத்து சங்க இலக்கியத்தாற் பெறப்படும். பொருளை ஈட்டுதல், செலவு செய்தல் ஆகிய எல்லாச் செயல்களிலும் அற நோக்கமே இருந்தது' என்கிறார் கு.வெ.பாலசுப்பிரமணியன் (சங்க இலக்கியத்தில் சமூக அமைப்புகள்:ப.120).

எனவே சங்கப் பொருளியல் சிந்தனை என்பது அறத்திற்கு உட்பட்ட ஒன்றாகவும் அறம் என்ற கட்டுமானத்தின் மேலேயே உருவாக்கப்படுவதாகவும் சித்தரிக்கப்படுவது குறிப்பிடத்தக்கத் தத்துவார்த்த அடிப்படையை வழங்குகிறது எனலாம்.

பொருள் திரட்டல்:

வினையே ஆடவர்க்கு உயிரே என்று மரபிலக்கியங்கள் வற்புறுத்தினாலும் உற்பத்தியிலிருந்து அல்லது உடல் உழைப்பிலிருந்து பெண்கள் விலக்கி வைக்கப்பட்டவர்கள் அல்லர். 'கண்ணுக்குத் தெரியாத உழைப்பு' என்றே அவர்களின் உழைப்பு சமகாலத்தில் பார்க்கப்படுகிறது. 'பொருளீட்டல்' என்ற வினையில் ஈடுபடும் ஆண்களை விட, அதிகமான அளவு உடல் உழைப்பைச் சிந்தும் சமூகப் பிரிவினராகப் பெண்களே இருக்கிறார்கள்.

சங்க காலப் பகுதியில் பெண்கள் எல்லாக் காலங்களையும் போலவே பொருளுற்பத்தி, வாணிகம் முதலான அடிப்படைகளில் பொருளீட்டுபவராகவும் உள்ளனர். உமணப் பெண்டிர் உப்பு விற்றுப் பொருளீட்டியமையை அகநானூறு சுட்டிக் காட்டுகிறது.

'நெல்லும் உப்பும் நேரே; ஊர்!' (அகம்.390)

கொள்ளீ ரோவெனச் சேரிதொறும் நுவலும்

அவ்வாங்கு உந்தி, அமைத்தோ ளாய்! (அகம்.390)

'உப்பு நொடை நெல்லின் மூரல் வெண் சோறு

அயிலை துழந்த அம்புளிச் சொரிந்து,

கொழுமீன் தனியொடு குறுமகள் கொடுக்கும்' (அகம்.60)

போன்றவை உமணர் பெண்டிர் உப்பு விற்றமைக்குச் சான்றுகள் ஆகும். இவை மட்டுமின்றிச் சங்க இலக்கியப் பரப்பில் விரிவான குறிப்புகள் உள்ளன.

முல்லை நிலப் பெண்கள் பால்வினைப் பயன்கள் விற்றுப் பொருளாதாரப் பயன் எய்தியமை சங்க இலக்கியத்தில் மிகுதியான இடங்களில் பதிவு செய்யப்பட்டுள்ளது.

'..... ஆய்மகள்

தயிர் கொடு வந்த தசம்பும், நிறைய

ஏரின் வாழ்நர் பேர் இல் அரிவையர்

குளக் கீழ் விளைந்த களக் கொள் வெண்ணெல்

மிகந்தனர் கொடுப்ப.....' (புறம்.33)

-எனவே பெண்கள் உப்புவிற்றும் பால்,மோர்,தயிர்,நெய் விற்றும் பொருளீட்டினர் என்பது புலப்படுகிறது.

உணவு சேகரித்தல், வேட்டையாடுதல் என்பதிலிருந்து உணவு உற்பத்தி செய்தல் என்று வளர்ந்தது மிக முக்கியமான பொருளுற்பத்திச் செயல்பாடு ஆகும். இனக்குழு வாழ்க்கையில் பெண்கள் கையில் இருந்த

விவசாய உற்பத்தி என்பதும் பிற்காலத்தில் அரசு உருவாக்கக் காலத்தில் புதிய தன்மைகளை எட்டியது. பாசனக் கட்டுமானங்கள், புதிய உற்பத்தி முறைமைகள் என அவை விரிவடைந்தன.

தனிச்சொத்து, குடும்பம் ஆகிய கட்டுமானங்கள் ஆண் தலைமையினை ஏற்றுக் கொள்வதாயின. ஆண்மை பெண்மை என்ற இருமை எதிர்வுகளில் 'பெருமையும் உரனும் ஆடுஉ மேன' (தொல்.) என்று பேச வேண்டிய அவசியம் ஏற்படுகிறது. எனவே பொருள் தேடுதல் உரனுடைய முயற்சியாக முன்வைக்கப்படுவது குறிப்பிடத் தக்கது.

பொருள் தேடுதலில் பெண்கள்:

'முந்நீர் வழக்கம் மகடுஉவோடில்லை' (தொல்.அகம்.34) என்று தொல்காப்பியம் குறிப்பிடுகிறது. தலைமகன் தன் தலைவியோடு கலத்திலேறிக் கடல் தாண்டிச் செல்வதில்லை என்பது அதன் செய்தி. ஆனால் இதற்குச் சிலர் பொருள் கொள்ளும் முறைமையினை எடுத்துக்காட்டி மறுத்துரைக்கிறார் தி.சு.பாலசுந்தரனார். அதாவது, 'தலைமகன் தன் தலைவியோடு கலத்திலேறிக் கடல் தாண்டிச் செல்வதில்லை; ஆயினும் காலிலேறி நாட்டிடையே செல்வதுண்டு' என்று தமக்கு வேண்டிய வகையாய்ப் பொருந்தாப் பொருளுரைத்துப் 'பொருள் பொருட்டுத் தலைவன் தலைவியோடு செல்லும் வழக்கம் பண்டு நிகழ்தலுண்டு' என்று உண்மையைத் திரித்துக் கூறுவாருமுளர்' (பாலசுந்தரனார்.தி.சு; பண்டைத் தமிழர் இன்பியல் வாழ்க்கை: ப.149) என்கிறார். மேற்குறித்த கருத்துக்கு இலக்கியச் சான்று ஏதுமிருப்பதை எடுத்துக்காட்டும் நச்சினார்க்கினியர் அதனைத் திட்டவாட்டமாக மறுத்துரைக்கிறார்.

தலைவன் தன் தலைவியையும் உடன் கூட்டிக் கொண்டு தன்னூர் நடந்து செல்வதெல்லாம், அவளுடன் யாறுங் குளனும் படிந்த நீர் விளையாடியும், குன்றும் பொழிலுந் தங்கிப் பூ விளையாடியும் அங்கெல்லாம் காணப்படும் புது மகிழ்ச்சியினை நுகர்ந்துறைதற்கேயா மென்று,

'யாறுங் குளனுங் காவும் ஆடிப்

பதியிகந்து நுகர்தலும் உரிய வென்ப' (தொல்.கற்பு.50)

என்று கற்பியற்கண் ஒரு நூற்பா இயற்றி நிறுத்துகின்றார் ' என்கிறார் அவர். (ப.149)

எனவே பொருள் நாடி வேற்று நாட்டிற்குச் செல்லும் தலைமகன் தன் தலைவியையும் உடன் கூட்டிச் செல்லல் பண்டைத் தமிழ் வழக்கன்றென்றே தெற்றென உணரல் வேண்டும் என்பார் அவர். எனவே பெண்கள் பொருள் தேடிப் புலம் பெயர்தலில்லை என்பதோடு, பொருள்தேடிச் செல்லும் தலைவனுடன் சேர்ந்து பயணப்படுதல் இல்லை எனலாம். அவ்வாறு இருப்பின் 'பொருள் வயிற் பிரிதல்' என்ற இலக்கிய உத்தியே பொருளற்றுப் போகும் என்பது பெறப்படுகிறது.

பொருள் தேடுதல் ஆடவர் இயல்பெனல்:

செய்பொருட்டு அகல்வது என்பது ஆடவர் பண்பு; அப்பிரிவை மகளிர் பொறுத்திருத்தல் கடமை என்று பேசுகிறது நற்றிணைப்பாடல் (24) ஒன்று. 'செயல்படு மனத்தர் செய்பொருட் ககல்வர் ஆடவரதுவதன் பண்பே' என்கிறது அது. எனவே 'வினையே ஆடவர்க்கு உயிரே' என்பதையே பண்டைய இலக்கியங்கள்

பல்வேறு வகைகளில் வற்புறுத்துவதைக் காணமுடிகிறது. 'உத்தியோகம் புருஷ லட்சணம்' என்னும் தற்காலச் சொல்வடையை நினைவுறுத்திக் கொள்ளலாம்.

பொருள் முயற்சி வகைகளும் பிரிவும்:

உலகத்தில் பொருள் தேடும் வழிகளாயுள்ள தொழில்களெல்லாம் அறிவு முயற்சியும் உடல் முயற்சியும் என இரு வகைப்படும் என்பார் தி.சு.பாலசுந்தரனார் (ப:155). அறிவு முயற்சி என்பது புலவர், அமைச்சர், கணக்கர் முதலியோர் தங்கள் அறிவுத் திறத்தாலும் புலமைத் திறத்தாலும் பொருளீட்டுவதாகும். உடல்முயற்சி என்பது இவை தவிர்ந்த உற்பத்தி, வாணிகம், போர் முதலியவை ஆகும்.

அறிவு முயற்சிக்கான பிரிவு என்பது திங்கள் நாட் கணக்கிலேயே அமைந்திருக்க வேண்டும். ஏனென்றால் அவை குறுகிய கால முயற்சியே ஆகும். ஆனால் உடல் முயற்சி என்பது பெரும்பாலும் திங்கள், பருவ (இருது)க் கணக்கிலேயே இருந்திருக்க வேண்டும்.

'பிரிவின் நீட்டம் நிலம்பெயர்ந் துறைவோர்க்

குரிய தன்றே யாண்டுவரை யறுத்தல்' (இறையனாரகப்பொருள்)

என்று குறிப்பிடப்படுவதும் பிற்கால வழக்கு எனலாம்.

பிரிவுக் காலம்:

தமிழ் மரபில் எடுத்துரைக்கப்பட்ட பிரிவுகள் அறுவகைப்படும்.

அவை, 1. உயர்கல்வி, 2. நாடு காத்தல், 3. போர் புரிதல், 4. பொருளீட்டல், 5. அரசனுக்கு உதவி, 6. பரத்தையர் நிமித்தம் பிரிதல்.

பொருள் வயிற் பிரிதல் என்பது பொருள் வயிற் பிரியும் தலைமகன் ஓராண்டுக்குள் திரும்புவான் என்பது இளம்பூரணர் கருத்தாகும் (190).

எக்காலத்தில் பிரிவு?:

இலக்கணிகளால் அடையாளப்படுத்தப்பட்ட ஆறு பெரும்பொழுதுகளில் பிரிதற்குரிய பொழுது வேனில் பருவமாகும். 'தலைவன் தலைவியர்க்குட் பிரிவு நிகழ்வதெல்லாம் தலைவன் நாடிடையிட்டுங் காடிடையிட்டும் வெளியே சென்று கருதிய தொழிலை முயன்று முடித்தற்கே யாதலின், அங்ஙனமொரு போர்ச்செயல் முதலான பெருஞ்செயல்களை மேற்கொண்டு முயன்று முடித்தற்கு உரிய காலம் அவற்கு வேனிற் பருவமேயாகும்' (தி.சு.பாலசுந்தரனார்;159) என்பர். ஏனைய பருவங்களெல்லாம் கருதிய வேலையை முடித்தற்கு மழையாலும் பனியாலும் இடையூறு பயப்பனவாகும்.

'உலகத்தில் நிகழும் புற முயற்சிகளெல்லாம் பெரும்பாலும் வேனிற் பருவத்திலேயே நிகழ்தலும், கார்ப்பருவத்தே நிறுத்தப்படுதலுங் கண்கூடாகும். எனவே ஒரு செயலையெடுத்து முயன்று ஆற்றவேண்டுந் தலைமகன் அது செய்தற்குரிய வேனிற்பருவத்தே பிரிந்து, அச்செயல் முயற்சி கார்காலந் தொடங்கியவுடன் நிகழமாட்டாமையின் அக்கார்காலத் தொடக்கத்தே அம்முயற்சியை முடித்துக் கொண்டோ அல்லதனை நிறுத்திக் கொண்டோ மீள்வனென்பது நன்கு பெறப்படும்' (தி.சு.பாலசுந்தரனார்;ப.159) என்பர்.

ஆகவேதான், 'நடுவுநிலைத் திணையே நண்பகல் வேனிலொடு...' (தொல்.அக.9) என்று பாலைத்திணைக்குரிய பெரும்பொழுதைக் குறிப்பிடுகிறது தொல்காப்பியம். இருத்தலை உரிப்பொருளாகக் கொண்ட முல்லைத்திணைக்கு, 'காரும் மாலையும் முல்லை' (தொல்.அகம்.6) என்கிறது.

பொருள் தேடும் முயற்சிக்கு வறுமை காரணமா?

அக இலக்கியங்களில் குறிப்பிடப்படும் தலைவன் வளமை குன்றியவனாகக் காட்டப்பெறவில்லை. 'நாடு கிழவோன், குன்று கிழவோன்' என்று வளமை மிகுந்தவனாகவே சிந்தரிக்கப்படுகிறான். அவ்வாறாயின் அவன் தனது மூதாதையர்களால் சேகரித்து வைக்கப்பட்ட பொருளியல் வளம் உடையவனாகவே தென்படுகிறான்.

தொல்காப்பியப் பொருளதிகாரத்தில் இளம்பூரணர், ஒருவனுடைய பொருள் வரவு நெறி என்று நான்கு முறையினைக் குறிப்பிடுகிறார் (217).

1. தாயத்தான் எய்துவன
2. ஒருவன் கொடுப்ப ஒருவன் பெறுவன
3. உழவு முதலிய வினையான் வருவன
4. பகைவரிடமிருந்து பெறுவன

தாயத்தால் எய்திய பொருளியல் வளத்தை உடையவனாகத் தலைவன் இருப்பின் அவற்றை வைத்து இல்லறத்தை இனிதுற நடத்திச் செல்லாமல் தலைவியைப் பிரிந்து துன்புற்றுப் பொருளீட்டும் முயற்சியில் தலைவன் ஏன் ஈடுபட வேண்டும் என்ற வினாவெழுகிறது.

'முன்னோர் தேடி வைத்த பொருளைச் செலவு செய்யாமல், தன் முயற்சியால் பொருள்தேடிச் செலவு செய்தல் குடும்பத் தலைவனுக்கு உரிய கடமையாக இருந்தது' என்று தனது ஓவச் செய்தியில் குறிப்பிடுகிறார் மு.வ.

பொருள்வயிற் பிரிதலென்பது நல்குரவு காரணமாகவன்று என்று எடுத்துரைக்கிறார் நக்கீரர். இறையனார் களவியல் உரையில் (36) பின்வருமாறு குறிப்பிடுகிறார்.

'இனிப் பொருள்வயிற் பிரியுமே யெனின் முன்னர்ப் பொருளிலனாயினானாம், ஆகவே எள்ளநர்ப் பணித்தலும் இரந்தோர்க் கீதலும் என்னும் இவையெல்லாம் பொருட்குறைபாடுடையார்க்கு நிகழாமையின் இக்குறைபாடுகளெல்லாம் உடையனாம்; அவை யுடையானது பொருவிறப்பு என்னையோ வென்பது... பொருட் பிணியென்பது பொருளிலனாய்ப் பிரியுமென்பதன்று, தன் முதுகுரவராற் படைக்கப்பட்ட பல்வேறு வகைப்பட்ட பொருளெல்லாங் கிடந்ததுமன், அது கொடு துய்ப்பது ஆண்மைத் தன்மை யன்றெனத் தனது தாளாற்றலாற் படைத்த பொருள் கொண்டு வழங்கி வாழ்வதற்குப் பிரியுமென்பது' என்று குறிப்பிடுகிறார்.

எனவே முன்னோர் பொருளைத் துய்த்தல் என்பது தாளாண்மைக்கு அழகாகாததாலும் அம்முன்னோரின் பெருஞ்செல்வம் தன் காலத்தில் தனக்கு உதவியது போலவே வருங்காலத் தனது சந்ததிக்கு உதவ வேண்டும் என்ற அடிப்படையிலும் பொருத்தமற்றது ஆகும். 'அம்முன்னோர் பணமென்பது தலைவனுக்குப் பொருள் தேடும் பருவமும் ஆற்றலும் வருந்துணையும் உதவியாய் நின்றற்குரியதேயன்றி அதற்கு மேலும் அவற்கு அஃது உதவியாறக் கன்றாமாதலாலும் தலைவன் தான் மேற்கொண்ட இவ்வாழ்க்கையினை நடத்துதற்குத் தானே முயன்று பொருள் தேடுதலை விரும்பினான்' (தி.சு.பாலசுந்தரனார்:ப.154) என்பர்.

திருமணத்துக்குமுன்ஏன்பொருள்தேடவில்லை?

தலைவியைத் தலைவன் வரைந்து கொள்ளுதற்கு முன்னர்ப் பொருள் தேடிச் செல்லுதல் பெருவழக்கில்லை. சிறார் பருவத்திலிருந்து வளர்ந்து இளைஞனாகத் தலைவன் உருமாறிய காலத்திலேயே தலைவியின் மீதான காதல் ஏற்படுகிறது. எனவே அக்காலகட்டத்தில் பொருளைத் தேடுதல் உரிய செயலன்று. தலைவன் திருமணம் செய்து கொள்ளுவதற்கு முன்னர்ப் பொருள் தேடியதுண்டு என்றும் அது தலைவியை வரைதற் பொருட்டே என்றும் தி.சு.பாலசுந்தரனார் குறிப்பிடுவார் (பண்டைத் தமிழர் இன்பியல் வாழ்க்கை;ப.153). திருமணத்திற்கான பொருளைத் தலைவன் ஈட்டினானே தவிர, திருமணத்துக்குப் பிந்தைய குடும்பத்திற்கான பொருளை ஈட்டவில்லை. எனவே தலைவியை அவன் மணம் செய்த பிறகு பொருள் தேடிச் செல்ல வேண்டிய கட்டாயம் உருவாகிறது எனலாம்.

'திருமணத்துக்கு முன்னால் பொருள் தேடும் ஆண்மைப் பருவமே அவன் வரப்பெற்றிலனாதலாலும் வரைதலுக்குப் பின்னால் நிகழ்விருக்கும் இல்வாழ்க்கையின் பொருட்டு அவன் முன்னமேயே பொருள் தொகுத்துக் கொள்ளுதற்கு இடமில்லை. எனவே திருமணஞ் செய்துகொண்டதன் பின்னர்த்தான் தலைவன் தனது இல்வாழ்க்கைக்கு வேண்டப்படும் பொருளைத் தேடுதற்கு இடம் பெற்றான்' என்பர் (ப:154).

எனவே திருமணத்திற்குப் பிறகே பொருள் தேடும் முயற்சி தீவிரம் பெறுகிறது என்பது கவனத்திற் கொள்ளத் தக்கது.

அறிவித்துப் பிரிதல்:

இறையனார் அகப்பொருள் பிரிதலை அறிவித்துப் பிரிதல், அறிவியாமல் பிரிதல் என்று இருவகையாகப் பகுக்கிறது. ஆனால், தலைவன் தலைவியைப் பிரிதலை அறிவித்துப் பிரிதலே சிறப்பு என்றும் குறிப்பிடுகிறது அது. எனவே தலைவன் தலைவியைப் பொருள்வயிற் பிரியப்போகிறேன் என்று அறிவிப்பதன் காரணமாகவே பிரிவதற்கான சூழலும் இலக்கியத் தளமும் கிடைக்கிறது எனலாம்.

பொருளா? புணர்வா?:

அறத்தையும் பொருளையும், அறத்தையும் இன்பத்தையும் எதிர் முரணாகச் சித்தரிக்கும் மரபு சங்க இலக்கியக்காலத்திலேயே தோற்றம் பெற்றுவிட்டதெனினும் அவற்றை இணைவுபடுத்தும் முயற்சிகளும் அக்காலகட்டத்திலேயே வெளிப்பட்டமையைக் காணமுடிகிறது. மேற்குறித்த எதிர்வு விதந்தோதப்பட்ட இலக்கியக்காலகட்டமாகப் பக்தி இலக்கியங்கள் இருக்கின்றன. பொருள் மற்றும் புணர்வு குறித்த தத்துவ விவாதம் சங்க அக இலக்கியங்களில் பொருள்வயிற் பிரிவின் நிமித்தம் மேற்கொள்ளப்பட்டிருக்கிறது.

'புணரின் புணராது பொருளே பொருள்வயின்

பிரியின் புணராது புணர்வே...' (நற்.16)

புணர்ச்சி இன்பத்திலீடுபட்டுப் பொருள்வயிற் பிரியாதிருப்பின் பொருள் புணராது என்பதும் பொருள்வயிற் பிரிந்து சென்றால் தலைவியின் புணர்வைப் பெறுதல் இயலாது என்பதுமான முரண் தர்க்கம் நுட்பமாகச் சொல்லப்பட்டுள்ளது.

தலைவியைப் பிரிதல் என்பது உலகியலார் வழங்கும் அறநெறியைப் புறக்கணித்ததாகும் என்று நற்றிணையில் (337) தோழி பேசுகிறாள். ஆனாலும் தோழிக்கான எதிர்க்குரலும் அக இலக்கியங்களில்

இல்லாமல் இல்லை. 'அறன் கடைப்படா வாழ்க்கையைப் பொருள் தருவதால் தலைவர் பிரிதல் சரியானதே' (அகம்.155) என்று தலைவன் கூறியதாகத் தலைவி கூறுவதும் கவனத்திற்குரியது. எனவே பொருள், புணர்வு குறித்த விவாதம் அக இலக்கியப் பொருள் வயிற் பிரிவில் நுட்பமாக நடைபெறுவது குறிப்பிடத்தக்கது.

பொருள் தேடுதலைப் பழித்துரைத்தல்:

பொருளின் இன்றியமையாமை வற்புறுத்தப்படினும் அகவாழ்க்கை அதனை ஏற்றல் எளிதில்லை. எனவே பொருள் தேடும் முயற்சியைப் பழித்தலும் பொருள் தேடும் தலைவனைப் பழித்தலுமான செயல்பாடுகள் எதிர்ப்படவே செய்கின்றன. எனவேதான் பொருள் தேடிச் செல்லும் தலைவனை 'அருள் இல்லாதவன்' என்றும் 'இரங்காதவன்' என்றும் (அகம் 75) குறிப்பிடுகின்றனர் பெண்டிர். 'பொருளையே நம்மினும் விரும்பினார் தலைவர்' (அகம்.53) என்றும் கடிந்துரைக்கின்றனர். கலித்தொகை 13 ஆம் பாடலில் 'பொருள் தேடுதலை வேண்டா முயற்சி எனக் கூறவந்த தோழியும், தன்னையறியாது, காதலர் வாழ்வுக்குப் பொருள் வேண்டுமென்பதையும், அது செந்நெறியாற் செய்யப்பட வேண்டுமென்பதையும் கூறினாள்' (கு.வெ.பாலசுப்பிரமணியன்:ப.120) என்பர்.

அக இலக்கியங்களில் பொருள் தேடும் முயற்சிகள் தடுத்து நிறுத்தப்பட்டன போலத் தோன்றினும் அவை செலவழங்கலையன்றிச் செலவு தவிர்தல் இல்லை' என்பார் கு.வெ.பாலசுப்பிரமணியன் (ப:120-121).

பிரிவின் விளைவுகள்:

பிரிவுச் செய்தி கேட்டுத் தலைவி நடுக்குறுதலும் அதைக்கண்டு தலைவன் நகுதலும் கலித்தொகையில் கூறப்படுகிறது (கலி.13). பிரிவினால் தலைவியின் எழில் கெடும் (அகம்.81), வளை நெகிழும் (நற்.26), மேனி பசப்புறும் (குறுந்.33), கவின் கெடும் (ஐங்.310), நோயுறும் (கலி.2) என்றெல்லாம் பிரிவின் விளைவுகள் குறிப்பிடப்படுகின்றன.

இதன் உச்சமாக 'சில நாட்களில் திரும்பி வருவதாகச் சொல்லும் தலைவனே, நீ வரும் வரையில் இவள் உயிர் வாழாள் என்பதை நன்கறிந்த பின் செல்க!' (நற்.19) என்று தோழி குறிப்பிடுவது கவனத்திற்குரியது. 'இன்னுயிர் தருதலும் ஆற்றுமோ' (கலி.7) என்றும் குறிப்பிடப்படுகிறது.

தலைவி, தலைவனின் பிரிவை ஏற்றுப் பேசும் புரிந்துணர்வு அம்சங்களும் சங்க இலக்கியப் பாடல்களில் உள (நற்.214). எனவே பொருள்வயிற் பிரிதல் என்பதைப் பழித்தலும் விளைவு கூறலும் தலைவனின் அன்பை மிகுவிக்கவே எனலாம்.

இலக்கியத்தின் தொழிற்பாடு:

பொருளின் இன்றியமையாமை குறித்துப் புறநானூறு முதலான பொது இலக்கிய நூல்களில் போதிக்கப்படும் அறவுரைகளை விட, மேற்குறித்த அக இலக்கியங்களே வாசிப்பாளனின் மனத்தில் நுண்ணிய தாக்கங்களை ஏற்படுத்துகின்றன. இலக்கியத்தின் வியத்தகு தொழிற்பாடும் அதுதான். கருத்தியல்களை நிலைநிறுத்த இலக்கியங்கள் உற்பத்தி செய்யப்படுகின்றன என்ற மார்க்ஸின் கூற்று இங்கு நினைவுகூரத்தக்கது.

பொருள்வயிற் பிரிதல், செலவழங்குவித்தல், ஆற்றியிருத்தல் என்பவை யாவுமே பொருளீட்டல் அதற்கான பொது ஏற்புநிலையை உருவாக்குதல் என்ற அடிப்படையிலிருந்தே உருவாக்கப்பட்டுள்ளன எனலாம்.

முடிவாக...

உடைமைச் சமூகத்தில் ஆண்கள் தலைமையிடம் பெற்றதன் பின்னணியில் பொருள் தேடுதலும் அவற்றுக்கு ஒரு பொதுநிலைப்பட்ட நோக்கத்தை வழங்குவதும் அதற்கான பொதுச் சமூகத்தின் ஏற்பைக் கோருவதுமே பொருள்வயிற் பிரிவு குறித்த இலக்கியச் செயல்பாட்டின் அடிப்படையாகின்றன.

பொருளின் இன்றியமையாமை, நிலையாமை என்ற எதிர் முரண்களும் பொருளினால் விளையும் பயன்கள், இழப்பவை பற்றிய எதிர்வுகளும் நிறுவ விரும்புவது பொருளின் ஏற்பைத்தான்.

கைப்பொருளை மெய்ப்பொருளாக்கும் தத்துவார்த்த முயற்சியில் அக இலக்கியங்கள் பெரும்பங்கு வகித்திருக்கின்றன எனலாம்.

முதன்மைச் சான்றாதாரங்கள்:

1. அகநானூறு
2. குறுந்தொகை
3. புறநானூறு
4. நற்றிணை
5. கலித்தொகை (அனைத்து நூல்களும் என்.சி.பி.எச் வெளியீடுகள், பதிப்பாசிரியர்கள்: அ.மா.பரிமணம், கு.வெ.பாலசுப்பிரமணியன்; ஏப்.2004)
6. தொல்காப்பியம் (மர்ரே எஸ்.ராஜம் பதிப்பு)

துணைமைச் சான்றாதாரங்கள்:

1. ----- 'இறையனார் களவியலுரை'; திருநெல்வேலி சைவசித்தாந்த நூற்பதிப்புக் கழகம்; 1963.
2. பாலசுப்பிரமணியன் கு.வெ; 'சங்க இலக்கியத்தில் சமூக அமைப்புகள்'; தமிழ்ப்பல்கலைக் கழகம், தஞ்சாவூர்;திசம்பர் 1994.
3. பாலசுந்தரனார் தி.சு; 'பண்டைத் தமிழர் இன்பியல் வாழ்க்கை'; திருநெல்வேலி சைவசித்தாந்த நூற்பதிப்புக் கழகம்; 1960.
4. வரதராசனார்.மு: 'ஓவச் செய்தி'; பாரிநிலையம், சென்னை;1980.

ஜி.நாகராஜன் - மாற்று ஒழுக்கத்தை முன்வைத்த கலைஞன்

சு.இரமேஷ்.

தமிழ்த்துறை, இந்துக் கல்லூரி, பட்டாபிராம், சென்னை- 72

புதுமைப்பித்தனில் தொடங்கிய நவீனத்துவ கதைசொல்லும் மரபு, தொடர்ந்து பல்வேறு கதைஞர்களின் முயற்சிகளின் ஊடாக அதன் ஆழத்தையும் விரிவையும் தேடி பயணப்பட்டது. ஒவ்வொரு காலகட்டத்திலும் தோன்றும் கதையாசிரியன் தன் பங்காக ஏதோ ஒரு சேதனை முயற்சியைத் தம் படைப்பின் வழியாகத் தேடுகிறான். அத்தேடுதல் ஒரு முற்றுபெறாத முடிவை நோக்கி அவனை நகர்த்திச் செல்கிறது. இவ்வாறாக முற்றுபெறாத மாற்று ஒழுக்கத்தின் தேடலை நோக்கி தம் புனைகதைகளைச் செலுத்திய மகத்தான கலைஞன்தான் ஜி.நாகராஜன்.

ஜி.நாகராஜன், 1929-ஆம் ஆண்டு செப்டம்பர் 1-ஆம் தேதி மதுரையில் பிறந்தார். தந்தை பெயர் கணேச அய்யர்; பழனியில் வழக்கறிஞர் தொழிலை மேற்கொண்டு வந்தார். ஜி.நாகராஜனின் நான்காவது வயதில் அவரது தாயார் எதிர்பாராதவிதமாக ஒரு பிரசவத்தின்போது இறந்துவிட்டார். ஜி.நாகராஜனுக்கு இரண்டு சகோதரிகள், ஓர் அண்ணன், ஒரு தம்பி என இருந்தனர். ஜி.நாகராஜனின் பிள்ளைப்பருவம் அவரது தாய்வழிப்பாட்டி வீட்டில் கழிந்தது. நான்காம் வகுப்புவரை மதுரை திருமங்கலத்தில் படித்தார். இளமையிலேயே ஜி.நாகராஜன் தமிழ், ஆங்கிலம் ஆகிய மொழிகளில் புலமை மிக்கவராக விளங்கினார். இவரின் ஆங்கில உச்சரிப்பைக் கண்டு பலரும் வியந்தனர். இவருக்குப் பிடித்த பாடம் கணிதமாக இருந்தது. சிலகாலம் ஜி.நாகராஜனின் தந்தை கணேச அய்யர் அவரைப் பள்ளிக்கு அனுப்பாமல் தாமே பாடங்களைச் சொல்லிக் கொடுத்தார். ஆனால், எட்டு மற்றும் ஒன்பதாம் வகுப்புகளை மீண்டும் மாமா வீட்டில் தங்கி திருமங்கலம் பி.கே.நாடார் உயர்நிலைப்பள்ளியிலும் பத்து, பதினொன்றாம் வகுப்புகளைத் தந்தையுடன் தங்கி பழனி எம்.ஹெச்.பள்ளியிலும் பயின்றார். இன்டர் மீடியட்டை மதுரைக் கல்லூரியில் படித்து, சிறப்பான முறையில் தேறினார். அப்போது கணிதத்தில் நூற்றுக்கு நூறு மதிப்பெண்கள் பெற்றதற்காக அறிவியல் அறிஞர் சி.வி.ராமணிமிருந்து ஜி.நாகராஜன் தங்கப் பதக்கம் பெற்றார் என்பது குறிப்பிடத்தக்கது.

கல்லூரிப் படிப்பை முடித்த ஜி.நாகராஜன், காரைக்குடி கல்லூரியில் ஒரு வருடம் டியூட்டராக பணியாற்றினார். தொடர்ந்து, சென்னை அக்கவுண்டன்ட் ஜெனரல் அலுவலகத்தில் சேர்ந்து ஒரு வருடம் பணிபுரிந்தார். இயல்பாகவே கற்பிக்கும் பணியில் அளவிலாத ஈடுபாடு கொண்டிருந்த ஜி.நாகராஜன், அங்கிருந்து விலகி மதுரை அமெரிக்கன் கல்லூரியில் விரிவுரையாளராகச் சேர்ந்தார். அமெரிக்கன் கல்லூரியில் பணியாற்றிய காலகட்டத்தில்தான் அவருக்குக் கம்யூனிஸ்ட் இயக்கத்தோடும் இலக்கியத்தோடும் தொடர்பு ஏற்பட்டது. பின்னாட்களில், 'என் உடம்பிலிருந்து உயிர் பிரிவது வரை நான் கம்யூனிஸ்ட்தான்' என்று அவருடைய நண்பரும் எழுத்தாளருமான சுந்தர ராமசாமியிடம் கூறும் அளவுக்கு ஜி.நாகராஜனுடைய கம்யூனிஸ்ட் பற்று இருந்திருக்கிறது.

ஜி.நாகராஜன் கணிதம் கற்பிப்பதில் மிகச்சிறந்தவாக அக்காலத்தில் இருந்திருக்கிறார். அறிவாற்றலும் கற்பிக்கும் திறனும் மாணவர்களிடையேயும் சக ஆசிரியர்களிடையேயும் நிர்வாகத்திடமும் அவருக்கு மிகுந்த மரியாதையைப் பெற்றுத்தந்தன. கம்பீரமான தோற்றமும் பொலிவும்கூடிய வசீகரமான தோற்றம் ஜி.நாகராஜனுடையது. வெண்மைநிற வேட்டியும் ஜிப்பாவும்தான் அவரின் அடையாளம். 'கம்பீரமும் பொலிவும்கூடி முயங்கிய வசீகரத் தோற்றம். உடல் பயிற்சிகளினால் திண்மம் பெற்ற உடல்வாகு. தன்னம்பிக்கை மிளிரும் முகம். ஒவ்வொரு

அசைவிலும் அணுகுமுறையிலும் பாந்தமாக வெளிப்படும் லயம். அவரைப்போல் ஆகவேண்டும் என்று என் லட்சிய மனிதனாக அவரை ஸ்வீகரித்திருந்தேன். நாலு முழ அகலக் கரை வேட்டியிலும் வெள்ளை ஜிப்பாவிலும் படு சுத்தமாக எப்போதும் தோற்றமளிப்பார்' (நடைவழிக் குறிப்புகள், பக்.61) என்று ஜி.நாகராஜனிடம் கணிதம் பயின்ற எழுத்தாளர் சி.மோகன் பதிவுசெய்கிறார்.

மாணவர்களுக்கு பாடம் நடத்தும் திறமையைக் கண்ட அமெரிக்கக் கல்லூரி நிர்வாகம், ஜி.நாகராஜனை அமெரிக்காவுக்கு அனுப்பவும் முடிவு செய்திருந்தது. ஆனால், கம்யூனிஸ்ட் இயக்கத்தோடு கொண்டிருந்த தொடர்பு காரணமாக நிர்வாகம் இவரை வேலை நீக்கம் செய்தது. பின்னர் வந்த நாட்களில் ஜி.நாகராஜன் கட்சிப் பணிகளில் ஈடுபட்டபடியே மாணவர்களுக்குத் தனியாகப் பாடம் கற்பித்துக் கிடைத்த வருமானத்தைக் கொண்டு நாட்களை நகர்த்தினார். பின்னர், கட்சித் தோழரான சங்கர நாராயணன் நடத்திய தனிப்பயிற்சிக் கல்லூரியில் சேர்ந்து, 1956 முதல் 1970-ஆம் வரை பணியாற்றினார். 'ஜி.நாகராஜன் எங்கள் கல்லூரியில் வகுப்பு எடுக்கிறார்' என்று திரையரங்குகளில் விளம்பர ஸ்லைடு காட்டும் அளவிற்கு இவரது கற்பிக்கும் திறன் இருந்திருக்கிறது.

1959-ஆம் ஆண்டு ஜி.நாகராஜன் ஆனந்தி என்ற பெண்ணைத் திருமணம் செய்துகொண்டார். ஆனால், துரதிர்ஷ்டவசமாக மணமான நான்காவது மாதத்தில் அவரது மனைவி ஸ்டவ் வெடித்து மரணமடைந்தார். மூன்றாண்டு இடைவெளிக்குப் பின்னர், 1962-ஆம் ஆண்டு ஜி.நாகராஜன் பள்ளி ஆசிரியையாகப் பணியாற்றிவந்த நாகலட்சுமியை இரண்டாந்தாரமாக மணந்துகொண்டார். இவர்களுக்கு ஆனந்தி, கண்ணன் என இரு குழந்தைகள் பிறந்தனர்.

1957-ஆம் ஆண்டு ஜூன் மாதம் 'அணுகும' என்ற முதல்சிறுகதை ஜனசக்தி வாரமலரில் பிரசுரமானது. இக்கதையிலிருந்துதான் ஜி.நாகராஜனின் படைப்புலகம் தொடங்குகிறது. சரஸ்வதி, சாந்தி, ஜனசக்தி, இரும்புத்திரை, ஞானரதம், கண்ணதாசன், கணையாழி, சதங்கை, இல்லஸ்டிரேட்டட் வீக்லி ஆப் இந்தியா போன்ற இதழ்களில் நாகராஜனின் எழுத்துக்கள் தொடர்ந்து வெளிவந்தன. ஆங்கிலத்திலும் சில சிறுகதைகள் எழுதியிருக்கிறார். *With Fate Conspires* என்றொரு ஆங்கில நாவலும் இவரின் படைப்புகளில் அடங்கும். சிறுகதை, நாவல், கட்டுரை தவிர *புற்றுக்குடிப் புலவர்* என்ற பெயரில் 'ஞானரதம்' இதழில் மூன்று கவிதைகளையும் எழுதியிருக்கிறார். இவருடைய மொத்தப் படைப்புகளையும் ராஜமார்த்தாண்டன் தொகுத்து 'ஜி.நாகராஜன் ஆக்கங்கள்' என்ற பெயரில் காலச்சுவடு பதிப்பகம் மூலமாக வெளியிட்டுள்ளார்.

ஜி.நாகராஜனின் முதல் புத்தகமாக வெளிவந்தது 'குறத்தி முடுக்கு' என்ற குறுநாவல்தான். 'பித்தன் பட்டறை' என்ற பதிப்பகமொன்றை ஆரம்பித்து 1963-ஆம் ஆண்டு ஜி.நாகராஜனே இதனைப் புத்தகமாகக் கொண்டு வந்தார். அக்கால கட்டத்தில் முறையாக கவனிக்கப்படாத எழுத்தாளராகவே ஜி.நாகராஜன் இருந்திருக்கிறார். இவரே 1971-ஆம் ஆண்டு, அதுவரை தாம் எழுதிய கதைகளிலிருந்து 14 கதைகளைத் தேர்ந்தெடுத்து 'கண்டதும் கேட்டதும்' என்ற பெயரில் ஒரு தொகுப்பைக் கொண்டு வந்தார். 1973-ஆம் ஆண்டு ஜனவரியிலிருந்து டிசம்பர் வரை 'ஞானரதம்' இதழில் இவருடைய மற்றொரு நாவலான, 'நாளை மற்றுமொரு நாளை' தொடராக வெளிவந்தது. இதனையும் 'பித்தன் பட்டறை' வெளியீடாக 1974-ஆம் ஆண்டு ஜி.நாகராஜனே புத்தகமாகக் கொண்டு வந்தார்.

ஜி.நாகராஜன் இந்த உலகில் வாழ்ந்த காலம் ஐம்பத்திரண்டு ஆண்டுகள்தான். இதில் அவர் உருவாக்கியப் படைப்புகள் மிகக்குறைவே. ஆனாலும் எக்காலத்திலும் பேசக்கூடிய பக்கங்களைத்

தொட்டுச் சென்றவர். ஜி.நாகராஜனின் கதை உலகம் இதுவரை தமிழ்ச்சூழல் கண்டிராத ஒன்று. சமூகத்தால் அங்கீகரிக்கப்படாத விளிம்புநிலை மக்களான பாலியல் தொழிலாளிகளைப் பற்றி எழுதி நவீன இலக்கியத்தின் பக்கங்களை விரிவாக்கியவர். இதில் ஜெயகாந்தனின் பங்கையும் மறுக்க முடியாது. ஆனாலும் ஜெயகாந்தனிலிருந்து முற்றிலும் வேறு திசையில் பயணித்தவர் ஜி.நாகராஜன். பொறுக்கிகளையும் உதிரிகளையும் தம் படைப்புகளில் பூரணத்துவம் பெறச் செய்தவர் ஜி.நாகராஜன். இடதுசாரிகளோடு கொண்ட தொடர்பும் விளிம்புநிலை மக்களோடு அவருக்கிருந்த நெருக்கமும் அவருடைய படைப்பை முழுமைபெறச் செய்தன. தான் எழுதிய 'குறத்தி முடுக்கு' என்ற குறுநாவலின் முதல்பக்கத்தில் ஜி.நாகராஜன் இவ்வாறு எழுதுகிறார்: "நாட்டில் நடப்பதைச் சொல்லியிருக்கிறேன். இதில் உங்களுக்குப் பிடிக்காதது இருந்தால் 'இப்படியெல்லாம் ஏன் நடக்கிறது?' என்று வேண்டுமானால் கேளுங்கள் 'இதையெல்லாம் ஏன் எழுத வேண்டும்?' என்று கேட்டுத் தப்பித்துக்கொள்ளப் பார்க்காதீர்கள். உண்மையைச் சொல்வதென்றால் முழுமையுந்தான் சொல்லியாக வேண்டும். நான் விரும்பும் அளவுக்குச் சொல்ல முடியவில்லையே என்பதுதான் என் வருத்தம்" என்று தன் வருத்தத்தைக் குறிப்பிடுகிறார். ஜி.நாகராஜனின் கதை உலகம் என்பது சமூகத்தால் கண்டுகொள்ளப்படாத தகுந்த அங்கீகாரமில்லாத நகரத்தின் இடுக்குகளில் வாழும் விளிம்புநிலை மக்கள் சார்ந்தது. தமிழ்ப் புனைவுகள் அதுவரைக் கண்டிராத ஓர் உலகத்தை தம் கதைகளின் வாழிலாகக் கட்டமைத்தார். அவர் கதைகளில் வரும் கதாபாத்திரங்கள் போலவே பிறர் தரும் மதிப்புக்கும் மரியாதைக்கும் முக்கியத்துவம் கொடுக்காத ஒரு நபராகவே இறுதிவரை ஜி.நாகராஜன் வாழ்ந்திருக்கிறார்.

தான் ஓர் எழுத்தாளன் என்ற பிம்பத்தை ஜி.நாகராஜன் எப்போதும் கொண்டிருக்கவில்லை. தன்னை ஒரு கம்ப்யூனிஸ்டாக கம்ப்யூனிஸ்ட் கட்சியைச் சார்ந்தவர்களே மதிக்கவில்லை என்பதையும் அவர் உணர்ந்திருந்தார். அது குறித்தும் அவர் கவலைப்பட்டதாகத் தெரியவில்லை. பாலியல் தொழிலாளிகளுடனான அவரது இயல்பான பழக்கம் அவரது நண்பர்களுக்கும் உறவுகளுக்கும் பெரும் சங்கடத்தையும் மனச்சோர்வையும் ஏற்படுத்தியது. பல எழுத்தாள நண்பர்கள் இவருடன் பழகுவதையே தவிர்த்திருக்கிறார்கள். இருந்தும் அவர்களுடன் பழகுவதை ஒரு குற்றவுணர்வாக ஜி.நாகராஜன் பார்த்ததாகத் தெரியவில்லை. இறுதிநாள் வரை தன் அடையாளத்தை மாற்றிக்கொள்ளாதவராகவே இருந்திருக்கிறார். 'அவர் செய்வது குறித்த குற்ற உணர்வோ, அவரது மனைவிபடும் துன்பம் பற்றிய பச்சாதாபமோ அவரிடம் ஒரு துளிகூட இருந்தது கிடையாது' (பக்.25) என்று ஜி.நாகராஜன் குறித்த நினைவோடையில் சுந்தர ராமசாமி குறிப்பிடுகிறார்.

தன் தோற்றத்தின் மூலமாகவே பலராலும் அடையாளம் காணப்பட்ட ஜி.நாகராஜன், ஒரு கட்டத்தில் கிழிந்துபோன ஆடைகளை அணிய ஆரம்பித்தார்; மழிக்காத முகத்தோடு வெறுமை படர்ந்து காணப்பட்டார். கஞ்சாவை சிகரெட்டில் கலந்து பிடிக்கும் பழக்கத்திலிருந்து விடுபட முடியாமல் தவிர்ந்தார். அவர் இறப்பதற்கு முந்தைய நாள் கூட சிகரெட்டில் கஞ்சாவைக் கலந்துப் பயன்படுத்த விரும்பியதாக இறக்கும் தருவாயில் அவருடனிருந்த சி.மோகன் குறிப்பிடுகிறார். அவருக்கு ஏற்பட்ட சில தவறான பழக்கங்களின் காரணமாக கடுமையான நோய்களுக்கு தன் உடலை உண்ணக் கொடுத்துவிட்டார். 'நாகராஜன் தன்னை அழித்துக்கொள்ள விரும்பி அப்படிச் செயல்பட்டு வருகிறார். ஆனால் அப்படித் தன்னை அழித்துக்கொள்ள விரும்பாதவர்களைச் சங்கடத்திற்குள்ளாக்குவதற்கு அவருக்கு எந்த உரிமையும் கிடையாது. ஆனால் அது பற்றி அவர் கவலைப்பட்டதே இல்லை' (பக்.73) என்று சு.ரா. மேலும் தம் நூலில் குறிப்பிடுகிறார்.

'சாவும் அதை எதிர்கொள்ள மனிதன் தன்னைத் தயார்படுத்திக் கொள்ளும்போதே வரும்' என்று கூறிய ஜி.நாகராஜன், 1981-ஆம் ஆண்டு பிப்ரவரி மாதம் 19-ஆம் தேதி நள்ளிரவில் மதுரை அரசு மருத்துவமனையில் காப்பாற்ற கதியற்று ஏறக்குறைய அநாதையாக இறந்துபோனார். தற்போது ஜி.நாகராஜனின் குடும்பம் சென்னையில் வசித்து வருகிறது.

இதுகாறும் நம்பப்பட்டு வந்த ஒழுக்கத்தையும் அதன் விதிகளையும் அதன் எல்லைவரைச் சென்று தன் கதைகளின் மூலமாகத் தகர்த்தெறிந்தவர் ஜி.நாகராஜன். கந்தன் என்ற சேரி மனிதனின் ஒருநாள் அனுபவத்தை 'நாளை மற்றொரு நாளே' என்ற குறுநாவலின் மூலமாக வெளிப்படுத்தினார். மரபுகளை மறு மதிப்பீடு செய்யும் இந்நாவல் ஏற்படுத்தும் அதிர்வுகள் அதுவரை தமிழ்ச்சூழல் கண்டிராத ஒன்று. ஜி.நாகராஜனை ஒரு மிகச்சிறந்த படைப்பாளியாக அறிமுகப்படுத்திய நாவல் நாளை மற்றொரு நாளே. இந்நாவலைத் தவிர்த்த ஜி.நாகராஜன் சாதாரண ஒரு படைப்பாளியாகவே அடையாளம் காணப்பட்டிருப்பார். இந்நாவலில் அவர் வெளிப்படுத்தும் அங்கதம் அபரிமிதமானது.

மனித சமூகத்தின் இனக்குழு அடையாளத்தைத் தன் 'குறத்தி முடுக்கு' என்ற நாவலின் மூலமாக மீட்டவர். புதுமைப்பித்தன் தன்னுடைய 'பொன்னகரம்' கதையின் மூலமாக கற்பு குறித்த ஒரு மாற்று கதையாடலின் தொடக்கத்தை ஏற்படுத்தினார். பொன்னகரம் அம்மாளுவின் நீட்சியை குறத்தி முடுக்கு தங்கத்திடம் காணமுடிகிறது. தான் கணவனாக நினைக்கும் நடராஜனுக்காக விபச்சாரியாக மாறுகிறாள் தங்கம். தங்கத்தின் கணவன் அவளை அத்தானிடம் நூறு ரூயாய்க்கு விற்றுவிட்டுப் போய்விடுகிறான். நடராஜன் தன்னை ஏமாற்றிவிட்டான் என்ற கோபமோ வெறுப்போ தங்கத்திடம் துளியும் இல்லை; மாறாக அவன் நிலை குறித்து அனுதாபப்படவே செய்கிறாள். தனக்காகத்தான் அவன் இவ்வாறெல்லம் செய்கிறான் என்ற குற்றவுணர்வே அவளிடம் மேலோங்கி காணப்படுகிறது. தான் புனைந்துகொண்ட தொழிலுக்கும் அவள் நேர்மையாக நடந்துகொள்கிறாள். தன்னைத் தேடி வருபவர்கள் கொடுக்கும் பணத்திற்கு தன்னால் முடிந்த அளவுக்கு அவர்களோடு நியாயமாக இருக்க முயற்சிக்கிறாள். இத்தகைய குணங்களால் கவரப்பட்ட பத்திரிகையாளன் தங்கத்தைத் திருமணம் செய்துகொள்ள முயற்சிக்கிறான். "நல்ல பெண்ணாப் பாத்து கல்யாணம் செய்துகிட்டு சொகமா இருங்க. நாங்க எல்லாம் கழுதைங்க" என்று தங்கம் அவளிடம் கூறுகிறாள். மேலும் அதே தங்கம் மற்றொரு இடத்தில், "குறத்தி முடுக்கிலே இருந்தா, அதனாலே தாலியறுந்தவளாயிடுமா?" என்று கேள்வி கேட்கிறாள். தன்னைப் பாலியல் தொழிலில் ஈடுபடுத்திய கணவன் வந்து அழைத்தவுடன் அவனுடனேயே சென்று விடுகிறாள்.

குறத்தி முடுக்கின் 'தங்கம்' ஜி.நாகராஜன் படைத்த பெண்களிலேயே மிகச் சிறந்தவள். புதுமைப்பித்தனின் 'அம்மாளு' சாதாரண பெண்; ஆனால் ஜி.நாகராஜனின் தங்கம் ஒழுங்கின்மைக்குள் நின்றுகொண்டு சில ஒழுங்குகளைக் கட்டமைப்பவள்; புனிதத்திற்கு எதிரான ஒழுங்குகளைச் சிதைப்பவள்; தான் செய்யக்கூடிய பாலியல் தொழிலுக்கும் சில புனிதங்களை உருவாக்குபவள் என பன்முகத் தன்மை வாய்ந்தவளாக இருக்கிறாள். தங்கத்தைப் பொறுத்தவரை ஜி.நாகராஜனின் கட்டுப்பாட்டிற்கு அப்பாற்பட்டவளாக அவரது பாத்திரம் இருக்கிறது. அக்கதாபாத்திரம் கதாசிரியனின் கட்டுப்பாட்டிலிருந்து இயல்பாகவே விலகிவிடுகிறது. ஜி.நாகராஜனும் அதனைக் கட்டுப்படுத்தவில்லை. இதேபோன்று மரகதம், செல்லம், செண்பகம், தேவையானை, மீனாட்சி என நாவலில் வரும் பெண்கள் அனைவரும் தங்களுக்கே உரிய வாழ்வின் சிக்கல்களுடனும் அதீத காதலுடனும் காமத்துடனும் உலா வருகிறார்கள். ஜி.நாகராஜன் ஒரு பார்வையாளராக மட்டுமே அவர்களிடம் நடந்துகொள்கிறார். ஆனால் ஜி.நாகராஜன், 'தான் விரும்பும் ஒரு பெண்ணைக் கதாபாத்திரங்களில் திணிக்கிறார். ஜி.நாகராஜனால் தன்னைக் கருவியாக்கும் ஓர் ஆண் சமூகத்தைத் தூக்கியெறிந்துவிட்டு புதிதாக வாழத்தொடங்கும் ஒரு பாலியல் தொழிலாளியை நினைத்துக்கூட பார்க்கமுடியவில்லை. ஆணுக்கு அடிமையாக இருக்கும்; எல்லா சுரண்டல்களையும் சகித்துக்கொண்டு நேர்மையைக் கடைபிடிக்கும் மரகதம், தங்கம், மீனா போன்ற பெண்களே அவருக்கு உவப்பானவர்கள்' என்ற விமர்சனமும் அவர்மீது உண்டு. 'அடுத்தது வருபவன் ஆணா, அலியா, கிழவனா, வாலிபனா, அழகனா, குரூபியா, முரடனா, சாதுவானவனா என்றெல்லாம் கவலைப்படாது அவனிடத்துத் தன்னைத் தானே ஒப்படைத்துக்கொள்கிறானே அந்தச் சிறுமியிடத்து யாரும் ஒரு தெய்வீக உணர்வைச் சந்திக்காமல் இருக்க முடியாது. சமுதாயம் அவ்வப்போது கற்பிக்கும் போலி ஏற்றத்தாழ்வு உணர்ச்சிகளுக்கு இரையாகாமல் இருப்பவன் ஒருவனே இதைப் புரிந்துகொள்ள முடியும். எது எப்படி இருப்பினும் 'தேவடியாள்' என்பதை ஒரு வசைச் சொல்லாகப்

பயன்படுத்த நியாயமே இல்லை' (ஜி.நாகராஜன் ஆக்கங்கள்) என்ற உயர்ந்த கருத்தை ஜி.நாகராஜன் கொண்டிருந்தார்; இந்தக் கருத்திலிருந்து கடைசிவரை மாறவில்லை. பாலியல் தொழிலாளிகளால் போற்றிப் பாதுகாக்கப்பட்டவர் ஜி.நாகராஜன் என்பதை அவருடன் பழகியவர்கள் நன்கு அறிவார்கள்.

ஜி.நாகராஜனின் சிறுகதைகளைவிட அவரது இரு நாவல்களுமே அதிகமாக கவனிக்கப்பட்டவை. தி.ஜா.வைப் போன்று நாவல்களின் மூலமாகவே அடையாளம் காணப்பட்டவர் ஜி.நாகராஜன். அவரது 'நாளை மற்றொரு நாளை' 'Tomorrow is One More Day' என்ற பெயரில் ஆங்கிலத்தில் மொழிபெயர்த்து வெளியிடப்பட்டுள்ளதையும் இங்கே குறிப்பிட வேண்டும். ஜி.நாகராஜனை மதிப்பீடு செய்பவர்கள் அவரது நாவல்களை மட்டுமே எடுத்துக்கொள்கின்றனர். அவரது நாவல்கள் அளவுக்கு அவரது சிறுகதைகள் கவனிக்கப்படவில்லை என்பது உண்மை. அவரது இரண்டு நாவல்களுக்கும் இணையான ஒரு சிறுகதை, 'கல்லூரி முதல்வர் மிஸ் நிர்மலா' என்ற கதை. ஐந்து பக்கங்களுக்கும் குறைவான இக்கதை கட்டியெழுப்பும் காமத்தின் பிம்பம் மிகப்பெரிது. மனிதர்களுக்குள் படிந்திருக்கும் காமத்தின் இயல்புக்கு முன்னர் வயது, பதவி, மனித மதிப்பீடுகள், சுயமரியாதை எல்லாம் சாதாரணமாக சரிந்து வீழ்வதை ஜி.நாகராஜன் அழகாகக் கதையாக்கியுள்ளார். இதேபோன்று ஜி.நாகராஜனின் இறப்புக்குப் பிறகு தொ.மு.சி.ரகுநாதனிடமிருந்து பெறப்பட்டு, 1988-ஆம் ஆண்டு காலச்சுவடில் பிரசுரிக்கப்பட்ட 'ஆண்மை' என்ற சிறுகதை ஜி.நாகராஜன் படைப்புகளில் உச்சம் என்று கூறும் அளவுக்கு மிகச்சிறந்ததொரு புனைவு. காலத்தின் சூழ்ச்சியின் காரணமாக பெரும் வீழ்ச்சியைச் சந்தித்த ஒரு தந்தை, தன் மனைவியின் மருத்துவச் செலவினங்களுக்காகவும் இழந்த வாழ்க்கையை மீட்டெடுப்பதற்காகவும் தன் இருபது வயது நிரம்பிய மகளை அலுவலகம் அனுப்புவதுபோல் பாலியல் தொழிலுக்கு அனுப்புகிறார். முப்பது ரூபாய் கொடுத்து அவளுடன் ஆண்மையை நிரூபிக்க நினைத்த ஒருவன், அவளின் நிலை கண்டு தான் ஓர் ஆண்மையற்றவனென வெளியேறுகிறான். தன் தந்தையாலேயே பாலியல் தொழிலுக்கு அனுப்பப்படும் ஒரு பெண்ணின் மனநிலையை இதைவிடச் சிறப்பாகச் சொல்லிவிட முடியுமென்று தோன்றவில்லை.

பாலியலை அறிவு நிலையிலிருந்து விடுதலை செய்யும் முயற்சிகளை ஆரம்பகாலத்தில் கு.ப.ரா.வும் தி.ஜானகிராமனும் மேற்கொண்டனர். ஜெயகாந்தன் இவர்கள் இருவரிலும் இருந்து வேறு பட்டவராகவே காணப்படுகிறார். 'காமந்தான் ஆணுக்கு அழகு. காமத்தை வைத்தே ஓர் ஆண் ஒரு பெண்ணை வெல்ல முயல வேண்டும். மற்ற எந்தச் சக்தியின் உதவியை நாடுவது ஆண்மைக் குறைவு, தோல்வி' என்று வெளிப்படையாகப் பேசும் தன்மை கொண்டவர். இவரது வாழ்க்கையைப் போலவே இவரது படைப்புகளும் அமைதியற்றவை; வாசகர்கள் மத்தியிலும் விமர்சகர்கள் மத்திலும் கடுமையான விமர்சனங்களை எதிர்கொண்டவை. ஜெயகாந்தனை ஏற்றுக் கொண்டவர்கள்கூட ஜி.நாகராஜனை ஏற்றுக்கொள்ள மறுத்தார்கள். அதிர்ச்சி மதிப்பீடுகளுக்காகவும் பரபரப்புக்காகவும் கிளர்ச்சிக்காகவும் ஜி.நாகராஜன் எழுதுவதாகக் கருதினார்கள். அவரின் தனிப்பட்ட வாழ்க்கையோடு சேர்த்து அவரது படைப்புகளையும் விமர்சித்தார்கள்.

ஜி.நாகராஜனின் ஒட்டுமொத்தப் படைப்புகளையும் வாசிக்கும்பொழுது அவர் பாலியல் தொழிலாளிகளை மட்டும் தம் படைப்புகளில் முன்னிலைப் படுத்தவில்லை என்பதைப் புரிந்துகொள்ள முடியும். இவரது புனைவுகள் ஒழுக்கமின்மைக்குள் ஓர் அழகியலைக் கட்டமைக்கின்றனர். 'மனிதாபிமான உணர்வில் மட்டும் உயர்ந்த இலக்கியம் உருவாவதில்லை. மனித துவேஷ உணர்வும் சிறந்த இலக்கியத்தைப் படைக்கவல்லது' (பக்.478) என்று ஜி.நாகராஜன் தம்முடைய பொன்மொழிகளில் குறிப்பிட்டுள்ளார். இதையே தம் புனைவுகளிலும் வெளிப்படுத்தினார். இவரது 35 சிறுகதைகளும் கிளர்ச்சிக்காகவோ பரபரப்புக்காகவோ எழுதப்பட்டவை அல்ல. வடிவநேர்த்தி கொண்ட பல கதைகளை இவர் எழுதியிருக்கிறார். வெகுமதி, தீராக் குறை, பச்சக்குதிரை, நடிகள் போன்ற பல கதைகளை இதற்கு உதாரணமாகக் கூறலாம். பெண்களின் உணர்வுகளை நுட்பமாக வெளிப்படுத்தும் தீராக்குறை கு.ப.ரா.வின்

கதைகளோடு ஒப்பிடத்தக்கது. 'யாரோ முட்டாள் சொன்ன கதை' இனக்குழு சமூகத்தின் எச்சமாக உள்ள பாக்கியம் என்ற பெண்ணின் இருப்பை வெளிப்படுத்தும் கதை; பாக்கியம், குடும்பம் என்ற அமைப்பை தன் நடவடிக்கைகளின் ஊடாக இயல்பாக கடந்து சென்று விடுகிறாள். 'ஜி.நாகராஜன் ஓர் ஆணாதிக்கவாதி' என்று அவரது நாவல்களை மட்டும் படித்துவிட்டு விமர்சிப்பவர்களுக்கு பதில் சொல்லும் கதை. ஜி.நாகராஜன் படைத்த பெண்களிலிருந்து வேறுபட்டவள் பாக்கியம். 'என் கதைகளில் முழுமையாக சிறுகதை இலக்கணத்தைப் பெற்றிருக்கும் ஒரே கதை 'யாரோ முட்டாள் சொன்ன கதை' மற்றவையெல்லாம் வெறும் முயற்சிகளே' (பக்.489) என்று தன்னுடைய 'கண்டதும் கேட்டதும்' சிறுகதைத் தொகுப்பிற்காக எழுதிய சுயவிமர்சனத்தில் ஜி.நாகராஜன் குறிப்பிடுகிறார். ஜி.நாகராஜன் தன்னுடைய படைப்புகள் குறித்தும் தன்னைக் குறித்தும் என்றுமே உயர்ந்த மதிப்பீடுகளைக் கொண்டிருந்ததில்லை என்பதையும் எண்ணிப்பார்க்க வேண்டும்.

தமிழின் மிகச்சிறந்த எழுத்தாளரான ஜெயமோகன் ஜி.நாகராஜனின் ஒட்டுமொத்த ஆக்கங்கள் குறித்தும் பின்வருமாறு மதிப்பிடுகிறார்.

அ. ஜி.நாகராஜன் அதுவரை கூறப்படாத ஓர் உலகத்தின் சித்திரத்தை அளித்தவர் அல்லர்.

ஆ. அவர் கூறிய உலகம் இலக்கியத்தின் தொடக்கம் முதல் தமிழில் இருந்து வந்ததுதான்.

இ. நவீன இலக்கியத்தில் ஒழுக்கப் பார்வை சார்ந்தும் கற்பனாவாத மனிதாபிமானப் பார்வை சார்ந்தும் முற்போக்கு மனிதாபிமானப் பார்வை சார்ந்தும் இவ்வுலகம் ஏற்கனவே கூறப்பட்டுள்ளது.

ஈ. ஜி.நாகராஜன் நவீனத்துவ அழகியலுடனும் நவீனத்துவ தத்துவப் பார்வையுடனும் அவ்வுலகை மீண்டும் சொன்னவர்.

உ. நவீனத்துவ அணுகுமுறையின் பலங்களான வடிவநேர்த்தி, மொழிக்கச்சிதம் அவரிடம் உள்ளது.

ஊ. நவீனத்துவ அணுகுமுறையின் பலவீனமான மனிதனை தனித்த இருப்பாக, அடிப்படை உணர்வுகளாலும் இச்சைகளாலும் மட்டும் உருவானவனாகக் குறுக்கும் போக்கு அவரிடம் உள்ளது. (நவீனத்துவத்தின் முகங்கள், பக்.54)

ஜி.நாகராஜன் தேர்ந்தெடுத்துக் கொண்ட வாழ்க்கைமுறை தொடர்ந்து விமர்சிக்கப்படும் ஒன்றாகவே இருந்து வருகிறது. அவரது வாழ்க்கையை ஒழுங்கீனத்தின் வெளிப்பாடாகப் பார்த்தவர்கள் அவரது படைப்புகளையும் அவ்வாறே எதிர்கொண்டனர். தனி மனிதன் மேல் சமூகமும் பண்பாடும் ஏற்றிவைக்கும் ஒடுக்குமுறைக்கு எதிரான ஒரு கலகக்குரலாகவும் ஜி.நாகராஜனைப் பார்த்தனர். உதாரணமாக ஜி.நாகராஜனைக் கடுமையாக விமர்சிக்கும் ஜெயமோகன், 'ஜி.நாகராஜனின் படைப்புகள் எப்போதும் நமது தீவிர இலக்கியத்தின் குறிப்பிடத்தக்க பகுதியாக இருந்து கொண்டதான் இருக்கும். நமது மரபில் என்றுமுள்ள பரத்தையர் உலகின் நவீனச் சித்தரிப்பு முறைகளில் நவீனத்துவம் சார்ந்த கோணம் அவருடையது. நமது நவீனத்துவப் படைப்பாளிகளில் அங்கதம், கச்சிதமான வடிவம் ஆகியவற்றின் மூலம் முக்கியத்துவம் பெறும் படைப்பாளி அவர்' (நவீனத்துவத்தின் முகங்கள், பக்.77) என்று இறுதியாக நிறைவு செய்கிறார். பாலியல் ஒடுக்குமுறைகள் குறித்து தீவிர விவாதங்களை உருவாக்கிய ஜி.நாகராஜன், சமூகத்தின் இறுக்கமான கட்டமைப்புகளைத் தகர்த்தெறிய அறியப்படாத இருண்ட பகுதிகளின்மீது தம் புனைவுகள் ஊடாக வெளிச்சம் பாய்ச்சினார். இவரது புனைவுகள் விளிம்புநிலை மக்களின் இனவரைவியலைத் தேடுபவை. ஜி.நாகராஜன் அடுத்து வரக்கூடிய எழுத்தாளர்களுக்கு நிறையவே வழிகாட்டிச் சென்றிருக்கிறார்; விட்டுச் சென்றிருக்கிறார். 'ஜி.நாகராஜனின் அருமையை உணர சமூக மதிப்பீடுகளின் கண்கள் கொஞ்சமும் உதவாது. இயல்புணர்ச்சிகளை நேசிக்கும் கண்களுக்கு மட்டுமே ஜி. நாகராஜனுடைய வாழ்வும் எழுத்தும், வசீகரமும் அழகும் கொண்டதாக வெளிப்படும்' (தீராந்தி, அக்.2010) என்ற சி.மோகனின் கருத்துதான் ஜி.நாகராஜனை விமர்சிப்பவர்களுக்கான பதில்.

உதவி நூல்கள்

- 1.ஜி.நாகராஜன் ஆக்கங்கள், ராஜமார்த்தாண்டன் (தொ.ஆ), காலச்சுவடு, மு.ப. டிச.2007
- 2.ஜி.நாகராஜன் நினைவோடை, சுந்தர ராமசாமி, காலச்சுவடு, மு.ப. நவ.2006
- 3.நவீனத்துவத்தின் முகங்கள், ஜெயமோகன், தமிழினி, மு.ப. செப்.2003
- 4.நடைவழிக் குறிப்புகள், சி.மோகன், அகரம், மு.ப. டிச.2000
- 5.தீராநதி, அக்.2010

Notes on the preparation of papers

Typescript

Text should be typed double spaced with 1" margin on all sides. Text with embedded graphics should be in Microsoft Word Format.

Title page

- (1) The title of the paper must be short and contain words useful for indexing
- (2) Name(s) of author(s) with initial(s) and the name and address of the institution where the work was done must be given. Present address (es) of author(s) may be given if different from the above.
- (3) An abbreviated running title of not more than 50 letters and spaces must also be given.

Abstract

All papers must have an abstract of not more than 200 words of the significant results reported in the paper. Presentation of numerical results should be avoided as far as possible in the abstract.

Keywords

Between 3 and 6 keywords must be provided for indexing and information retrieval.

Text

The paper must be divided into sections starting preferably with 'Introduction' and ending with 'Conclusions'. Main sections should be numbered 1, 2 etc., sub-sections 1.1, 1.2 etc. and further sub-sections (if necessary) 1.1a, 1.1b etc.

Tables

All tables must be numbered consecutively in Arabic numerals in the order of their appearance in the text. Tables should be self-contained and have a descriptive title.

Figures

All figures including photographs should be numbered consecutively in Arabic numerals in the order of their appearance in the text. Figure captions must be typed on a separate sheet.

References

References should be cited in the text as superscript numbers in order of appearance. References at the end of the paper should be listed in serial order to match their order of appearance in the text. References should be listed in the following manner. Author(s) name(s), followed by initial(s), year of publication, name of the journal (abbreviated according to the World List of Scientific Periodicals, Butterworths, London) volume number, and number of the first page. References to books should include: name(s) of author(s), initials, year of publication, title of the book, edition of not the first, initials and name(s) of editor(s), if any, preceded by "ed(s)", place of publication, publisher and chapter or pages referred to. References to theses must include the year, the title of the thesis, the degree for which submitted, the name of the university and the city where it is located. References to reports and unpublished conference proceedings should include the title of the report/paper.

Footnotes

Footnotes to the text should be avoided if possible but when necessary should be numbered consecutively, and typed on a separate sheet.